The Effect of α-Tocopherol on the Membrane Dipole Potential

Sterenn Le Nen Davey MPhys

Submitted by Sterenn Le Nen Davey, to the University of Exeter as a thesis for the degree of Doctor of Philosophy in Physics, March 2011

Abstract

α-Tocopherol has a well known antioxidant action but is also considered likely to exert significant non-antioxidant effects in cell membranes. Due to its lipophilic nature α-tocopherol inserts into biological membranes where it influences the organisation of the component lipids and may therefore influence biophysical parameters including the membrane dipole potential. The dipole potential has been demonstrated to modulate the function of several membrane associated proteins and perturbation of this physical parameter by α-tocopherol may prove to be a significant non-antioxidant mechanism underlying several of its cellular effects. This study investigates the influence of α-tocopherol, and the non-antioxidant structural analogue α-tocopherol succinate, on the membrane dipole potential employing fluorescence spectroscopy techniques with the dipole potential sensitive probe Di-8-ANEPPS. Similar techniques are utilised with the surface potential sensitive probe FPE to investigate the interaction of the charged α-tocopherol succinate molecule with membranes. α-Tocopherol and α-tocopherol succinate are shown to decrease the dipole potential of egg-phosphatidylcholine vesicles and Jurkat T-lymphocyte cell membranes. This effect is placed in the context of the significant influence of membrane cholesterol oxidation on the dipole potential. 7-ketocholesterol, an oxidised form of cholesterol, significantly influences several cellular processes and is thought to mediate these effects, in part, through its physical effects on the cell membrane. These include altering the composition, and therefore biophysical properties, of rafts; structures which are considered to support the function of a host of membrane proteins. This study attempts to correlate the effect of 7-ketocholesterol on the dipole potential of microdomains with the influence of the oxysterol on the function of two microdomains associated receptors: P-glycoprotein and the insulin receptor, assessed by determining the extent of ligand binding using flow fluorocytometry. α-Tocopherol has been suggested to inhibit the raft-mediated effects of 7-ketocholesterol and the influence of this molecule on the effect of 7-ketocholesterol on the dipole potential are investigated as a potential mechanism for this inhibition. It is hypothesized that α-tocopherols may protect against the deleterious effects of cholesterol oxidation in cell membranes by excluding 7-ketocholesterol from specific microdomains, of which rafts are a subset, acting to preserve their dipole potential and maintain the function of the proteins they support. However, where significant cholesterol oxidation has previously occured the concurrent changes in the microdomain landscape of the membrane is suggested to prevent α-tocopherol succinate from eliciting this protective effect.

Acknowledgements

I would first like to thank my supervisors Prof. Peter Winlove and Dr Peter Petrov for the opportunity to undertake this PhD and their support and guidance, both academic and pastoral, throughout my studies. I would also like to convey my deep gratitude to Prof. Paul O'Shea, my acting supervisor at the Institute of Biophysics, Imaging and Optical Science (IBIOS), University of Nottingham, where the work presented in this thesis was conducted, and without whose understanding and generosity this thesis would not exist. I extend my thanks to members past and present of the Biomedical Physical Group, University of Exeter, particularly; Ellen Green, Dick Ellis, Dr. Natalie Garrett, Dr. Elly Martin, Dr. Sarah Carr, Dr. Mike Chu, Dr. Jess Mansfield, Dr. Sharon Jewell, Dr. John Hale, Dr. Kenton Arkill, Amanda Lindsay and Rachel Palfrey for their friendship and support. Thanks also to members past and present of the Cell Biophysics group and IBIOS, University of Nottingham, particularly; Prof. Mike Somekh, Dr Mark Pitter, Dr Kevin Webb, Dr Joanna Richens, Dr Mark Tilley, Dr Ken Hsu, Ben Davis, Kelly-Ann Vere and Graeme McKenzie. Thank you all for your support during the PhD process.

I would like to thank Dr Jackie Whatmore (Peninsula College of Medicine and Dentistry) for her time and patience in introducing a clueless physicist to cell culture technique and to Rebecca Wordsworth, Ben Davis and Dr Kenton Arkill for 'babysitting' cultures from time to time. I would also like to thank members of the vascular interthematic network (University of Exeter) for many interesting discussions and introducing me to a fascinating interdisciplinary outlook of vascular research.

I would like to thank my family and prospective family in-law without whose love and support I wouldn't have been able to complete this process. A special thank you to my parents, my sister Maela, my future parents in-law, Anna and Steve, and my fiancé Ben (who not only offered endless encouragement and helped me to keep perspective during the last months of the PhD, but as a fellow biophysics PhD student has discussed the contents of this thesis at length) to whom I'd like to dedicate this thesis. Finally a big thank you to my friends including; Tanya Eves-Browning, Emma Richards, Martin Cardoza, Loveday Trinick-Rowe, Steve Rowe, Becki Wordsworth, Natalie Garrett, John Tyler, Ben Ayliffe, Paul Hegarty, Chris Higman and Nick Jones for always being there and being understanding of my long silences (this is what I've been up to!).

Finally I would like to thank the EPSRC for funding this project.

Table of Contents

List of Figures

List of Tables

Abbreviations

AF-488	Alexa Fluor 488
S488	Streptavidin-Alexa Fluor 488
^{125}I-Insulin	^{125}I radioligand conjugated insulin
6-KC	6-ketocholestanol
7-KC	7-ketocholesterol
A_l	integral area of long-wavelength component of Di-8-ANEPPS excitation spectrum
apoA-I	apolipoprotein A1
A_s	integral area of short-wavelength component of Di-8-ANEPPS excitation spectrum
BI	biotinylated insulin
B_{max}	maximum change in fluorescence signal
Ca^{2+}	calcium ions
Caco2	epithelial cell line
CARS	coherent anti-stokes raman scattering
C_B	concentration of deprotonated FPE
C_{HB}	concentration of protonated FPE
Chol	Cholesterol
CMC	critical micelle concentration
Di-8-ANEPPS	(*1-(3-sulphonatopropyl)-4-[β[2-(di-n-octylamino)-6-naphthyl]vinyl]pyridium betaine*)
DLPC	1,2-dilauroyl-sn-3-glycerophosphatidylcholine
DMPC	Dimyristoylphosphatidylcholine
DNA	deoxyribosenucleic acid
DOPC	Dioleoylphosphatidylcholine
DOPE	Dioleoylphosphatidylethanolamine
DOPS	Dioleoylphosphatidylserine
DPBS	Dulbecco's phosphate buffered saline
DPH	1,6-diphenyl-1,3,5-hexatriene
DPPC	Dipalmitoylphosphatidylcholine
DRM	detergent resistant membranes
DSC	differential scanning calorimetry
egg-PC	egg-phosphatidylcholine
ESR	Electron spin resonance
FBS	Foetal bovine serum
FI, fitc-I	fluorescein isothiocyanate labelled insulin
FPE	fluorescein phosphatidylethanolamine
FRAP	fluorescence recovery after photobleaching
FRET	Forster resonance energy transfer
FSC	forward scattered light
FTIR	Fourier transform infrared spectroscopy
GM1	Monosialotetrahexosylganglioside
GM2	Ganglioside GM2
GM3	Ganglioside GM3
GPI	Glycophosphatidylinositol
HC	4-heptadecyl-7-hydroxy-coumarin
HUVEC	human umbilical vein endothelial cells
h	hill coefficient

I	Insulin
IR	insulin receptor
K_d	binding affinity or dissociation constant
K_{eff}	molar efficiency of titrated substance in modulating the surface or dipole potential
L_α	pseudocrystalline phase
L_β	gel phase
l_c	liquid crystalline phase
l_d	liquid disordered phase
LDL	low density lipoprotein
l_o	liquid ordered phase
LogD	Distribution coefficient
LogP	Octanol/water partition coefficient
MD	molecular dynamics
MβCD	methyl-β-cyclodextrin
NMR	nuclear magnetic resonance
P_β	ripple phase
PA	phosphatidic acid
PC	Phosphatidylcholine
PE	Phosphatidylethanolamine
Pe	Phycoerythricin
PG	Phosphatidylglycerols
P-gp	P-glycoprotein
PI	Phosphatidylinositol
PI	propidium iodide
pK_a	apparent pK
Pk_{aB}	apparent pK in bulk aqueous medium
pK_{as}	apparent pK at membrane surface
POPC	1-palmitoyl-2-oleoyl-*sn*-3-glycerophosphatidylcholine
PS	Phosphatidylserine
PUFA	poly unsaturated fatty acid
R	ratio of fluorescence emission of Di-8-ANEPPS at 460nm and 520nm excitation
ROS	reactive oxygen species
Saq	Saquinavir
SPT	single particle tracking
SSC	side scattered light
Swiss 3T3 cells	fibroblast cell line
$T_{1/2}$	temperature at which an assymetrical phase transition is one-half complete
TB	trypan blue
T_m	main (gel-liquid crystalline) transition temperature
TPGS	Tocopheryl polyethylene glycol 1000 succinate
$X^\bullet$	denotes a radical
$X^{\delta+}$-$X^{\delta-}$	denotes a dipole
α-toc, toc	α-tocopherol
α-TS, TS	α-tocopherol succinate
α-TTP	α-tocopherol transfer protein
ΔF	change in fluorescence
ΔR	change in ratio of fluorescence emission of Di-8-ANEPPS at 460nm and 520nm

	excitation
$\Delta\nu$	spectral shift
$\Delta\Psi$	transmembrane potential
λ_l	wavelength peak of long-wavelength component of Di-8-ANEPPS excitation spectrum
λ_s	wavelength peak of short-wavelength component of Di-8-ANEPPS excitation spectrum
μ	dipole moment
Ψ_d	membrane dipole potential
Ψ_s	membrane surface potential
ω	stern potential

1. Introduction

The cell membrane is a double layered polymeric structure of amphipathic lipids that entirely encloses a cell acting as a boundary to its external environment. This section introduces the species of lipid present in biological membranes and the structural characteristics that drive the formation, and determine the physical properties, of membranes. The additional elements that, together with the lipid bilayer, comprise the cell membrane are then outlined and their influence alongside that of the lipids on the functions of the cell membrane is discussed.

1.1. Lipid membranes

Lipid membranes formed from selected synthetic or natural extracted lipids in aqueous solution are widely used as a simple model of biological membranes to study the behaviour of lipids in these polymeric structures. This section outlines the lipids present in biological membranes and reviews their collective behaviours, which can be correlated with their structural characteristics, determined by studies with lipid membrane models.

1.1.1. Lipid membrane composition

Membrane lipids are amphipathic molecules possessing a polar (hydrophilic) headgroup and a non-polar (hydrophobic) tail. There are three predominant categories of lipids within biological membranes; phospholipids, subcatergorised into glycerphospholipids and sphingolipids, sterols and minor or simple lipids. The structure of these lipids is outlined in the following section.

1.1.1.1. *Phospholipids*

Phospholipids comprise the principle lipid component of biological membranes and consist of a phosphate containing headgroup and two fatty acid chains covalently linked via a structural backbone, the identity of which determining their sub-categorisation.

Glycerophospholipids consist of an L-glycerol core which is tri-substituted with a phosphate, forming the basis of the headgroup, and two fatty acid chains. Several types of structural group may then be bound, via an ester linkage, to the phosphate to form the headgroup, as presented in Figure 1.1.1. These include choline, ethanolamine, serine, inositol or simply a hydrogen atom, resulting in phosphatidylcholine, phosphatidylethanolamine and phosphatidylserine, the three most abundant phosphoglycerides in the cell membrane, and phosphatidylinositol, which is present in smaller amounts, respectively. The substitution of a hydrogen atom results in phosphatidic acid which can be readily reverted back to the diacylglycerol by lipid phosphate phosphohydrolases as the concomitant step in the production of the other glycerophospholipids mentioned above. Cardiolipin, a significant component of the inner mitochondrial membrane, is

also classed as a glycerophospholipid and consists of two phosphatidylglycerols linked via a third glycerol backbone to form the dimeric structure (Hauser and Poupart, 2005).

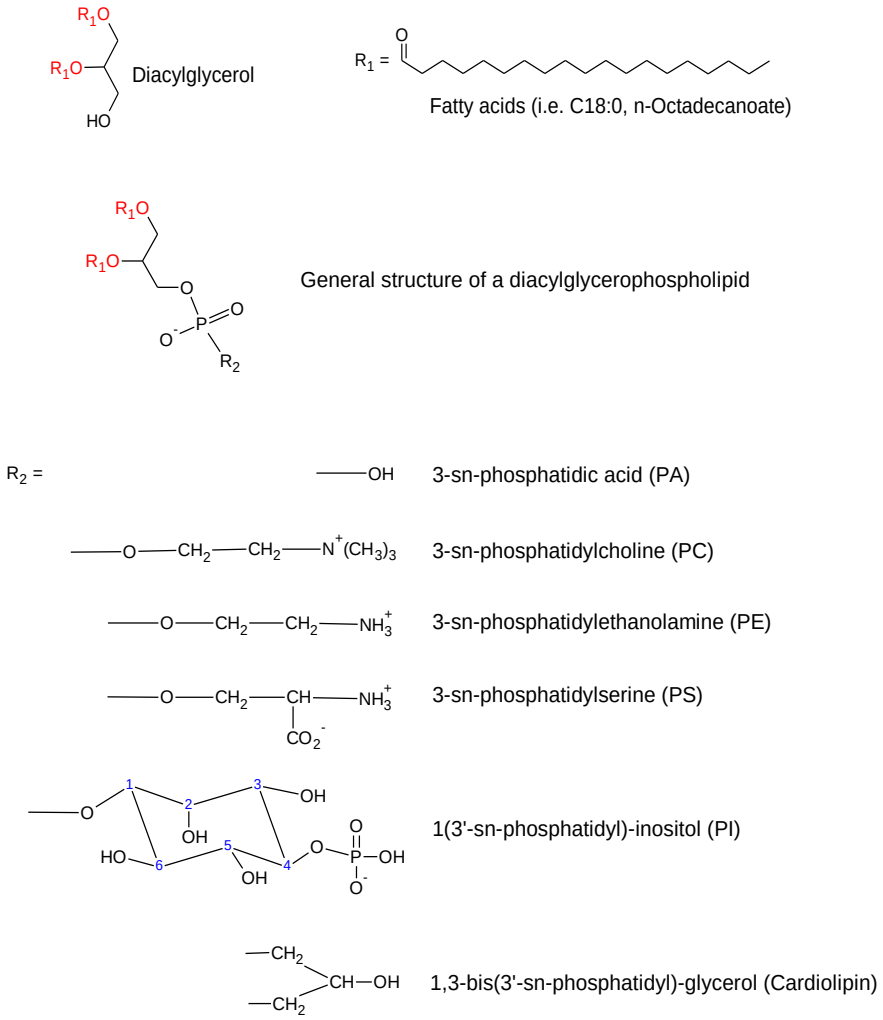

Figure 1.1.1: A depiction of the di- substitution of glycerol with fatty acids, forming diacylglycerol, and the third substitution of the phosphate containing group to give a diacylglycerophospholipid. The chemical structures which, together with the phosphate moiety, form the headgroups of diacyglycerophospholipids commonly found in biological membranes are also shown. Adapted from (Hauser and Poupart, 2005).

The two fatty acid moieties linked to the glycerol backbone generally possess, in eukaryotic membranes, acyl chains of an even number of carbon atoms. These are usually between 14 and 24 carbons in length, with fatty acids of 16 to 18 carbon atoms the most common (Berg et al., 2002, Hauser and Poupart, 2005). These molecules frequently also contain one or more double bond, generally in the *cis* conformation. The most abundant fatty acids in eukaryotic membranes are listed in Table 1.1.1.

Name	Number of carbons	Systematic designation	Formula
Laurate	12	*n*-Dodecanoate	$CH_3(CH_2)_{10}COO^-$
Myristate	14	*n*-Tetradecanoate	$CH_3(CH_2)_{12}COO^-$
Palmitate	16	*n*-Hexadecanoate	$CH_3(CH_2)_{14}COO^-$
Stearate	18	*n*-Octadecanoate	$CH_3(CH_2)_{16}COO^-$
Arachidate	20	*n*-Eicosanoate	$CH_3(CH_2)_{18}COO^-$
Behenate	22	*n*-Docosanoate	$CH_3(CH_2)_{20}COO^-$
Lignocerate	24	*n*-Tetracosanoate	$CH_3(CH_2)_{22}COO^-$
Palmitoleate	16	*cis*-Δ^9-Hexadecenoate	$CH_3(CH_2)_5CH{=}CH(CH_2)_7COO^-$
Oleate	18	*cis*-Δ^9-Octadecenoate	$CH_3(CH_2)_7CH{=}CH(CH_2)_7COO^-$
Linoleate	18	*cis,cis*-Δ^9, Δ^{12}-Octadecadienoate	$CH_3(CH_2)_4(CH{=}CHCH_2)_2(CH_2)_6COO^-$
Linolenate	18	all-*cis*- Δ^9, Δ^{12}, Δ^{15}-Octadecatrienoate	$CH_3(CH_2)_2(CH{=}CHCH_2)_3(CH_2)_6COO^-$
Arachidonate	20	all-*cis*- Δ^5, Δ^8, Δ^{11}, Δ^{14}-Eicosatetraenoate	$CH_3(CH_2)_4(CH{=}CHCH_2)_4(CH_2)_2COO^-$

Table 1.1.1: The most common saturated and unsaturated fatty acids of eukaryotic cell membranes. The notation Δ^n refers to the presence of a double bond at the n^{th} carbon. Adapted from (Berg et al., 2002).

1.1.1.2. ***Sphingolipids***

Sphingolipids are lipids which have sphingosine, a sphingoid backbone with a single fatty acid chain attached via an amide linkage, as a basis. The addition of a second fatty acid via amide linkage to the sphingoid transforms the molecule into a ceramide which, with the addition of a headgroup, forms a sphingolipid, as shown in Figure 1.1.2. They are less abundant in eukaryotic membranes than their glycerophospholipid counterparts but three main forms are present to notable extents which are sphingomyelins, glycosphingolipids and gangliosides. Sphingomyelins possess an ester linked phosphocholine or phosphoethanolamine bound to the sphingosine 1-hydroxyl group. Glycosphingolipids contain one or more sugars in their headgroup and gangliosides, such as GM2 or GM3, are based on glycosphingolipids with an oligosaccharide chain possessing at least one sialic acid residue (Hauser and Poupart, 2005).

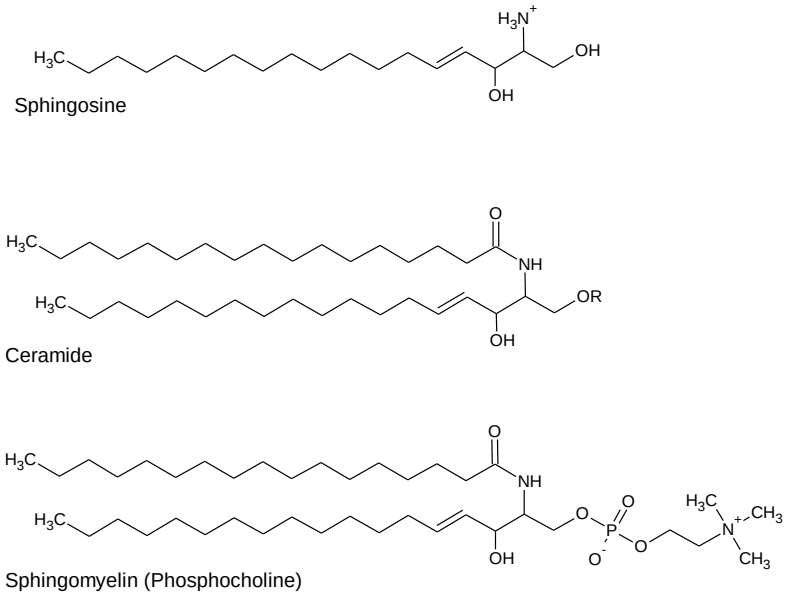

Figure 1.1.2: The chemical structure of sphingosine which is di- substituted with a fatty acid, giving ceramide, and a phosphate containing headgroup (e.g. phosphocholine) forming sphingomyelin. Adapted from (Hauser and Poupart, 2005).

1.1.1.3. ***Sterols***

Sterols describe the category of lipids which possess a fused 4-ring structure consisting of three 6-membered rings and a 5-membered ring with a hydroxyl group in the 3-position of the A-ring as illustrated in Figure 1.1.3. Due to the variation in the degree of saturation and substitution around the fused ring structure many forms of sterol exist however cholesterol (cholest-5-en-3β-ol) is by far the most abundant in mammalian cell membranes (Hauser and Poupart, 2005). The four rings of cholesterol are fused in the *trans* conformation resulting in a relatively flat structure enabling the high packing density of the molecule in biological membranes. This property contributes to the ability of cholesterol to create phase-separated domains in lipid membranes (Demel and de kruijff, 1976, Yeagle, 1988).

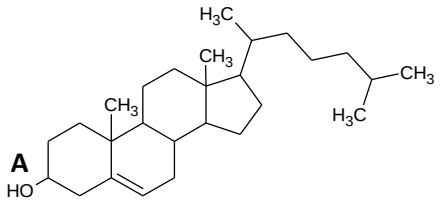

Figure 1.1.3: The structure of cholesterol, a member of the sterol family of lipids characterised by the fused ring structure of three 6-membered rings and a 5-membered ring with a hydroxyl group in the 3-position of the A ring.

1.1.1.4. ***Minor (simple) lipids***

This group of lipids represents those that are present in the membrane in relatively small quantities and includes long-chain alcohols and fatty acids. Retinol, a derivative of vitamin A which is enriched in retinal membranes with an essential role in vision is an example. Other minor lipids include hydrocarbon chains of odd carbon number which accumulate in membranes due to their lipophilic nature but serve no known biological function (Fox and Keith, 1972).

1.1.2. Membrane organisation

The bilayer structure of biological membranes was first proposed by Gorter and Grendel (Gorter and Grendel, 1925) who observed that erythrocytes contained a sufficient quantity of lipid to coat the cell in two lipid monolayers (De Weer, 2000). This structure arises as a result of the interactions of the amphipathic lipid molecules with water, as described by the hydrophobic effect.

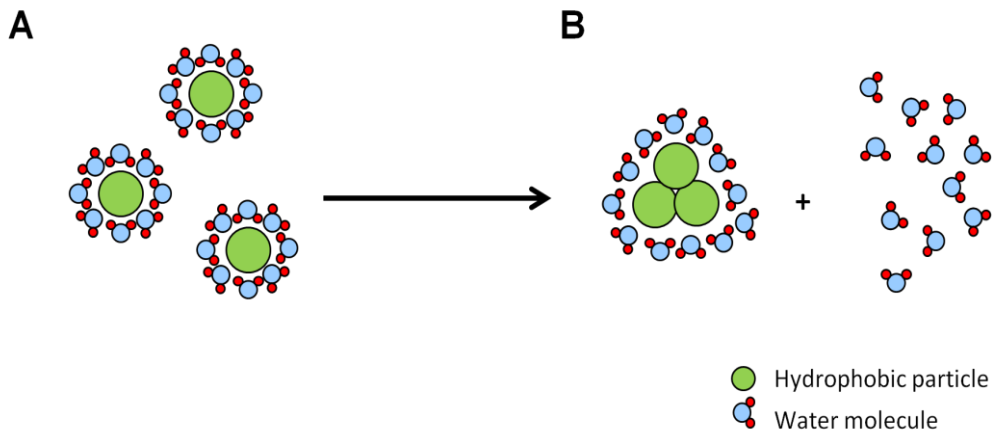

Figure 1.1.4: A diagrammatic demonstration of the hydrophobic effect. **A** depicts hydrophobic particles (green) surrounded by a hydration shell of water molecules (blue/red). The clustering of these molecules (**B**) reduces the total hydrophobic surface area minimising thermodynamically unfavourable hydrophobic-water interactions and relinquishing water molecules to the energetically more favourable water-water interactions.

The hydrophobic effect describes the tendency of water to exclude non-polar molecules resulting in the clustering of these molecules in aqueous solution, as illustrated in Figure 1.1.4. This is thought to be a predominantly entropic process in which the clustering of the non-polar (hydrophobic) molecules is the result, not of the van der Waals attraction of these molecules, but of the preferential association of water molecules (Tanford, 1980). This can be illustrated with consideration to the free energies of attraction associated with the combination of water and the hydrophobic hydrocarbon, octane. The free energy of attraction between octanol and water is around -0.04Jm^{-2} and is closely similar to that between molecules of octanol. The free energy of attraction between molecules of water is significantly greater at -0.144 Jm^{-2} such that this interaction is thermodynamically preferable and drives the minimisation of water/non-polar molecular contact (Tanford, 1980). More recently, involvement of van der Waals interactions in the hydrophobic effect has been reported. In particular this attractive force is thought to have a role in the stabilisation of the clusters of small hydrophobic molecules which only cause relatively slight perturbation of the hydrogen bonding lattice of water compared with their larger non-polar molecules (Chandler, 2005).

Phospholipids are amphipathic molecules with a hydrophilic headgroup counteracting the effect of the hydrophobic fatty acid tails (see Figure 1.1.5A). The result of this amphipathic nature is the formation of higher order, non-covalent, structures in an aqueous environment as illustrated in Figure 1.1.5. In the presence of two phases with different dielectric constants, such as the air-water interface, phospholipids accumulate at the interface, positioned with their hydrophobic fatty acid tails exposed to the air shielded from the aqueous environment by the hydrophilic headgroups (Figure 1.1.5 B). The result of this is a decreasing surface tension with increasing phospholipid concentration at the water surface; a parameter that enables the detection of such lipid films via surface tensiometry (Purdon et al., 1976). If the concentration of phospholipids in

an aqueous environment exceeds a critical threshold, known as the critical micelle concentration, the lipids form one of several organised structures which are classed as lamellar and non-lamellar lipid phases. The nature of the lipid phase formed, and the critical micelle concentration above which it occurs, is dependent on the structure of the lipid monomer (Israelachvili et al., 1976). There are several methods for the determination of the critical micelle concentration of amphiphilic molecules, the most recently proposed technique employs dynamic light scattering to detect the onset of the occurrence of micelles on increasing concentration of lipid in aqueous solution (Davis et al., 2011 *submitted*). The type of organised structures formed above the critical micelle concentration depends on the overall dynamic shape of the lipid (Israelachvili and Mitchell, 1975, Israelachvili et al., 1980, Gruner et al., 1985, Cullis and Dekruijff, 1979, Janmey and Kinnunen, 2006). Phosphatidylcholine, for example, can be considered to have a roughly cylindrical shape as the radius of the volume of the headgroup approximately matches that of the volume occupied by the fatty acid tails. Lipids of this shape form stable lamellar phases including bilayers (Figure 1.1.5 C) or, above the critical micelle concentration, vesicles (Figure 1.1.5D). Lipids such as phosphatidylethanolamine (Cullis and Dekruijff, 1978) and cardiolipin (Vasilenko et al., 1982) possess a headgroup which occupies a volume of smaller radius relative to that of their fatty acid tails giving rise to a roughly conical molecular shape. Lipids of this shape give rise to less stable lamellar structures as they impart a negative curvature stress to the bilayer (Figure 1.1.5 G) and are thermodynamically driven to form non-lamellar structures such as the cubic phase or the type II hexagonal phase (Figure 1.1.5 H). Likewise, lipids of an inverted conical shape, such as lysophospholipids (Fuller and Rand, 2001), form unstable lamellar bilayers under positive curvature strain (Figure 1.1.5 E) and the formation of non-lamellar micelles is thermodynamically preferable (Figure 1.1.5 F).

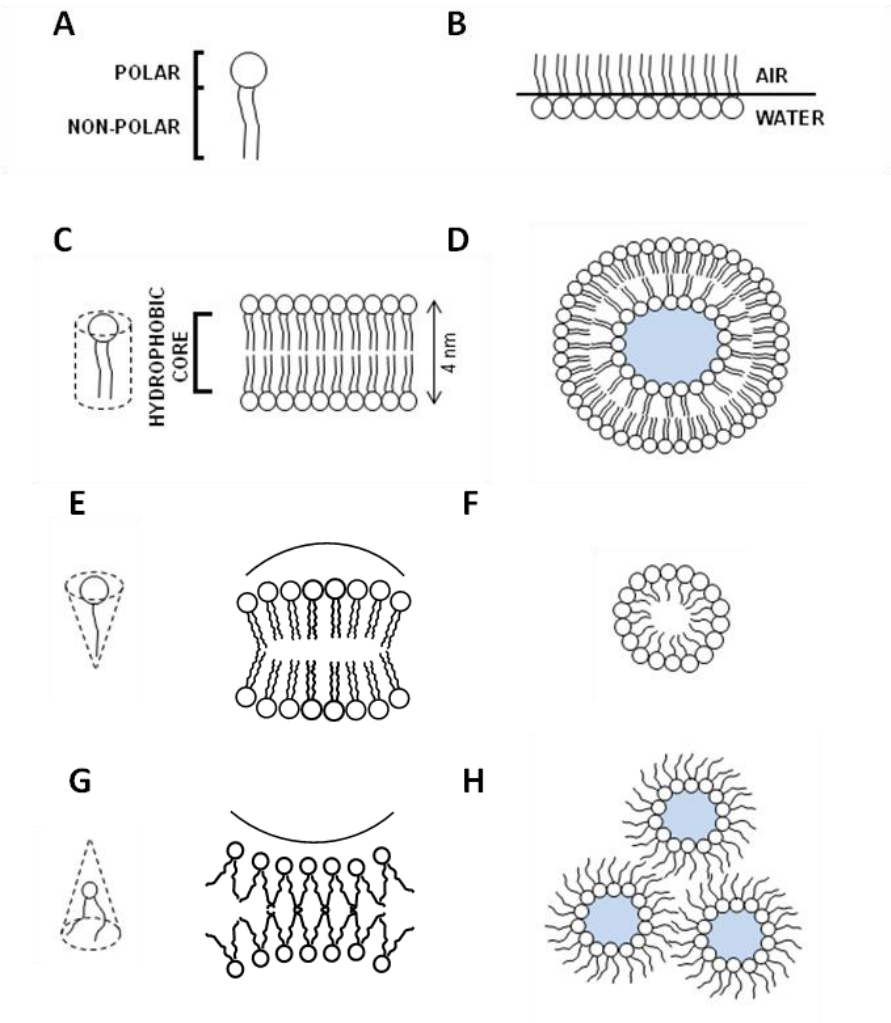

Figure 1.1.5: The amphiphillic nature of phospholipids (**A**) and their orientation at an air-water interface (**B**), and an illustration of the cylindrical (**C**), inverted conical (**E**) and conical (**G**) overall shapes of lipids and the resulting lamellar bilayers and non-lamellar (**D**,**F**,**H**) structures formed in an aqueous environment.

Biological membranes are composed of a variety of lipids which independently promote the formation of lamellar and non-lamellar phases but which collectively adopt a bilayer structure. The presence of non-lamellar lipids, among the lamellar lipids that promote the stable bilayer, imparts a curvature stress on the membrane. The extent to which a lipid is likely to induce curvature stress is determined by the spontaneous radius of curvature of the lipid; a constant specific to a defined set of conditions which include the identity of the other lipids and ions present, the hydration of the membrane and the pH and temperature of the environment. Table 1.1.2 gives the experimentally determined spontaneous radii of curvature of several membrane lipids. Lamellar lipids, such as dioleoylphosphatidylcholine (DOPC), have a large absolute radius of curvature and result in little inherent curvature of a bilayer structure. Lipids such as dioleoylphosphatidylethanolamine (DOPE) and cholesterol posses a relatively low absolute radius of curvature and are likely to induce a negative curvature stress when added to stable lamellar bilayers. This increases the free energy of the bilayer rendering it more susceptible to deformation than the more stable bilayer by lowering the elastic bending modulus; the energy required to deform the membrane (Atkinson et al., 2008). Membrane curvature stress has been

implicated in membrane fusion (Chernomordik and Zimmerberg, 1995, Haque and Lentz, 2004) and, under the guise of "membrane tension" or lipid "packing stresses", has been identified as a potential regulatory mechanism for the activity of membrane bound proteins and enzymes (Brink-van der Laan et al., 2004, Epand, 1998, Morris et al., 2004, de Kruijff, 1997, Kinnunen, 1996).

Lipid	Spontaneous radius of curvature	Reference
Dioleoylphosphatidylcholine (DOPC)	-80 to -200	(Chen and Rand, 1997)
Dioleoylphosphatidylserine (DOPS)	+150	(Fuller et al., 2003)
Dioleoylphosphatidylethanolamine (DOPE)	-28.5	(Leikin et al., 1996)
Cholesterol	-22.8	(Chen and Rand, 1997)
Lyso-phosphatidylcholine	+38 to +68	(Fuller and Rand, 2001)

Table 1.1.2: The spontaneous radius of curvature of various lipids. After (Atkinson et al., 2008).

1.1.3. The phase behaviour of membrane lipids

The bilayer structure adopted by a physiologically relevant combination of lipids can exist in multiple phases dependent on the precise lipid composition and hydration of the membrane as well as the temperature, pressure, ionic strength and pH of the environment (Lewis and McElhaney, 2005). The temperature dependent-, and to a small extent the hydration dependent-, phase behaviour of lipids within a lamellar structure are the most relevant to biological membranes and are discussed below.

1.1.3.1. *The thermotropic phase behaviour of membrane phospholipids*

Simple bilayers composed of a single lipid species can exist in one of four phases; the pseudocrystalline, gel, ripple or liquid disordered phases as illustrated in Figure 1.1.6. The transition between these phases occurs with increasing temperature (at constant pressure, ionic strength and pH) as a result of overcoming the steric and van der Waals interactions predominating at the lower temperature phases by thermally induced rotational excitations. Such thermotropic phase transitions can be detected using differential scanning calorimetry (DSC) to measure the excess specific heat associated with the transition. The phase transition temperature, T_m, is defined as the temperature at which the excess specific heat reaches a maximum and signifies the point at which a symmetrical phase transition is one-half complete. For asymmetrical transitions the $T_{1/2}$ is often reported in place of the T_m (Lewis and McElhaney, 2005).

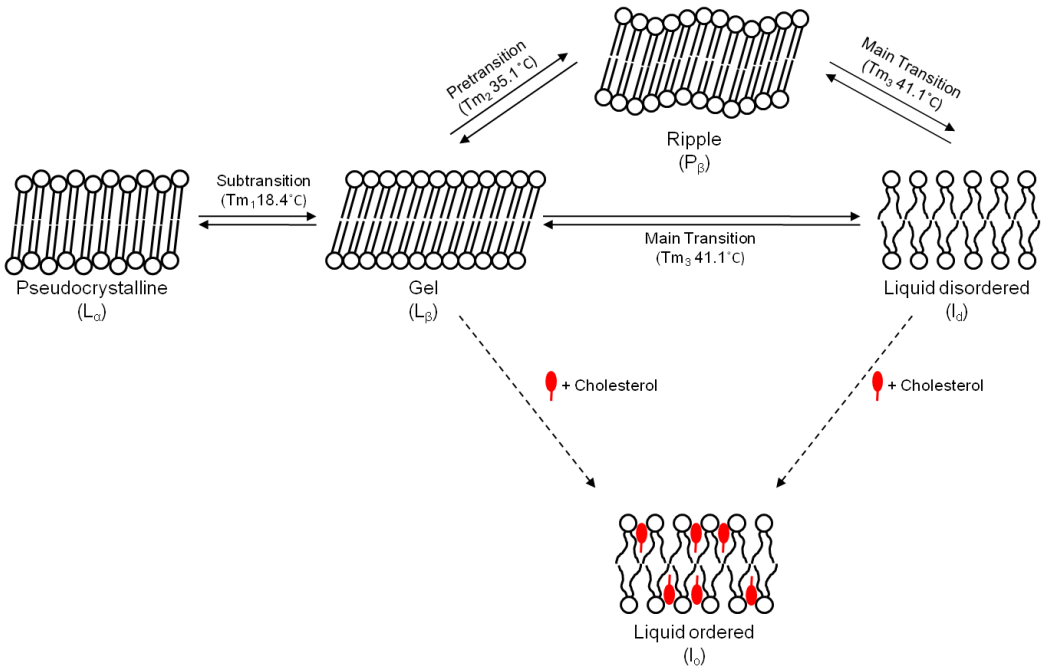

Figure 1.1.6: The phases exhibited by pure DPPC and DPPC with cholesterol bilayers and the transitions between them. The figure is adapted from (Davis, 2011) after (Lewis and McElhaney, 2005) with transition temperatures reproduced from (Chen et al., 1980).

Each phase possesses distinct structural features which have been determined largely using nuclear magnetic resonance (NMR) and X-ray diffraction (Gruner, 2005, Lewis and McElhaney, 2005). The pseudocrystalline phase exhibits highly ordered fatty acid chains which are oriented at a tilt with respect to the axis perpendicular to the bilayer surface and are severely restricted in long axis rotation. The polar headgroups of the lipids are minimally hydrated and also severely restricted in motion (Lewis and McElhaney, 2005). With increasing temperature, thermally induced rotational excitations of the fatty acid chains gradually overcome the interchain interactions that stabilise the pseudocrystalline phase resulting in a transition to the gel phase at the subtransition temperature. In this phase the fatty acid chains are organised in a distorted orthorhombic lattice and oriented with an increased tilt with respect to the bilayer normal. The polar headgroups are more hydrated and the lipids, with the decrease in lipid packing, are capable of slow rotational and diffusional motion.

On increasing the temperature further a pronounced lateral expansion of the bilayer is apparent with a concomitant decrease in bilayer thickness. An increase in the number of gauche conformers of the fatty acid chains, previously predominantly in rigid extended all-trans conformation, also occurs. The transition from the gel to the liquid crystalline (or liquid disordered) phase is defined as the point where the decrease in cohesive energy arising from the lateral expansion of the bilayer and the energy expenditure in forming gauche conformers in the fatty acid chains is balanced by the entropic reduction in free energy due to fatty acid chain isomerisation (Lewis and McElhaney, 2005). An intermediate phase between the gel and liquid crystalline phases, known as the ripple phase, sometimes occurs. In this phase the fatty acid

chains, organised in a hexagonal lattice, retain their tilted orientation but exhibit a greater rotational freedom. The degree of hydration of the polar headgroups is not thought to change. Further increase in temperature results in the increasing formation of gauche conformers within the fatty acid chains. When the transition temperature is reached and 'chain melting' occurs each fatty acid contains an average of four gauche bonds (Mendelsohn et al., 1989). This results in a marked increase in the cross sectional area per lipid causing the lateral expansion and reduction in thickness of the bilayer associated with the liquid crystalline phase. Lipids in this phase are well hydrated and oriented perpendicular to the plane of the membrane forming a loosely hexagonal lattice structure where they exhibit rapid rotational and diffusional motion.

It should be noted that the nature of this transition is dependent on the fatty acid chain lengths of the lipids comprising the bilayer (Lewis and McElhaney, 2005). For example, phosphatidylcholines with saturated short chain (10-13 carbon) fatty acids form very stable pseudocrystalline phases which melt directly into the liquid crystalline phase. Phosphatidylcholines with linear saturated 14 or 15 carbon length chains undergo transitions from the pseudocrystalline to ripple phases and then to the liquid crystalline phase whereas those with very long chained fatty acids exhibit pseudocrystalline to gel phase and gel to liquid crystalline phase transitions. Phosphatidylcholines with 16 to 21 carbon length fatty acid chains demonstrate all four phases on increasing temperature from 0 to 100^{o}C and the phase transition temperatures of dipalmitoylphosphatidylcholine (DPPC), with saturated 16-carbon fatty acids, are shown as an example in Figure 1.1.6.

The length of the fatty acid chains not only affects the phases exhibited but also the main transition temperature, T_m, at which the liquid crystalline phase occurs. T_m increases progressively, but non-linearly, with increasing chain length however, this is a relatively modest effect with an approximately 7-14^{o}C increase in T_m per methylene group observed for lipids with 16-18 carbon length fatty acids (Lewis and McElhaney, 2005). A more significant effect is observed with changes in the chemical structure of the fatty acids. Phospholipids with two linear saturated fatty acids have high transition temperatures which decrease with increasing unsaturation due to the perturbation of lipid packing by unsaturated fatty acids. The isomerisation of the double bond is also important with a more pronounced perturbation of lipid packing resulting from a bond in the *cis* than the *trans* formation (Lewis and McElhaney, 2005). The location of a double bond on the fatty acid chain is also significant in the degree to which the T_m is modulated by unsaturation. A *cis* double bond in the centre of a fatty acid chain severly perturbs the interaction of the polymethylene regions either side of it significantly decreasing the thermal energy required to induce the main phase transition (Wang et al., 1995, Marsh, 1999, Barton and Gunstone, 1975). Table 1.1.3 gives the main transition temperature of several phosphatidylcholines of varying chain length and unsaturation for comparison.

Fatty acid chain structure	T_m (^oC)	Reference
14:0	23.9	(Lewis et al., 1987a)
15:0	34.7	(Lewis et al., 1987a)
16:0	41.4	(Lewis et al., 1987a)
17:0	49.8	(Lewis et al., 1987a)
18:0	55.3	(Lewis et al., 1987a)
18:1tΔ9	9.5	(van Dijck et al., 1976)
18:1cΔ9	-17.3	(Lewis et al., 1987b)
18:2cΔ9Δ12	-53	(Avanti)
18:3cΔ9Δ12Δ15	-60	(Avanti)

Table 1.1.3: The transition temperatures of phosphatidylcholines with fatty acids of increasing chain length and unsaturation. The effect of the *cis* or *trans* isomerisation of the double bond is also shown. Chain structures are annotated as 'carbon number:number of unsaturations' with c for *cis* and t for *trans* isomerisation and Δn defining the location of the unsaturation.

The influence of the chemical structure of the lipid headgroup on the phase behaviour of a bilayer is complex. A combination of the size and charge of the headgroup as well as the extent of hydrogen bonding are likely to contribute in influencing phase behaviour. However, it is unlikely that consideration purely of these factors will give a complete picture as the extent of the polar and hydrophobic interactions actually occurring at the bilayer surface are the result of a compromise between competing forces. The geometric conditions required to maximise the polar and hydrophobic interactions are not often met due to the competing requirements of the van der Waals interactions of the fatty acid chains. Due to the near impossibility of finding a set of lipids in which the headgroup changes but the fatty acid composition, which is likely to influence headgroup interactions, remains constant it is extremely difficult to study the effect of phospholipid headgroup size or charge in isolation. Trends in the effect of headgroup size or charge on the main transition temperature have, however, been identified. Headgroups with a small cross sectional area are associated with high transition temperatures (T_m) as they promote interactions between lipids stabilising the gel phase. Large headgroups conversely increase the separation between fatty acid chains, decreasing the strength of interactions and decreasing T_m. The protonation and deprotonation of ionisable headgroups by varying pH has been demonstrated to cause significant changes in T_m. Altering the charge of the headgroup alters the attractive/repulsive interactions between them affecting the relative stability of the gel phase and the thermal energy required to induce the transition to the liquid crystalline phase (Trauble and Eibl, 1974, van Dijck et al., 1975). The binding of specific ions to bilayers of lipids with charged headgroups has also been shown to influence T_m; increasing the ionic strength of the aqueous environment of phosphatidylserine bilayers increases T_m (Cevc et al., 1981) as does the binding of Ca^{2+} to negatively charged bilayers (Demel et al., 1987). This is thought to be due to the shielding of the charge of the headgroup resulting in its partial or total effective neutralisation which then promotes lipid packing, stabilising the gel phase and increasing T_m.

The backbone region of the phospholipid, linking the headgroup and fatty acid chains, can also influence the phase behaviour within bilayers. For example, sphingomyelins and glycosphingolipids, with a sphingoid backbone, have an amide group as opposed to the ester

group of the glycerol backbone of glycerophospholipids. As a result they exhibit higher transition temperatures due to the stronger hydrogen bonding associated with the amide, as opposed to the ester, in the interfacial region of the phospholipid (Lewis and McElhaney, 2005).

1.1.3.2. *A brief note on the lyotropic phase behaviour of phospholipids*

The number and types of phases exhibited by phospholipids within a lamellar bilayer structure depends on the degree of hydration of the lipids. Considering dipalmitoylphosphatidylcholine (DPPC) again as an example, it has been shown that anhydrous DPPC undergoes a single transition into the liquid crystalline phase at a temperature in excess of 100^{o}C whereas the fully hydrated form, considered in Figure 1.1.6, undergoes three distinct transitions below 50^{o}C (Lewis and McElhaney, 2005). The main transition temperature, T_m, decreases with increasing hydration up until a point after which adsorption of further water molecules does not further alter T_m. In the former regime the adsorption of water molecules in the interfacial region of the bilayer decreases the strength of interaction between adjacent lipids reducing the thermal energy required to induce the phase transition to the liquid crystalline phase. An approximately 10wt% increase in bound water has been detected for DPPC between the gel or ripple phase and the liquid crystalline phase correlating to a 17:1 and 27:1 ratio of water molecules per DPPC molecule in these phases, respectively (Janiak et al., 1979, Jendrasiak and Mendible, 1976a). The extent to which hydration modulates the phase behaviour of a bilayer depends on the composition of lipids within the lamellar structure, in particular the chemical structure of the polar headgroups. Phosphatidylserine and phosphatidylethanolamine both bind fewer water molecules in the liquid crystalline phase than phosphatidylcholine (Jendrasiak and Mendible, 1976b).

1.1.3.3. *The effect of cholesterol on the thermotropic phase behaviour*

Cholesterol in phospholipid bilayers intercalates between the fatty acid chains of lipids with its hydrocarbon chain penetrating the hydrophobic interior of the bilayer and the polar 3β-hydroxyl group, at the opposite extremity of the fused ring system, preferring the hydrated interfacial region (Yeagle, 2005) where it forms hydrogen bonds with the carboxyl oxygen of adjacent lipids (Rietveld and Simons, 1998). This places the rigid fused 4-ring system in the region of the upper part of the fatty acid chains of the phospholipids where it has significant impact on the ordering and motion of these structures. For bilayers in the gel phase the intercalation of cholesterol between the phospholipids reduces the cohesive forces between fatty acid chains increasing their motion (Yeagle, 1988). In the liquid crystalline phase cholesterol increases the order and reduces the motion of the fatty acid chains of phospholipids (Demel and de kruijff, 1976). The result is a distinct intermediate phase between the gel and liquid crystalline phases known as the liquid ordered phase (Chapman, 1975b), illustrated in Figure 1.1.6.

Differential scanning calorimetry (DSC) and deuterium nuclear magnetic resonance (^{2}H NMR) have been used in several attempts to map the phase behaviour of cholesterol in a binary system with dipalmitoylphosphatidylcholine (DPPC) (Vist and Davis, 1990, McMullen and McElhaney, 1995). The map, or phase diagram, produced by Vist and Davis (Vist and Davis, 1990) later modified by Sankaram and Thompson (Sankaram and Thompson, 1991) (Figure 1.1.7) most closely matches the prior theoretical studies of Ipsen *et al.* (Ipsen et al., 1987) and is therefore considered the most accurate.

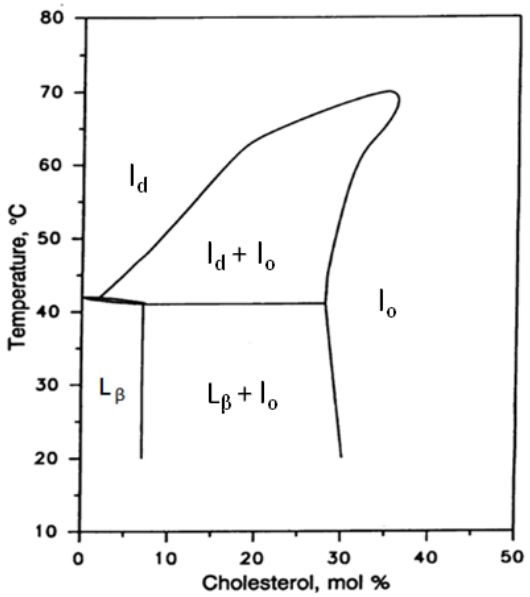

Figure 1.1.7: The phase diagram for the binary DPPC-Cholesterol system adapted from (Sankaram and Thompson, 1991).

For DPPC in both the gel phase (L_β) and liquid crystalline (l_d) phase (below and above 41.4^{o}C, respectively (Lewis et al., 1987a)) a region of coexistence with the liquid ordered phase, l_o, exists in the presence of approximately 10-30mol% cholesterol with respect to total lipid concentration. The onset of liquid ordered phases occurs at ~7mol% cholesterol when the system is in the gel phase and between 5mol% and 30mol%, increasing with temperature, in the liquid crystalline phase also referred to as the liquid disordered phase. At low cholesterol concentrations (<5mol%) the liquid ordered phase is absent and at concentrations >30-35mol% the gel or liquid disordered phases are abolished in favour of the liquid ordered phase which persists at all temperatures in the measured range (20-80^{o}C). The thermotropic phase behaviour of the binary system with, for example, 80mol%DPPC and 20mol% cholesterol is to present coexisting gel and liquid ordered phases until the transition temperature of DPPC is reached (T_m~41^{o}C) above which the liquid disordered and liquid ordered phase coexist. This phase coexistence persists until ~65^{o}C where thermally excited molecular motions overcome the cohesive interactions between cholesterol and DPPC and the liquid ordered phase ceases in favour of the liquid disordered phase.

As mentioned previously the fatty acid chain length and degree of unsaturation alters the gel to liquid crystalline transition temperature of the phospholipid bilayer and likewise affects the temperature range at which liquid ordered/gel phase and liquid disordered/liquid ordered phase coexistence occurs in binary systems with cholesterol. For example the phase diagram produced by Almeida *et al.* (Almeida et al., 1992) for the dimyristoylphosphatidylcholine (DMPC)/cholesterol binary system (Figure 1.1.8) resembles that for the DPPC/cholesterol system (Figure 1.1.7) but is centered at a lower temperature. DMPC has shorter fatty acid chains than DPPC (14 carbons in length as opposed to 16) and as a result a lower main transition temperature of 23.9^{o}C compared with 41.4^{o}C for DPPC (Lewis et al., 1987a).

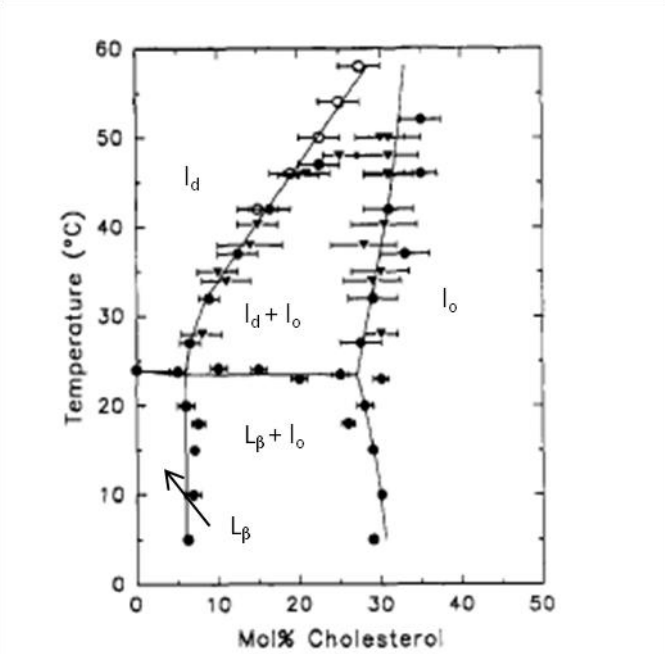

Figure 1.1.8: The phase diagram for the binary DMPC-Cholesterol system adapted from (Almeida et al., 1992).

Comparison of the phase diagrams of Figures 1.1.7 and 1.1.8 also reveals differences in cholesterol concentration dependence of the temperature range between the gel+liquid ordered to liquid disordered+liquid ordered phase coexistence boundary and that marking the transition to the purely liquid disordered phase. This suggests that the dependence of the phases on the cholesterol concentration and changes in the temperature may vary slightly with fatty acid chain length as well as the distinct effect on the temperature at which the gel+liquid ordered to liquid disordered+liquid ordered transition occurs.

Partial phase diagrams for the binary system of cholesterol with 1-palmitoyl-2-oleoyl-*sn*-3-glycerophosphatidylcholine (POPC), a phosphatidylcholine with a 16-carbon saturated and 18-carbon unsaturated fatty acid, have also been formed both by Thewalt and Bloom (Thewalt and Bloom, 1992) and de Almeida *et al*. (de Almeida et al., 2003). These place the gel+liquid ordered and liquid disordered+liquid ordered coexistence regions at around -10^{o}C and 15^{o}C respectively at cholesterol concentrations between 10mol% and 30mol%. Again, this is

consistent with the boundary between these regions occurring at roughly the transition temperature of the pure phospholipids (-2^{o}C for POPC) and reinforce the notion that both fatty acid chain length and degree of unsaturation significantly influence the thermotropic phase behaviour of phosphatidylcholine/cholesterol binary lamellar systems.

Biological membranes invariably contain phospholipids with a mixture of fatty acids which has lead to the study of the phase behaviour of ternary phase systems, containing two phospholipid species and cholesterol. Figure 1.1.9A is the phase diagram for 1,2-dilauroyl-sn-3-glycerophosphatidylcholine (DLPC)/DPPC/cholesterol bilayers at 25^{o}C produced by Silvius *et al.* (Silvius et al., 1996) from data presented by Vist and Davis (Vist and Davis, 1990) and van Dijck *et al.* (van Dijck et al., 1977) for binary DPPC/cholesterol and DPPC/DLPC systems accompanying their own experimental observations. A striking difference from the binary systems is the presence of a three phase region occurring as a result of the different phase behaviour of each phospholipid with increasing cholesterol concentration at this temperature. DLPC possesses short chain fatty acids (12 carbons) relative to DPPC (16 carbons) and, for example, with a fixed 30mol% cholesterol exhibits coexisting liquid ordered and liquid disordered phases (l_d+l_o) at 25^{o}C which is above its transition temperature (-1^{o}C (Avanti)). Increasing the proportion of longer chained fatty acids promotes the coexistence of three phases (l_o+l_d+L_β) at a 1:1 ratio of DLPC to DPPC as although DLPC is above its transition temperature DPPC is not. The onset of the (l_o+L_β) two phase regime occurs when longer chain fatty acids comprise 70% of the total fatty acids exceeding the concentration of shorter chained fatty acids to an extent where their preferred liquid disordered phase is no longer supported. The higher the proportion of longer chained fatty acids in this system, the higher the concentration of cholesterol required to entirely disrupt the gel phase with the liquid ordered phase only existing at over ~38mol% cholesterol where the proportion of DPPC exceeds 70%.

Figure 1.1.9B is a similar phase diagram for the DOPC/DPPC/cholesterol ternary phase system formed by de Almeida *et al.* (de Almeida et al., 2007) combining their experimental data with the findings of Lentz and co-workers (Lentz et al., 1976, Lentz et al., 1980), McMullen and McElhaney (McMullen and McElhaney, 1995)), Sankaram and Thompson (Sankaram and Thompson, 1991), Veatch *et al.* (Veatch et al., 2004) and Elliot *et al.* (Elliott et al., 2005). It is interesting to note that the l_o phases occur at a higher percentage of DPPC in the total PC fraction in the system shown in Figure 1.1.9B than in 1.1.9A. This is due to the fact that unsaturation within the fatty acids of a phospholipid has a greater effect in reducing lipid packing than the length of the fatty acid, as reflected by their relatively lower transition temperatures (see Table 1.1.3), such that a greater proportion of DPPC is required to form stabilised l_o or L_β domains. Figure 1.1.9B also indicates the predicted location of a tie-line; along this line the relative extent of each phase is constant despite the changing lipid composition.

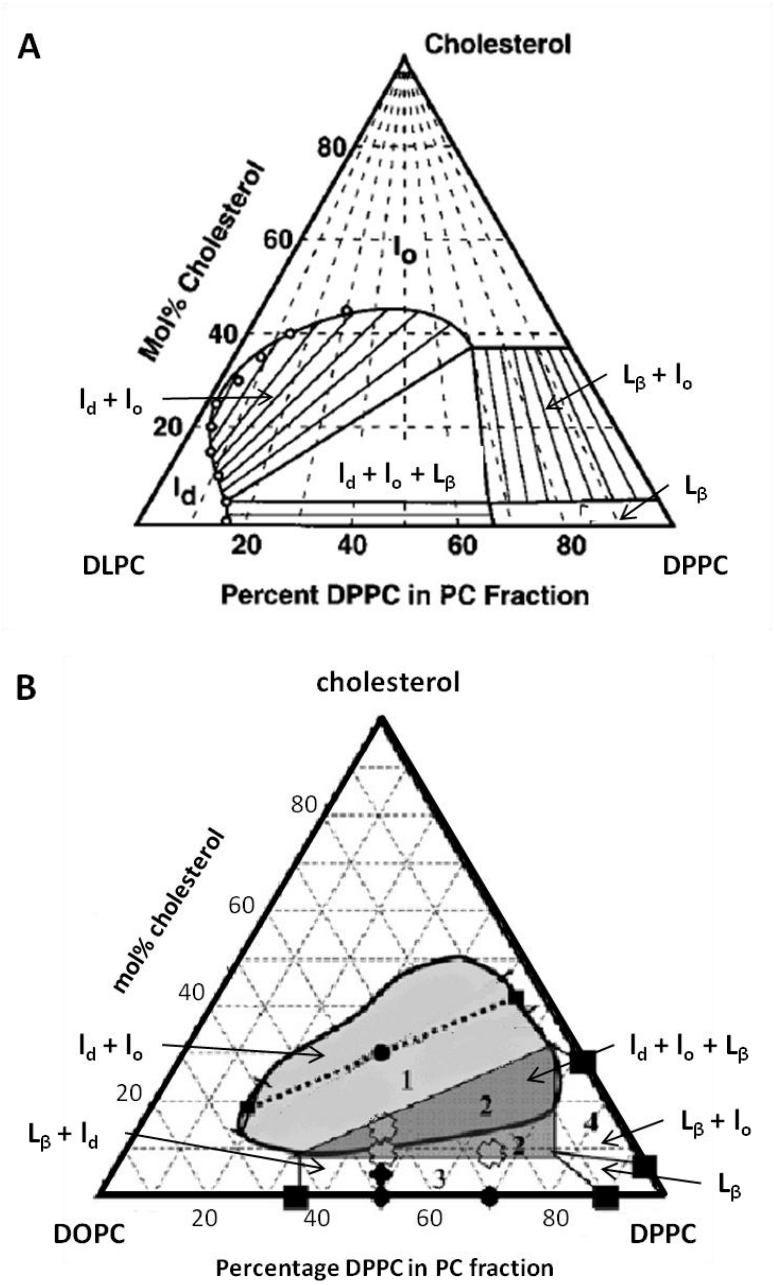

Figure 1.1.9: **A** The ternary phase diagram for DLPC:DPPC:cholesterol mixed membranes at 25°C after (Silvius et al., 1996) **B** The phase diagram for DOPC:DPPC;cholesterol mixed membranes reproduced from (de Almeida et al., 2007). The proportion of all three components at which the gel-phase (L_β), liquid ordered phase (l_o) and liquid disordered phase (l_d) exist, and regions of phase coexistence, are indicated. The dotted line in **B** represents a tie-line. The diagrams are described in detail in the text.

1.1.4. Membrane lipid dynamics

Phospholipids within biological membranes can undergo a variety of motions such as gauche-trans isomerisation and bond oscillation within a phospholipid molecule, rotation about the long axis, lateral diffusion and transbilayer "flip flop" of the molecule, and collective motions such as the undulation of a section of membrane, as illustrated in Figure 1.1.10. The extent of these motions reflects the phase the phospholipids are in, as mentioned briefly in the previous section, and is a function of the thermal energy and specific lipid composition of the system (Gawrisch, 2005).

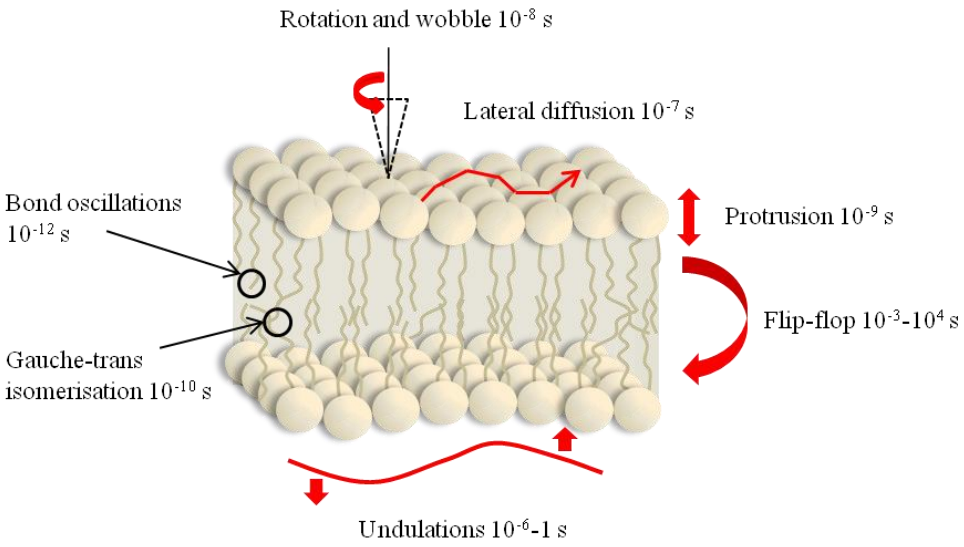

Figure 1.1.10: An illustration of the dynamic motions of lipids in membranes and their approximate correlation times. Adapted from (Gawrisch, 2005).

These motions endow a fluid-like property to the membrane and so the term membrane fluidity was introduced to reflect the collective effects of lipid motions. Traditionally, fluidity is considered the reciprocal of viscosity and therefore a decrease in membrane fluidity can be thought of as an increase in the viscous drag experienced by the lipids in the dynamic motions of the molecules (lateral diffusion and rotation) (Gawrisch, 2005). For example, the incorporation of cholesterol into a membrane is reported to decrease fluidity due to the resistance to lipid motion imposed by their ordering into l_o domains (Cooper, 1978, van Blitterswijk et al., 1987). Due to the number of motional parameters, membrane fluidity summarises the results of a variety of measurements including; the order and motional correlation times of lipid molecular bonds and membrane-imbedded probes, lateral diffusion rates, membrane permeability, and phase transition temperatures. As a result the term 'membrane fluidity' is vague with the association of these measurements with viscous restriction to lipid motion often quite obscure (Gawrisch, 2005, Atkinson et al., 2008, Marguet et al., 2006) and caution should be taken in their comparison and interpretation.

1.1.5. Phosphatidylcholine membranes used in this study

The artificial membrane systems used in this study are composed of egg-phosphatidylcholine which consists of lipids with a variety of fatty acid chain length and degree of unsaturation. Figure 1.1.11 details the average fatty acid composition.

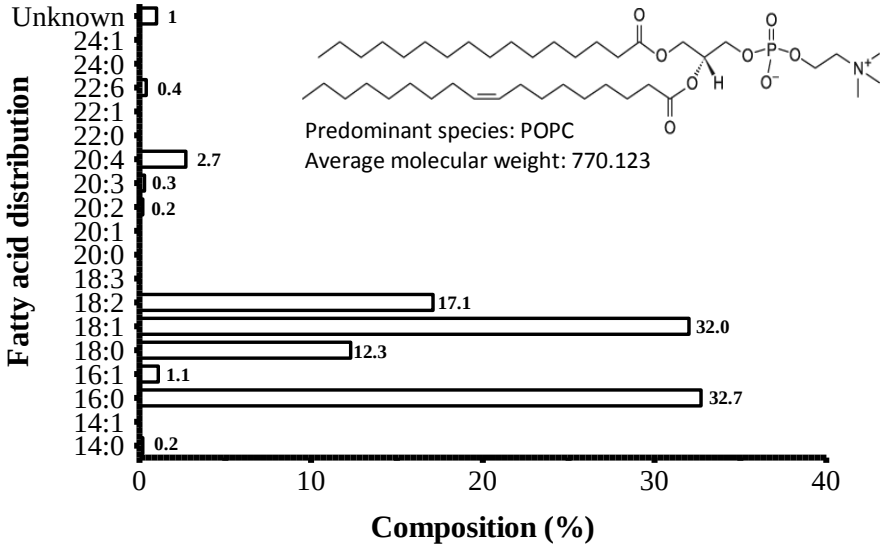

Figure 1.1.11: The fatty acid distribution within egg-phosphatidylcholine. The structure of the predominant lipid species is 1-palmitoyl-2-oleoyl-sn-glycero-3-phosphocholine (POPC) with 16-carbon saturated and 18-carbon single unsaturated fatty acids. After (Avanti).

The likely phases exhibited by the egg-PC membranes can be estimated from the phase diagrams shown above based on the knowledge that egg-PC comprises approximately 53% unsaturated fatty acids. Inspection of the phase diagram for cholesterol with a saturated and unsaturated PC (Figure 1.1.9B) suggests the membranes to exhibit l_d and L_β phases. On inclusion of ~10-20% cholesterol the membrane will have three distinct phases, $l_d + l_o + L_\beta$ and at cholesterol concentrations between 20-30mol% the gel phase is likely to cease leaving only the l_d and l_o phases. It should be noted, however, that the phase diagram in Figure 1.1.9B was formed at 25^{o}C whereas in this study the membranes were observed at 37^{o}C. The likely effect of increased temperature on the phase diagram is to increase the % DPPC in total PC fraction at which gel phases occur so it is possible that the gel phase ceases at lower cholesterol concentration in egg-PC membranes at 37^{o}C, or may not exist at all.

1.2. Composition and organisation of cell membranes

The cell membrane is the outermost component of the cell, completely enclosing cellular structures, forming a selectively permeable barrier and point of contact between intra- and extra-cellular environments (Berg et al., 2002, Alberts, 1994, Becker, 2003). The lipid bilayer structure discussed above forms the basis of the cell membrane with several additional components which are introduced in this section.

The lipid bilayer of the cell membrane is supported by a network of cytosolic structural proteins forming the cytoskeleton and an extracellular matrix surrounding the exocytosolic surface. There are also many proteins associated with the cell membrane which enable the selective transport of ions and large molecules across the membrane and are also responsible for catalysing a host of cellular processes. In most cases, these elements combine to form a 6-10nm thick membrane structure, of which ~4nm corresponds to the lipid bilayer (Becker, 2003, Berg et al., 2002, Alberts, 1994).

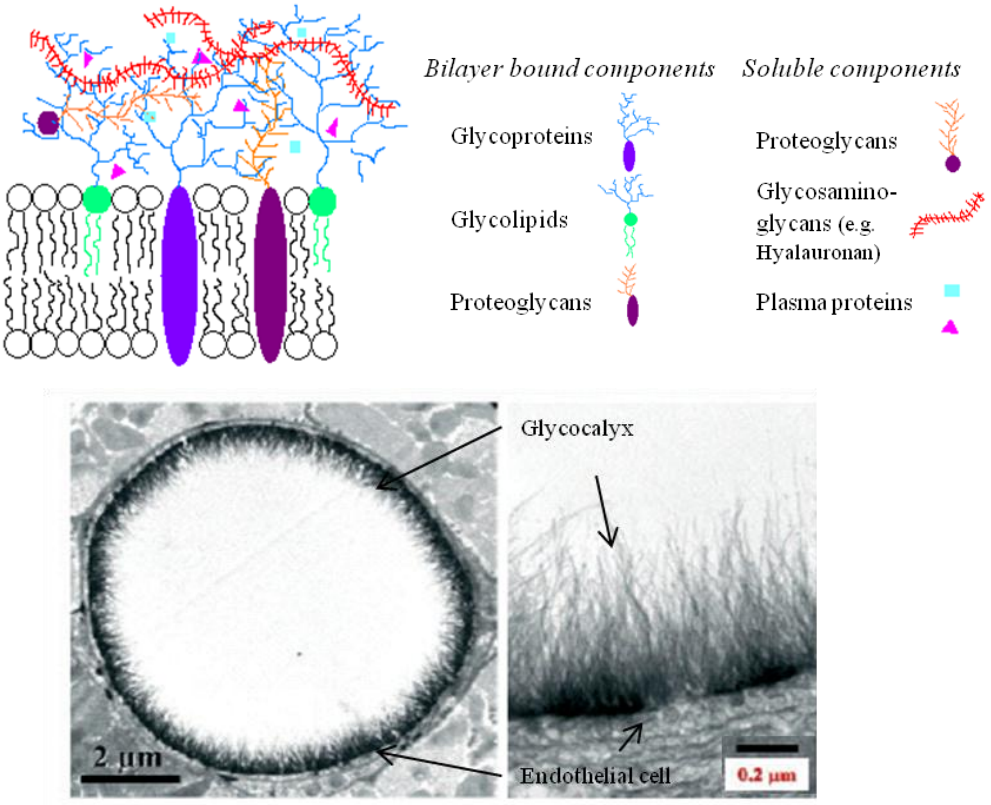

Figure 1.2.1: A diagrammatic representation (*top*) and electron micrographs (After (Gouverneur et al., 2006b) (*bottom*) of the endothelial glycocalyx.

The extracellular matrix of endothelial cells lining the luminal surface of the vasculature and of circulating blood cells is known as the glycocalyx. This is a negatively charged, hydrated matrix of proteoglycans, glycosaminoglycans and associated plasma proteins among the carbohydrate chains extending from the glycoproteins and glycolipids of the lipid bilayer (Tarbell et al., 2005, Tarbell and Pahakis, 2006, Pries et al., 2000). Endothelial cells have been demonstrated to have a substantial glycocalyx measuring 0.2-3µM (depending on visualisation method, vessel and

tissue type (Tarbell et al., 2005)) whereas red blood cells have a minimal glycocalyx. The glycocalyx has several functions including; acting as a permeability barrier based on charge and size exclusion, providing a lubrication layer assisting the movement of red blood cells in the microcirculation, and regulating a host of ligand-receptor interactions (Tarbell and Pahakis, 2006).

The association of proteins with the cell membrane was first suggested by Danielli and Davson (Danielli and Davson, 1935) and later described in detail by the fluid mosaic model of Singer and Nicolson (Singer and Nicolson, 1972). This model proposed that cell membranes contain globular proteins embedded within, and often spanning, the lipid bilayer which in effect 'float in a sea of phospholipids' of the fluid membrane bilayer. The proteins are suggested to position in the membrane so that their hydrophobic residues are within the hydrophobic core of the bilayer with their polar residues exposed to the aqueous cytosolic or extracellular environment, maintaining the membrane in the lowest energy state achievable in the aqueous environment. In recent years, analysis of protein structure has identified membrane associated proteins with hydrophobic domains that do not match the hydrophobic dimension of the bilayer suggesting the lipids of the membrane distort to accommodate these proteins (Engelman, 2005). These studies have also demonstrated that the fraction of the membrane surface occupied by proteins is significantly larger than originally considered and includes proteins that can have ectodomains spanning several times the membrane surface area of their transbilayer component (Engelman, 2005). Figure 1.2.2 illustrates the resulting view of the cell membrane in comparison with that of the fluid mosaic model.

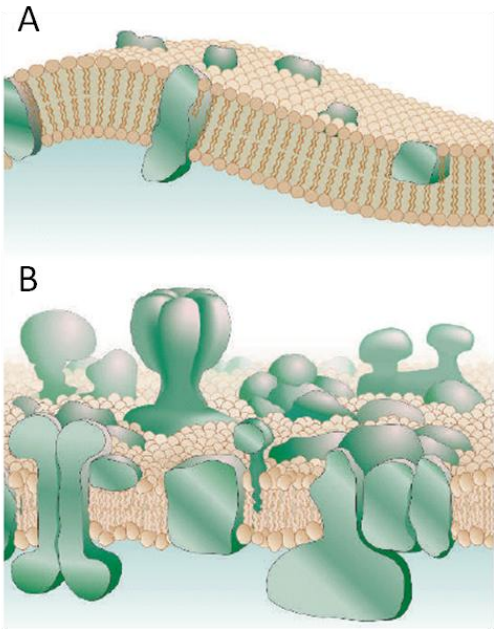

Figure 1.2.2: Depictions of **A**: the fluid mosaic model of the cell membrane, **B**: a more recent view of the cell membrane illustrating a larger protein concentration, protein ectodomains and a protein mediated variation in the bilayer width. After (Engelman, 2005).

Singer and Nicolson (Singer and Nicolson, 1972), although not explicity discussing the spatial and temporal heterogeneity of lipids in the proposed fluid mosaic model, did speculate the possibility of small domains within the fluid membrane. Evidence of the existence of these transient microdomains, possessing distinct lipid order and motions, has led to the most significant amendment to the fluid mosaic hypothesis which otherwise still forms the basis of our understanding of cell membrane structure.

1.2.1. Structure and function of membrane microdomains

Microdomains are regions of the bilayer that exhibit distinct lipid ordering and motions from the surrounding lipid environment. A clear example of this is the formation of liquid ordered (l_o) domains as a result of phase separation in cholesterol containing mixed phospholipid membranes discussed in the previous section. These l_o domains were found to be insoluble in cold non-ionic detergents, such as Triton-X100, leading to their definition as detergent resistant membrane (DRM). Their detergent resistance enables their extraction by detergent treatment of membranes followed by sucrose gradient centrifugation (Brown and Rose, 1992). The observation of a cholesterol enriched fraction of lipids in cell membranes that are also detergent insoluble suggested the presence of domains with the characteristics of the l_o phase in cell membranes known as rafts. These are the most widely recognised subset of membrane microdomain and the focus of the following discussion.

Analyses of the composition of DRM extracted from cells have confirmed they are rich in cholesterol with sphingomyelins, gangliosides and glycophosphatidylinositol (GPI) anchored proteins also present. Sphingomyelin, introduced in an earlier section, is a lipid with relatively long saturated fatty acid chains and a high transition temperature of 40^{o}C (Boesze-Battaglia, 2005). This results in its preferential association with cholesterol promoting the formation of rafts and stabilising these liquid ordered microdomains by means of a hydrogen bond between the cholesterol 3β-hydroxyl and the amide group of the spingomyelin (Bittman et al., 1994). Not surprisingly, gangliosides which are based on the same ceramide structure with its long saturated fatty acids also localise in these microdomains. Many proteins have been observed to localise in DRM microdomains, including caveolins and flotillins, kinases (e.g. src kinases) and low density and heterotrimeric G-proteins (and associated G-protein coupled receptors) (reviewed in (Pike, 2003)) and this led Simons and Ikonen (Simons and Ikonen, 1997) to speculate that rafts are involved in protein trafficking and membrane signalling events. They propose rafts act as functional platforms that concentrate or sequester proteins and other signalling molecules, promoting or inhibiting specific signalling events.

Following over a decade of research into these structures, the definition of membrane rafts has been agreed as “small (10-200nm), heterogeneous, highly dynamic, sterol- and sphingolipid-

enriched domains that compartmentalize cellular processes. Small rafts can sometimes be stabilized to form larger platforms through protein-protein and protein-lipid interactions" (Pike, 2006). Interestingly, this definition purposefully omits reference to DRM due to the variation in the composition of microdomains isolated due to the limitations of the detergent-extraction technique (Reviewed by (Shogomori and Brown, 2003)). These limitations include the changes in phase behaviour likely to occur at the low temperatures at which detergent extraction is conducted and the observation that the incorporation of detergent into membranes can result in microdomain rearrangement prior to their isolation. It has also been observed that small differences in the manipulation of the sample between detergent treatment and sucrose gradient centrifugation can result in the presence or absence of receptors (e.g. epidermal growth factor receptors) from the DRM fraction (Pike, 2003).

The size of membrane rafts places them beyond the diffraction limit, and therefore resolution, of conventional light or laser scanning microscopy and these microdomains can therefore not be directly visualised in cell membranes. Several indirect fluorescence based methods have been employed to observe the nature of these structures including microdomain clustering and observations based on the restricted diffusion of membrane lipids and proteins by rafts and the enhanced proximity of raft-associated molecules in these structures (Sharma, 2006).

Microdomain clustering is one of the earlier techniques employed to visualise rafts, which are not otherwise visible due to their size, by clustering them to form larger domains detectable via fluorescence microscopy. This is achieved by clustering raft markers, such as GPI-anchored proteins or gangliosides, using antibodies; for example GM1 gangliosides pre-capped with cholera-toxin B subunit are clustered on exposure to (fluorescent) anti-cholera antibodies. These raft markers have been observed to be uniformly distributed over the membrane (Brown and London, 1998b, Jacobson and Dietrich, 1999) however their distribution becomes heterogeneous on clustering with an antibody and other raft markers, unaffected by the antibody, have been shown to colocalise with the clustered markers (Viola et al., 1999, Harder et al., 1998). As both markers are known to prefer the l_o phase of rafts, this has been taken as evidence of the existence of rafts in cell membranes. However, there is some ambiguity in the interpretation of these observations as it is not clear whether the raft markers initially appear homogeneously distributed due to their raft-association being undetectable under the resolution of optical microscopy and upon clustering this becomes visible, or that rafts do not constitutively exist and are formed as a result of the clustering (Brown and London, 2000).

The indirect detection of rafts through differences in the rates of diffusion of membrane components in rafts and the surrounding more fluid membrane has been achieved through fluorescence microscopy techniques including fluorescence recovery after photobleaching

(FRAP) and single particle tracking. For example, Oliferenko *et al.* (Oliferenko et al., 1999) have used FRAP to compare the diffusion of a proposed transmembrane-anchored raft marker and a marker not associated with rafts showing that the former was distinctly immobilised with respect to the latter. Cholesterol depletion significantly increased the mobile fraction of the proposed raft-associated marker confirming that it does reside in rafts where the high ordering reduces its mobility. FRAP of GPI-anchored proteins has also conferred the presence of rafts (Jacobson et al., 1995). Several single particle tracking studies of fluorescently tagged GPI-anchored proteins have offered estimates of the size of rafts ranging from around 200-300nm (Sheets et al., 1997, Simson et al., 1998) to as small as ~26nm (Pralle et al., 2000). Single particle tracking of fluorescently labelled lipids incorporated into the cell membrane has, however, yielded a much larger estimate of 0.2-2μM (Schutz et al., 2000). These authors also suggest that rafts comprise ~13% of membranes from their observations.

Forster resonance energy transfer (FRET) is another technique to determine the presence of rafts relying on the close proximity of raft-associated molecules when localised in rafts. Kenworthy *et al*. found this technique to provide no evidence in support of the presence of stable rafts and suggest that these structures are either transient, or if stable only comprise a minor fraction of the total membrane surface (Kenworthy and Edidin, 1998, Kenworthy et al., 2000).

The inability to directly visualise rafts and the inconsistency of data from several indirect methods utilised to infer the existence and nature of rafts has sparked a small but intense debate as to the physiological significance of these structures (Hancock, 2006). The main criticism of the raft hypothesis was whether the estimated size and stability of rafts in cell membranes, an environment far from equilibrium (Mayor and Rao, 2004, Lenne et al., 2006), were sufficient to enable these structures to influence protein function. A response to this criticism is the hypothesis that, while the majority of spontaneously forming rafts have been predicted by FRET and single particle tracking to be transient structures of <30nm in diameter and <0.1ms lifetime, they may be stabilised by lipid-anchored or transmembrane proteins and coalesce to form larger rafts of up to 200nm (Mayor and Rao, 2004, Hancock, 2006). The raft stabilising proteins may in turn be associated with elements of the extracellular matrix (Garner and Baum, 2008) or the actin cytoskeleton (Langhorst et al., 2007) resulting in the creation of larger stabilised rafts which have been implicated in protein function.

As well as their ability to colocalise or sequester molecules to promote or inhibit protein activity, as mentioned above, rafts may also influence protein function as a result of their unique physical characteristics. The influence of the decreased fluidity of rafts on protein function is well understood (Lucero and Robbins, 2004, Barenholz, 2002) but the elevated dipole potential of these liquid ordered structures (Starke-Peterkovic et al., 2006, Duggan et al., 2008) may also

influence the behaviour of raft-associated proteins (O'Shea, 2003, O'Shea, 2005). For example, Asawakarn *et al.* (Asawakarn et al., 2001) have demonstrated the ligand binding of P-glycoprotein, a receptor known to associate with rafts (Demeule et al., 2000, Hinrichs et al., 2004), to be increased or decreased by agents that increase or decrease the dipole potential, respectively. Furthermore, they found ligand binding to be significantly reduced following raft depletion by methyl-β-cyclodextrin treatment and propose the elevated dipole potential of rafts as an underlying factor promoting ligand binding to the raft associated P-glycoprotein (Asawakarn et al., 2001). The molecular origin and measurement of the dipole potential will be discussed in the following section.

Although this discussion has focussed principally on membrane rafts, due to the wide variety of lipids and proteins present the cell membrane is likely to display complex phase behaviours potentially resulting in the formation of many species of transient and stabilised microdomains, of which rafts are just a subset. The notion of the existence of microdomains other than rafts in the membrane is reflected in the coining of the phrase 'non-raft microdomains' by Shaikh and Edidin (Shaikh and Edidin, 2006) as a label for all membrane heterogeneities that do not possess the composition and physical characteristics of rafts. Microdomains within this subset will have their own unique compositions and physical properties and have also been identified to influence protein function (Popik and Alce, 2004, Fukano et al., 2007). The microdomain landscape of the membrane my therefore prove to be a complex mechanism for the regulation of a host of membrane protein activities closely controlled by the cell through variation in membrane composition.

1.3. Membrane electrostatic potentials

Due to the composition of membranes and their surrounding intra- and extra- cellular aqueous environments, and the specific electrostatic behaviours of these molecular and ionic components, several electrostatic potentials are associated with membranes. The most significant of these are the transmembrane potential $\Delta\Psi$, the surface potential, Ψ_s, and the dipole potential, Ψ_d and the profile of these potentials in relation to the phospholipid bilayer is demonstrated in Figure 1.3.1. The molecular origin of these potentials, their detection and physiological relevance is discussed in this section.

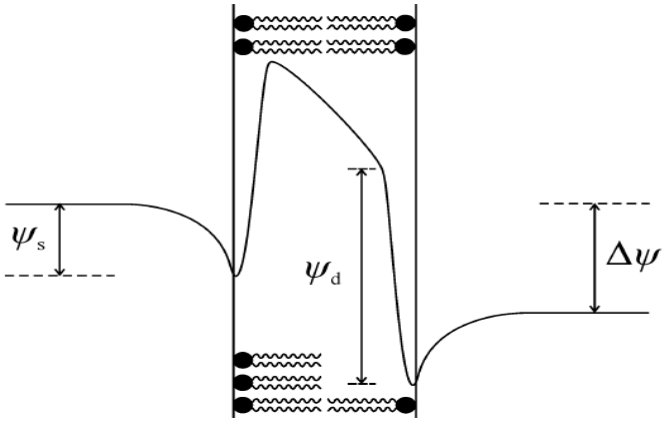

Figure 1.3.1: The profile of the principle membrane electrostatic potentials across a phospholipid bilayer. The transmembrane potential, $\Delta\Psi$, is a consequence of the different charge of the intra- and extra- cellular fluid phases separated by the membrane. The surface potential, Ψ_s, is the result of charges at the membrane surface and the dipole potential, Ψ_d, arises from the orientation and distribution of lipid and water dipoles in the hydrated headgroup region of each leaflet. *After* (Clarke, 1997).

1.3.1. The transmembrane potential

The transmembrane is the most documented of these potentials and is associated with the gradient of electric charge across the membrane bilayer due to differences in the intra- and extra- cellular cationic and anionic concentrations. The magnitude of $\Delta\Psi$ across cell membranes is around -70mV with the cell interior the more negative environment (Cevc, 1990). This potential is maintained by potassium (K^+), sodium (Na^+) and chloride (Cl^-) ion gradients generated by their protein mediated active transport across the membrane as well as electron transport (Clarke, 2001, O'Shea, 2005). Several techniques have been employed to measure $\Delta\Psi$ in cells including patch clamping and the use of fast or slow response fluorescence probes. Fast response probes undergo changes to their electronic structure in response to $\Delta\Psi$ exhibiting changes in their fluorescence with millisecond resolution and are used with excitable cells such as neurons (Zhang et al., 1998). Slow response probes change their transmembrane distribution in response to $\Delta\Psi$ detecting average changes in the potential resulting, for example, from ion channel activation in non-excitable cells (Haugland, 2005).

1.3.2. The surface potential

The surface potential, Ψ_s, arises as a consequence of the incomplete quenching of the net negative charge at the membrane surface by counter-ions in the surrounding aqueous milieu. This net negative charge originates from the charged moieties of membrane lipids and proteins and additional charged species absorbed onto the membrane surface. Where a significant glycocalyx is present the charge associated with this structure also contributes. As a result, this potential exists from the membrane surface (the lipid headgroup/aqueous interface) diminishing to an infinitely distant electroneutral point in the surrounding bulk aqueous medium, as illustrated in Figure 1.3.2, and is usually around -60mV in magnitude (McLaughlin, 1989, Cevc, 1990, O'Shea, 1988).

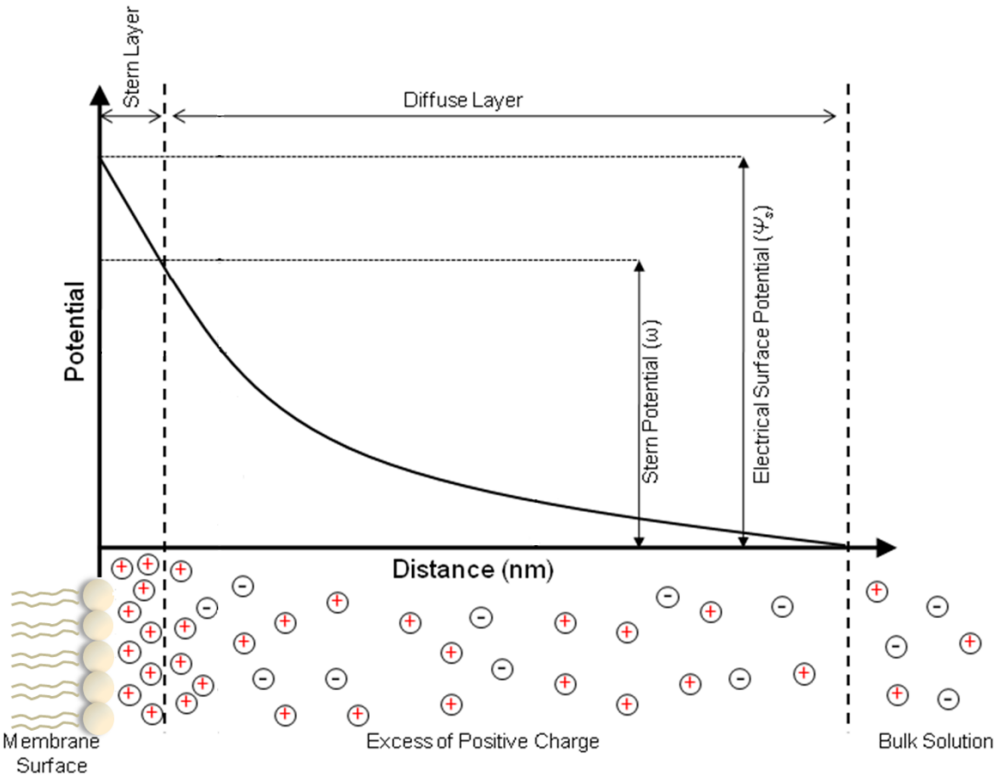

Figure 1.3.2: The profile of the surface potential which exists from the membrane surface to an infinitely distant electroneutral point in the surrounding bulk aqueous milieu. Adapted from (O'Shea, 2005).

The negative charge of the membrane surface influences the distribution of ions in the immediate aqueous phase, resulting in the absorption of dehydrated counter-ions from the bulk aqueous environment onto the membrane surface and the repulsion of co-ions. This plane of ions at the interface of the membrane surface is known as the inner Helmholtz plane and is surrounded by a layer of ordered water molecules (the outer Helmholtz plane) together forming the Stern layer. This layer of counter-ions is insufficient to completely quench the charge of the membrane surface resulting in the presence of an excess negative charge at the membrane-aqueous medium interface and an electrical potential, the surface potential, therefore exists between the membrane surface and bulk aqueous milieu. Beyond the Stern layer, ions in

solution are under the influence of columbic interactions with the charged membrane surface coupled with their thermal motion resulting in the formation of a diffuse layer which, together with the Stern layer, comprises the double layer over which the surface potential exists.

The behaviour of ions in aqueous solution with distance from the membrane surface is essentially analogous to that of an electrode-solution system. Gouy and Chapman propose the Poisson-Boltzman approach best describes this effect where free diffusion of ions restricted by columbic interaction with the charged surface results in a concentration profile with distance from the surface resembling a Boltzman distribution. A limitation of the Gouy-Chapman model, however, is that it assumes ions behave as point charges and therefore places no physical limits for ions in their approach to the surface. This is not the case as the hydration radius of ions in the diffuse layer prevents them from moving within a finite distance of the membrane surface without becoming partially or fully dehydrated and absorbed onto the surface. The Stern layer, and associated Stern potential, was therefore proposed as a modification to the Gouy-Chapman model. This layer, immediately adjacent to the surface, precedes the diffuse layer which remains described by the Gouy-Chapman model (O'Shea, 2004). The resulting Gouy-Chapman-Stern model replaces the previous model in describing the behaviour of ions in the context of the membrane surface potential, continuing the analogy between the biological membrane and the electrode-solution system. This analogy leads to the assumption that the membrane surface is similar to the solid surface of an electrode and fails to consider the fluid nature and structural heterogeneity of the membrane. This description of the membrane surface potential therefore remains an approximation with attempts at improvement ongoing (e.g. (Domene et al., 2003)). A more in-depth account of the origin of the Gouy-Chapman-Stern model and its application to the membrane surface potential, including the derivation of the expressions describing this effect, can be found in (O'Shea, 2004).

A change in the surface potential, for example on the interaction of a charged species with the membrane, can be detected with the probe Fluorescein phosphatidylethanolamine (FPE). The quantum yield of fluorescein is dependent on its protonation state; neutral fluorescein is non-fluorescent and deprotonation to monoanion and dianion states results in fluorescent forms with increasing quantum yield (Figure 1.3.3). Fluorescein can therefore be used to detect changes in pH and of the charge density of its immediate environment (Wall et al., 1995b).

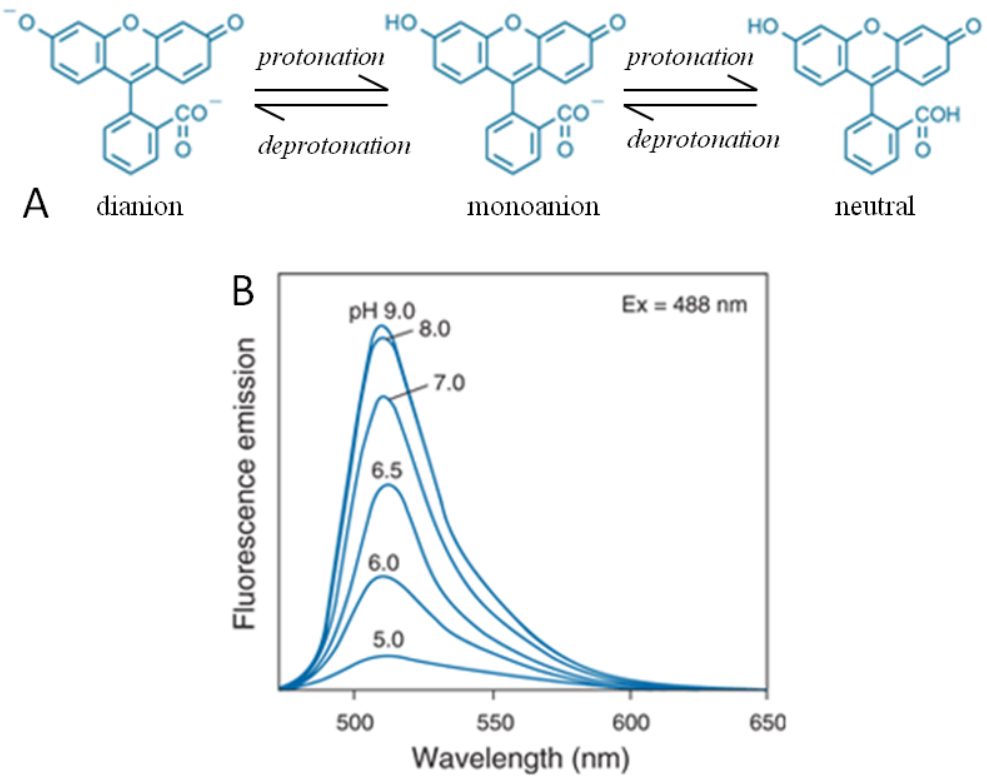

Figure 1.3.3: **A** The protonation states of Fluorescein. Neutral fluorescein is non-fluorescent and the monoanion and dianion are fluorescent with increasing quantum yield, respectively. **B** demonstrated the increasing intensity of the emission spectra due to the increased deprotonation of fluorescein with increasing pH. Images adapted from (Johnson and Spence, 2011).

The conjugation of fluorescein to phosphatidylethanolamine enables the probe to insert into the membrane bilayer with the fluorescein moiety located at the lipid water interface where it is sensitive to variation in the charge density at the membrane surface associated with changes in the surface potential. The sensitivity of FPE to the surface potential is described by the Henderson-Hasselbach equation with the substitution of the expression $pK - \frac{F\varphi_s}{RTln10}$ which can be considered to reflect the apparent *pK* (pK_a) for the proton binding of an acid-base couple of the fluorophore (Equation 1.3.1) (O'Shea, 2005).

$$log\left(\frac{C_B}{C_{HB}}\right) = pH - \left[pK - \frac{F\varphi_s}{RTln10}\right] \qquad \textit{Equation 1.3.1}$$

Here C_B and C_{HB} denote the concentrations of deprotonated and protonated FPE respectively and according to this expression changes in the surface potential at constant pH will alter the protonation state of FPE detected as a change in the fluorescence intensity. For example, the addition of a positive charge to the membrane surface decreases the net negative charge of the membrane with respect to the bulk aqueous environment and therefore decreases the surface potential. This increases the apparent *pK* of FPE resulting in its deprotonation and an increase in fluorescence intensity. The equation can be represented more simply as Equation 1.3.2 denoting

that the pK_a of FPE at the membrane surface (pK_{as}) is equal to the Pk_{aB} of FPE in the bulk aqueous medium plus the effect of the surface potential (O'Shea, 2003).

$$\Delta pK_{as} = pK_{aB} + \Delta\varphi_s \qquad \textit{Equation 1.3.2}$$

The change in FPE fluorescence as a result of a change in the surface potential can be utilised to study the kinetics of interaction of charged species with the membrane. As the surface potential decreases, for example by the binding of a negatively charged molecular species to the membrane, FPE has a lower propensity to ionise (resulting in an increased *pK* value). A higher fraction of FPE at the membrane-surface interface is therefore in semi- or non- ionised states (monoanionic or neutral fluorescein configurations) and so the fluorescence quantum yield, hence intensity, decreases (Fitchen et al., 2003).

This effect can be utilised to study the kinetics of the interaction of charged species with both artificial phospholipid membranes and cell membranes. Examples include the interaction of the cytochrome c oxidase signal sequence (p25) with phospholipid vesicles (Wall et al., 1995b, Golding et al., 1996), the interaction of the HIV fusion peptide gp41 with both phospholipid vesicles and Jurkat T-lymphocytes (Cladera et al., 2001) and the interaction of the extracellular matrix protein fibronectin with osteoblasts (Sim et al., 2004).

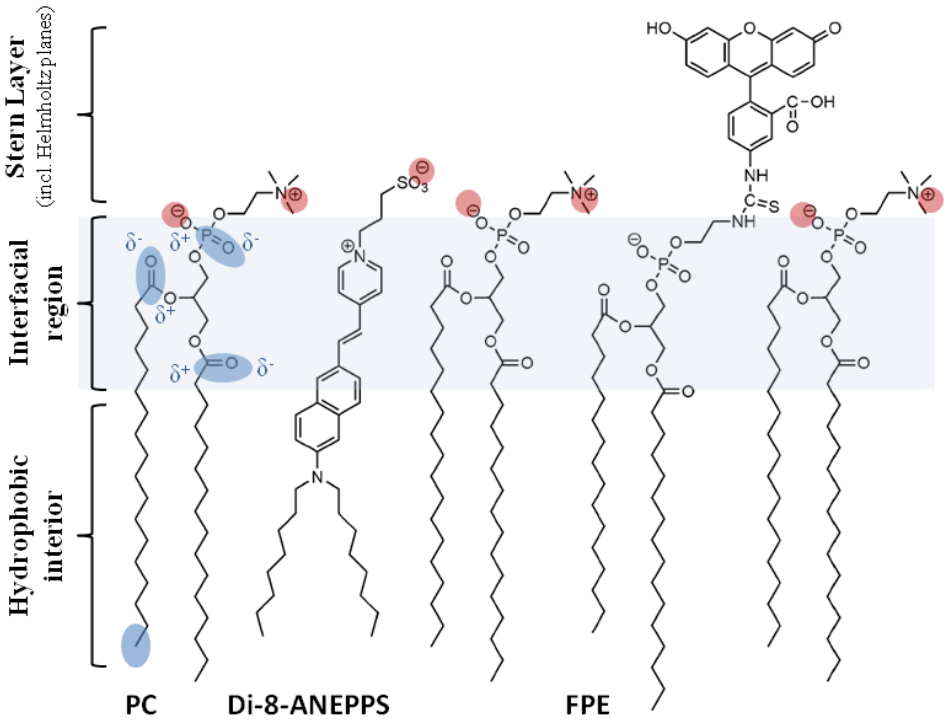

Figure 1.3.4: The structures and orientation of FPE and Di-8-ANEPPS in a phosphatidylcholine membrane leaflet. The dipoles thought to contribute to the dipole potential (blue) and the surface charges resulting in the surface potential (red) are highlighted. The dipole potential manifests between the hydrophobic interior and the exterior of the membrane and the surface potential exists between the membrane surface and the distant bulk aqueous phase. Adapted from (Matos et al., 2008).

1.3.3. The dipole potential

The membrane dipole potential originates from the alignment of the molecular dipoles within lipids, predominantly in the interfacial region of the bilayer, with contribution from the orientationally restricted water molecules adjacent to these groups and within the outer Helmholtz plane (Bechinger and Seelig, 1991, Brockman, 1994, Gawrisch et al., 1992). Contributing dipoles include those found in the lipid headgroups (with a dipole moment, μ, of approximate value μ=20D (Shepherd and Buldt, 1978)), for example $P^{\delta+}$-$O^{\delta-}$, the glycerol ester moieties ($C^{\delta+}$=$O^{\delta-}$, μ≈1.8D (Flewelling and Hubbell, 1986)) and, with a relatively minor contribution, the terminal methyl groups of the fatty acid tails (μ≈0.35D (Vogel and Mobius, 1988)), as identified in Figure 1.3.4. The P^{-}-N^{+} dipole present in phosphatidylcholine (PC) and phosphatidylethanolamine (PE) may also contribute (Starke-Peterkovic et al., 2006). It should be noted that the values of μ are very approximate due to limitations in the methods used to derive them and are given to demonstrate their relative magnitudes only.

These dipolar groups are thought to be organised such that their combined effect, resolved parallel to the membrane normal, endows the hydrophobic interior of the membrane bilayer with a positive dipolar charge relative to the exterior. This manifests in a potential over the interfacial region of the membrane bilayer with a magnitude between 220-300mV, depending on the membrane composition (Brockman, 1994, Clarke, 1997, O'Shea, 2005, Starke-Peterkovic et al., 2006). Figure 1.3.5 illustrates the profile of this potential with respect to the membrane, compared to that of the surface potential discussed above.

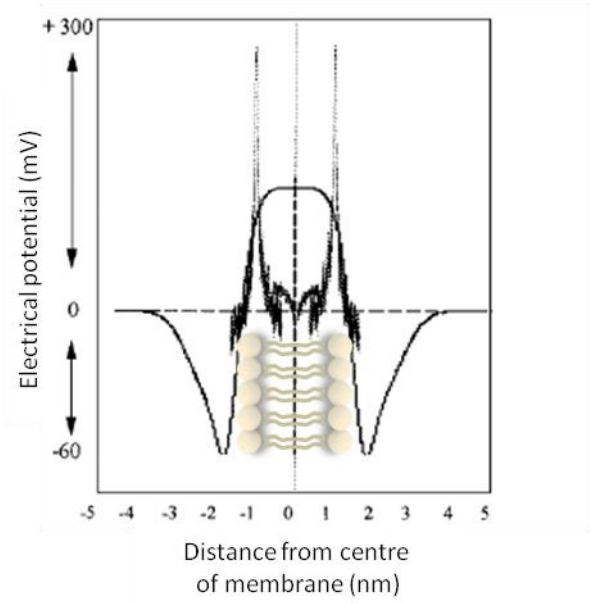

Figure 1.3.5: Computationally derived profiles of the dipole potential and surface potential with respect to the membrane. The dipole potential exists over the headgroup region of each leaflet of the membrane bilayer with a magnitude ~300mV and the surface potential is negative (around -60mV) at the membrane surface decreasing with distance into the surrounding aqueous environment. Adapted from data presented in O'Shea 2003 (O'Shea, 2003).

Variation in the lipid packing density is also reported to contribute to the magnitude of this potential which is greatest in highly ordered bilayers of lipids with saturated fatty acid chains, decreasing with increasing unsaturation (Clarke, 1997, Le Goff et al., 2007). As discussed previously (Section 1.1.3), cholesterol intercalates between lipids increasing the lipid packing density and forming highly ordered l_o phase regions in membranes which have an elevated dipole potential with respect to the surrounding membrane (O'Shea, 2003, Starke-Peterkovic et al., 2006, Duggan et al., 2008).

The relative contribution of these factors to the dipole potential is unclear with many studies providing conflicting reports. The molecular dipole moment of molecules in the membrane has been reported to have both a significant and negligible effect on the dipole potential. For example, Phloretin was observed to significantly decrease the dipole potential at low molar concentration where it does not influence lipid packing or hydration, leading to the suggestion that this decrease arises from the molecular dipole of the molecule (Bechinger and Seelig, 1991). Molecular dynamic simulations have also demonstrated the molecular dipole of cholesterol to significantly affect the dipole potential (Smondyrev and Berkowitz, 2001) and, conversely, to have negligible effect (Hofsass et al., 2003). Interestingly, Starke-Peterkovic *et al.* (Starke-Peterkovic et al., 2006), based on calculations from the computationally derived molecular dipole moment for cholesterol, suggest this only contributes 10-30% of the increase in dipole potential observed of cholesterol experimentally. They attribute a further 8.7% to the increased dipole density due to the equivalent percentage increase in lipid packing and order promoted by cholesterol (Almeida et al., 1992), and assign the remaining, dominant, proportion of the change to occur due to the oriented water molecules (Starke-Peterkovic et al., 2006). However, although confirming through molecular dynamics simulations that the oriented water molecules in the interfacial region of the membrane do provide a significant contribution to the dipole potential, Robinson *et al.* (Robinson et al., 2010) also show that this contribution does not change on the inclusion of cholesterol in the membrane. Experimental studies where the amount of oriented water in the interfacial region has been reduced by replacing water molecules hydrogen-bonded to the lipid phosphate or carbonyl dipoles with hydroxyl-rich molecules (e.g. trehalose) have demonstrated this effect to significantly alter the dipole potential. Again this suggests the importance of hydrating water molecules. The extent to which each of the dipoles within the lipids contributes is also unclear. The P^--N^+ dipole of PC is considered not to have a significant contribution as, due to the orientation of the dipole with the negatively charged phosphate nearer the membrane interior, it would cause the dipole potential to be negative which is not observed (Starke-Peterkovic and Clarke, 2009). Conversely, PE which also possesses the P^--N^+ moiety significantly increases the dipole potential which may result from the movement of this dipole to a position more parallel to the membrane surface as the headgroup of PE is overall less bulky than that of PC (Starke-Peterkovic and Clarke, 2009).

The orientation of the P^-N^+ moiety has been reported to vary up to 40^o depending on the surface charge of the membrane (Semchyschyn and Macdonald, 2004, Seelig et al., 1987). Interestingly phosphatidic acid (PA), which does not possess a P^-N^+ group, also causes a significant increase in the dipole potential suggesting that the P^-N^+ moiety may not provide a major contribution. The charged moieties present on phosphatidylserine (PS) and phosphatidylglycerols (PG), in contrast, have only very minor effects on the dipole potential as the charges are thought to reside too far into the surrounding aqueous environment, away from the interfacial region, to significantly influence the dipole potential (Starke-Peterkovic and Clarke, 2009). The importance of the carbonyl dipoles was demonstrated on replacing the ester bonds on which they occur with ether moieties which significantly decreased the dipole potential however, a significant potential still persisted which was attributed to the associated oriented water molecules (Gawrisch et al., 1992). Fatty acid chain length has been reported to influence the dipole potential due to associated changes in lipid packing (Clarke, 1997) but has also been shown to have a negligible effect (Peterson et al., 2002).

The relative contributions from lipid molecular dipoles, oriented water molecules and the fatty acid composition of lipids are therefore undefined and likely to vary significantly with the specific composition of a membrane. The factors resulting in a change in the dipole potential are also likely to vary depending on the effectors of the change and the membrane composition. Despite the ambiguity in the exact mechanism underlying an observed change in the dipole potential of a membrane, these changes have been identified to play a significant role in physiological processes within cell membrane (reviewed later) and as such have been widely studied.

Changes in the dipole potential can be detected using the electrochromic fluorescent probe Di-8-ANEPPS (*1-(3-sulphonatopropyl)-4-[β[2-(di-n-octylamino)-6-naphthyl]vinyl]pyridium betaine*) developed by Loew *et al.* (Loew et al., 1979). Two hydrocarbon chains ensure the probe locates within the membrane bilayer with the polar zwitterionic end positioned in the region of the lipid polar headgroups, as shown in Figure 1.3.4. When Di-8-ANEPPS absorbs a photon of the appropriate wavelength a change in the electronic distribution within the molecule occurs; the effect of which is that negative charge, normally situated at the aniline nitrogen, moves along the length of the conjugated ring system to the pyridinium nitrogen (as demonstrated in Figure 1.3.6). Upon relaxation the negative charge returns towards the aniline nitrogen and a photon is emitted as fluorescence.

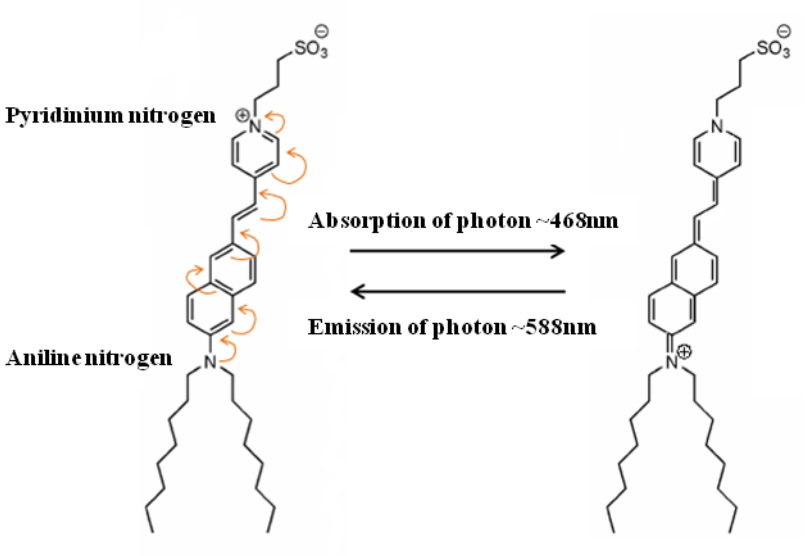

Figure 1.3.6: The electronic redistribution within Di-8-ANEPPS (orange arrows) upon absorption of an exciting photon and prior to emission of a photon as fluorescence.

Di-8-ANEPPS is sensitive to the local electric field associated with the dipole potential which influences the electronic distribution within the molecule; changes in the dipole potential therefore alter the energy levels and, consequently, the energy of the photon required to excite the probe (Loew et al., 1979). This manifests as a shift in the excitation spectrum of Di-8-ANEPPS in response to changes in the dipole potential. The spectral shift, $\Delta\nu$, of the chromophore is related to the local electric field, *E*, by expression 1.3.3 (Gross et al., 1994):

$$\Delta\nu = -\frac{1}{h}\Delta\vec{\mu}.\vec{E} - \left(\frac{1}{2h}\right)\Delta\alpha\vec{E}^2 \qquad \textit{Equation 1.3.3}$$

Here $\Delta\mu$ denotes the change in the dipole moment and $\Delta\alpha$ the change in polarisibility of Di-8-ANEPPS. For field strengths relevant to biological membranes, the first term of this expression dominates and the relationship between the spectral shift of the chromophore and the local electric field it experiences as a result of the dipole potential is essentially linear (Gross et al., 1994).

Di-8-ANEPPS is highly sensitive to the dipole potential by virtue of its position within the membrane bilayer placing the electrochromic conjugated ring system of the molecule within the small region in which the dipole potential manifests. Considering the shorter distance over which it acts and the greater magnitude of the dipole potential relative to the transmembrane potential (that translates into the electric field that influences the chromophore by the expression $\vec{E} = -\Delta\vec{\varphi}$) it is evident that Di-8-ANEPPS, positioned as it is, is significantly less sensitive to the transmembrane potential than the dipole potential (Gross et al., 1994). Conveniently the position of the probe also renders it unable to detect the surface potential (Gross et al., 1994) and this has been confirmed experimentally by (Cladera and O'Shea, 1998) who demonstrate

negligible change in the spectroscopic properties of Di-8-ANEPPS in phospholipid vesicles on addition of calcium ions which are previously reported to decrease the surface potential (Wall et al., 1995b). Changes in the ionic strength of the aqueous solution surrounding a membrane may, however, influence the dipole potential indirectly by perturbing the oriented water molecules within the Stern layer which contribute to the dipole potential (Brockman, 1994).

An example of the spectral shift exhibited by Di-8-ANEPPS as a result of the decrease or increase in the dipole potential induced by phloretin and 6-ketocholestanol, respectively, in DOPC membranes is shown in Figure 1.3.7. The inclusion of 15mol% phloretin in the membranes causes a red shift in the excitation spectrum, relative to that of Di-8-ANEPPS in 100mol% DOPC membranes, and the associated decrease in dipole potential is thought to occur a result of two effects. The molecular dipole of phloretin (~5D) resolved along the axis parallel to the membrane normal acts anti-parallel to the likewise resolved dipolar contributions of the membrane lipids, therefore counteracting their contribution to the dipole potential. Phloretin also reduces the density of water dipoles within the hydration layer at the bilayer-water interface by preferentially forming hydrogen bonds with the phosphate of the lipid headgroups in place of the water (Bechinger and Seelig, 1991, Franklin and Cafiso, 1993). The presence of 15mol% 6-ketocholestanol in the DOPC membranes causes a relative blue shift of the excitation spectrum of Di-8-ANEPPS. This corresponds with the increase in dipole potential occurring as a result of the component of the molecular dipole of 6-ketocholestanol (~1.6D) resolved parallel to the membrane normal contributing to the effect of the collective components of the membrane lipids in this direction (Franklin and Cafiso, 1993).

A dual-wavelength ratiometric method has been developed enabling real-time monitoring of changes in the dipole potential within membranes (Gross et al., 1994). This involves recording the emission (~590nm) of Di-8-ANEPPS in membranes at two excitation wavelengths (usually around 460nm and 520nm) and taking the ratio of the intensities obtained. A decrease or increase in the ratio reflects a red shift or blue shift of the excitation spectrum, and decrease or increase in the dipole potential, respectively. This technique has significant advantages over single-wavelength determination of excitation spectral-shift; the ratio obtained is insensitive to changes in the emission intensity, for example as a result of photobleaching (irreversible photochemical destruction of a fluorophore rendering it non-fluorescent) or small differences in the partition coefficient of Di-8-ANEPPS between the membrane and aqueous solution (where it is non-fluorescent) (Cladera and O'Shea, 1998). A limitation of the technique, however, is that a rigorous calibration method has yet to be established to correlate the ratio recorded with actual dipole potential values (Matos et al., 2008).

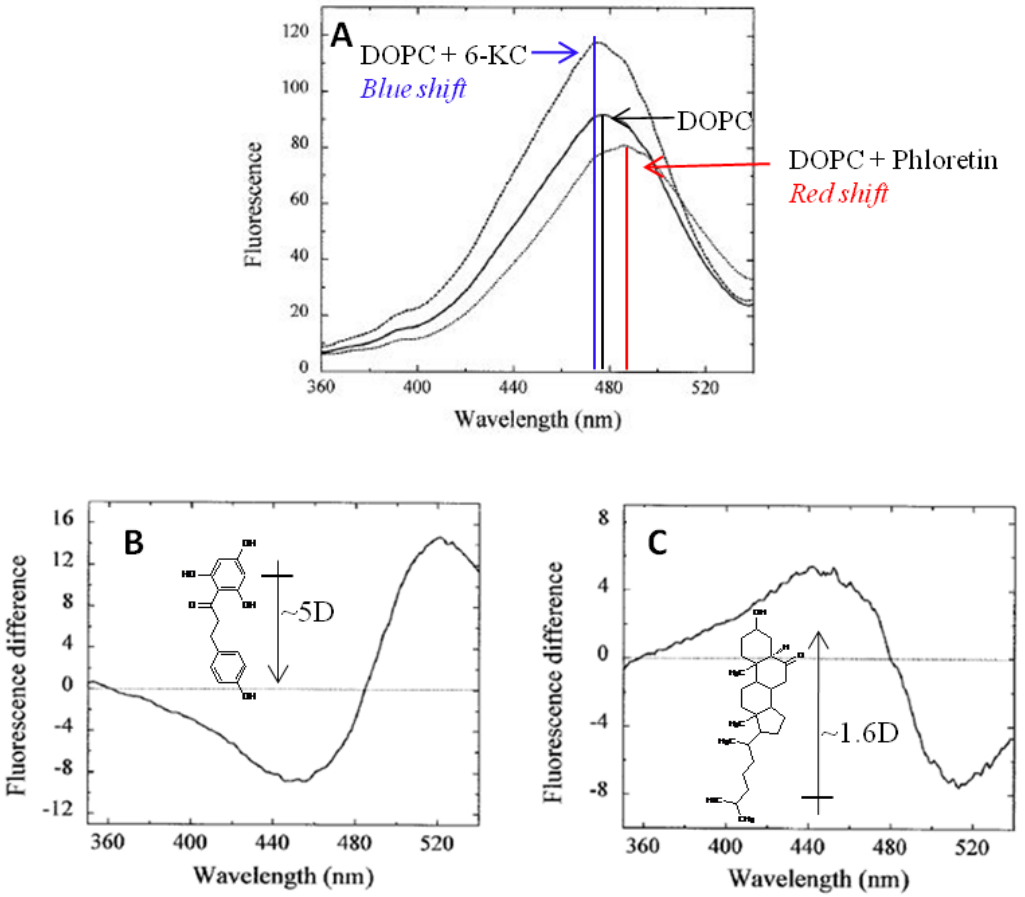

Figure 1.3.7: **A** the excitation spectrum of Di-8-ANEPPS in DOPC vesicles and the red shift or blue shift of this spectrum on inclusion of 15mol% Phloretin or 6-Ketocholestanol (6-KC). The difference spectra obtained by subtracting the excitation spectrum of Di-8-ANEPPS in DOPC vesicles from that in DOPC+15ml%Phloretin (**B**) or DOPC+15mol%6-KC (**C**) vesicles, clearly demonstrating the resultant spectral shifts, are also shown. Adapted from data presented in (Cladera and O'Shea, 1998).

A further shortcoming, highlighted by Clarke and Kane (Clarke and Kane, 1997), is that the excitation spectrum of Di-8-ANEPPS, and therefore the ratio, is influenced by the fluidity of the membrane. They observe significant effects on the ratio of Di-8-ANEPPS in DMPC vesicles (at 420nm and 520nm excitation) with increasing temperature if emission was observed at 580nm however; this effect was significantly reduced if emission was detected at 670nm. This result was interpreted to suggest that, under the wavelengths normally chosen, the ratiometric method is sensitive to the fluidity in addition to the dipole potential. There is some ambiguity in this interpretation as it cannot be assumed that the increasing temperature does not influence the dipole potential; the increasing molecular motion may alter the magnitude of the lipid dipole moments resolved parallel to the membrane normal due to reorganisation of the molecular dipoles and hydration may also be affected. Therefore, confidence in this interpretation can only be gained on de-coupling the changes in fluidity and dipole potential occurring which is not a straightforward task. Interestingly, Cladera and O'Shea (Cladera and O'Shea, 1998) observed no difference in the ratio (at 460nm and 520nm excitation) of emission intensities detected at 580nm or 630nm with the presence of phloretin or 6-ketocholestanol in egg-phosphatidylcholine vesicles, both of which alter membrane fluidity (Valenta et al., 2004).

A dual-*emission* ratiometric method has been employed by Bullen and Saggau (Bullen and Saggau, 1999) to investigate changes in the transmembrane potential induced by an externally applied electric field. Vitha and Clarke have recently evaluated this technique in comparison with the dual-excitation ratiometric method for the detection of the dipole potential (Vitha and Clarke, 2007). They report that, unless used with membranes within a defined lipid phase and at a specific excitation wavelength, the emission ratio obtained with Di-8-ANEPPS does not correlate well with known changes in the dipole potential. This is as a result of the significant influence of membrane fluidity on the emission spectrum. Fluorescence emission is of a longer wavelength than excitation as a result of the Stoke's shift; the decrease in excited state energy due to solvent relaxation (in this case molecular reorganisation of the lipids surrounding the probe acting to stabilise the excited state). This effect depends on the orientational polarisibility of lipids and therefore reflects the dipole potential, however, the rate of solvent relaxation also influences the excitation spectrum (a slow rate decreases the probability of emission from higher energy states shifting the excitation spectrum to lower wavelengths) and this is affected by the fluidity of the membrane surrounding the probe (Vitha and Clarke, 2007).

The dual-excitation ratiometric method is therefore the most appropriate technique employing Di-8-ANEPPS in the investigation of the dipole potential and has been widely used to demonstrate the significance of this membrane potential in cellular physiology. For example, the dipole potential has been reported to be involved in the activity of phospholipase A_2 (Maggio, 1999) and Na^+ K^+ ATPase (Starke-Peterkovic et al., 2006) and with the control of redox reactions on the membrane surface (Alakoskela and Kinnunen, 2001). The insertion and secondary structure formation of the mitochondrial signalling sequence P25 in membranes has also been demonstrated to be influenced by the dipole potential (Cladera and O'Shea, 1998). The dipole potential is also thought to be involved in several pathological processes as fusion peptides, such as the simian immunodeficiency virus peptide (Cladera et al., 1999), the HIV GP41 peptide (Buzon and Cladera, 2006, Cladera et al., 2001) and regions of the S2 domain in SARS-CoV glycoprotein (Guillen et al., 2008), which promote the fusion of viral and cellular membranes influence, and are influenced by, the dipole potential. In addition, signalling molecules from both *Escherichia coli* (Voglino et al., 1998) and *Pseudomonas Aeruginosa* (Davis et al., 2010) have also been demonstrated to modulate the dipole potential on interaction with membranes. Recently, attention has focussed on the effects of xenobiotic agents, for example anaesthetics such as Pregnanolone (Alakoskela et al., 2004) and Lidocaine (Hogberg and Lyubartsev, 2008) on the membrane dipole potential. Interestingly, it has also been observed that ligand binding to the multi-drug transporter P-glycoprotein alters the dipole potential (Asawakarn et al., 2001) and, conversely, modulating the dipole potential also influences the activity of this receptor (Asawakarn et al., 2001, Cattelotte et al., 2009).

1.4. Oxidative stress and oxidation of membrane lipids

Redox reactions are involved in several cellular processes, such as signalling mechanisms and glucose metabolism, however, the normal redox state of the cell can become disrupted resulting in an imbalance between the rate of production of reactive oxygen species and the rate at which the cell destroys them and their reactive intermediates. The resulting damage, that the cell is unable to protect from or repair, manifests as oxidative stress. The consequent diverse and dramatic effects has lead to the association of oxidative stress with many pathological states including neurodegenerative disease, such as Alzheimer's and Parkinson's disease (e.g. (Smith et al., 2000, Jenner, 2003)), cardiovascular disease, such as atherosclerosis (e.g. (Harrison et al., 2003)), and diabetes (e.g. (Maritim et al., 2003)). The cellular effects of oxidative stress are perpetrated by free radicals, including reactive oxygen species (ROS), which are collectively defined as "any species capable of independent existence that contains one or more unpaired electrons" (Halliwell and Gutteridge, 1999). The superoxide anion, $O_2^{\bullet-}$, readily formed by the acceptance of a single electron by molecular oxygen, mainly arising from the mitochondrial electron transport chain, is an example of a cellular reactive oxygen species which itself promotes the formation of hydroxyl radicals ($OH^{\bullet}$). The unpaired electron(s) render these molecules highly reactive and on interaction they cause significant structural alteration to many susceptible biomolecules affecting their function, molecular interactions and collective physical properties on a sub-cellular level (Catala, 2010, Fruhwirth et al., 2007, Girotti, 1998). The resulting significant impact on cellular physiology has lead oxidative stress to be considered a precursor and common underlying mechanism linking cardiovascular disease and diabetes (Ceriello and Motz, 2004). This was based on the earlier observation, proposed by Stern in the "common soil hypothesis" (Stern, 1995), that these diseases, which often occur together, must have common antecedents. The remainder of this section is dedicated to describing the structural effects of free radical attack on the molecular components of the cell membrane, specifically membrane lipids, and the consequences on the biophysical properties of the membrane. Further information on the occurrence of free radicals and their involvement in cellular physiology and the aetiology of oxidative stress can be found in (Halliwell and Gutteridge, 1999).

1.4.1. Protein oxidation

Oxidative damage to proteins can significantly impair their function as a result of the direct modification of active site residues or indirectly by inducing a change in the active site conformation. For example, the thiol group of cysteine residues are targeted by ROS resulting in the formation of disulfide cross-linkages which modify protein conformation. Likewise, the oxidation of histidine residues results in cross-linking. Tryptophan and tyrosine residues are also susceptible to oxidation, in the case of tyrosine leading to the tyrosine radical, TyrO•, which is

involved in the formation of dityrosine groups. Hydroperoxide groups can also form on the backbone and side-chains of residues, particularly valine, and can decompose in the presence of O-O cleaving transition metals resulting in gross structural changes to the protein conformation. The presence of dityrosine and hydroperoxide groups on protein residues are deemed as an indicator of oxidative stress (Halliwell and Gutteridge, 1999).

As radicals can form on both DNA and lipids, DNA-bound and membrane-bound proteins are susceptible to oxidation. DNA-bound proteins are targets for free radical mediated cross-linking with DNA and the propagation of the lipid radical chain following peroxidation of membrane lipids likewise results in the modification of membrane bound proteins (Halliwell and Gutteridge, 1999).

1.4.2. Lipid peroxidation

Lipid oxidation can occur through three mechanisms; enzymatic oxidation, non-enzymatic non-radical oxidation and non-enzymatic free radical mediated oxidation (Niki et al., 2005). When the free-radical associated chain reactions occur uncontrolled by the cell the resulting oxidation manifests as oxidative stress (Halliwell and Gutteridge, 1999). Figure 1.4.1 outlines the free radical mediated oxidation of a lipid fatty acid with single unsaturation. The reaction is initiated by the abstraction of a hydrogen atom from the fatty acid by a free radical (in this case the ROS hydroxyl radical) forming a lipid radical [1]. The lipid radical reacts with molecular oxygen to create a lipid peroxyl radical [2] in a process that is freely reversible by fragmentation of the lipid peroxyl radical producing oxygen and the original lipid radical [3]. The unstable lipid peroxyl radical can then abstract a hydrogen atom from a nearby lipid forming lipid peroxide and in the process propagating the radical chain reaction by initiating the process in the lipid from which it took the hydrogen [4]. The resulting lipid hydroperoxide (having a hydrogen atom as one of the functional groups of the R-O-O-R' peroxide group) is a major primary product of lipid peroxidation and provides the substrate for several secondary reactions, for example the reduction to the corresponding hydroxide (Halliwell and Gutteridge, 1999, Niki et al., 2005).

A further step occurs for lipids with fatty acids containing more than three sites of unsaturation involving cyclization of the lipid peroxyl radical forming a cyclic peroxide or cyclic endoperoxide (illustrated in Figure 1.4.2). The further oxidation or hydrolysis of cyclic endoperoxide leads to the formation of malondialdehyde and fatty acid chain shortening (Halliwell and Gutteridge, 1999, Niki et al., 2005).

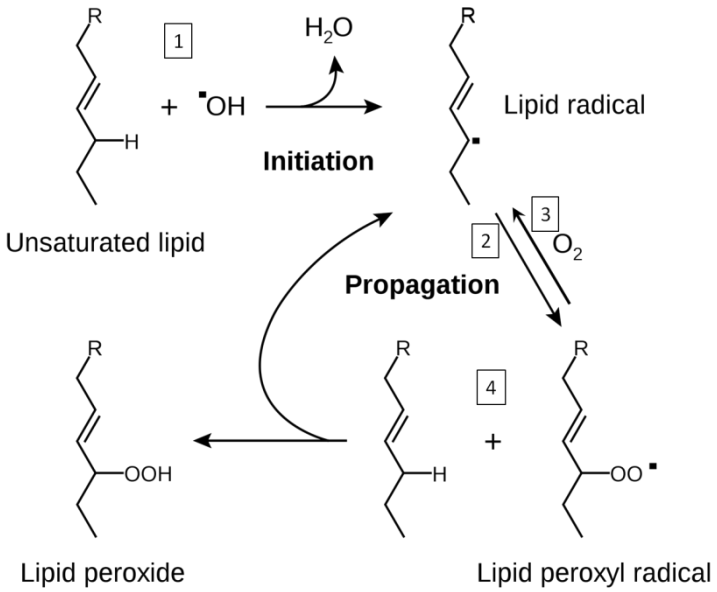

Figure 1.4.1: A diagram demonstrating the free radical mediated oxidation of unsaturated lipids. One unsaturated fatty acid of the lipid is shown for clarity with R representing the glycerol backbone with attached head-group and second fatty acid tail, forming the complete lipid. Each step of the process, involving initiation and propagation of the free radical chain reaction and the formation of the resulting lipid peroxide end product, is described in the text. Adapted from (Vickers, 2007) after (Young and McEneny, 2001).

.

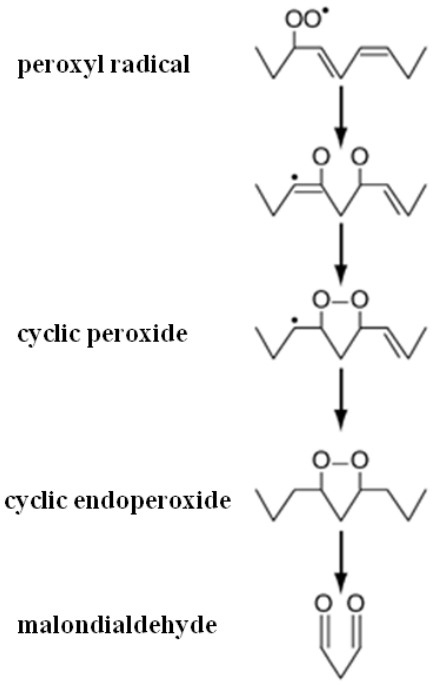

Figure 1.4.2: The formation of cyclic peroxide, cyclic endoperoxide and malondialdehyde from a lipid peroxyl radical formed in step [2] of the oxidation process detailed in Figure 1.4.1 from a PUFA. The formation of the malondialdehyde results in the shortening of the fatty acid chain length. After (Hall and Bosken, 2009).

Lipid peroxidation preferentially occurs in regions of high electron density and therefore poly-unsaturated fatty acids (PUFAs) are prime targets in cell membranes. The relative susceptibility of membrane fatty acids to oxidation has been reported to decrease with decreasing levels of fatty acid unsaturation in the order 22:6>20:4>18:2>>18:1>16:0 (where fatty acid structure is

represented as chain length (no. of carbons):no of unsaturation sites) with a significant reduction between poly- and mono-unsaturated fatty acids (Noguchi et al., 1998, Niki et al., 2005).

The structural modifications occurring as a result of lipid peroxidation, outlined above, significantly influence the physical properties they collectively endow on the membrane which are highly sensitive to fatty acid structure (discussed in detail in Sections 1.1.3 & 1.1.4). For example, oxidative stress has been reported to promote the disordering of phospholipids, increasing fluidity of saturated-lipid rich phases, and influence the phase behaviour of membranes (Megli and Sabatini, 2003, Megli et al., 2005, Ayuyan and Cohen, 2006).

1.4.3. Sterol oxidation

Cholesterol, like phospholipids, can be oxidised via enzymatic, non-radical or radical mediated mechanisms and the resulting modified structures are known as oxysterols. In cellular membranes, cholesterol oxidation is most likely to be mediated by ROS derived from metabolic pathways (Bjorkhem and Diczfalusy, 2002) with 7-ketocholesterol (7-KC) a major product of this process (Lyons and Brown, 1999). The resulting oxysterols although structurally similar to cholesterol, exhibit very different physical behaviour in membranes to their unoxidised precursor. If the substitution resulting from oxidation occurs at the sterol nucleus, for example, the order and packing of the upper part of the fatty acid chains is thought to be affected altering the phase behaviour of the membrane (Rooney et al., 1986). Oxysterols are, however, thought to preferentially form ordered domains in a similar manner to cholesterol, perhaps as a result of their unfavourable solubility among lipids where repulsion between the polar moieties of the oxysterol and of the fatty acids may occur (Rooney et al., 1986). The extent to which ordered domains are promoted and the nature of these phases is highly dependent on the structure of the oxysterol (Li et al., 2003, Wenz and Barrantes, 2003, Wang et al., 2004, Massey and Pownall, 2006). The remainder of this section will focus on the influence of 7-ketocholesterol on the physical properties of membranes.

1.4.3.1. *The effect of 7-ketocholesterol on the physical properties of phosphatidylcholine membranes*

The formation of 7-ketocholesterol by the oxidation of cholesterol is outlined in Figure 1.4.3. 7-Ketocholesterol differs structurally from cholesterol only by a ketone functional group present at the 7-position (Lyons and Brown, 1999). This relatively minor structural modification, however, significantly influences the behaviour of the oxysterol in membranes where unsaturated lipids are present (Massey and Pownall, 2005).

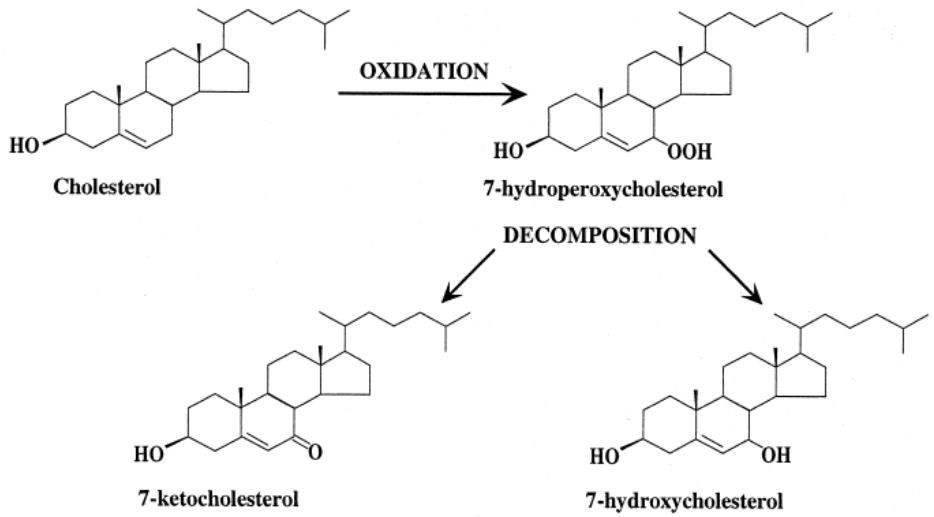

Figure 1.4.3: The oxidation of cholesterol forming 7-hydroxycholesterol and, principally, 7-ketocholesterol via the unstable 7-hydroperoxycholesterol. After (Lyons and Brown, 1999).

Among saturated phosphatidylcholines 7-ketocholesterol promotes the formation of ordered domains in a similar manner to cholesterol (Rooney et al., 1986). These domains, like the liquid ordered (l_o) domains formed by cholesterol, are detergent resistant (Wang et al., 2004, Massey and Pownall, 2005). However, through fluorescence quenching and general polarisation studies it has been observed that they exhibit lower lipid packing density and therefore decrease hydration and polarity to a lesser extent (Wang et al., 2004, Massey and Pownall, 2005) confirming earlier observations arising from differences in glucose permeability of cholesterol- and 7-ketocholesterol containing membranes (Theunissen et al., 1986). Analysis of detergent resistant membrane fractions of DPPC membranes with equivalent concentrations of cholesterol or 7-ketocholesterol has determined that the sterols promote the formation of the ordered phase to equal extent (Wang et al., 2004). This is consistent with the observations that, for DPPC or DMPC membranes below T_m, cholesterol and 7-ketocholesterol equally disrupt the tight fatty acid chain packing of the gel phase resulting in the coexistence of the gel (L_β) and 'l_o' phases. Above T_m the sterols similarly order the lipids promoting the phase separation of the l_c phase to coexisting l_d and 'l_o' phases (Massey and Pownall, 2005).

Among unsaturated lipids, however, 7-ketocholesterol exhibits very different behaviour from cholesterol. Neither sterol forms highly ordered domains of the sort observed with saturated lipids, but weaker phospholipid-sterol interactions persist (weakened by the lower packing density as a result of unsaturated fatty acid chains) enabling the sterols to have a slight ordering effect (Wang et al., 2004). In X-ray diffraction studies of POPC membranes, 7-ketocholesterol was found to condense the membrane, by increasing lipid packing, to a lesser extent than cholesterol (Phillips et al., 2001). Interestingly, 7-ketocholesterol was observed to order fatty acid chains much less than cholesterol but exhibit a greater influence on the glycerol backbone

and headgroups of the lipids. This suggested that 7-ketocholesterol does not penetrate as deeply into the bilayer as cholesterol, most likely as a result of the entropically favourable hydrogen bonding of the additional polar moiety with interfacial water at the membrane surface (Phillips et al., 2001). The differences in the ordering of unsaturated lipids is thought to result from the distinct position of 7-ketocholesterol in the membrane with respect to cholesterol (Phillips et al., 2001).

The difference in the behaviour of 7-ketocholesterol among saturated and unsaturated lipids and the fact that biological membranes generally contain both lipid species led to the study of the influence of 7-ketocholesterol in ternary systems. As discussed in detail in Section 1.1.3, cholesterol disrupts the L_β phase and induces phase separation of the l_c phase by promoting the formation of the l_o phase to an extent dependent on the proportion of cholesterol, saturated lipid and unsaturated lipid in the membrane (defined in the cholesterol:DPPC:POPC phase diagram of Figure 1.1.9) (Veatch et al., 2004, de Almeida et al., 2007). 7-ketocholesterol similarly induces the formation of ordered domains in a dose dependent manner in 7-KC:DPPC:DOPC membranes however, lipid packing and hydration are altered to a lesser extent (Massey and Pownall, 2005). Comparison of the detergent insoluble fraction of mixed membranes with equal concentrations of either cholesterol or 7-ketocholesterol demonstrate the latter to form ~50% less DRM than cholesterol suggesting 7-ketocholesterol to have a significantly lower affinity for forming ordered domains with DPPC than cholesterol in the presence of DOPC (Massey and Pownall, 2005, Wang et al., 2004). 7-Ketocholesterol was also observed to have significantly less influence on fatty acid chain ordering and to decrease polarity in the interfacial region to a much lesser extent than cholesterol. This indicates that the 7-ketocholesterol molecules, or at least a population of 7-ketocholesterol, does not position in the bilayer with the same penetration depth as cholesterol and resides closer to the membrane surface, as was suggested to occur among unsaturated lipids (Massey and Pownall, 2005).

A similar position, closer to the membrane-water interface, is thought to be held by 6-ketocholestanol (6-KC) which is structurally similar to 7-ketocholesterol but with the ketone moiety at the 6-position. This was suggested to position with the ketone group (as well as the hydroxyl group) oriented towards, and hydrated by, the aqueous phase by Simon *et al.* (Simon et al., 1992) following a comparison of the effects of cholesterol and 6-ketocholestanol on the compressibility modulus (an indicator of the extent of lipid packing) and hydration of egg-phosphatidylcholine membranes. This concept was later supported by Smondyrev and Berkowitz (Smondyrev and Berkowitz, 2001) with molecular dynamics simulations of the localisation of 6-ketocholestanol in DPPC membranes who then went on to propose that 7-ketocholesterol is likely to position in the same way.

Following from the speculations of Smondyrev and Berkowitz and in consideration of the evidence presented above for the behaviour of 7-ketocholesterol in membranes, Massey and Pownall proposed a model for the orientation of 7-ketocholesterol in mixed saturated/unsaturated lipid membranes (Figure 1.4.4) (Massey and Pownall, 2005).

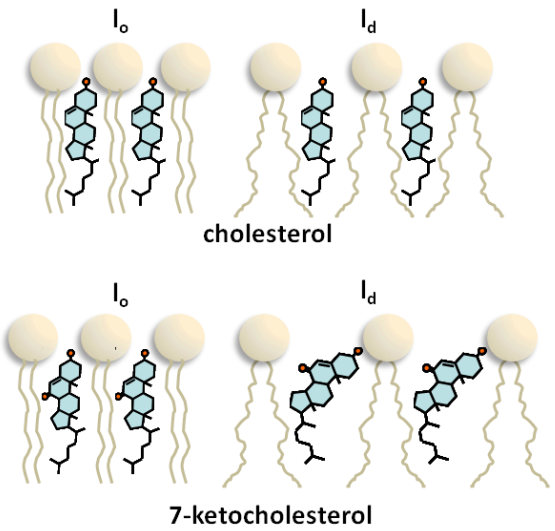

Figure 1.4.4: A diagrammatic representation of the model for the orientation of 7-ketocholesterol in mixed saturated/unsaturated lipid membrane proposed by Massey and Pownall (Massey and Pownall, 2005). The proposed depth and orientation of the sterol ring structure of 7-ketocholesterol in the liquid ordered (l_o) and liquid disordered (l_d) phases are compared to that of cholesterol. After (Massey and Pownall, 2005).

In the saturated-lipid rich l_o phase 7-ketocholesterol is proposed to adopt a similar orientation to cholesterol although, due to the presence of the ketone group, it does not increase the lipid density as much as cholesterol. The lower lipid packing density of the unsaturated lipid rich l_d phase is thought to enable the re-orientation of 7-ketocholesterol to a more thermodynamically favourable position where the additional polar moiety can form hydrogen bonds with interfacial water at the membrane surface. The resulting tilt of the 7-ketocholesterol molecule reduces the depth of penetration of the sterol ring structure into the membrane bilayer causing significantly less ordering of the lipids than cholesterol. The effect of the presence of two polar moieties in the interfacial region is to increase the extent of hydration of the membrane surface relative to that with cholesterol. As the tilted orientation of 7-ketocholesterol is thermodynamically preferable, the oxysterol has a stronger tendency to partition into the less densely packed l_d phases resulting in a lower extent of the l_o phase persisting with 7-ketocholesterol than with the equivalent concentration of cholesterol (Massey and Pownall, 2005). It is thought that the oxidation of membrane cholesterol into 7-ketocholesterol would therefore lead to the destabilisation of membrane rafts (Massey and Pownall, 2005) and the significance of this is discussed below.

1.4.3.2. *The influence of 7-ketocholesterol on the membrane dipole potential*

In light of its effects on lipid ordering and hydration, 7-ketocholesterol can be considered very likely to modulate the membrane dipole potential. 6-Ketocholestanol, structurally similar to 7-ketocholesterol but with the ketone group in the 6-position, is widely reported to increase the dipole potential (Franklin and Cafiso, 1993, Cladera and O'Shea, 1998, O'Shea, 2005) partly as a result of the location of this function group in the interfacial region of the membrane. It was therefore speculated that 7-ketocholesterol, which places its ketone moiety in the interfacial region when in the tilted orientation, should similarly alter the dipole potential (Massey and Pownall, 2005). Starke-Peterkovic *et al.*, however, observe that 7-ketocholesterol decreases the dipole potential of DMPC membranes (Starke-Peterkovic et al., 2006). This was the opposite effect to that observed with cholesterol, although the magnitude of the change in dipole potential on inclusion of either sterol to DMPC membranes was similar. The reverse effect of 7-ketocholesterol on the dipole potential to that of cholesterol or 6-ketocholestanol is attributed to the component of its molecular dipole moment resolved to the membrane normal acting anti-parallel to the likewise resolved molecular dipole moments of cholesterol and 6-ketocholestanol (Starke-Peterkovic et al., 2006). The ratio of the resolved dipole moment magnitudes of cholesterol and 7-ketocholesterol, determined computationally, were found to correlate well with the experimentally derived relative effects of the sterols on the dipole potential, confirming the significant influence of the molecular dipole moments (Starke-Peterkovic et al., 2006). As for cholesterol, the effect of 7-ketocholesterol on lipid packing and on hydration of the interfacial region of the membrane are also likely to contribute to the overall influence of this oxysterol on the dipole potential.

1.4.3.3. *Cellular effects of 7-ketocholesterol*

7-ketocholesterol has pro-oxidant, pro-inflammatory and cytotoxic effects in vivo (Vejux et al., 2008) and, as a result, is considered to have a significant role in the development of cardiovascular disease such as atherosclerosis (Brown and Jessup, 1999). These effects are mediated on a cellular level through several mechanisms. For example, 7-ketocholesterol promotes the production of reactive oxygen species (Myoishi et al., 2007) and can cause the oxidation of low density lipoproteins (Rosenblat and Aviram, 2002) which are then involved in the pathogenesis of atherosclerosis. 7-Ketocholesterol also disrupts reverse cholesterol transport, an important cardioprotective process, by inhibiting apoA-I mediated cholesterol efflux from cells (Gaus et al., 2001, Gaus et al., 2004). 7-Ketocholesterol has also been demonstrated to alter several signalling processes (Berthier et al., 2004, Myers and Stanley, 1999, Millanvoye-Van Brussel et al., 2004). The pro-apoptotic effects of 7-ketocholesterol are widely reported (e.g.(Jang and Lee, 2011, Huang et al., 2010, Leonarduzzi et al., 2006, Pedruzzi et al., 2004) and occur through a variety of mechanistic pathways. One such proposed

mechanism involves the 7-ketocholesterol stimulated incorporation of the calcium channel component, Trpc-1, into rafts which induces the calcium mediated activation of calcineurin leading to the dephosphorylation of the pro-apoptotic protein BAD, part of the mitochondrial pathway of apoptosis (Berthier et al., 2004, Berthier et al., 2005, Lemaire-Ewing et al., 2005). Interestingly, 7-ketocholesterol has been reported to be present in detergent resistant membranes (DRM) following exposure of cells to the oxysterol (Royer et al., 2009, Myers and Stanley, 1999) and it has also been identified in the DRM of macrophage foam cells found in atherosclerotic plaques (Maor et al., 2000). It therefore likely acts to alter the composition (and consequently the biophysical properties) of rafts and as these structures support the function of a host of membrane proteins (Brown and London, 1998a, Simons and Ikonen, 1997) this is thought to be mechanistically associated with its diverse pathological effects.

1.5. α-Tocopherol

Vitamin E was discovered almost 90 years ago by Evans and Bishop (Evans and Bishop, 1922) as a dietary factor essential for reproduction in rats. Since then, it has been identified as being composed of four tocopherol and four tocotrienol analogues (denoted α-, β-, γ-, and δ-) with the α-tocopherol form most preferentially absorbed from the diet in humans and almost exclusively recognised by α-TTP (the α-tocopherol transfer protein) which is responsible for maintaining plasma levels of the vitamin (Hosomi et al., 1997). α-Tocopherol has a widely recognised anti-oxidant action and, as a lipid-soluble molecule, is thought to exert its free radical scavenging action within cell membranes protecting primarily poly unsaturated fatty acids (PUFAs) which are highly susceptible to oxidative attack (Azzi, 2007, KamalEldin and Appelqvist, 1996, Atkinson et al., 2010). Several reviews discuss the uptake and transport of α-tocopherol and the mechanisms of its anti-oxidant action in detail (for example: (Herrera and Barbas, 2001, KamalEldin and Appelqvist, 1996, Hacquebard and Carpentier, 2005)). This section, however, will focus on the physical properties of α-tocopherol in membranes and introduce the notion that α-tocopherol may also have significant non-antioxidant biological actions.

1.5.1. Physical behaviour of α-tocopherol in membranes

A host of measurements of the concentration of α-tocopherol in biological membranes, collated by McMurchie and McIntosh (McMurchie and McIntosh, 1986), suggest α-tocopherol is present at concentrations ranging from 0.1-1mol% corresponding approximately to one molecule of α-tocopherol for every 100-1000 phospholipids. More recently determined concentrations in human platelets have reported a ratio of α-tocopherol to phospholipid as 220:1 which is in good agreement with the earlier estimations (Leray et al., 2002). α-Tocopherol is therefore present in cellular membranes at relatively low concentrations suggesting that, in order to effectively exert its biological activity in membranes, it may not be homogeneously distributed. This has led to many studies on the localisation of α-tocopherol in membranes and the resulting physical effects which are described below (Atkinson et al., 2008).

1.5.1.1. *Position of α-tocopherol in lipid bilayers*

The molecular structure of α-tocopherol consists of a long hydrocarbon chain which preferentially resides in the hydrophobic core anchoring the molecule within the lipid bilayer. A polar hydroxyl group in the 6-position of the chromanol fused ring structure ensures this part of the molecule positions within the hydrated interfacial region. Based on considerations of its antioxidant activity in membranes, for example that the molecule must be able to access both peroxidising lipids in the bilayer and aqueous reductants, Fukuzawa *et al.*(Fukuzawa et al., 1993) proposed three models for the position of α-tocopherol in the membrane (Figure 1.5.1).

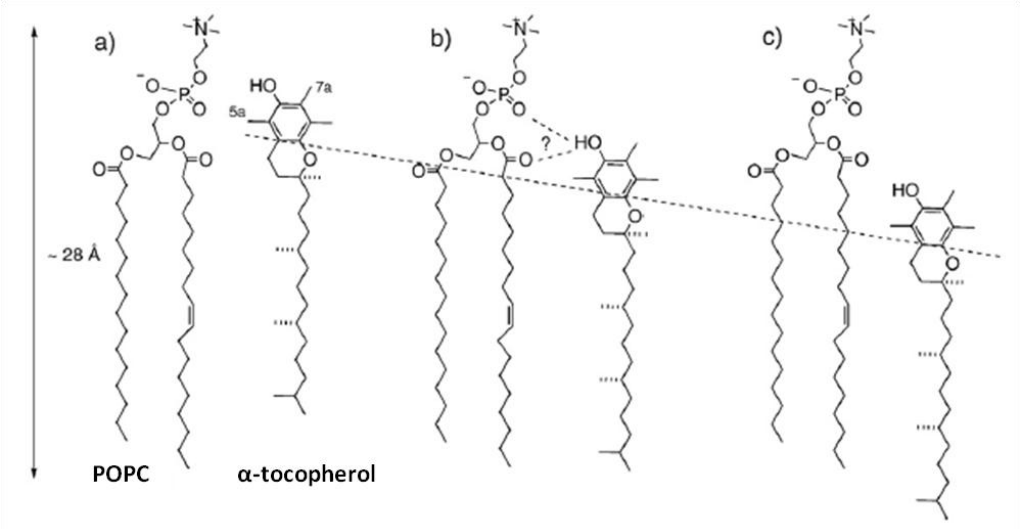

Figure 1.5.1: Representation of the three possible locations of α-tocopherol in the membrane proposed by Fukuzawa *et al.*(Fukuzawa et al., 1993). Palmitoyloleoylphosphatidylcholine (POPC) is used as a representative phospholipid. Adapted from (Atkinson et al., 2008).

In model A the phenol (chromanol) hydroxyl group of α-tocopherol is located near the membrane surface in the hydrated interfacial region (where it would be accessible by aqueous reductants). Model B shows the molecule positioned deeper into the membrane where hydrogen bonding may potentially occur between the phenol hydroxyl and the carboxyl and phosphate-oxygen polar moieties of phospholipids. In model C the chromanol group is positioned deeper within the hydrophobic core of the membrane in proximity to the sites of unsaturation of the fatty acid chains of lipids which generate peroxyradicals during lipid peroxidation (Fukuzawa et al., 1993). The depth of the chromanol group and its orientation within the bilayer has been studied with a variety of techniques. These include methods based on the interaction of cholesterol with membrane-resident probes that are located at varying depths in the bilayer, indicating a position between models B and C (Stillwell et al., 1992, Aranda et al., 1989, Kagan and Quinn, 1988), and nuclear magnetic resonance (NMR) experiments either with ^{13}C or ^{19}F which suggest locations closer to model A and B respectively (Perly et al., 1985, Urano et al., 1993). An alternative model was proposed by van Ginkel *et al*. (van Ginkel et al., 1992) where the chromanol resides in the interfacial region but is oriented such that the hydroxyl moiety is in close proximity to the 'bobbing' lipid peroxyl radical, thus satisfying the condition for an antioxidant action against lipid peroxidation (see Figure 1.5.2). Interestingly, neutron diffraction studies of deuterium labelled α-tocopherol has demonstrated that it resides higher in POPC membranes than DOPC membranes (Atkinson et al., 2008).

These studies collectively suggest that an average position of α-tocopherol in the membrane may be considered between that indicated by models B and C however, it is clear that α-tocopherol does not occupy a single environment with the chromanol group likely residing at

different depths, and possibly with different orientations, depending on the species of the surrounding lipids (Atkinson et al., 2008).

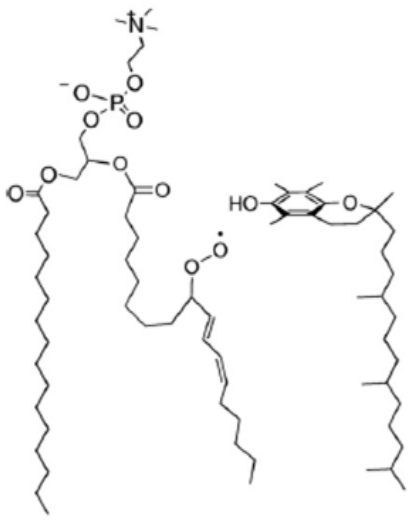

Figure 1.5.2: The alternative orientation of α-tocopherol in membranes proposed by (van Ginkel et al., 1992) where the chromonal, located in the interfacial region, is oriented such that the hydroxyl moiety can attain close proximity to the 'bobbing' peroxyl radical of a PUFA containing lipid. After (Atkinson et al., 2008).

1.5.1.2. *Hydrogen bonding of α-tocopherol with membrane lipids*

In the models of α-tocopherol localisation discussed above it is indicated that the hydroxyl moiety present on the chromanol ring of α-tocopherol may form hydrogen bonds with polar moieties present in the upper part of phospholipids forming the hydrated interfacial region. This has been widely investigated using several different methods which have provided conflicting results. For example, Fourier transform infrared spectroscopy (FTIR) of DPPC, DOPC and DMPC membranes have shown hydrogen bonding to occur with the carbonyl but not to the phosphate-oxygen moieties (Gomez-Fernandez et al., 1989, Lefevre and Picquart, 1996) of the phospholipds. Further evidence for the hydrogen bonding to the ester carbonyl has been provided by Urano *et al*. who observed the changes in membrane fluidity as chromate ions, capable of breaking the hydrogen bonds to form complexes with α-tocopherol, were passed through the membrane. In egg-PC membranes a greater change in fluidity was seen on addition of chromate ions compared to membranes composed of an ether analogue-PC with no carbonyl moiety. This difference was ascribed to the disruption of the hydrogen bonds of α-tocopherol to the carbonyl in egg-PC membranes by the chromate ions (Urano et al., 1992). Using ^{13}C NMR to monitor the polarity dependent chemical shifts of α-tocopherol in DPPC membranes Srivastava *et al.* suggest that the hydroxyl group of α-tocopherol is more likely to form hydrogen bonds with either the phosphate oxygens or water at the membrane surface (Srivastava et al., 1983). Fukuzawa *et al.*, however, found that the P=O and C=O stretching bands of DMPC were not changed by the incorporation of α-tocopherol using FTIR indicating that there is no hydrogen bonding occurring between these moieties and the hydroxyl group of

α-tocopherol (Fukuzawa et al., 1992). The evidence is, therefore, far from conclusive with parallel claims that the hydrogen bonding of α-tocopherol with either the carbonyl or phosphate-oxygen dipolar groups of phospholipids may or may not occur (Atkinson et al., 2008).

1.5.1.3. ***Dynamic behaviour of α-tocopherol in membranes***

α-Tocopherol can undergo a variety of motions within the lipid bilayer similar to those of membrane lipids (discussed in Section 1.1.4). Figure 1.5.3 summarises these motions.

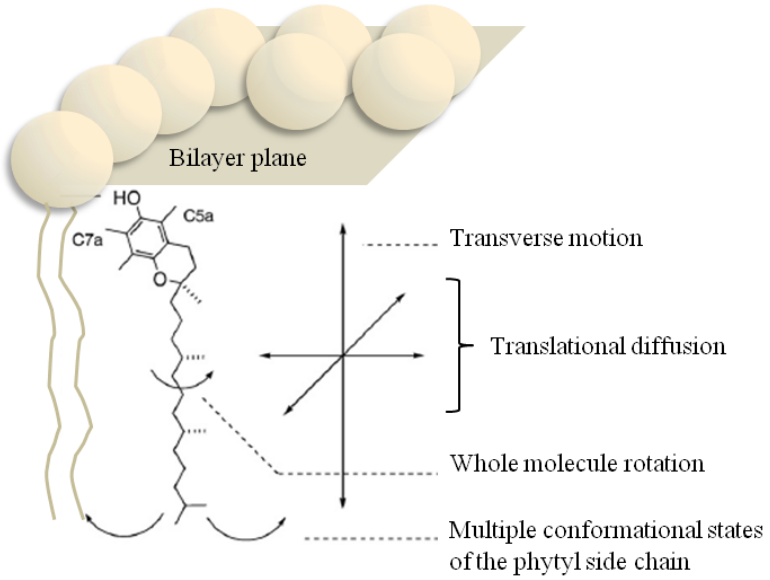

Figure 1.5.3: A representation of the motions of α-tocopherol in the phospholipid bilayer. Adapted from (Atkinson et al., 2008).

The hydrocarbon tail of α-tocopherol, as with those present in lipids, exhibits considerable conformational freedom (SanchezMigallon et al., 1996, Fukuzawa et al., 1992). NMR studies have indicated the presence of *gauche* conformers (Figure 1.5.4) and observed an increasing disorder of the hydrocarbon chain from the 5th carbon atom towards the end (Ekiel et al., 1988, Urano et al., 1993).

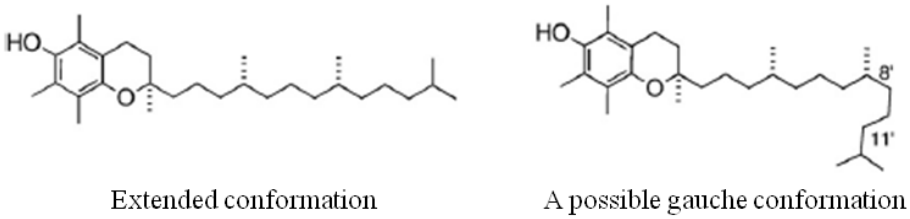

Figure 1.5.4: The extended conformation of α-tocopherol and one of several possible *gauche* conformations occurring between carbons 8' and 11'. After (Atkinson et al., 2008).

The chromanol group, conversely, displays limited conformational flexibility due to the rigidity of the fused ring structure. The evidence outlined above indicating the molecule may reside at several different depths in the bilayer does, however, suggest that the chromanol group is capable of movement, perpendicular to the membrane surface, positioning it closer to, or further away from the membrane surface (Atkinson et al., 2008). The molecule as a whole has been

observed to undergo axial rotation although, interestingly, the axis wobbles more than that of cholesterol which similarly possesses a fused-ring structure and hydrocarbon chain (Perly et al., 1985, Ekiel et al., 1988). α-Tocopherol also diffuses laterally within the membrane bilayer at a rate of $9x10^{-8}$ cm^2s^{-1} which is within the range of lipid diffusion (discussed in section 1.1.4). Transbilayer 'flip-flop' of α-tocopherol occurs very slowly over the time frame of hours which is also in contrast to that of cholesterol which is reported to occur with a half-life <1min (Tyurin et al., 1986, Backer and Dawidowicz, 1981, Lange et al., 1981).

1.5.1.4. *Effect of α-tocopherol on the order and phase behaviour of lipid bilayers*

α-Tocopherol has long been observed to have a 'stabilizing' effect in membranes reducing their fluidity (Diplock and Lucy, 1973, Diplock et al., 1977, Lucy, 1972). α-Tocopherol has been reported to decrease the fluidity of arachidonic acid (a PUFA of 20-carbon length and 4 unsaturations) containing membranes (Urano et al., 1988b). It has also been demonstrated to increase fatty acid chain order of saturated lipids above their transition temperature (Wassall et al., 1986) for example, increasing molecular packing and decreasing fluidity in l_c-phase DPPC membranes (Srivastava et al., 1983). That α-tocopherol increases order in l_c phase membranes has been widely reported using ^2H NMR (Wassall et al., 1986, Wassall et al., 1990, Stillwell et al., 1990, Suzuki et al., 1993), electron spin resonance (ESR) (Wassall et al., 1991) and fluorescence (Massey, 2001) techniques. In the gel phase however, FTIR, X-ray diffraction and fluorescence techniques have demonstrated the presence of α-tocopherol to disrupt fatty acid chain packing (Severcan, 1997, Quinn, 2004, Stillwell et al., 1992, Wang and Quinn, 2002, Wang and Quinn, 2000c). As a result, α-tocopherol disrupts the gel-phase and stabilises the l_c phase with respect to the gel-phase manifesting as a decrease in the gel-l_c transition temperature (see section 1.1.3). This has been detected using differential scanning calorimetry (DSC) in DMPC membranes (Massey et al., 1982) where a broadening of the transition and decrease in the enthalpy of transition was also noted (Massey et al., 1982, McMurchie and McIntosh, 1986). A similar broadening of the transition and decrease in enthalpy, such that the temperature at the onset of the transition is lower but the completion temperature is constant, has been demonstrated in DPPC membranes (McMurchie and McIntosh, 1986, Quinn, 2004). Comparatively, the influence of α-tocopherol on the gel-l_c phase transition with unsaturated lipids is relatively minor with respect to that in saturated lipid membranes (Fukuzawa et al., 1979). This is consistent with the observation that α-tocopherol increased the order of saturated DMPC bilayers to a greater extent than the poly-unsaturated di-arachidonoyl-PC bilayers which is attributed to the fact that the looser packing of the unsaturated phase more easily accommodates α-tocopherol with minimal perturbation (Wassall et al., 1991).

Following from these observations, α-tocopherol has been suggested to perform a similar structural role in the membrane to cholesterol (Wassall et al., 1986, Stillwell et al., 1996),

although it is present at much lower concentrations (Atkinson et al., 2008). However, α-tocopherol has been observed to partition in the membrane very differently from cholesterol which has a strong propensity for the saturated lipid phase where it similarly disorders the gel phase and orders the l_c phase, as discussed previously (Section 1.1.3) (Vist and Davis, 1990).

α-Tocopherol preferentially associates with PUFAs in mixed saturated/unsaturated lipid membranes (Stillwell et al., 1992, Wassall et al., 1991), even in the presence of an excess of saturated lipid (Stillwell et al., 1992). Sanchez-Migallon *et al.* (SanchezMigallon et al., 1996), using heteroacid-PC with an 18:0 fatty acid in the sn1 position and an 18:1, 18:2, 18:3 or 20:4 fatty acid in the sn2 position, have demonstrated that the influence of α-tocopherol on the gel-l_c thermotropic behaviour increases with degree of unsaturation. They also observed a lateral phase separation and the formation of domains containing different concentrations of α-tocopherol in the fluid phase (SanchezMigallon et al., 1996). α-Tocopherol has been demonstrated to have a larger effect on lipid order than cholesterol in PUFA-containing membranes where the first double bond occurs before the Δ9 position on the fatty acid chain (Stillwell et al., 1996). This is thought to result from the smaller fused-ring structure of α-tocopherol than cholesterol. In the absence of unsaturated fatty acids, α-tocopherol is observed to induce phase separation with a preference for the lipid component of lowest gel-l_c transition temperature (Ortiz et al., 1987).

The preferential association of α-tocopherol with PUFA containing lipids is thought to arise from the favourable conditions of phases rich in these lipids; for example the lower packing density as a result of the flexible fatty acid chains of PUFAs provides an ideal environment for the motion of the α-tocopherol flexible hydrocarbon chain (Atkinson et al., 2008, Atkinson et al., 2010). However, α-tocopherol has also been suggested to form complexes with PUFAs (Diplock and Lucy, 1973, Kagan, 1989, Erin et al., 1985, Erin et al., 1984) with Urano and co-workers proposing that the chromanol methyl groups fit into the Z-double bonds of poly unsaturated lipids (Urano et al., 1988a, Urano et al., 1987). This association of α-tocopherol with PUFA chains is also thought to underly the partitioning of α-tocopherol into different phases (Kagan et al., 1990).

α-Tocopherol has a higher negative radius of curvature (-13.7Å) (lower absolute value) than cholesterol or DOPE (see table 1.1.2) and will place a membrane under significant negative curvature stress where present in relatively high concentrations (Bradford et al., 2003). Interestingly, endogenous α-tocopherol in neurons has been observed to be most abundant in highly curved regions of the cell membrane occurring at the soma-neurite junctions (Monroe et al., 2005). This property of α-tocopherol is also likely to influence its localisation in membranes as it may avoid partitioning into regions containing a significant proportion of other lipids that

impart a high negative curvature stress (Atkinson et al., 2008). This phenomena has been observed on the addition of α-tocopherol to POPE (Wang and Quinn, 2006) or DPPE (Wang and Quinn, 1999) membranes where it formed an α-tocopherol rich hexagonal phase separated from the bulk lipid which is maintained in the lamellar state. The same effect is seen with cholesterol in PE membranes (van Dijck et al., 1976, McMullen and McElhaney, 1997). Interestingly, in mixtures of DOPE with DOPC or DMPC the hexagonal phase is not observed suggesting that α-tocopherol prefers to associate with the PC element which has a very high radius of curvature supporting lamellar phases (Quinn, 2004). This is also observed in saturated PC/PE mixed membranes (Wang and Quinn, 2000a, Wang and Quinn, 2000b).

1.5.1.5. ***The localisation of α-tocopherol in biological membranes***

Atkinson *et al*. (Atkinson et al., 2010) propose a model for the localisation of α-tocopherol in biological membranes in which it preferentially localises and orders PUFA rich regions forming stabilized non-raft domains in a parallel manner to the role of cholesterol in forming saturated lipid rich rafts (Figure 1.5.5). The resulting concentration amplification of α-tocopherol in domains rich in PUFAs, which are most susceptible to oxidation, is thought to optimize the protective action of the free-radical scavenger from the deleterious effects of oxidation.

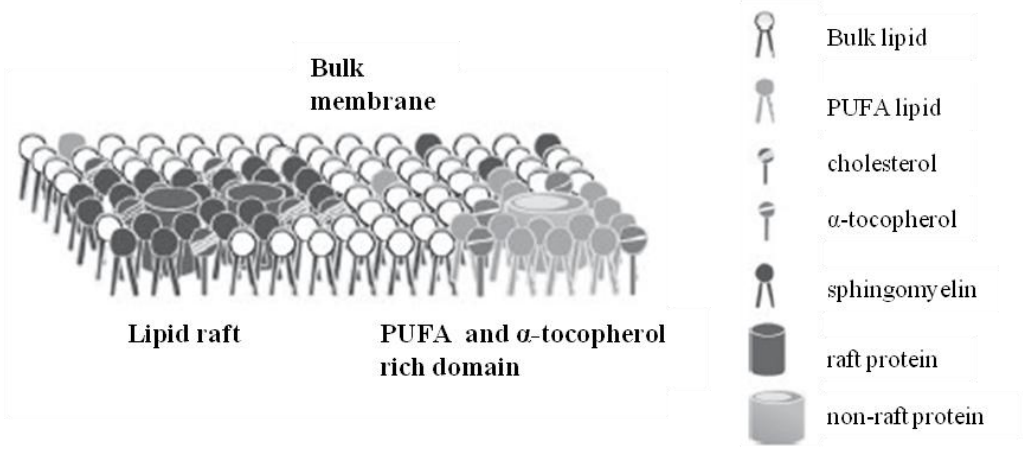

Figure 1.5.5: An illustration of the model proposed by Atkinson *et al*. (Atkinson et al., 2010) for the localisation of α-tocopherol in poly unsaturated fatty acid (PUFA) rich domains akin to the localisation of cholesterol with saturated lipids and sphingomyelin forming rafts. After (Atkinson et al., 2010).

Interestingly, α-tocopherol has been identified in detergent resistant membrane fractions corresponding to membrane rafts in an aortic smooth muscle cell line (A7R5) following α-tocopherol treatment (Royer et al., 2009). It has also been observed that many enzymes known to be regulated by α-tocopherol are raft-associated and modulate raft-embedded signalling pathways which had led to speculation that α-tocopherol may modulate signalling processes via a raft-related mechanism (Brigelius-Flohe, 2009, Lemaire-Ewing et al., 2010).

It therefore seems possible that α-tocopherol influences both raft and non-raft regions of cellular membranes and, in a similar manner to the influence of cholesterol in rafts, may affect proteins within these domains modulating the functional processes of the membrane.

1.5.2. Does α-tocopherol have non-antioxidant actions?

α-Tocopherol has been observed to elicit a host of cellular functions including the activation or inhibition of many enzymes (reviewed in (Zingg, 2007)) and the regulation of several genes (reviewed in (Zingg and Azzi, 2004)). In an attempt to reconcile the variety of cellular effects of α-tocopherol with its anti-oxidant action Traber and Atkinson (Traber and Atkinson, 2007) propose that these effects stem from the protection of PUFAs in cell membranes from free radical attack. This prevents the structural alteration of these lipids as a result of oxidation thereby preserving the physical properties they endow upon the membrane, such as fluidity and phase behaviour, and consequently the microdomain landscape of the membrane. Such physical parameters have been associated with membrane protein function, including signalling proteins, and this mechanism therefore represents an indirect antioxidant action of α-tocopherol (Traber and Atkinson, 2007).

A conflicting review by Azzi *et al.* (Azzi, 2007), however, presents evidence to strongly suggest that α-tocopherol has significant non-antioxidant effects and includes several reports of observed cellular effects of the vitamin which cannot be attributed, directly or indirectly, to its proposed free radical scavenging ability (reviewed in (Azzi, 2007)).

All tocopherol vitamers exhibit free-radical scavenging capability but, remarkably, only α-tocopherol is retained by the body in significant quantity (Traber and Kayden, 1989). This is as a result of the high specificity of α-TTP, the hepatic α-tocopherol transfer protein responsible for the distribution of the vitamin to extra-hepatic tissues, for α-tocopherol with negligible affinity for the other forms (Hosomi et al., 1997). This is suggestive of a specific requirement for α-tocopherol that is not associated with its anti-oxidant nature. Additionally, α-tocopherol uniquely influences several cellular processes in a manner not shared by other anti-oxidants (see (Azzi, 2007) and references therein). These diverse effects include: inhibition of smooth muscle proliferation, preservation of endothelial cell integrity, inhibition of monocyte-endothelial adhesion, inhibition of platelet adhesion and aggregation and the inhibition of monocyte cytokine and ROS release. α-Tocopherol has also been observed to modulate the expression of several genes (see (Azzi et al., 2004) and references therein) but interestingly, the deficiency of α-tocopherol does not promote the upregulation of genes that express anti-oxidants adding to the growing speculation that cells do not rely on its anti-oxidant activity. In light of the specificity of the biological actions inhibited by α-tocopherol, it seems unlikely that these numerous effects can be mediated by the uncontrolled free radical chain reaction and therefore prevented by the anti-oxidant (Azzi, 2007).

There is also much *in vivo* evidence that the principle action of α-tocopherol is not as a free radical scavenger. For example, analysis of several biomarkers of oxidative damage has

demonstrated no anti-oxidant benefit of α-tocopherol in oxidative stress (Dragsted, 2008, Prieme et al., 1997, Mastaloudis et al., 2006). α-Tocopherol supplementation has also been observed to increase plasma and LDL concentrations of the anti-oxidant but offer no protection against copper- catalysed LDL oxidation at physiological concentrations (Prieme et al., 1997). Additionally, a relatively large concentration of α-tocopherol has been identified to be present in atherosclerotic plaques yet a significant proportion of oxysterols was also found. This suggests α-tocopherol is eliciting negligible anti-oxidant action and providing little protection from the oxidative stress mediated development of atherosclerotic lesions (Suarna et al., 1995).

α-Tocopherol has received much attention as a potential preventative or therapeutic agent in oxidative stress associated pathologies, including cardiovascular disease and diabetic complications (e.g. (Maritim et al., 2003, Harrison et al., 2003). However, extensive clinical trials have demonstrated α-tocopherol to be of negligible benefit, or to even increase mortality, indicating not only a lack of *in vivo* anti-oxidant effect but suggesting non-antioxidation based mechanisms of action may be occurring (e.g. (Golbidi et al., 2011, Pazdro and Burgess, 2010, Saremi and Arora, 2010, Clarke et al., 2008).

Although the non-antioxidant effects of α-tocopherol have been investigated for over 20 years, the mechanism of this action is still unclear. Azzi *et al.* (Azzi, 2007) propose that α-tocopherol acts as a ligand to receptors and transcription factors which are associated with the regulation of the signalling events and gene expression observed to be modulated by the vitamin. A receptor that specifically binds α-tocopherol, however, has not as yet been identified and the search for a common transcription factor for all genes regulated by the vitamin has also not yet proven successful (Brigelius-Flohe, 2009). Many of the enzymes and other signalling molecules influenced by α-tocopherol are membrane associated and, as discussed above, α-tocopherol has been demonstrated to significantly affect the biophysical parameters of membranes. This has led to the suggestion that the influence of α-tocopherol on lipid organisation and order, in particular the formation of complexes or domains with PUFAs, may mediate some of its non-antioxidant effects (Brigelius-Flohe, 2009). Microdomains are considered to provide platforms for various signalling events (Brown and London, 1998a) and it has been suggested that the formation of these structures by α-tocopherol may serve to promote its interaction with proteins that reside within them (Brigelius-Flohe, 2009).

It is evident that, whether mediated as a result of the molecular structure of α-tocopherol itself, or by its protection of the structure of PUFAs, α-tocopherol is considered to significantly influence the physical properties of the cell membrane. The modulation of membrane biophysical parameters by α-tocopherol may prove to be the underlying mechanism mediating many of its observed biological effects.

1.6. The Present Study

α-Tocopherol has a well known free radical scavenging action and, as a lipid soluble vitamin, is thought to exert this anti-oxidant effect in cell membranes. Oxidative stress in cells is considered an underlying factor in the development of many pathological states including neurodegenerative and cardiovascular diseases and diabetes. α-Tocopherol has therefore been widely approached as a preventative or therapeutic agent in oxidative stress associated disease but, despite encouraging evidence in vitro, has demonstrated little benefit and even negative effects in vivo. The resulting failure of several clinical trials and the growing body of evidence demonstrating cellular effects of α-tocopherol which cannot be attributed to its anti-oxidant action has led to the suggestion that this molecule may also have significant non-antioxidant roles.

Due to its lipophilic nature and the structural similarities with cholesterol, α-tocopherol has long been considered likely to influence the physical properties of membranes. Over the last three decades this has been explored extending the analogy with cholesterol with similarities in their effects on the phase behaviour and negative curvature stress of membranes. The effects of α-tocopherol on lipid packing and order suggest it is likely to influence the membrane dipole potential; a physical parameter of membranes which has been demonstrated to modulate the function of several membrane-associated proteins. Alteration of the dipole potential may prove to be a significant non-antioxidant mechanism of α-tocopherol underlying several of its cellular effects.

This present study investigates the influence of α-tocopherol on the membrane dipole potential and places this in the context of the effect of cholesterol oxidation on this physical parameter. This is firstly explored in egg-phosphatidylcholine vesicles which provide a simple membrane model (Chapter 3) before investigating this effect in the more complex cellular membrane of Jurkat T-lymphocytes (Chapter 4).

7-Ketocholesterol, an oxidised form of cholesterol, has significant impact on several cellular processes and is considered to mediate these effects, in part, through its physical effects on the cell membrane. For example, 7-ketocholesterol has been demonstrated to alter the lipidic and protein content, and consequently the biophysical parameters, of membrane rafts; structures which are considered to support the function of a host of membrane proteins. It has recently been suggested that α-tocopherol inhibits the effect of 7-ketocholesterol on rafts, thereby limiting the influence of the oxysterol on raft-associated proteins. This study considers the effect of 7-ketocholesterol on the unique dipole potential of membrane microdomains and the influence that α-tocopherol may have on this effect. This is correlated with the effects of 7-ketocholesterol on the function of two microdomain-associated receptors, the multi-drug efflux

pump P-glycoprotein and the insulin receptor, and the impact of α-tocopherol treatment prior to, or following, exposure to the oxysterol (Chapter 5).

2. Materials and Methods

2.1. Materials

D-α-tocopherol, D-α-tocopherol succinate, cholesterol, 7-ketocholesterol and Insulin (human, 10mg ml^{-1} solution in 25mM Hepes pH8.2) were obtained from Sigma-Aldrich (Gillingham, Dorset, UK). Biotinylated insulin (bovine, biotin content 1:1 mol/mol insulin), saponin, methyl-β-cyclodextrin, triton-X 100 and calcium chloride were also obtained from this same supplier. The P-glycoprotein ligand, Saquinavir, was from Roche (Hertfordshire, UK). Vesicles were made with Grade 1 Egg Phosphatidylcholine from Lipid Products (Nutfield, Kent, UK). Cell cultures were sourced from The European Collection of Cell Cultures (ECACC, Salisbury, UK) and The American Type Culture Collection (ATCC, through LGC Standards, Teddington, Middlesex UK). Cell culture reagents including RPMI 1640, C-SC medium for endothelial cell lines, foetal bovine serum (FBS), penicillin-streptomycin mixture, L-glutamine, heparin (porcine, sodium salt grade I-A), endothelial cell growth supplement (from bovine neural tissue), trypsin-EDTA, poly-l-lysine solution, Dulbecco's phosphate buffered saline (DPBS) and trypan blue (0.4% solution) were from Sigma-Aldrich (Gillingham, Dorset, UK). Ham's F12-K was from ATCC (through LGC Standards, Teddington, Middlesex, UK). Gelatin solution (1%, attachment factor 1x) was from Invitrogen (Paisley, UK). The buffered, osmotically balanced solutions used in this study contained trizma base, Hepes sodium salt, sucrose, glucose, magnesium sulphate, sodium acetate, calcium chloride hexahydrate, hydrochloric acid and human serum albumin from Sigma-Aldrich (Gilligham, UK), sodium chloride and sodium hydroxide from Fisher Scientific (Loughborough, UK), and potassium chloride from BDH (VWR international, Poole, UK). Fluorescent probes included Di-8-ANEPPS ((1-(3-sulfonatopropyl)-4-[β[2-(di-n-octylamino)-6-naphthyl]vinyl] pyridinium betaine), FPE (N-(fluorescein-5-thiocarbamoyl)-1,2-dihexadecanoyl-sn-glycerol-3-phosphoethanolamine) and streptavidin-Alexa Fluor 488 conjugate from Invitrogen (Paisley, UK), Insulin FITC conjugate (bovine insulin, fluorescein isothiocyanate labelled) from Sigma-Aldrich (Gillingham, Dorset, UK) and Propidium Iodide (1mg ml^{-1} solution) from Fluka (through Sigma-Aldrich, Gilligham, UK). AlamarBlue was from Invitrogen (Paisley, UK). Solvents used included DMSO (>99.9%), Ethanol (>99.9%) and Methanol (>99.9%) from Sigma-Aldrich (Gillingham, Dorset, UK) and Chloroform (>99.9%) from Fisher Scientific (Loughborough, UK). Nitrogen and carbon dioxide gases were from BOC Gases (Manchester, UK). All chemicals were used at the highest purity available and, where appropriate, cell-culture tested and sterile.

2.2. Equipment

A pressure extruding bomb used to produce phospholipid vesicles was from Lipex Biomembranes Inc. (Vancouver, Canada) and was used in conjunction with 25mm diameter polycarbonate filters of 100nm pore size from Nucleopore Filtration Products (CA, USA). Phospholipid solutions were maintained at 37^{o}C in a desktop incubator from Grant Instruments (Cambridgeshire, UK) during fluorescent labelling and prior to experiments. Sephadex PD-10 columns from Amersham Biosciences (UK) were used to remove excess FPE from solutions of labelled phospholipid vesicles.

Cell cultures were maintained at 37^{o}C with 5%CO_2 and 90% humidity in a Nuaire Autoflow IR water Jacketed CO_2 incubator from Triple Red Laboratory Technology (Buckinghamshire, UK) and manipulated within a Hera Safe KS12 Class II tissue culture hood (Thermo Electron Corporation now Thermo Fisher Scientific, Massachusets USA). Media were warmed in a water bath at 37^{o}C from Fisher Scientific (Loughborough, UK) and cells in suspension were retrieved by centrifugation using an AccuSpin 1R or AccuSpin Micro17R also from Fisher Scientific (Loughborough, UK). Cell cultures were checked routinely under a light microsope. Cell culture densities were determined and trypan blue exclusion viability assays performed using a Haematocytometer from BDH (Teddington, Middlesex, UK). A double walled vacuum vessel by Statebourne Cryogenics (Tyne and Wear, UK) was used for the long term storage of cells under the gaseous phase of liquid nitrogen.

Excitation and emission spectra, time course fluorescence measurements and measurements of 90^{o} light scattering were obtained using a FluoroMax-4 spectrofluorimeter from HORIBA Jobin-Yvon (Japan) running the Datamax Intrument Control Centre software (version 2.2.10, Jobin-Yvon Inc. Japan) and FluorEssence software (version 3.1.0.22 Horiba Jobin-Yvon, Japan) with Origin (Version 8.0.988 Origin Lab Corporation MA, USA). UV grade disposable 3.5ml cuvettes from Sigma-Aldrich (Gillingham, UK) were used for fluorescence spectroscopy. AlamarBlue viability assays were read using the plate reader attachment of a LS-55 Fluorescence Spectrophotometer from Perkin-Elmer (MA, USA).

Flow cytofluorometry was conducted using a BD FacsCanto flow cytometer (BD Biosciences, Oxford, UK) with BD FacsDiva software Version 5.0.3 and Filmware version 1.14. Samples were prepared in 5ml polystyrene round-bottom tubes from BD Falcon (MA, USA) for flow cytometry. Data was analysed using Weasel Version 2.7.4 (Walter and Eliza Hall Institute for Medical research, Victoria, Austalia).

Images of fluorescently labelled adherent cells, cultured in Fluorodish 35mm coverglass-bottomed culture dishes (WPI, FL, USA), were obtained with a Nikon TiE microscope with NIS imaging software (Nikon Instruments Europe B.V., Amstelveen, The Netherlands).

Predicted values of the pKa, LogP, LogD and aqueous solubility of α-tocopherol and α-tocopherol succinate were obtained using the ACD/I-Lab Web services ACD/pKa 12.0, ACD/LogP 12.0, ACD/LogD 12.0 and ACD/Aqueous solubility 12.0 respectively. The predicted charge of insulin at pH7.4 and pH8.2 was determined using Protein Calculator version 3.3 (C.D. Putnam at the Scripps Research Institute, CA, USA) on inputting the protein sequence obtained from UniProtKB/Swiss-Prot protein knowledgebase version 155. Graphing and statistical tests were performed using Prism version 5.02 from GraphPad Inc. (CA, USA).

2.3. Preparation of phosphatidylcholine vesicles

Large unilamellar phosphosphatidylcholine vesicles were formed using the method of rapid extrusion of frozen and thawed vesicles pioneered by Mayer *et al*. (Mayer et al., 1986). Volumes of phosphatidylcholine, cholesterol, 7-ketocholesterol and α-tocopherol, prepared in chloroform/methanol (5:1 ratio) at 100mg/ml, were combined at the desired proportions in a round bottomed flask. After briefly mixing by vortex the solvent was evaporated by gentle rotation under a stream of nitrogen gas and the resulting thin lipid film was resolvated in a tris buffered sucrose solution (280mM sucrose 10mM tris in distilled H_20 300mOsmol, pH 7.4 with HCl) filtered with a 0.2μm diameter pore filter. The solution of multilamellar vesicles was then subject to five freeze-thaw cycles using liquid nitrogen and running water >45^oC to promote the formation of unilamellar vesicles. Finally, these vesicles were extruded ten times through the 100nm pores of a polycarbonate filter at 45^oC with nitrogen gas in a pressure extruding bomb. This gives rise to a 13mM solution of monodispersed, ~100nm diameter unilamellar vesicles. The vesicle solution is stable for up to one month stored at 4^oC under nitrogen gas (Gubernator et al., 1999) and was used for experiments within this time frame.

The phosphatidylcholine used to form vesicles for this study, derived from egg yolk, contains acyl chains of varying degrees of saturation and chain length and was chosen so that the resulting artificial membranes more closely reflect the lipid environment of cell membranes. Cholesterol, 7-ketocholesterol and α-tocopherol were also incorporated into the vesicles but a minimum 70mol% concentration of phosphatidylcholine was maintained to support lipid phases similar to those present in cell membranes.

2.3.1. Labelling phospholipid vesicles with Di-8-ANEPPS

Di-8-ANEPPS was prepared as a 2mM stock solution in ethanol and stored, protected from light, at 4^oC. The required volume of the 13mM vesicle solution was incubated with 30μM Di-8-ANEPPS at 37^oC, protected from light, for 2hrs. The labelled vesicle solution was then diluted to a concentration of 400μM in tris-buffered sucrose solution (280mM sucrose 10mM tris pH7.4, 0.2μm-pore filtered), warmed to 37^oC, for spectroscopy. Labelled vesicle solutions were used within 8 hours.

2.3.2. Labelling phospholipid vesicles with FPE

Vesicles were labelled with fluorescein-phosphatidylethanolamine (FPE) using the method outlined by Cladera *et al*. (Cladera et al., 2001) which achieves exclusive labelling of the outer leaflet of the vesicle membrane bilayer. FPE was prepared as a 2mM stock solution in chloroform/methanol at a 5:1 ratio and stored, protected from light, at -20^oC. Gentle rotation under a stream of nitrogen gas was used to evaporate the solvent from a volume of FPE

equating to 30μM once later added to the vesicle suspension. The resulting FPE lipid film was resuspended in an equal volume of ethanol and added to the desired volume of 13mM vesicle suspension which was then incubated at 37^{o}C for 90mins protected from light. After this time the FPE labelled vesicle suspension was passed through a Sephadex PD-10 column, pre-equilibrated with tris buffered sucrose solution (280mM sucrose 10mM tris pH 7.4, 0.2μm-pore filtered), in order to separate the vesicles from free FPE in solution. The concentration of the FPE labelled vesicle suspension collected from the PD-10 column was presumed to be 6.5mM; half that of the solution entered into the column to take into account lipid retention and dilution in the column. Labelled vesicles were stored, protected from light, under nitrogen gas at 4^{o}C and were used within one week.

2.4. Cell culture and preparation

2.4.1. Jurkat T-Lymphocytes and IM9 B-Lymphocytes

Jurkat T-lymphocytes (E6-1 clone, ECACC) and IM9 B-lymphocytes (ECACC), both from a human source, were cultured in suspension in RPMI 1640 supplemented with 2mM L-glutamine, 100 U ml^{-1} penicillin-streptomycin and 10% v/v heat inactivated foetal bovine serum. Cells were cultured at 37°C in a humidified incubator with 5% CO_2 (95% air) and the populations were maintained between 10^5 and 10^6 cells ml^{-1} by passage every third day. The viable cell population was estimated prior to each experiment using a haematocytometer and the trypan blue exclusion assay.

2.4.2. Human umbilical vein endothelial cells (HUVEC)

The human umbilical vein cell line, HUV-EC-C (CRL-1730, ATCC), were cultured in ATCC formulation F-12K basal medium supplemented with 0.1mg ml^{-1} heparin, 0.03mg ml^{-1} endothelial cell growth supplement and 100 U ml^{-1} pencillin-streptomycin with 10% v/v heat inactivated foetal bovine serum. Cells were propagated in 75cm^2 tissue culture flasks that were gelatin coated immediately prior to seeding the culture and maintained at 37°C in a humidified incubator with 5% CO_2 (95% air). Gelatin coating was achieved by adding 3mls of a 0.1% gelatin solution to each flask, ensuring the solution completely covered the surface, and incubating the flask at 37°C for 30 minutes. Cells were subcultured at a ratio of 1:3 when approximately 80% confluent by washing twice in DPBS pre-warmed to 37°C to remove traces of serum and then adding 3ml of trypsin-EDTA solution (0.25% v/v trypsin and 0.53mM EDTA). Cells were incubated with the trypsin-EDTA solution until the majority of cells were observed to have detached from the culture surface using an inverted light microscope (typically 5-10 minutes). 10ml of complete growth medium was then swiftly added to neutralise the activity of trypsin and the aspirated cell suspension was then centrifuged (300g, 5min) to pellet the cells. The cells were then resuspended in 10ml of fresh complete growth medium by gentle aspiration and added to a gelatin-coated culture flask immediately following removal of the 0.1% gelatin coating solution. The flask was gently rocked to ensure the cell suspension entirely coated the culture area and the cells were evenly distributed over the surface.

2.4.3. Cryopreservation of cells and establishing culture

Cell cultures were established from frozen stocks by rapid thawing of the frozen cell suspension followed by immediate (10x) dilution of the freezing medium with the appropriate complete growth media. The cell suspension was then centrifuged (300g, 5min) and the pellet resuspended in fresh growth media warmed to 37°C and transferred to a culture flask. Cultures were left to establish for a minimum of one week prior to experiments. Cultures were propagated to yield an excess of cells which were reserved as frozen stocks. Excess cells were

centrifuged (300g, 5min) and resuspended in cell freezing medium (10% DMSO in 90%FBS) at a concentration of 10^6-10^7 cells ml^{-1} for HUVEC or lymphocytes respectively. The cell suspensions are gradually cooled to -80°C at a rate of 1°C min^{-1} in an isopropyl alcohol filled container and then stored long term in the vapour phase of liquid nitrogen.

2.4.4. Labelling suspension cells with Di-8-ANEPPS

Suspension cultured cells were labelled with Di-8-ANEPPS according to the method outlined in Asawakarn *et al.* (Asawakarn et al., 2001). After establishing the viable cell population the required volume was removed from the confluent culture and cells were washed twice by centrifugation in Dulbecco's phosphate buffered saline (DPBS) warmed to 37°C. Cells were resuspended at $0.5x10^6$ cells ml^{-1} in a pre-warmed labelling solution of 2μM Di-8-ANEPPS (from a 2mM stock in ethanol) in tris buffered sucrose solution (280mM sucrose 10mM tris pH7.4, 0.2μm pore filtered) and incubated at 37°C in a humidified incubator with 5% CO_2 for 90 minutes protected from light. To prevent settling, labelling cell suspensions were gently agitated every 20 minutes during incubation. Experiments were conducted within 3hrs of labelling.

2.4.5. Labelling suspension cells with FPE

Suspension cultured cells were labelled with fluorescein-phosphatidylethanolamine (FPE) according to the method of Cladera and O'Shea (Cladera et al., 2001). The solvent was evaporated from a volume of a FPE (2mM stock in a 5:1 ratio of chloroform/methanol) required to give a 10μM labelling solution by gentle rotation under a steam of nitrogen gas. The resulting FPE film was resolvated in an equal volume of ethanol and added to tris buffered sucrose solution (280mM sucrose 10mM tris pH7.4, 0.2μm pore filtered) at 37°C. The concentration of ethanol in the labelling solution does not exceed 0.5%. The volume of culture containing the required number of viable cells was taken from a confluent culture and washed twice in Dulbecco's phosphate buffered saline (DPBS) warmed to 37°C. Cells were resuspended at $0.5x10^6$ cells ml^{-1} in the labelling solution and placed in a humidified incubator with 5% CO_2 at 37°C for 1hr protected from light. Labelling cell suspensions were gently agitated every 20 minutes to prevent cells settling. After this time cells were washed twice in DPBS at 37°C by centrifugation (300g, 5min) to remove unbound FPE, resuspended at $0.5x10^6$ cells ml^{-1} in tris buffered sucrose solution and maintained at 37°C. FPE labelled cells were used in experiments within 3 hrs of labelling.

2.4.6. Labelling suspension cells with fitc-Insulin

Two different protocols were used to label suspension cultures with fitc-insulin. The volume of culture containing the required number of viable cells was taken from the confluent culture and washed twice with Dulbecco's phosphate buffered saline (DPBS) by centrifugation. Cells were either resuspended in DPBS with 10% FBS and labelled with 1μM fitc-insulin for 30 minutes at either 37°C or 4°C, as required, after Murphy *et al.* (Murphy 1982) or resuspended in an assay buffer (100mM Hepes, 120mM $NaCl_2$, 5mM KCl, 1.2mM $MgSO_4$, 10mM NaN_3, 10mM D-glucose, 1%BSA, pH7.8, 0.2μm pore sterile filtered) and labelled with 0.01μM fitc-insulin for 90 minutes at 15°C after Zeigler *et al.* (Ziegler et al., 1994). Cells were then washed twice in DPBS by centrifugation, resuspended in the respective assay buffer for each protocol and transferred to 5ml round bottom polycarbonate tubes for flow cytometry. All samples were assessed by flow cytometry immediately following labelling.

2.4.7. Labelling suspension cells with biotin-insulin and streptavidin- Alexa fluor 488

The volume of suspension culture containing the required number of viable cells was taken from the confluent culture and washed twice with Dulbecco's phosphate buffered saline (DPBS) by centrifugation. Cells were resuspended in assay buffer at $1x10^6$ cells in 100μl per sample (100mM Hepes, 120mM $NaCl_2$, 5mM KCl, 1.2mM $MgSO_4$, 10mM NaN_3, 10mM D-glucose, 1%BSA, pH7.8, 0.2μm pore sterile filtered) and labelled with 0.1μM biotinylated insulin at 15°C for 90 minutes. Following this, cells were washed twice in DPBS by centrifugation and resuspended in 100μl streptavidin-Alexa Fluor 488 labelling solution consisting of a 1:500 dilution of 1mg ml^{-1} streptavidin-Alexa Fluor 488 in assay buffer. Cells were incubated at 4°C for 30 minutes in this labelling solution. Labelled cells were then washed twice in DPBS by centrifugation and resuspended in 1ml of assay buffer ($1x10^6$ cells ml^{-1}) in 5ml round bottom polycarbonate tubes in preparation for flow cytometry.

2.4.8. Depletion of membrane cholesterol in Jurkat T-lymphocytes

Methyl-β-cyclodextrin was used to remove cholesterol from Jurkat T-lymphocyte cell membranes, in order to disrupt lipid rafts, using a method adapted from Rouquette-Jazdanian *et al*. (Rouquette-Jazdanian et al., 2006). This method reports complete removal of cholesterol from rafts with little depletion of non-raft cholesterol and negligible effect on cell viability. Following fluorescent labelling cells were washed twice in DPBS at 37°C by centrifugation (300g, 5min) before exposure to 10mM methyl-β-cyclodextrin in tris buffered sucrose solution (280mM sucrose 10mM tris pH7.4, 0.2μm pore filtered) for 1min. Cells were then immediately centrifuged (500g, 2mins) and resuspended in fresh tris buffered sucrose solution at 37°C. Methyl-β-cyclodextrin treated cells were used for experiments within 90minutes.

2.4.9. Determination of cell viability using AlamarBlue

An AlamarBlue resazurin reduction assay was used to determine the number of viable and proliferating cells in the presence of cholesterol, 7-ketocholesterol and α-tocopherol succinate at concentrations relevant to this study. This assay is based on the fluorimetric detection of the reduction of the non-fluorescent resazurin salt into the fluorescent (λ_{em}=590nm) resorufin salt, as illustrated in Figure 2.4.1, by metabolic processes within viable cells (Mosmann, 1983, Magnani and Bettini, 2000, Zhang et al., 2004).The assays were performed in a 96 well plate and in accordance with the manufacturer's instructions. After the appropriate incubation of cells with cholesterol, 7-ketocholesterol and α-tocopherol succinate AlamarBlue was added to each well to a final concentration for 10%v/v. The cells were then incubated for 4hrs at 37°C in a humidified incubator with 5% CO_2 protected from light. A negative control containing culture medium with AlamarBlue and without cells was included along with experimental controls consisting of untreated cells and cells treated with equivalent volumes of solvent. Fluorescence measurements were made at 590nm emission after excitation at 550nm using a LS-55 plate reader. The results of the assays can be found in Appendix A.

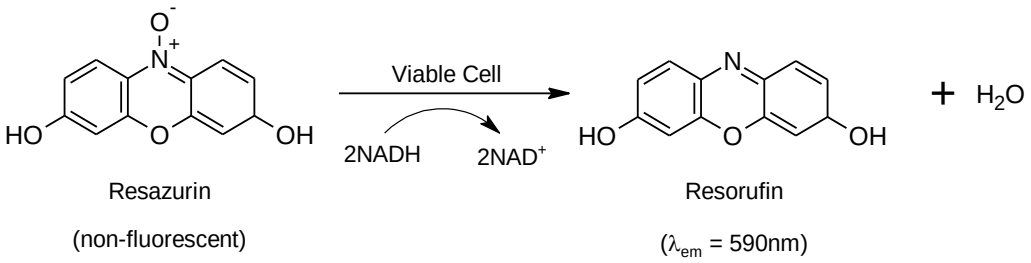

Figure 2.4.1: The mechanism of the reduction of non-fluorescent Alamar Blue (Resazurin) producing Resorufin which is fluorescent (λ_{em}=590) catalysed by mitochondrial, microsomal and cytosolic oxidoreductases in metabolically active (viable) cells.

2.4.10. Culturing adherent cells on glass-bottomed dishes for imaging

HUVEC were cultured in Fluorodish coverglass-bottomed culture dishes in preparation for imaging. The coverslip of the dish was coated with gelatin following treatment to adjust the charge of the glass to yield a more stable gelatin layer. This was achieved through a 3-step process involving treatment of the coverslip with three solutions (1M HNO_3, 1M NaOH, 10mM $MgCl_2$) added in 500-1000µl volumes to form a meniscus entirely covering the coverslip but not encroaching on the surrounding plastic of the dish. The coverslip was incubated at room temperature for 5 minutes under each solution with two washes in distilled H_2O (0.2µm sterile filtered) between each treatment. The wash following the final treatment was followed by two washes with 70% ethanol in distilled H_2O (0.2µm sterile filtered) and the dishes were left to air dry. 500µl of a 0.1% gelatin solution was then added, again forming a meniscus completely covering the coverslip, and the dishes were incubated with this solution for 30 minutes at 37°C.

The cells to be seeded onto the dishes were detached from the culture surface of their flask by trypsin-EDTA treatment as described in section 2.4.2. The number of cells per unit volume of the resulting cell suspension was determined using a haematocytometer with the trypan blue exclusion assay employed to identify non-viable cells which were not counted. Cells were then seeded onto the coverslip of the Fluorodish, immediately following removal of the gelatin solution, at approximately 10^4 cells cm^2. Cells were added in a volume of 500µl of growth medium, ensuring the suspension remained on the coverslip only, and the dishes were placed in a 37°C humidified incubator with 5% CO_2. After a minimum of 2hrs the attachment of the cells to the coated coverslip of the dish was checked under a light microscope and an additional 1ml of growth medium added. The cells were imaged within 24-48hrs of seeding.

2.4.11. Labelling adherent cells with Di-8-ANEPPS

Confluent HUVEC on Fluorodishes were gently washed twice in DPBS pre-warmed to 37°C. A labelling solution of Di-8-ANEPPS (2µM) was prepared in basal Ham's F-12K at 37°C and 1ml was added to each Fluorodish which was then incubated in a 37°C humidified incubator with 5%CO_2 for 90 minutes. After this time the cells were washed twice in DPBS at 37°C and 1ml of C-SC medium supplemented with 5% BSA, a phenol-red free medium suitable for fluorescence imaging, was added.

2.5. Spectroscopy

2.5.1. Determination of the Critical Micelle Concentration of α-tocopherol succinate

The critical micelle concentration of α-tocopherol succinate was determined using the technique of Davis *et al.* (Davis et al., 2011 *submitted*) which is based on the methods utilising 90° Rayleigh-Debye light scattering to determine the presence of aggregates of a compound in solution described by Hobden *et al.* (Hobden et al., 1995). Serial addition of α-tocopherol succinate (stocks prepared in ethanol) were made to a cuvette containing 2ml of tris buffered sucrose solution (280mM sucrose 10mM tris pH7.4, 0.2μm pore filtered) resting in the cuvette holder of a Fluoromax-4 Spectrofluorimeter. The cuvette was maintained at 37°C by temperature control of the cuvette holder connected to a circulating water bath and protected from light. The scattering at 90° was detected at 400nm with a band pass of 2nm and recorded on equilibration of the signal following each addition. A control experiment recording the effects of serial addition of equivalent volumes of ethanol without α-tocopherol succinate on the scattered signal was conducted under the same conditions.

At constant wavelength the intensity of scattered light detected at a fixed angle from the incident is proportional to the radius of the scattering particles to the power if six as well as directly proportional to the concentration of scattering particles. As the size of α-tocopherol succinate micelles is expected to be considerably greater than that of monomeric α-tocopherol succinate, much larger increases in intensity with increasing concentration would occur above the critical micelle concentration than below it. If the critical micelle concentration is passed in the concentration range of the experiment a plot of scattering intensity against α-tocopherol succinate concentration would best fit two linear expressions with the intersection of the higher gradient line with the concentration axis equal to the critical micelle concentration (Figure 2.5.1). For Rayleigh-Debye scattering in a system containing essentially identical spherical particles measured at a constant angle from the incident radiation of fixed wavelength;

$$I_s = \varepsilon_s . c$$

where I_s is the intensity of scattered light, ε_s is the scattering coefficient, a constant, and c is the concentration of particles (Hobden et al. 1995).

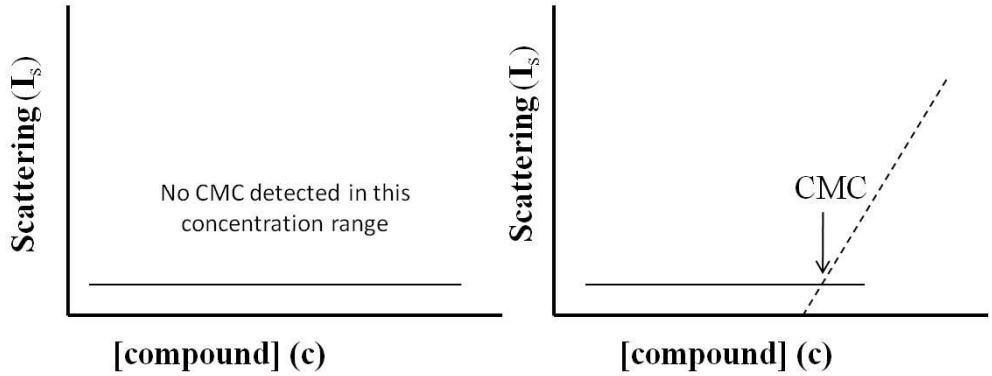

Figure 2.5.1: A diagrammatic representation of the measurement of the critical micelle concentration (CMC) by 90° Rayleigh-Debye light scattering of the micelles once formed. Below the critical micelle concentration a constant baseline scattering intensity is observed (—) and above CMC (----) the intensity of scattered light increases as the number of scattering particles increases with the concentration of the compound in the aqueous environment. *Left* no CMC is detected in the concentration range. *Right* the CMC is detected and is determined as the concentration at which the lines intersect.

2.5.2. Characterisation of fluorescent probes

2.5.2.1. ***Di-8-ANEPPS***

To determine if vesicle or cell membranes had been successfully labelled with Di-8-ANEPPS the excitation and emission spectra of the labelled membranes were compared to reference samples. Di-8-ANEPPS labelled vesicles or cells were diluted to 400μM or $4x10^4$ cells ml^{-1} respectively with tris buffered sucrose solution (280mM sucrose 10mM tris pH7.4, 0.2μm pore filtered) warmed to 37°C up to a final volume of 2ml in a cuvette. The cuvette was placed in the heated cuvette holder of a Fluoromax-4 Spectrofluorimeter maintained at 37°C by a connected circulating water bath. Excitation spectra were taken between 350nm and 550nm with emission at 590nm and emission spectra between 500 and 700nm with 460nm excitation using Datamax-4 software. Di-8-ANEPPS possesses a significantly lower quantum yield in water than in non-polar environments such as biological membranes (Fluhler et al., 1985) and as a result excess of the probe in solution after labelling can remain without affecting the fluorescence detected during experiments (Figure 2.5.2).

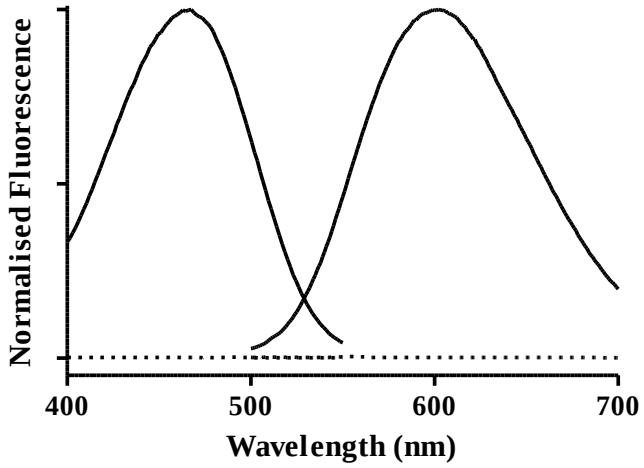

Figure 2.5.2: The excitation and emission spectra of Di-8-ANEPPS in aqueous solution (10μM in 10mM tris, 280mM sucrose pH 7.4) (----) or bound to phosphatidylcholine vesicles (400μM vesicle suspension labelled as detailed in section 2.3.1) (—) at 37°C. Di-8-ANEPPS is non fluorescent in aqueous solution and fluorescent with peak excitation at ~460nm and peak emission at ~600nm when present in membranes.

2.5.2.2. ***FPE***

Successful labelling of vesicle or cell membranes with fluorescein phosphatidylethanolamine (FPE) was determined by comparing the emission spectra (λ_{ex}=490nm, peak emission at 520nm) of the probe in labelled membranes with that of the fluorophore in tris buffered sucrose alone (fluorescein sodium salt, emission peak 510nm). FPE labelled vesicles or cells were diluted to 400μM or $4x10^4$ cells ml^{-1} respectively with tris buffered sucrose solution (280mM sucrose 10mM tris pH7.4, 0.2μm pore filtered) warmed to 37°C up to a final volume of 2ml in a cuvette. The cuvette was placed in the heated cuvette holder of a Fluoromax-4 Spectrofluorimeter maintained at 37°C by a connected circulating water bath. Emission spectra were taken using FluorEssence software. The red shift in the emission peak of fluorescein in the membrane compared with respect to that in solution is reported to occur due to differences in the dielectric permittivity of these environments (Wall et al 1995a, 1995b).

A second technique used to confirm the successful labelling of vesicle and cell membranes with FPE involved the modulation of the membrane surface potential with calcium ions. A single addition of 2mM Ca^{2+} ($CaCl_2$ 1M stock solution) was made to a suspension of 400μM vesicles or $4x10^4$ cells ml^{-1}, FPE labelled, in tris buffered sucrose solution (280mM sucrose 10mM tris pH7.4 0.2μm pore filtered). The subsequent increase in fluorescence intensity, recorded at 520nm following excitation at 490nm using a Fluoromax-4 Spectrofluorimeter with FluorEssence software, was taken to indicate the successful labelling of the membranes. The addition of Ca^{2+} to membranes reduces the net negative charge at the membrane surface decreasing the magnitude of the surface potential. The fluorescein moiety of membrane bound FPE is positioned at the membrane surface where an increasing proportion of the probe becomes deprotonated as the surface potential decreases leading to an increase in fluorescence

intensity. The membrane surface potential is highly localised and, at constant pH, an increase in fluorescence intensity of FPE would only occur on modulation of the surface potential if the probe were present in the outer leaflet of the biological membrane. Both techniques are demonstrated in Figure 2.5.3.

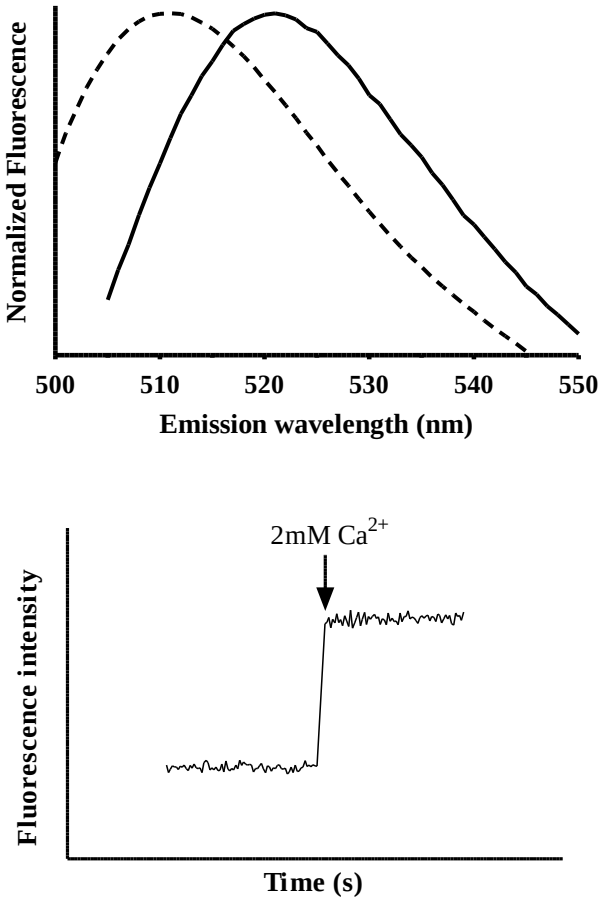

Figure 2.5.3: *Top* The fluorescence emission spectra of fluorescein sodium salt (10μM in aqueous solution) (----) and FPE labelled phosphatidylcholine vesicles (400μM vesicle suspension labelled as outlined in section 2.3.2) (—) with 490nm excitation. The spectra are normalised such that their peak emission is of equivalent intensity for comparison. The spectrum of FPE present in lipidic membranes is red shifted with respect to that in aqueous solution (peak emissions 520nm and 510nm, respectively). *Bottom* The increase in fluorescence intensity on addition of 2mM Ca^{2+}, in the form of $CaCl_2$, to FPE labelled phosphatidylcholine vesicles (400μM vesicle suspension labelled as outlined in section 2.3.2) (λ_{ex}=490nm λ_{em}=520nm). The arrow denotes the point at which the addition was made. Fluorescein sodium salt or FPE labelled vesicles were suspended in 10mM tris 280mM sucrose, pH7.4 and measurements were taken at 37°C.

2.5.3. Determination of the relative membrane dipole potential of sterol- and α-tocopherol-containing phosphatidylcholine vesicles

The spectral sensitivity of membrane bound Di-8-ANEPPS to the dipole potential was used to determine the dipole potential of phosphatidylcholine vesicles containing cholesterol, 7-ketocholesterol and α-tocopherol relative to that of 100% phosphatidylcholine vesicles. Labelled vesicles were diluted to 400μM in tris buffered sucrose solution (280mM sucrose 10mM tris pH7.4. 0.2μm pore filtered), pre-warmed to 37°C, up to a final volume of 2ml in a cuvette. The cuvette was placed in the temperature controlled cuvette holder of a Fluoromax-4

Spectrofluorimeter maintained at 37^{o}C using a heated circulating water bath. Excitation spectra were taken between 400nm and 550nm with a resolution of 1.5nm and recorded at an emission wavelength of 590nm using Datamax software. Each excitation spectrum for vesicles with cholesterol, 7-ketocholesterol and α-tocopherol was normalised with respect to their integral prior to subtracting the normalised spectrum for the 100% phosphatidylcholine membrane reference. The resulting difference spectra amplify the subtle shifts of the excitation spectrum of Di-8-ANEPPS in response to the dipole potential of the environment of the probe. The excitation spectra exhibit a red shift in membranes of decreased dipole potential with respect to the 100% PC membrane reference and a blue shift in membranes with an increased dipole potential relative to the reference (Figure 2.5.4) (Gross et al., 1994, Cladera and O'Shea, 1998, Cladera et al., 1999, Asawakarn et al., 2001).

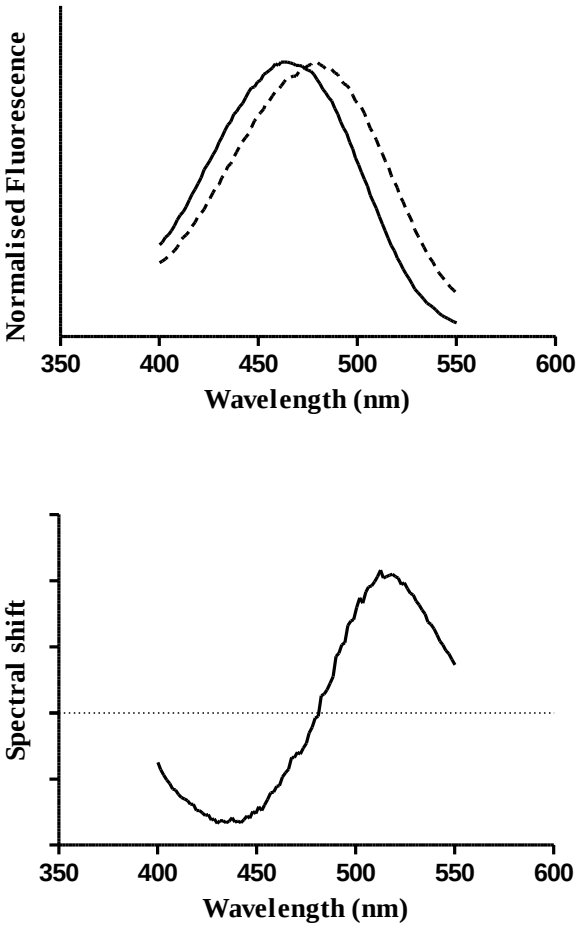

Figure 2.5.4: *Top* The excitation spectra of Di-8-ANEPPS in 100% phophatidylcholine (PC) vesicles (─) and in vesicles containing a lipophilic compound that decreases the dipole potential of the membrane (----) where the excitation spectrum is red shifted with respect to that to 100% PC vesicles. *Bottom* The corresponding difference spectrum obtained by subtracting the excitation spectrum of Di-8-ANEPPS in 100% PC vesicles with that in the vesicles of lower relative dipole potential.

2.5.4. Measuring changes in the dipole potential with titration of sterols and α-tocopherols to Di-8-ANEPPS labelled biological membranes using a dual-wavelength ratiometric method

A dual wavelength ratiometric technique pioneered by Gross *et al.* (Gross et al., 1994) was used to observe, in real time, the spectral shifts of Di-8-ANEPPS in response to changes in the dipole potential on serial addition of sterols or α-tocopherol to a suspension of labelled vesicles or cells. A cuvette was prepared with 2mls of a suspension of labelled vesicles (400μM) or labelled cells (40,000 cells ml^{-1}) in tris buffered sucrose solution (280mM sucrose 10mM tris pH7.4, 0.2μm pore filtered), pre-warmed to 37°C. The cuvette was placed in the temperature controlled cuvette holder of a Fluoromax-4 Spectrofluorimeter maintained at 37°C using a heated circulating water bath. The sample was alternately excited at 460nm and 520nm and the ratio of emission intensities ($R=I_{460}/I_{520}$), recorded at 580nm, was displayed at a period of 1.744s using the timedrive function of the Datamax software. In this way the real-time changes in the dipole potential on the interaction of a known concentration of sterol or α-tocopherol added to the cuvette with the membranes could be observed. Cholesterol, 7-ketocholesterol, α-tocopherol and α-tocopherol succinate were titrated to the Di-8-ANEPPS labelled membranes up to a final concentration above which further addition had negligible observable effect on the ratio. Experimental data was corrected for the effects of photobleaching and the solvent (ethanol) used to introduce the sterols and α-tocopherols by performing a titration with the solvent of equivalent volume additions to the experiment over a comparable timeframe. The ratio over the time course of the control titration was then subtracted from the experimental data. The final concentration of solvent added to the vesicle or cell suspension was minimised as far as possible and did not exceed 1% v/v.

2.5.5. Determination of changes in the surface potential on titration of α-tocopherol succinate or insulin to FPE labelled biological membranes

A sample of 400μM labelled vesicles or 40,000 cells ml^{-1} was prepared as a 2ml suspension in tris buffered or Hepes buffered sucrose solution (10mM tris or 10mM Hepes, with or without 10mM glucose, adjusted to 300mOsmol with sucrose (1mM=1mOsmol) pH7.4, 0.2μm pore filtered), pre-warmed to 37°C, in a cuvette. The cuvette was then placed in the temperature controlled cuvette holder of a Fluoromax-4 Spectrofluorimeter maintained at 37°C using a heated circulating water bath and the fluorescence of the labelled membranes recorded over time at 520nm emission following excitation at 490nm. Once the signal had stabilised to a constant intensity, indicating that the sample was in equilibrium, α-tocopherol succinate or insulin (both negatively charged at physiological pH) was titrated into the membranes and the change in fluorescence following each addition recorded. Experimental data was corrected for the effects of photobleaching and the solvent used to introduce the α-tocopherol succinate or insulin by performing a titration with the solvent of equivalent volume additions to the

experiment over a comparable timeframe. The fluorescence over the time course of the control titration was then subtracted from the experimental data. The final concentration of solvent added to the vesicle or cell suspension was minimised as far as possible and did not exceed 1% v/v.

2.5.6. Analysis of titration data

The average ratio or fluorescence intensity before the titration and following each addition is determined from a minimum of 100 readings after the signal has stabilised to a constant value. Following correction with control data, the change in FPE fluorescence (ΔF) or change in Di-8-ANEPPS fluorescence ratio (ΔR) relative to the starting value was plotted versus the cumulative concentration of the titrated substance (Figure 2.5.5). A minimum of 3 repeat experiments were averaged to produce each titration curve which was then fitted to simple hyperbolic (Equation 2.2) or sigmoidal (Equation 2.3) binding models, using Prism version 5.02. These models are commonly used to describe enzyme kinetics but have also been used to reflect the interaction of substances with membranes detected through changes in the surface and dipole potentials (Wall et al., 1995a, Wall et al., 1995b, Asawakarn et al., 2001, Fitchen et al., 2003, Davis et al., 2010).

$$y = \frac{B_{max}\, x}{(K_d + x)} \qquad \textit{Equation 2.2}$$

$$y = \frac{B_{max} x^h}{(K_d^h + x^h)} \qquad \textit{Equation 2.3}$$

In these models y is the change in fluorescence signal (ΔF orΔR) and x denotes the cumulative concentration of the titrated substance. B_{max} is the maximum change in the fluorescence signal achieved when the membranes are saturated with the substance such that further addition causes no change in the signal. This represents the binding capacity of the membrane for the substance with titrations performed with FPE labelled membranes however its interpretation is more complex with Di-8-ANEPPS labelled membranes as the change in dipole potential elicited per molecule of titrated substance is not necessarily constant. The concentration of substance at which half this maximum change in signal occurs, K_d, reflects the affinity of the substance for the membrane in both cases and is sometimes referred to as the dissociation constant. The sigmoidal model contains an additional term, h, known as the Hill coefficient which was first employed by Hill (Hill, 1910) to describe the cooperative nature of the binding of oxygen molecules to haemoglobin and the fit of this model to the data indicates that the titrated substance interacts cooperatively with the membranes.

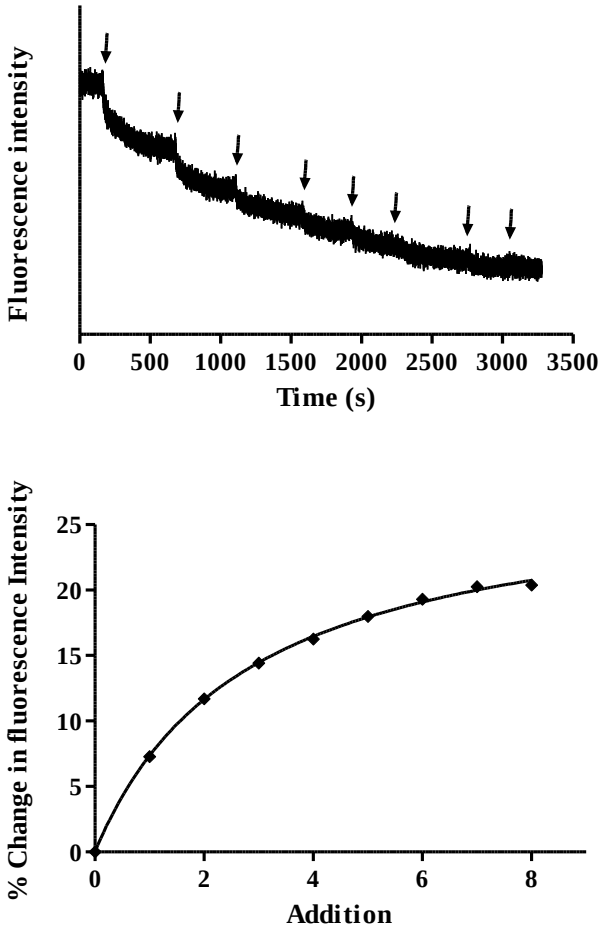

Figure 2.5.5: *Top* A time course of the fluorescence intensity of FPE labelled phosphatidylcholine vesicles on titration of a negatively charged compound that binds with the membranes. The arrows denote the times at which the 8 sequential additions of equal concentration were made. *Below* The corresponding titration curve obtained by plotting the modulus of the percentage change in intensity of FPE once equilibrated following each addition with respect to the initial intensity. A hyperbolic binding model is fitted to the data.

A sum of squares F-test (equation 2.4) was employed in order to determine which of the two models best fit the data.

$$F = \frac{(SS_1 - SS_2)/SS_2}{(DF_1 - DF_2)/DF_2} \qquad \textit{Equation 2.4}$$

Here, SS refers to the residual sum of squares (the sum of the square of the vertical distances of each data point from the curve) for the simpler hyperbolic curve ($_1$) or the more complex sigmoidal curve ($_2$) and DF is the number of degrees of freedom of each model. The goodness of fit of a model, denoted R^2, can be determined by the residual sum of squares normalised against the (total) sum of squares of the vertical distances of data points from a horizontal line through the mean signal (SS_{tot}):

$$R^2 = 1 - \frac{SS}{SS_{tot}}$$ *Equation 2.5*

When the data correlates well with the proposed model the ratio of the residual sum of squares to the total sum of squares is small and R^2 approaches 1. However the residual sum of squares decreases as the degrees of freedom decreases with increasing complexity of the model such that the more complex model nearly always fits the data better when determined by R^2 even when the simpler model suffices. The F-test enables the goodness of fit of the simpler and more complex model to be compared by accounting for the effect of the greater degrees of freedom of the complex model. If the F ratio is close to 1 the simpler model better fits the data. If the F ratio is >> 1 then the P value is approached; if P<0.05 the more complex model better represents the data and if P>0.05 the probability that random scatter of data points led to the higher goodness of fit for the more complex model is significant suggesting no compelling evidence exists that the data fits this model and the simpler model is accepted.

To compare the interactions of sterols and α-tocopherols with membranes, or the interactions of these substances with vesicles of different composition or cell membranes following different treatments, t-tests and one or two way analysis of variance (ANOVAs) were employed to compare the binding affinities (K_d) and, where appropriate, the binding capacities (B_{max}). The molar efficiencies (K_{eff}) of the titrated substances in modulating the surface or dipole potentials of the various vesicle membranes or differently treated membranes, described by equation 2.6, were also compared.

$$K_{eff=\frac{B_{max}}{K_d}}$$ *Equation 2.6*

This equation originates from the concept of molecular activity in enzyme kinetics allowing determination of the moles of substrate transformed per minute per mole of enzyme under optimum conditions (Segel, 1976).

2.5.7. Fluorescence quenching of fitc-insulin and Streptavidin- Alexa Fluor 488 with Trypan Blue

The quenching of streptavidin-Alexa Fluor 488 and fitc-insulin by trypan blue was visualised by the titration of trypan blue to a solution of the fluorescent probe at the equivalent concentration used for the labelling of suspension cells (1μM fitc-insulin, 1:500 dilution of 1mg ml^{-1} streptavidin-Alexa Fluor 488, outlined in sections 2.4.6 & 2.4.7). Solutions were made in DPBS equilibrated to room temperature and 2mls was transferred to a cuvette which was then placed in the cuvette holder of a Fluoromax-4 Spectrofluorimeter at room temperature. The titration

was performed once the fluorescence signal at 520nm, excited at 490nm, had stabilised to a constant intensity indicating the system was in equilibrium. The emission and excitation spectra of the fluorophores were taken prior to and following the titration and, in some cases, during the titration, to observe changes in the spectra with quenching. The percentage decrease in fluorescence with increasing cumulative concentration of trypan blue was plotted and used to determine the concentration of trypan blue later used to quench the surface-bound fluorescence of labelled cells (section 2.5.7).

2.6. Flow Cytometry

2.6.1. Preparation of cell samples for flow cytometry

Cells were labelled with fitc-insulin or biotinylated insulin and streptavidin-Alexa Fluor 488 as described in sections 2.4.6 and 2.4.7 above and the following additions were made to the cell preparation protocol as required.

2.6.1.1. *Identifying non-viable cells with propidium iodide*

In order to distinguish viable and non-viable cells in flow cytometry 3µM of propidium iodide (*PI*) was added to the prepared cell sample in the round bottom polycarbonate tube at room temperature at least 5 minutes prior to measurement. *PI* is a nucleic acid stain that is impermeable to viable cells but is able to penetrate the compromised membranes of non-viable cells and intercalate between the bases of DNA becoming fluorescent (λ_{em}=617nm) once bound. *PI* is non-fluorescent in solution and was therefore left in the solution of prepared cells to minimise the time between insulin labelling and flow cytometry measurement by avoiding unnecessary washing steps.

2.6.1.2. *Determining the extent of non-specific binding of fluorescently tagged insulins*

Cells were incubated with an excess (10µM) of unlabelled insulin for 30 minutes at 37^{o}C prior to fitc-insulin labelling after Murphy *et al.* (Murphy et al., 1982) or for 90 minutes at 15^{o}C prior to incubation with biotinylated insulin followed by streptavidin-Alexa Fluor 488 labelling after Zeigler *et al.* (Ziegler et al., 1994). This occupied insulin-specific binding sites with unlabelled insulin preventing the binding of fluorescently tagged insulins to these sites. Any fluorescence detected by flow cytometry was then attributed to non-specific binding of the fluorescently tagged insulin.

The non-biotin specific binding of streptavidin-Alexa Fluor 488 was determined by labelling cells with the fluorophore-conjugated streptavidin without prior incubation with biotinylated-insulin.

2.6.1.3. *Determining the extent of fluorophore internalisation using trypan blue quenching of cell surface bound fluorescence*

Trypan blue is a quenching agent for both fluorescein and Alexa Fluor 488 and, as it is impermeable to viable cells, can be used to quench the fluorescence of these fluorophores bound to the cell surface whilst preserving the fluorescence of internalised fluorophore (Ma and Lim, 2003, Loike and Silverstein, 1983). Following labelling with fitc-insulin or biotinylated insulin and streptavidin-Alexa Fluor 488 cells were washed twice in DPBS by centrifugation and resuspended in 100µM trypan blue in DPBS for 1 minute at room temperature (determined to

quench the fluorescence of these probes by the method outlined in section 2.5.7). The cells were then washed twice in DPBS to remove free trypan blue and resuspended in the appropriate assay buffer ($1x10^6$ cells in 1ml) for flow cytometry.

2.6.1.4. *Investigating the effect of 7-ketocholesterol or α-tocopherol succinate on insulin binding*

Prior to labelling with biotinylated insulin and streptavidin-Alexa Fluor 488 washed cells were treated with 7-ketocholesterol (10μM, 10 minutes 37°C) or α-tocopherol succinate (3.77μM, 10 minutes 37°C). Cells were then labelled as detailed in section 2.4.7 with the exception that the biointinylated insulin labelling solution also contained either 7-ketocholesterol (10μM) or α-tocopherol succinate (3.77μM).

2.6.1.5. *Investigating the influence of α-tocopherol succinate on the effect of 7-ketocholesterol on insulin binding*

The effect of α-tocopherol succinate treatment prior to exposure to 7-ketocholesterol on insulin binding was determined by incubating cells with 3.77μM α-tocopherol succinate for 10 minutes at 37°C followed by incubation with 10μM 7-ketocholesterol with 3.77μM α-tocopherol succinate (10 minutes, 37°C). To determine the effect of α-tocopherol succinate treatment after exposure to 7-ketocholesterol cells were first incubated with 7-ketocholesterol (10μM, 10 minutes 37°C) followed by treatment with α-tocopherol succinate with 7-ketocholesterol (3.77μM and 10μM respectively, 10 minutes, 37°C). Cells were then labelled as described in section 2.4.7 with the addition of 10μM 7-ketocholesterol and 3.77μM α-tocopherol succinate to the biotinylated insulin labelling solution.

2.6.2. Measurement of cell fluorescence by flow cytometry

The voltages of the photomultiplier tubes in the forward scattered (FSC) and side scattered (SSC) directions were optimised to 50 and 400mV respectively to ensure that the FSC and SSC recordings from the majority of Jurkat and IM-9 cells fell within the range of 0-250,000 intensity units. This was determined using a real time SSC vs FSC dot plot and, as forward scattered light represents the volume of the cell and side-scattered light inner complexity such as the shape of the nucleus and cytoplasmic granules, a distinct population from a sample of cells is apparent on the plot corresponding to largely viable cells.

The voltages of the photomultiplier tubes for both the fitc fluorescence channel (530/30nm bandpass filter) and the PE fluorescence channel (585/42nm bandpass filter) were optimised to 400mV. This placed the auto-fluorescence of unlabelled cells excited with a 488nm coherent sapphire solid state laser centred over 10^2 of the logarithmic intensity scale determined by a real time cell count vs logarithmic amplified intensity plot for both fluorescence channels.

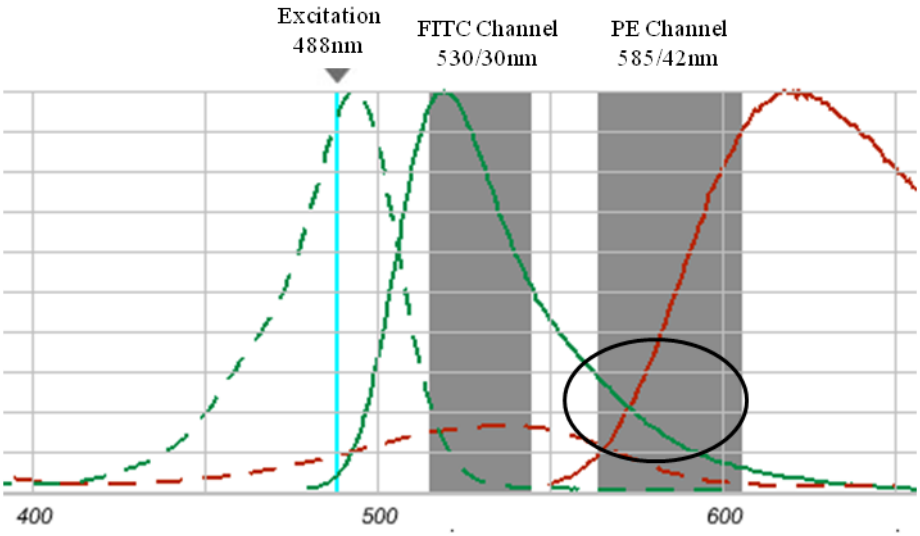

Figure 2.6.1: The excitation spectra (dashed lines) and emission spectra (solid lines) of Alexa Fluor 488 (AF 488)(Green) and propidium Iodide (*PI*)(Red). The 488nm excitation line and the central wavelength and bandpass of the filters (shaded) of the FITC and PE detection channels are shown. There is significant spectral overlap of AF 488 into the detection channel for *PI* (circles) resulting in the detection of this fluorophore as well as *PI* through this channel. Image constructed using the Fluorescence Spectra Viewer available on www.invitrogen.com.

With cell samples labelled with both Alexa Fluor 488 and *PI* it was necessary to compensate for the contributions of each fluorophore to the detected intensity in the channel designated for the other fluorophore due to the overlap of their emission spectra with respect to the bandpass filters of each channel (Figure 2.6.1). Compensation was applied to the raw data automatically by the software used in conjunction with the flow cytometer (BD FacsDiva) after creating compensation controls by defining the fluorescence intensities detected by each channel using unlabelled cells and Alexa Fluor 488 labelled- or saponin permeabilised (0.1% in assay buffer) *PI* labelled- cells as single stained control samples (Figure 2.6.2). The spectral overlap is determined by the software and raw data is compensated for this using calculated correction factors.

For each sample data was collected for 10,000 cells at a medium flow rate with compensation applied where necessary. A minimum of 3 samples were analysed for each experimental and control condition.

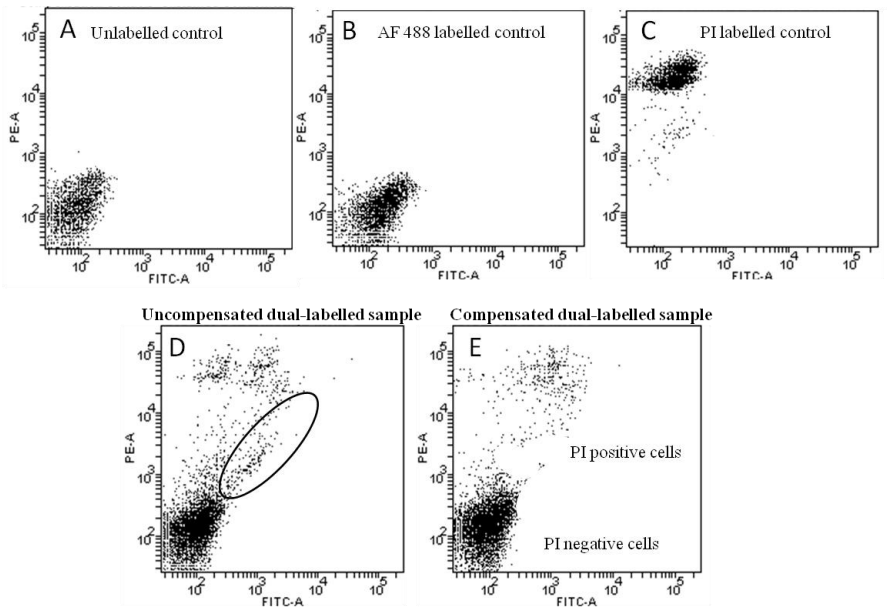

Figure 2.6.2: An illustration of the benefit of compensating for the spectral overlap of two fluorophores in a dual labelled sample. The plots shows the distribution of intensities of 10,000 cells detected by the PE channel vs the FITC channel PMTs for unlabelled cells (**A**), Alexa Fluor 488 (AF 488) labelled cells (**B**) and Propidium Iodide (*PI*) labelled cells (**C**). The distribution of detected intensities of data from a sample labelled with both AF 488 and *PI* that is uncompensated (**D**) or compensated (**E**) is shown with the characteristic profile of intensity of uncompensated data circled.

2.6.3. Analysis of flow cytometry data

Flow cytometry data was analysed using Weasel version 2.7.4. For each sample a FSC vs SSC dot plot was graphed and the viable cell population, excluding as many *PI* positive cells as possible, was gated (Figure 2.6.3). A fluorescence histogram for the fitc channel of cell counts vs. intensity on a log scale was then plotted for the gated population and the median intensity calculated excluding the fluorescence from any *PI* positive cells within the gated population (generally <10%). For each set of samples representing one repeat of an experiment with relevant controls the fluorescence intensities were normalised between that of unlabelled cells (0%) and fitc-insulin or biotinylated-insulin and Streptavidin Alexa Fluor 488 labelled cell (100%). The average normalised fluorescence intensities (n≥3) were then graphed in Prism with the standard error of the mean as error bars.

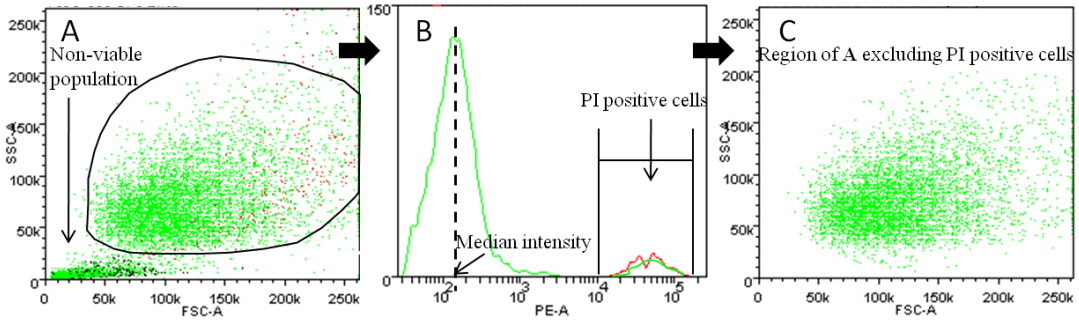

Figure 2.6.3: Demonstration of the analysis of flow cytometry data for Alexa Fluor-488 (AF 488) and Propidium Iodide (*PI*) labelled cells. A 'live-cell' population is identified in a forward-scattered (FSC) vs side-scattered (SSC) intensity plot (**A**) and an intensity histogram for the FITC-channel and PE-channel plotted for cells within this region (**B**). Non-viable cells, which show positive for *PI*, are identified and any AF 488 fluorescence from these is excluded. The median AF 488 intensity from the remaining cells, representing viable cells within the 'live cell' population (shown in **C**) is then determined.

2.7. Imaging of fluorescently labelled HUVEC

HUVEC labelled with Di-8-ANEPPS as described in section 2.4.11 were imaged within 2hrs of labelling using a Nikon TiE fluorescence microscope. Cells were illuminated with a mercury lamp source with the TRITC filter set in place. Images were captured with the CCD camera supplied with the system and viewed using the Nikon NIS imaging software. Images were analysed using ImageJ version 1.44 (Rasband, W.S., ImageJ, U.S. National Institute of Health, Bethesda, Maryland, USA http://imagej.nih.gov/ij/, 1997-2011).

3. Interactions of α-tocopherol with artificial membranes

α-Tocopherol is a lipophilic molecule that has been shown to insert into phospholipid membranes where it influences the phase behaviour of the constituent lipids (Massey et al., 1982, SanchezMigallon et al., 1996, Wang and Quinn, 2002). This is as a result of its effect on lipid ordering (Severcan, 1997, Wang and Quinn, 2000a) and it is therefore likely that this molecule may alter the membrane dipole potential. The influence of α-tocopherol on the membrane dipole potential of egg-phosphatidylcholine vesicles is investigated in this chapter.

The effects of α-tocopherol in the membrane have previously been compared to those of cholesterol (Atkinson et al., 2010) which is well documented to increase the membrane dipole potential (Asawakarn et al., 2001, Starke-Peterkovic et al., 2006). Interestingly 7-ketocholesterol, an oxidised counterpart of cholesterol, has been reported to elicit the opposite effect on the dipole potential (Starke-Peterkovic et al., 2006). As α-tocopherol is well known for its antioxidant action its influence on the dipole potential will be placed in the context of the likely effects of membrane oxidation. The relative effects of cholesterol and 7-ketocholesterol are quantified in the egg-phosphatidylcholine vesicle system and compared with previously reported findings in Section 3.1 (3.1.1 and 3.1.2). The effect of membrane cholesterol oxidation on the dipole potential is then explored (Section 3.1.3). Section 3.2 investigates the influence of α-tocopherol on the dipole potential and compares this effect with that of cholesterol and 7-ketocholesterol (3.2.1). Alteration to the influence of α-tocopherol on the dipole potential in the presence of cholesterol or 7-ketocholesterol are explored as these ternary systems are likely to exhibit different phase behaviour to that of α-tocopherol in egg-PC vesicles (Sections 3.2.2 and 3.2.3).

α-Tocopherol has been shown to modulate several biological effects that cannot be attributed to its free radical scavenging capability (Azzi and Stocker, 2000, Azzi et al., 2002, Brigelius-Flohe, 2009). Modulation of the dipole potential may prove to be a non-antioxidant action of α-tocopherol in membranes that may later prove to underlie some of these effects. To explore this notion the effect of α-tocopherol succinate on the dipole potential, a structural analogue with no anti-oxidant action, was compared with that of α-tocopherol (Section 3.3.2). The charge associated with the succinate moiety also enables the effect of this molecule on the membrane surface potential to be explored (Section 3.3.1).

.

3.1. The effect of cholesterol and its oxidised counterpart, 7-ketocholesterol, on the membrane dipole potential of phosphatidylcholine vesicles

The structure of cholesterol promotes its interaction with phospholipids forming phase separated domains characterised by high order and tight lipid packing (Ipsen et al., 1987, Vist and Davis, 1990, Chapman, 1975b). These liquid ordered (l_o) domains significantly alter the physical landscape of the membrane affecting properties such as fluidity (Chapman, 1975a) and the dipole potential (Starke-Peterkovic et al., 2006). Membrane cholesterol is susceptible to oxidation (Niki et al., 2005); a process which causes slight alteration to the molecular structure yet results in significantly different effects of the sterol on membrane organisation (Massey and Pownall, 2006, Rooney et al., 1986). It is likely that physical properties such as the dipole potential, therefore, are altered as a result of cholesterol oxidation. This section begins by comparing the influence of cholesterol and its oxidised counterpart, 7-ketocholesterol, on the dipole potential in the egg-phosphatidylcholine (PC) vesicle system (sections 3.1.1 and 3.1.2). A model of membrane cholesterol oxidation, in which the cholesterol fraction of the liposome composition is gradually replaced by 7-ketocholesterol, is then used to explore the likely effect of oxidation on the dipole potential (section 3.1.3).

3.1.1. The effect of cholesterol on the dipole potential of phosphatidylcholine vesicles

Cholesterol has been shown to cause an increase in the dipole potential of phospholipid membranes (Starke-Peterkovic et al., 2006) which is associated, at least partly, with the liquid ordered (l_o) domains formed in cholesterol enriched membranes. The influence of cholesterol on membrane organisation, however, is dependent on the specific fatty acid composition of the membrane lipids (Silvius et al., 1996, Veatch et al., 2004). The effect of cholesterol on the dipole potential of the egg-phosphatidylcholine (PC) membranes used in this study therefore needs to be quantified.

The difference spectra of figure 3.1.1 represent the shift in the excitation spectrum of Di-8-ANEPPS, reflecting differences in the dipole potential of the environment of the probe, between PC and PC-cholesterol vesicles. The increase in height of the positive part of the difference spectra at lower wavelengths is the result of a blue-shift of the excitation spectrum of Di-8-ANEPPS in response to an increase in dipole potential. As the concentration of cholesterol in the vesicles is increased, the dipole potential is increased with respect to that of cholesterol-free 100% PC vesicles.

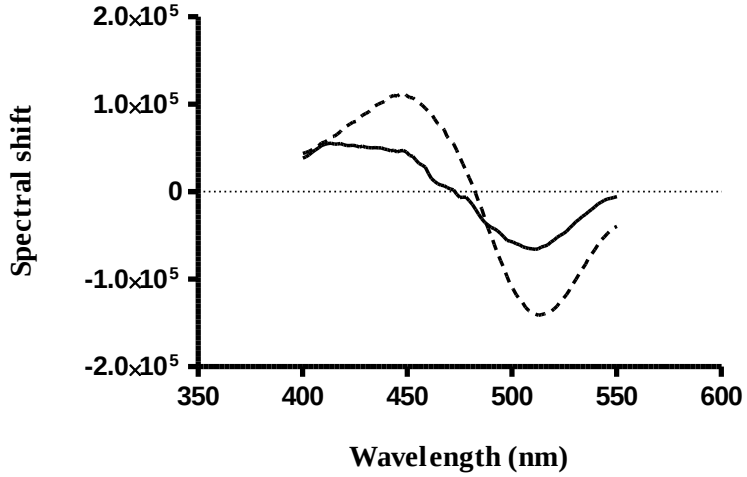

Figure 3.1.1: Difference spectra obtained by subtracting the excitation spectrum of Di-8-ANEPPS (λ_{em}=580nm) in 100% phosphatidylcholine (PC) vesicles from that in 90mol%PC-10mol%Cholesterol (—) and 70mol%PC-30mol%Cholesterol (----) vesicles. Excitation spectra were obtained with n=3 for each vesicle composition and the difference spectra shown are the average of the 3 resulting difference spectra. Data is smoothed by a 4-point moving average to clarify the overall shape of the spectra.

The increase in the dipole potential due to the presence of cholesterol in PC membranes is thought to arise from several factors. These include contributions from the dipole moment of the cholesterol molecule and from the increased motional ordering and lipid packing density, and decreased hydration of the bilayer, resulting from phase separation into liquid ordered (l_o) cholesterol-rich domains (Starke-Peterkovic et al., 2006).

Phosphatidylcholine (PC) has a total molecular dipole resulting from the sum of dipoles associated with the phosphate headgroup ($\mu \approx 20D$ (Shepherd and Buldt, 1978)), the carbonyl bonds of the ester linkages to the acyl chains (μ=1.8D (Flewelling and Hubbell, 1986)), and the terminal methyl groups of these chains (μ=0.35D (Vogel and Mobius, 1988)). The dipole potential of a pure PC bilayer arises from the component of these dipoles resolved parallel to the membrane normal with contribution from the oriented water molecules in the interfacial region (Brockman, 1994, Gawrisch et al., 1992, Peterson et al., 2002). Replacing 30mol% PC with cholesterol in the membrane introduces the molecular dipole of cholesterol ($\mu_{\perp}$=1.5D parallel to the membrane normal (Starke-Peterkovic et al., 2006)) in place of that of PC, altering the dipole potential of the membrane. The contribution of the cholesterol molecular dipole to the dipole potential has been suggested to be negligible compared to that of DPPC in a molecular dynamic (MD) simulation by Hofsass *et al.* (Hofsass et al., 2003). However, Smondyrev and Berkowitz (Smondyrev and Berkowitz, 2001) found cholesterol's molecular dipole to have a significant effect on the dipole potential in their MD calculations. The contribution of PC relies strongly on the orientation of the headgroup (Bechinger and Seelig, 1991), therefore slight differences in the tilt of the headgroup with respect to the membrane normal in these simulations can dramatically alter the resulting effect of PC on the dipole potential relative to that of cholesterol.

A characteristic effect of cholesterol in membranes is to promote phase separation into liquid ordered (l_o) cholesterol- and saturated lipid-rich domains with significant consequences on the dipole potential. The l_o phase displays high lipid packing with respect to the liquid crystalline (l_c) phase of cholesterol-free PC membranes. This increase in lipid packing due to cholesterol causes an increase in the dipole density, increasing the local dipole potential. The highly ordered nature of the l_o phase may also increase the magnitude of the molecular dipole of PC that is resolved parallel to the membrane normal also contributing to an increase in the dipole potential.

The hydration of the membrane is reduced as the tighter phospholipid-cholesterol packing reduces the penetration depth of water into the bilayer (Simon and McIntosh, 1986) and the membrane surface 'condensation' by increased lipid density reduces the amount of interfacial water (Parasassi et al., 1994). These effects, combined, result in an increase in the dipole potential of PC-cholesterol membranes with respect to pure PC membranes, shown in Figure 3.1.1.

Although the consensus is that the incorporation of cholesterol into a phospholipid bilayer increases the dipole potential (Starke-Peterkovic et al., 2006, Robinson et al., 2010, Buzon, 2006, Asawakarn et al., 2001), which is consistent with the result shown in Figure 3.1.1, the relative importance of the molecular dipoles of cholesterol and PC, and the increase in dipole density and decrease in hydration with lipid packing, to the dipole potential is controversial.

Starke-Peterkovic *et al.* (Starke-Peterkovic et al., 2006) compare a calculated change in dipole potential, based on a computationally derived value for the dipole moment of cholesterol, with experimental results for 40mol% cholesterol in a DMPC membrane. They conclude that the dipole moment, and associated electric field, of cholesterol must only account for 10-30% of the total change in the dipole potential seen experimentally. An additional 8.7% increase in dipole potential is expected from direct correlation to the equivalent percentage decrease in lipid packing density, quantified by Almeida *et al.* (Almeida et al., 1992) who report a drop in the area per DMPC molecule from 58.5Å^2 to 53.8 Å^2 in the presence of 40mol% cholesterol. The remaining discrepancy from the experimental values is assigned to the decrease in the depth of penetration of water into the bilayer with cholesterol. This results in a significant change in the polarity in the region of the ester carbonyls of PC, where water is no longer reaching, causing an increase in the dipole potential (Simon and McIntosh, 1986)).

Using molecular dynamics simulations, Robinson *et al.* (Robinson et al., 2010) confirm that the orientation of water molecules around the lipid headgroups at the bilayer surface provides the dominant contribution to the dipole potential in a pure DPPC bilayer. This contribution,

however, is shown to be approximately the same in pure DPPC and mixed DPPC/30mol% cholesterol bilayers suggesting that the difference in dipole potential that arises from increased lipid packing by cholesterol is solely due to the increase in lipid dipole density. The differences in these studies may lie with the limitations of the molecular dynamics simulations used in the latter. For example, due to the length of simulation time this would require the modelled bilayer studied may not have been in thermodynamic equilibrium and the subtleties of cholesterol domain formation and the associated changes in hydration not fully represented. Interestingly, Robinson *et al.* (Robinson et al., 2010) have also demonstrated by simulation that Di-8-ANEPPS, due to its location within the bilayer, is unlikely to be directly sensitive to changes in membrane surface hydration. As changes in hydration, however, impact on the orientation of lipid molecular dipoles (Ulrich and Watts, 1994), to which Di-8-ANEPPS is sensitive, it is possible that a change in hydration results in a spectral shift through indirect effects.

It should also be considered that the influence of cholesterol on the dipole potential is highly likely to be dependent on the phospholipid composition of a membrane. In egg-PC membranes on inclusion of 40mol% cholesterol Lecuyer and Dervichi. (Lecuyer and Dervichi, 1969) report a decrease in the area per molecule from 61 $Å^2$ to 49 $Å^2$ which is greater than that reported in DMPC membranes by (Almeida et al., 1992). This suggests that the increase in lipid packing, and therefore increase in dipole density, due to cholesterol is greater in egg-PC than pure DMPC membranes which may result in a larger increase in dipole potential. Egg-PC membranes contain both saturated and unsaturated fatty acid chains in a variety of lengths, both of which affect the magnitude of the dipole potential (Clarke, 1997) and this initial dipole potential endowed by the lipid species present may also influence the subsequent effect of cholesterol.

3.1.2. Comparison of the effects of cholesterol and 7-ketocholesterol on the dipole potential of phosphatidylcholine vesicles

Membrane cholesterol is highly susceptible to oxidation causing structural changes to the molecule which are likely to result in differences in its influence on the membrane dipole potential. Figure 3.1.2 shows the difference spectra derived from the excitation spectra of Di-8-ANEPPS in 7-ketocholesterol containing PC vesicles. The increase in height of the positive part of the difference spectra at higher wavelengths is the result of a red-shift of the excitation spectrum of Di-8-ANEPPS in response to a decrease in dipole potential, thus 7-ketocholesterol decreases the dipole potential. Comparison of Figure 3.1.1 and 3.1.2, noting the 5x larger scale in spectral shift in the later, reveals that the magnitude of change in the dipole potential due to 7-ketocholesterol is considerably greater than that due to cholesterol.

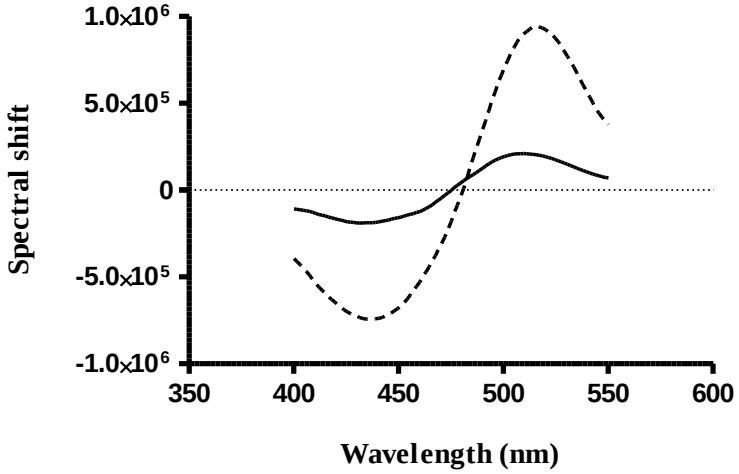

Figure 3.1.2: Difference spectra obtained by subtracting the excitation spectrum of Di-8-ANEPPS (λ_{em}=580nm) in 100% phosphatidylcholine (PC) vesicles from that in 90mol%PC-10mol%7-ketocholesterol (—) and 70mol%PC-30mol%7-ketocholesterol (----) vesicles. Excitation spectra were obtained with n=3 for each vesicle composition and the difference spectra shown are the average of the 3 resulting difference spectra. Data is smoothed by a 4-point moving average to clarify the overall shape of the spectra.

7-ketocholesterol, like cholesterol, promotes phase separation in the presence of saturated lipids into ordered domains. The tendency of 7-ketocholesterol to form these domains, and the degree of lipid packing and order within them, are lower than that of cholesterol l_o domains. The contribution to the dipole potential due to the lipid dipole density and hydration effects associated with these domains is therefore very different. Another contribution of 7-ketocholesterol to the dipole potential is thought to arise from its molecular dipole, which opposes that of cholesterol, and the effects of the presence of this dipole on properties of the bilayer such as hydration (Starke-Peterkovic et al., 2006, Massey and Pownall, 2005). The result is a lower magnitude of the dipole potential of 7-ketocholesterol containing PC membrane compared with pure PC membrane, as shown in figure 3.1.2. Starke-Peterkovic *et al.* (Starke-Peterkovic et al., 2006) also report the incorporation of 7-ketocholesterol into DMPC bilayers to decrease the dipole potential.

The relationship between the concentration of sterol (cholesterol or 7-ketocholesterol) in the vesicles and the dipole potential was further explored with the results shown in figure 3.1.3. In this figure the spectral shift exhibited by Di-8-ANEPPS is expressed as the change in the ratio (R) of fluorescence intensity at 460nm and 520nm excitation in PC vesicles containing increasing concentrations of sterol (5-30mol%) from that of a 100% PC vesicles reference (Equation 3.1.1):

$$\Delta R = \left(\frac{I_{460}}{I_{520}}\right)_{sterol+\ PC} - \left(\frac{I_{460}}{I_{520}}\right)_{PC} \qquad \textit{Equation 3.1.1}$$

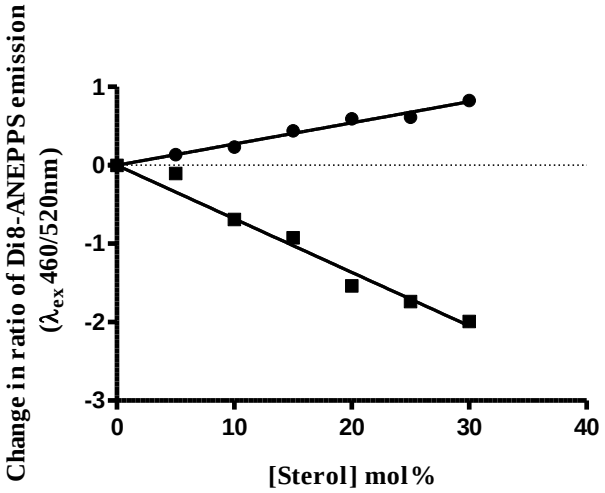

Figure 3.1.3: The change in the ratio of Di-8-ANEPPS fluorescence intensity at 460nm and 520nm excitation ($R=I_{460}/I_{520}$) with increasing cholesterol (●) or 7-ketocholesterol (■) concentration from a 100%PC vesicle baseline ratio. The data represents the average of 3 repeats with the standard error of the mean shown as error bars. The data is fitted to a straight line constrained to intercept at the origin yielding $r^2=0.98$, slope=0.0270±0.0005mol%$^{-1}$ and $r^2=0.97$, slope=-0.068±0.001mol%$^{-1}$ for cholesterol and 7-ketocholesterol containing vesicles respectively. Both slopes are significantly non-zero (P=0.0003 for cholesterol and P=0.0005 for 7-ketocholesterol, one sample t-test).

A linear relationship best describes the change in ratio with sterol concentration and the magnitude of the slope represents the magnitude of the change in dipole potential in each case. A two-tailed t-test of the slope magnitudes confirms that the change in the dipole potential due to cholesterol and 7-ketocholesterol are significantly different ($P<0.0001$, $R^2=0.99$). Taking the ratio of the magnitude of the slopes, we see the magnitude of the change in dipole potential with increasing 7-ketocholesterol concentration is 2.52±0.06 times greater than that caused by equivalent increase in cholesterol concentration.

The change in fluorescence ratio with increasing cholesterol or 7-ketocholesterol concentration in DMPC bilayers reported by Starke-Peterkovic *et al.* (Starke-Peterkovic et al., 2006) also follow an approximately linear relationship between 0% and 30mol% sterol. Although the direction of the change in ratio, and therefore change in dipole potential, is consistent with the data shown here, the magnitude of the change per unit concentration of each sterol (as determined by the slope of the linear relations) is much smaller. This could be due, in part, to the excitation wavelengths chosen for the ratiometric determination of spectral shift. Starke-Peterkovic *et al.* take the ratio of emission intensity at 670nm from 420nm and 520nm excitation which lie at the left and right tails of the approximately gaussian Di-8-ANEPPS excitation spectra and as a result reduce the sensitivity of their measurements. Our measurements take the ratio of emission intensity at 580nm after excitation at 460nm and 520nm which fall near the peak and right tail of the Di-8-ANEPPS excitation spectra affording maximum sensitivity. The different emission wavelengths chosen may influence the relative intensity of fluorescence detected in each study, but it does not impact the ratio.

Cholesterol has a marginally greater effect than 7-ketocholesterol (1.04x greater) based on the ratio of slopes estimated from data in (Starke-Peterkovic et al., 2006). This difference is much smaller than in the present study which also shows 7-ketocholesterol, not cholesterol, to have the greater effect. These discrepancies are likely to result from the different PC compositions of the bilayers used in these studies.

A significant contribution towards the dipole potential is associated with the highly ordered l_o domains present in cholesterol containing membranes. The formation, extent and nature of these domains is dependent on the acyl chain length and proportion of unsaturated chains in the membrane lipid composition (de Almeida 2007, Chiu 2002). In membranes composed of DOPC, which has unsaturation in both acyl chains, cholesterol does not form l_o domains (Veatch et al., 2004). From inspection of the phase diagrams presented by Veatch *et al.* and de Almeida *et al.* (Veatch et al., 2004, de Almeida et al., 2007) replacing roughly a quarter of the DOPC with DPPC, a fully saturated counterpart, supports the existence of l_o domains with 10mol% cholesterol. The concentration of cholesterol required for the onset of l_o domain formation increases as the fraction of DPPC to DOPC is increased suggesting that the presence of unsaturated lipids in a saturated/unsaturated lipid mixture promotes l_o domain formation. This variation in the cholesterol concentration at which l_o domains occur also implies that at 30mol% cholesterol, for example, a membrane with 2:1 DOPC:DPPC has a higher proportion of the l_o phase than a membrane with 1:2 DOPC:DPPC. Recently the fraction of the bilayer in the l_o phase has been reported to dictate the size of the l_o domains present; the higher this is, the larger the domains (de Almeida 2005). Typically thermokinetic considerations determine domain size, for example the rate at which the temperature of a membrane is changed affects the size of l_o domains (Blanchette et al., 2008).

The nature of these domains is also affected by the chain length of the saturated lipids within them. Acyl chains of greater than 14 carbons extend deeper into the bilayer than cholesterol and are thought to induce tighter packing by the folding of the lower part of the chains under the cholesterol tail (Chiu et al., 2002).The length of acyl chains have also been suggested to cause variation in the concentration of cholesterol at which l_o domains occur (Silvius et al., 1996).

In their comparison of the effects of cholesterol and 7-ketocholesterol on the dipole potential, Starke-Peterkovic *et al.* use DMPC which has fully saturated 14-carbon fatty acid chains resulting in the relatively high transition temperature of 23^{o}C. Their experiments were conducted at 30^{o}C where the DMPC bilayers would be in the liquid crystalline phase. The egg-PC system used here contains lipids with a mixture of saturated and unsaturated acyl chains varying in length from 14 to 26 carbons with the predominant species being POPC with a 16-carbon saturated and 18-carbon unsaturated fatty acid chain.

The influence of cholesterol on the l_o domains in these systems are therefore likely to be very different and further complicated by the fact that the egg-PC/cholesterol system at 37°C is a ternary phase system and at low cholesterol concentrations may exhibit gel (L_β), liquid ordered (l_o) and liquid disordered (l_d) phases, whereas the DMPC/cholesterol system is binary consisting of only l_o and l_d phases. Differences in the formation, proportion and lipid packing of the l_o domains between the egg-PC/cholesterol and DMPC/cholesterol systems are likely to cause differences on the influence of cholesterol on the dipole potential. 7-ketocholesterol, like cholesterol, forms ordered domains with saturated lipids (Rooney et al., 1986) and it is possible that the effect it has on the dipole potential is also influenced by the fraction of saturated to unsaturated lipids in the membrane.

The orientation of 7-ketocholesterol in the ordered domains it forms with saturated lipids is similar to that of cholesterol in l_o domains, however, its molecular dipole acts in the opposite direction to that of cholesterol. The opposing changes in the dipole potential by cholesterol and 7-ketocholesterol in saturated DMPC membranes are attributed to the difference in the direction of their dipole moments by Starke-Peterkovic *et al.* (Starke-Peterkovic et al., 2006). They find that the ratio of computationally determined dipole moments resolved parallel to the membrane normal for cholesterol and 7-ketocholesterol correlates well with the ratio of experimentally determined changes in the dipole potential due to these sterols.

The behaviour of 7-ketocholesterol in the unsaturated-lipid rich l_d phase of egg-PC mixed membranes is very different. 7-ketocholesterol, compared to cholesterol, has a greater preference for the l_d phase where the carbonyl group, its main structural difference from cholesterol, is oriented towards the aqueous phase by hydration causing the axis of 7-ketocholesterol to be tilted with respect to the bilayer normal (Smondyrev and Berkowitz, 2001, Massey and Pownall, 2005). This is consistent with the observation that 7-ketocholesterol orders the l_d phase much less than cholesterol (Wang et al., 2004) and the relative strength of the hydrogen bonding between the carbonyl group and the surface polar groups in the l_d phase compared to the van der Waals attractive interaction driving the formation of l_o phase domains accounts for the reduced affinity of 7-ketocholesterol to form l_o domains relative to cholesterol. This tilted orientation in the l_d phase both reduces the lipid packing density (therefore decreasing dipole density and increasing hydration) and orients the molecular dipole of 7-ketocholesterol at an even greater angle away from the positive axis perpendicular to the bilayer surface, such that a greater magnitude is resolved anti-parallel to the membrane normal. These effects result in a considerably larger reduction in the dipole potential when unit mol% 7-ketocholesterol is in a bilayer containing unsaturated lipids than in a saturated lipid bilayer.

The differences in behaviour of cholesterol and 7-ketocholesterol in saturated and unsaturated lipid environments described above account for the much greater effect of 7-ketocholesterol than cholesterol in changing the magnitude of the dipole potential the egg-PC vesicles used in this study than that observed by Starke-Peterkovic *et al.* (Starke-Peterkovic et al., 2006) in DMPC bilayer systems. The fatty acid composition and temperature of the membrane, with respect to the transition temperatures of the lipids, also dictate the phases present in the absence of sterol. These define the degree of order, both in terms of lipid packing and headgroup orientation, and therefore the magnitude of the dipole potential of the membrane which is likely to influence the further effect of either sterol on the dipole potential. It is clear that the phase profile of a membrane may significantly influence the effect of cholesterol oxidation into 7-ketocholesterol on the dipole potential.

To further investigate the influence of the phases present in a membrane on the effect of 7-ketocholesterol on the dipole potential, the change in Di-8-ANEPPS fluorescence ratio with increasing 7-ketocholesterol concentration was compared for PC-10mol%cholesterol vesicles (with coexisting L_β, l_o and l_d phases) and 100% PC vesicles (with L_β and l_c phases) at 37°C (figure 3.1.4).

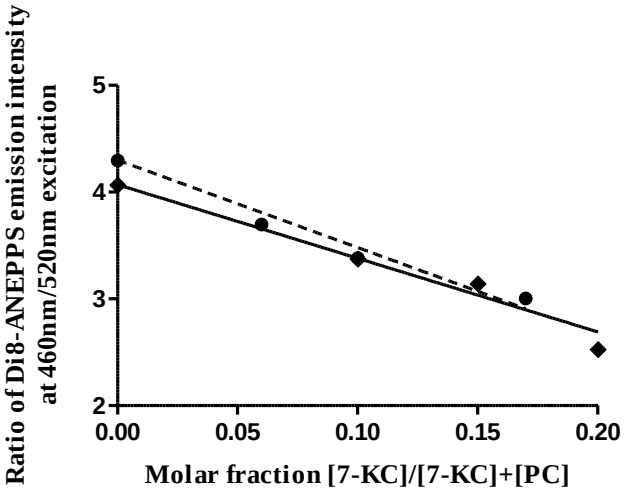

Figure 3.1.4: The ratio of Di-8-ANEPPS fluorescence intensity at 460nm and 520nm excitation ($R=I_{460}/I_{520}$ λ_{em}=580nm) with increasing 7-ketocholesterol (7-KC) concentration, represented as the ratio of % mol concentration [7-KC]/[7-KC +PC], in PC (♦) and PC-10mol%cholesterol (●) vesicles . Each data point is the average of 3 repeats with the standard error of the mean as error bars. Fitting linear regressions to the data gives r^2=0.98 and slope=-6.9±0.1 for 7-ketocholesterol-PC liposome ratios (----) and r^2=0.96 and slope=-8.2±0.3 for 7-ketocholesterol-cholesterol-PC vesicles (—). Both slopes are significantly non-zero (P=0.001 and P=0.003 respectively, one sample t-test).

The initial ratio (at x=0) for PC-10mol%cholesterol vesicles is higher than that for PC vesicles reflecting the increase in the magnitude of the dipole potential due to the presence of cholesterol. Comparison of the slopes shows the effect of 7-ketocholesterol on the dipole potential to be significantly greater in PC-cholesterol vesicles than pure egg-PC vesicles (two-tailed t test P=0.01 R^2=0.84). This suggests that the change in the phase profile, and subsequent

change in the dipole potential, of egg-PC membranes with the inclusion of 10mol% cholesterol has a significant effect on the influence of 7-ketocholesterol on the dipole potential.

As the effect of 7-ketocholesterol on the dipole potential depends on the phases it occupies, this suggests that 7-ketocholesterol may partition differently between the ordered saturated lipid phase and the unsaturated lipid- rich phase. The presence of cholesterol forming ordered (l_o) domains with saturated lipids may increase the tendency of 7-ketocholesterol for the disordered (l_d) phase where its tilted orientation results in a higher contribution from its molecular dipole to the dipole potential. An increased proportion of 7-ketocholesterol in the l_d phase would therefore result in a greater decrease in the dipole potential in the cholesterol-containing membrane. Alternatively, 7-ketocholesterol may be disrupting the order of the gel (L_β) phase or the cholesterol-rich l_o phase to form its own less-ordered domains and the resulting changes in lipid packing and hydration are reflected in the greater decrease in dipole potential.

3.1.3. A model of membrane cholesterol oxidation and the dipole potential

Section 3.1.2 shows cholesterol and its oxidation product, 7-ketocholesterol, to have very different effects on the dipole potential of egg-PC vesicles. To investigate the relative influences of cholesterol and 7-ketocholesterol on the dipole potential in the context of membrane oxidation a model was used where the 30mol% cholesterol component in egg-PC vesicles was increasingly replaced with 7-ketocholesterol. The influence of 7-ketocholesterol on the dipole potential was shown to be significantly different in the presence of 10mol% cholesterol in the previous section (Section 3.1.2) and is thought to depend on the phase profile and initial magnitude of the dipole potential of the membrane. In this model the molar fraction of cholesterol to egg-PC is changing resulting in changes to the extent of the liquid ordered (l_o) phase and contributions to the dipole potential associated with cholesterol. This may potentially affect the influence of the increasing molar fraction of 7-ketocholesterol on the dipole potential in this model compared with egg-PC vesicles, and this is also investigated.

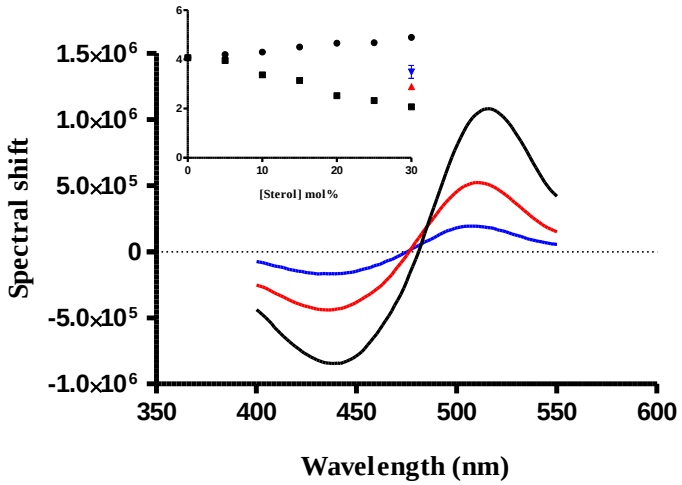

Figure 3.1.5: *Main*: Difference spectra obtained by subtracting the excitation spectrum of Di-8-ANEPPS in 70mol%PC-30mol%Cholesterol vesicles from that in 70mol%PC-25mol%Cholesterol-5mol%7-ketocholesterol (—), 70mol%PC-15mol%Cholesterol-15mol%7-ketocholesterol (—) and 70mol%PC-30mol%7-ketocholesterol (—) vesicles. *Inset*: The ratios of Di-8-ANEPPS fluorescence intensity at 460nm and 520nm excitation in the above vesicles added to the plot of Figure 3.1.3 for reference.

Figure 3.1.5 shows a series of difference spectra resulting from the model of membrane oxidation demonstrating an increasing red-shift of the Di-8-ANNEPS excitation spectra from that of 70mol%PC-30mol%cholesterol vesicles as the fraction of cholesterol replaced with 7-ketocholesterol increases. This suggests that the oxidation of membrane cholesterol is likely to result in a significant decrease in the dipole potential.

Figure 3.1.6 shows the spectral shifts of Di-8-ANEPPS in the vesicles of the cholesterol oxidation model expressed as the change in the ratio, R ($R=I_{460}/I_{520}$ at λ_{em}=580nm), with reference to the 30mol%cholesterol-PC ('un-oxidised') vesicles.

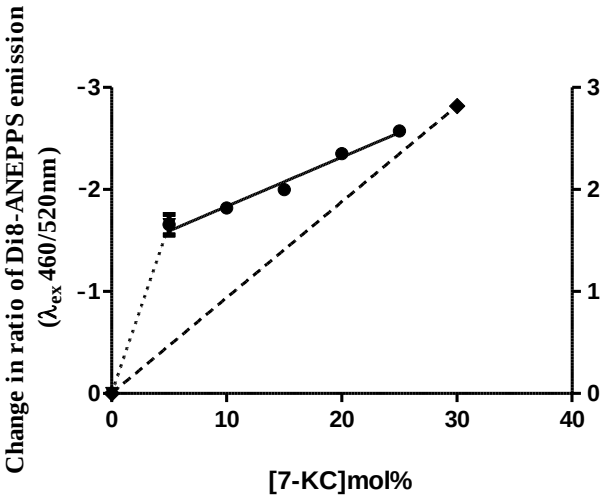

Figure 3.1.6: The change in ratio (ΔR) of Di-8-ANEPPS fluorescence intensity at 460nm and 520nm excitation ($R=I_{460}/I_{520}$ λ_{em}=580nm) from a PC-30mol%cholesterol reference as the concentration of 7-ketocholesterol is increased (5-25mol%) whilst maintaining a fixed 30mol% of non-PC component. The modulus of the change in ratio is shown on the right y-axis. The data is fit to two straight lines (— & …) indicating the two possible regimes present. A straight line fit between PC-30mol% cholesterol and PC-30mol%7-ketocholesterol (----) denotes the relationship expected if the change in ratio caused by cholesterol and 7-ketocholesterol were simply additive.

This data deviates significantly from the course expected if the effects of cholesterol and 7-ketocholesterol on the membrane dipole potential were purely additive. This indicates that a level of interaction exists between the sterols influencing the resulting changes in the dipole potential. Two regimes are clearly apparent in this effect, one below and one above the 25mol%cholesterol-5mol%7-ketocholesterol vesicle composition. The first regime shows a large change in the dipole potential which may or may not be linear as shown in figure 3.1.6. The subsequent changes in the dipole potential, in the second regime, are much less and follow a linear increase. The regimes correlate roughly with the two regimes of phases likely to be occurring between the egg-PC and cholesterol components. Above a molar ratio of cholesterol to egg-PC of approximately 0.25 l_o and l_d phases will be present and below this the gel phase (L_β) may persist alongside the l_o and l_d phases. The liposome composition at the border of the regime has a molar ratio of cholesterol to egg-PC of 0.26 and so it is likely the phase profile of the membranes is having a significant effect on the influence of 7-ketocholesterol on the dipole potential. Di-8-ANEPPS molecules localised within the different phases are likely to report different ratios due to the different dipole potential experienced by the probe in each phase as a result of its physical properties (e.g. lipid ordering and hydration). Changes in the phase profile of a membrane are therefore likely to result in changes in the ratio reported by Di-8-ANEPPS for the membrane as a whole with significant changes likely to occur at phase boundaries.

To explore the concept that the influence of 7-ketocholesterol on the dipole potential may depend on the phase landscape of the membrane, the data of Figure 3.1.6 is expressed as the molar ratio of 7-ketocholesterol to total PC+7-ketocholesterol and compared for the cholesterol-containing oxidation model vesicle series and a cholesterol-free egg-PC series (Figure 3.1.7).

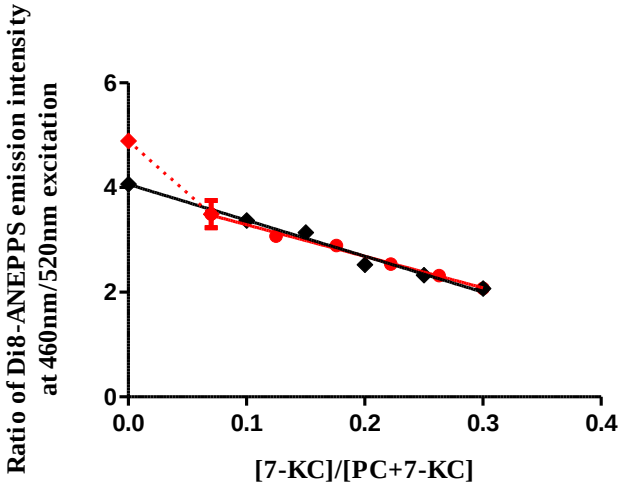

Figure 3.1.7. The ratio of Di-8-ANEPPS fluorescence intensity at 460nm and 520nm excitation ($R=I_{460}/I_{520}$ λ_{em}=580nm) with increasing 7-ketocholesterol (7-KC) concentration, represented as the ratio of mol% concentration [7-KC]/[7-KC+PC], in PC vesicles (♦) and PC-cholesterol vesicles of the oxidation model (●) . Each data point is the average of 3 repeats with the standard error of the mean as error bars. Fitting linear regressions to the data gives r^2=0.98 and slope=-6.8±0.2 for 7-ketocholesterol-PC liposome ratios (—) and r^2=0.90 and slope=-6.0±0.5 for the 2nd regime of 7-ketocholesterol-cholesterol-PC vesicles (—).Both slopes are significantly non-zero (P=0.001 and P=0.007 respectively, one sample t-test). The large change of the 1st regime, although not necessarily linear, is also fitted to a straight line (…).

From this figure it is evident that the influence of 7-ketocholesterol on the dipole potential in the ascribed $L_\beta+l_o+l_d$ regime of the cholesterol-oxidation model vesicles is very similar to that in egg-PC vesicles which are speculated to possess the L_β and liquid crystalline (l_c) phases. A two-tailed t-test confirms the slopes, representing the efficacy of 7-ketocholesterol in changing the dipole potential, are not significantly different (P=0.2 R^2=0.37).

An explanation for the behaviour in the first regime is that the significant proportion of l_o phase domains present sequester saturated lipids from 7-ketocholesterol, driving it to partition more preferentially in the l_d phase. The higher tendency of 7-ketocholesterol for the l_d phase results in a greater proportion of 7-ketocholesterol in the tilted orientation causing a greater decrease in the dipole potential. In the second phase the lower cholesterol concentration results in a lower proportion of l_o phase domains resulting in a greater availability of non-l_o saturated lipids with which 7-ketocholesterol can form ordered domains. The similarity in the influence of 7-ketocholesterol on the dipole potential in this second regime and in cholesterol-free egg-PC vesicles suggests that 7-ketocholesterol may partition between ordered and disordered phases to similar extent in both cases. However, it is also possible that 7-ketocholesterol is partitioning into cholesterol-rich ordered domains but the resulting changes in lipid packing and hydration only count towards a minor contribution to the change in dipole potential compared to that of the molecular dipole moment of 7-ketocholesterol. If this is the case, any disruption of cholesterol-rich l_o domains in the cholesterol oxidation model may not be detected by this technique and, if the proportion of 7-ketocholesterol in the tilted to non-tilted orientation is

similar in egg-PC, 7-ketocholesterol would be observed to have the same effect on the dipole potential in both systems.

The vesicles of the cholesterol oxidation model contain lipids with fatty acid tails of varying degrees of unsaturation and chain length as well as cholesterol and 7-ketocholesterol resulting in a complex system with many co-existing domains. The above explanation is most likely a gross oversimplification and the overall dipole potential of the membranes is likely to be a balance of many contributing factors. These include the lipid packing and hydration of these domains as well as contributions from the molecular dipole moments of cholesterol and 7-ketocholesterol which are likely to vary depending on their microenvironment. The work presented above, however, does provide evidence to suggest that the phase landscape of the membrane, and subsequently the magnitude of the membrane dipole potential, may influence the effect of 7-ketocholesterol on the dipole potential.

3.2. The effect of α-tocopherol on the dipole potential of phosphatidylcholine vesicles with cholesterol and 7-ketocholesterol

α-Tocopherol has a well established antioxidant action and, due to its lipophilic nature, is said to direct this action within membranes protecting unsaturated lipids from oxidation (Azzi, 2007). It is structurally similar to cholesterol, both having a conjugated ring structure with a polar moiety at one end and a hydrocarbon chain at the other. This structure endows cholesterol with unique physical properties in membranes, notably lipid ordering effects promoting the phase separation of saturated lipids into liquid ordered (l_o) domains (Ipsen et al., 1987, Chapman, 1975b, Vist and Davis, 1990). In the previous section it was shown that this effect, as well as the molecular dipole of cholesterol, results in an increase in the dipole potential on inclusion of cholesterol to phosphatidylcholine (PC) vesicles (Section 3.1.1). α-Tocopherol similarly orders membrane lipids forming domains of increased lipid density with unsaturated lipids (Atkinson et al., 2010). As a result of this ordering effect, and of its own molecular dipole, α-tocopherol is likely to modulate the membrane dipole potential. The following section reports the changes in the dipole potential elicited by α-tocopherol in phosphatidylcholine vesicles in comparison to cholesterol and its oxidised counterpart, 7-ketocholesterol, discussed in the previous section. The effect of α-tocopherol on the dipole potential of membranes containing cholesterol or 7-ketocholesterol is then investigated and discussed in terms of the phase profiles, and resulting initial dipole potential, of these membranes.

3.2.1. The effect of α-tocopherol on the dipole potential of phosphatidylcholine vesicles

A series of egg-phosphatidylcholine (PC) vesicles containing α-tocopherol at concentrations up to 30mol% of total lipid were labelled with the dipole potential sensitive fluorescent probe, Di-8-ANEPPS. The difference spectra, reporting the degree of spectral shift of Di-8-ANEPPS, shown in figure 3.2.1 compare the change in dipole potential when 10mol% α-tocopherol, cholesterol or 7-ketocholesterol is incorporated into PC vesicles. α-Tocopherol decreases the dipole potential which is the same effect caused by 7-ketocholesterol. This is an interesting observation in the context of α-tocopherol's antioxidant action; α-tocopherol, in the protection of cholesterol from oxidation, prevents the decrease in dipole potential associated with 7-ketocholesterol, yet α-tocopherol itself decreases the dipole potential. The magnitude of the change, however, is much smaller than that of 7-ketocholesterol and closer to that caused by cholesterol in the opposite direction.

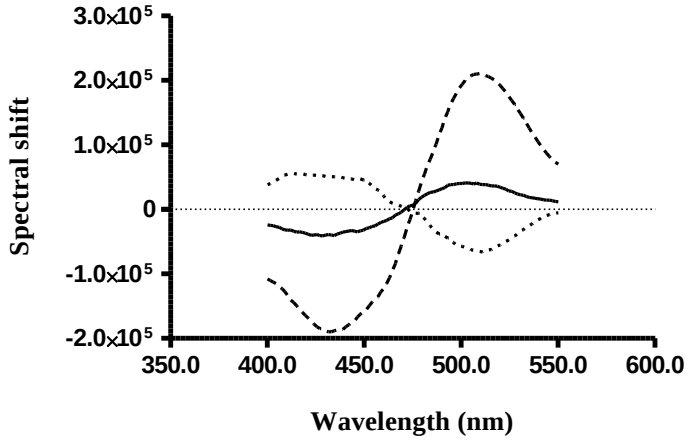

Figure 3.2.1: Difference spectra obtained by subtracting the excitation spectrum of Di-8-ANEPPS (λ_{em}=580nm) in 100% egg-phosphatidylcholine (PC) vesicles from that in 90mol%PC-10mol%α-tocopherol (—). The difference spectra for 90mol%PC-10mol%cholesterol (…) and 90mol%PC-10mol%7-ketocholesterol (----) from section 3.1.2 are also shown for comparison. Excitation spectra were obtained with n=3 for each vesicle composition and the difference spectra shown are the average of the 3 resulting difference spectra. Data is smoothed by a 4-point moving average to clarify the overall shape of the spectra.

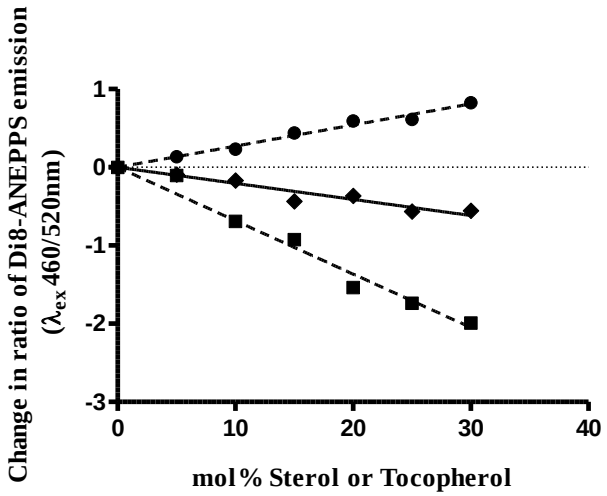

Figure 3.2.2: The change in ratio (R) of Di-8-ANEPPS fluorescence intensity at 460nm and 520nm excitation ($R=I_{460}/I_{520}$ λ_{em}=580nm) with increasing α-tocopherol (♦) concentration. The change in ratio with increasing cholesterol (●) and 7-ketocholesterol (■) concentration from section 3.1.2 are also shown for comparison. Increasing the α-tocopherol concentration linearly decreases the change in ratio indicating a decrease in dipole potential. The data are fitted to straight lines constrained to intercept at the origin yielding r^2=0.91 slope= -0.0206±0.0008mol%$^{-1}$ for PC-α-tocopherol vesicles and, r^2=0.98 slope= 0.0270±0.0005 and r^2=0.97 slope= -0.068±0.001 for PC-cholesterol and PC-7-ketocholesterol vesicles respectively. All slopes are significantly non-zero (P<0.01, one-tailed t-tests).

The relationship between the concentration of α-tocopherol (between 5mol% and 30mol%) and the dipole potential of PC vesicles is shown in figure 3.2.2 with that for cholesterol and 7-ketocholesterol also shown for comparison. The relationships are best represented by straight lines where the slope reflects the molar effectiveness of α-tocopherol, cholesterol or 7-ketocholesterol in changing the dipole potential. The magnitudes of the slopes are significantly different for the PC-α-tocopherol and PC-cholesterol vesicle series and the PC-α-tocopherol and PC-7-ketocholesterol vesicle series (one way ANOVA (P<0.0001, F=2204, R^2=0.999) followed

by Tukey's multiple comparison test, $P<0.05$ both cases). The ratio of the slope of the PC-α-tocopherol vesicle series with that of the PC-cholesterol and PC-7-ketocholesterol vesicle series are 0.76±0.03 and 0.30±0.01 respectively. The change in the dipole potential of PC vesicles by α-tocopherol is, therefore, approximately three-quarters of that caused by the equivalent concentration of cholesterol in the opposite direction, and approximately one-third of that caused by 7-ketocholesterol.

The polar moiety on the chromanol ring structure and hydrophobic carbon chain of α-tocopherol causes the molecule to insert into the bilayer perpendicular to the membrane surface, in a similar manner to cholesterol, with the hydrophobic tail alongside those of the phospholipids. The chromanol group is thought to locate in the interfacial region, or partially in the aqueous phase of the membrane (Fukuzawa et al., 1993) placing it slightly higher in the membrane than the ring system of cholesterol. The exact position of α-tocopherol in the membrane, however, is not clear and it is likely it has several depths of insertion depending of the lipid composition, and resulting hydration, of its environment (Atkinson et al., 2008). The depth of insertion is likely to influence the effect of α-tocopherol on lipid packing and its other interactions with membrane lipids, such as hydrogen bonding, and therefore its influence on the dipole potential, discussed in more detail below.

In the bilayer α-tocopherol preferentially associates with unsaturated fatty acids with preference increasing with degree of unsaturation (Stillwell et al., 1996). This causes a lateral phase separation with ordered α-tocopherol rich domains occurring in the liquid crystalline membrane (SanchezMigallon et al., 1996) confirmed by a broadening and lowering of the phase transition temperature of poly-unsaturated fatty acid containing membranes. This is consistent with earlier work showing α-tocopherol to both decrease the fluidity (in the context of acyl chain motion) (Urano et al., 1988b) and increase order (Wassall et al., 1986, Stillwell et al., 1990, Wassall et al., 1990, Suzuki et al., 1993) of the liquid crystalline phase of unsaturated PCs. These effects are attributed to a 'stabilisation' of the lipids by association or complex formation through hydrogen bonding of the hydroxyl (Erin et al., 1985) or methyl (Urano et al., 1988b) groups of α-tocopherol with moieties on the phospholipids (Atkinson et al., 2010).

In the mixed saturated/unsaturated lipid environment of the egg-PC membranes used in this study, α-tocopherol is likely to separate into PUFA- and α-tocopherol- rich domains in the liquid crystalline phase in a comparative way to the phase separation of cholesterol into saturated-lipid rich domains (Atkinson et al., 2010, Atkinson et al., 2008). As discussed in section 3.1.1 the tight packing of the lipids, increasing the dipole density, and the reduced depth of penetration of water in cholesterol- rich liquid ordered domains are likely to contribute to the increase in dipole potential elicited by cholesterol in the egg-PC membrane. α-Tocopherol,

however, decreases the dipole potential despite the increase in lipid order and packing within the liquid crystalline phase. This suggests that the dipole moment of α-tocopherol may have a component anti-parallel to the membrane normal, acting in the opposite direction to that of the surrounding lipids, providing a significant contribution towards decreasing in the dipole potential.

A similar argument is used by Bechinger and Seelig (Bechinger and Seelig, 1991) in explaining the origin of the decrease in dipole potential induced by a low concentration of phloretin in POPC bilayers. Low molar ratios of phloretin are not thought to affect the phase properties, and therefore lipid packing, of the bilayer and ^{2}H NMR experiments have detected no change in the ordering of water (hydration) around the lipid headgroups. The decrease in dipole potential is therefore ascribed to the arrangement of phloretin dipoles in an anti-parallel way to the carbonyl at the sn2 position of the phospholipids. The phloretin dipoles therefore neutralise this carbonyl dipole which has previously been shown to be the primary contribution from lipids to the dipole potential due to its orientation normal to the bilayer (Franklin and Cafiso, 1993, Gawrisch et al., 1992).

Interestingly, the ability of a simple sugar molecule to change the dipole potential of a DPPC membrane has been correlated with the extent of hydrogen bonding between the hydroxyl moiety of the sugar molecule and the sn2 carbonyl of the phospholipid (Diaz et al., 1999). This indicates that hydrogen bonding of a molecule with the carbonyls or phosphate oxygen, phospholipid moieties whose dipoles form the basis of the membrane dipole potential, is likely to alter the dipole potential. There is evidence that the phenol of α-tocopherol hydrogen bonds with the polar groups of phospholipids (discussed in Section 1.5.1) however, it should be noted that conflicting results have rendered this far from conclusive with parallel claims that it may not occur (Atkinson et al., 2008).

There are therefore several mechanisms by which α-tocopherol can decrease the dipole potential of egg-PC vesicles. Although the magnitude and direction of the change in dipole potential can be compared with that elicited by cholesterol and 7-ketocholesterol, it is not possible, without knowledge of the magnitude and direction of its molecular dipole, to speculate on the extent to which these difference may depend on the molecular dipole of α-tocopherol, its lipid ordering and hydration effects or the potential effects of its binding to dipolar moieties of the lipids.

3.2.2. The effect of α-tocopherol with cholesterol on the dipole potential of phosphatidylcholine membranes

In the previous section it was shown that α-tocopherol decreases the dipole potential of egg-phosphatidylcholine (PC) vesicles. As α-tocopherol has been shown to induce phase separation in phosphatidylcholine membranes forming α-tocopherol-rich ordered domains (Quinn, 2004) it is likely the dipole potential is not homogeneous over the membrane with these domains poised at a lower dipole potential than the bulk membrane. Similarly, cholesterol forms highly ordered (l_o) domains with saturated lipids which are thought to possess a higher dipole potential relative to the bulk membrane (Section 3.1.1). The changes in the dipole potential when α-tocopherol is incorporated with cholesterol into egg-PC vesicles are explored in the following figures and are interpreted in the context of the phase behaviours of α-tocopherol and cholesterol.

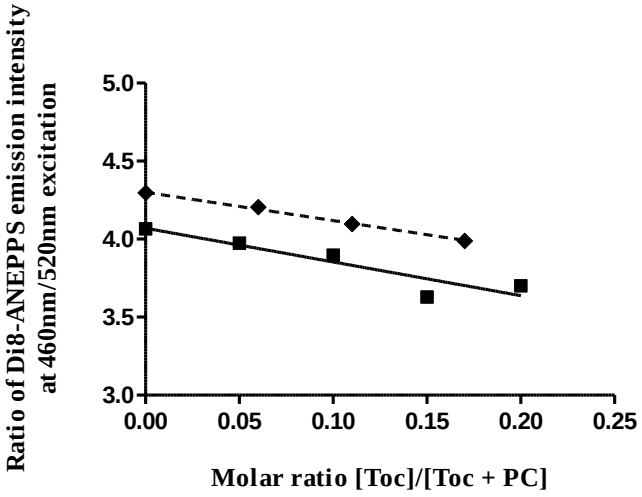

Figure 3.2.3: The ratio of Di-8-ANEPPS fluorescence intensity at 460nm and 520nm excitation ($R=I_{460}/I_{520}$ λ_{em}=580nm) with increasing α-tocopherol concentration, represented as the ratio of % mol concentration [Toc]/[Toc +PC], in PC (■) and PC-10mol%cholesterol (♦) vesicles . Each data point is the average of 3 repeats with the standard error of the mean as error bars. Fitting linear regressions to the data gives r^2=0.85 and slope=-2.2±0.1 for α-tocopherol-PC vesicle ratios (—) and r^2=0.99 and slope=-1.81±0.04 for α-tocopherol-cholesterol-PC vesicles (----). Both slopes are significantly non-zero (P=0.0043 and P=0.0004 respectively, one sample t-test).

Figure 3.2.3 shows the decrease in the dipole potential of a series of PC-10mol%cholesterol vesicles with increasing concentration of α-tocopherol (5-20mol%). The trend with increasing α-tocopherol concentration is similar in both PC-cholesterol and pure PC vesicles although the y-intercept is at a higher ratio for the PC-cholesterol vesicles series reflecting the higher initial magnitude of the dipole potential due to the presence of cholesterol. Comparing the slopes of the linear relationships of the two vesicle series reveals that the effectivity of α-tocopherol in decreasing the dipole potential in cholesterol containing PC vesicles is not significantly different from that in pure PC vesicles (one-way ANOVA P=0.0003, F=44.55, R^2=0.94 followed by Tukey's multiple comparison test, P>0.05). The effects of cholesterol and α-tocopherol on the dipole potential appear to be additive in this system, and the presence of 10mol% cholesterol has no effect on the extent to which α-tocopherol changes the dipole potential. This data suggests that, at 10mol% cholesterol, a high enough proportion of saturated

and unsaturated lipids in the liquid crystalline phase are not associated with cholesterol rich ordered domains allowing their ordering by α-tocopherol to occur to similar extent as in 100%PC vesicles, unperturbed by the presence of cholesterol.

As discussed in section 3.1.1, higher concentrations of cholesterol (>20mol%) result in larger cholesterol-rich domains and as the concentration is increased a phase transition resulting in the disruption of gel-phases and the co-existance of only the l_o and l_d phases occurs (Veatch et al., 2004, de Almeida et al., 2005, de Almeida et al., 2007). It is therefore interesting to see if these effects have any influence on the dipole potential changes elicited by α-tocopherol in the egg-PC membrane.

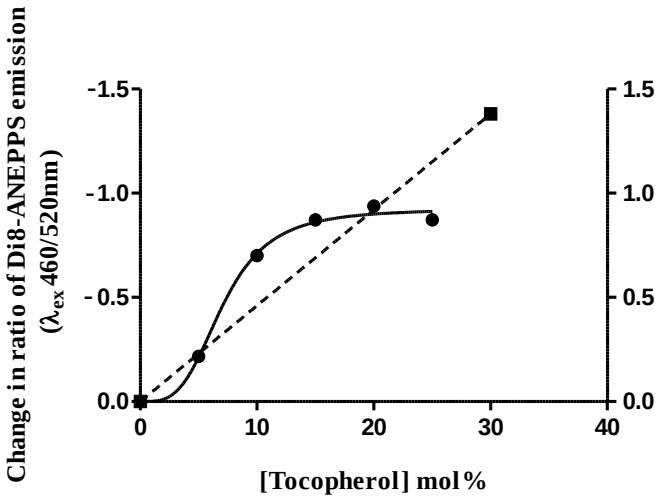

Figure 3.2.4: The change in ratio (R) of Di-8-ANEPPS fluorescence intensity at 460nm and 520nm excitation ($R=I_{460}/I_{520}$ λ_{em}=580nm) from a PC-30mol%cholesterol reference as the concentration of α-tocopherol is increased (5-25mol%)whilst maintaining a fixed 30mol% of non-PC component. The modulus of the change in ratio is shown on the right y-axis. The data is fitted to a sigmoidal curve showing the greatest change in dipole potential per unit increase in α-tocopherol concentration to occur between 5 and 10mol% α-tocopherol corresponding to 20-25mol% cholesterol. A straight line fit between PC-30mol% cholesterol and PC-30mol%α-tocopherol (----) denotes the relationship expected if the change in ratio caused by cholesterol and α-tocopherol were simply additive.

Figure 3.2.4 shows the change in ratio of Di-8-ANEPPS fluorescence at 460nm and 520nm excitation for a series of vesicles consisting of 70mol% PC and varying concentrations of α-tocopherol (0-25%) and cholesterol (5-30%) in the non PC component. The non-PC component is fixed at 30mol%, so as the concentration of α-tocopherol increases that of cholesterol decreases. The dotted line denotes the expected relationship if the effects of cholesterol and α-tocopherol on the dipole potential were additive as they were in Figure 3.2.3. The data, however, follows a sigmoidal relationship with an inflection between 5mol% and 10mol% α-tocopherol which may reflect a phase transition. De Almeida *et al*. (de Almeida et al., 2005) have used the steady state anisotropy of DPH and the lifetime weighted quantum yield of trans-parinaric acid to detect the l_o and l_d phase boundaries in ternary DOPC:PSM:Chol mixtures. Their data appears sigmoidal, however, it has been fit to three straight lines, the intercepts of which coincide with the phase boundaries of the system denoted in a phase diagram produced

previously by same group (de Almeida et al., 2003). Steady state anisotropy and lifetime weighted quantum yield are both properties of fluorescent probes that reflect the degree of order of their environment and as the dipole potential is affected by lipid packing density and hydration- parameters concurrent with order- it is likely that spectral shifts in Di-8-ANEPPS fluorescence may also reflect phase transitions.

In order to eliminate the event that the sigmoidal shape of figure 3.2.4 is an artefact of the changing relative concentration of cholesterol to PC this data is re-plotted with the molar fraction of cholesterol to total (cholesterol + PC) on the abscissa. For comparison the data for PC-cholesterol (5-30mol%) vesicles from figure 3.2.2 is also shown and this follows a single linear relationship consistent with all vesicle compositions existing in a single region of a phase plot (l_d + l_o). The data for cholesterol with α-tocopherol in egg-PC vesicles, however, best follows two straight lines of distinct slope which suggests that the compositions of the vesicles used may pass through a phase boundary.

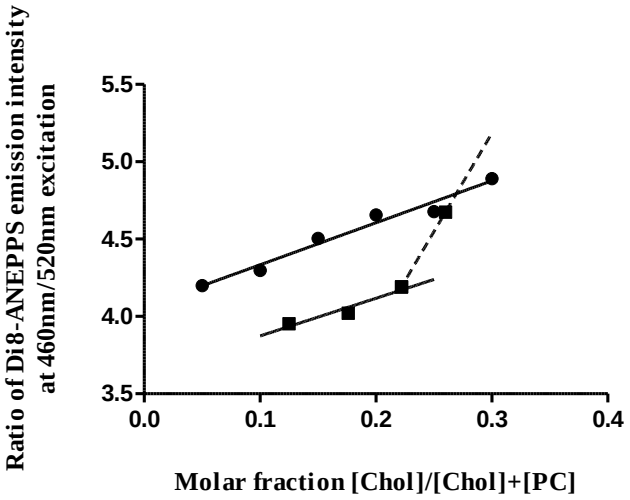

Figure 3.2.5 The ratio of Di-8-ANEPPS fluorescent intensity at 460nm and 520nm excitation in PC-Cholesterol vesicles (●) and PC-Cholesterol-α-tocopherol vesicles (■) represented as a molar fraction of cholesterol in total (cholesterol + PC) concentrations. The cholesterol-PC vesicles are fit to a straight line as originally shown in Figure 3.1.3. The PC-cholesterol-α-tocopherol data can be fit to two straight lines of distinct slopes which is thought to be as a result of a phase transition.

α-Tocopherol is known to decrease the temperature of the gel to liquid crystalline transition in saturated-PC membranes (Massey et al., 1982). Similar effects have also been shown by Fukuzawa *et al*. (Fukuzawa et al., 1979) in saturated lecithin membranes and, to a lesser extent, in mixed saturated/unsaturated egg-lecithin membranes, however, little effect is seen in soybean-lecithin membranes which possess a higher degree of unsaturation. This suggests that, although α-tocopherol preferentially localises with PUFAs in the liquid crystalline phase, in membranes which still possess a certain extent of saturated lipids, it is able to reduce the gel to liquid crystalline transition temperature of the saturated lipids. Figure 3.2.5 indicates that increasing cholesterol up to 30mol% does not induce a phase transition detected by Di-8-

ANEPPS spectral shifts, but the presence of 5mol% α-tocopherol with 25mol% cholesterol does. It is possible the presence of cholesterol-rich l_o phases, in reducing the fraction of membrane available to α-tocopherol and thus increasing the molar fraction of α-tocopherol to egg-PC, facilitates the decrease in gel to liquid crystalline transition temperature of the saturated lipid fraction.

Figure 3.2.6 presents the ratio data for PC vesicles containing both α-tocopherol and cholesterol in terms of the molar fraction of α-tocopherol in each vesicle composition and compares it to the ratios of a set of vesicles with increasing molar fraction of α-tocopherol in PC. α-Tocopherol alone in egg-PC membranes up to 30mol% does not induce a phase transition detectable with Di-8-ANEPPS however the situation is again very different in the presence of cholesterol. At lower molar fractions the membrane is exhibiting a very different trend in the changes to the dipole potential with increasing α-tocopherol concentration than at higher molar fractions perhaps reflecting the transition between two different phase landscapes.

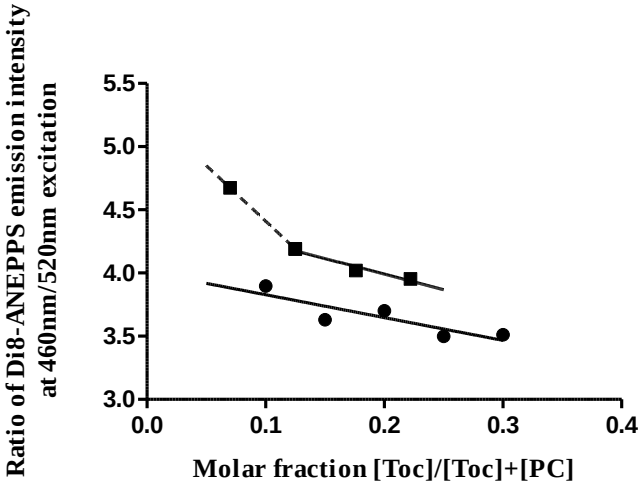

Figure 3.2.6: The ratio of Di-8-ANEPPS fluorescent intensity at 460nm and 520nm excitation in PC-α-tocopherol vesicles (●) and PC-cholesterol-α-tocopherol vesicles (■) represented as a molar fraction of α-tocopherol in total (α-tocopherol + PC) concentrations. The α-tocopherol-PC vesicles are fit to a straight line as originally shown in figure 3.2.2. The PC-cholesterol-α-tocopherol data can be fit to two straight lines of distinct slopes which is thought to be as a result of a phase transition.

These data demonstrate that, at concentrations of cholesterol above a molar fraction of ~0.25, the presence of cholesterol in the membrane significantly influences the effect of α-tocopherol on the membrane dipole potential perhaps by altering the changes in the phase landscape occurring with α-tocopherol.

3.2.3. The effect of α-tocopherol with 7-ketocholesterol on the dipole potential of phosphatidylcholine membranes

7-ketocholesterol has very different behaviour in membranes than its unoxidised precursor. Although it forms ordered domains with saturated lipids in a similar manor to cholesterol, its influence on the dipole potential is significantly greater and acting in the opposite direction to

that of cholesterol. This may be attributed to larger contribution of the molecular dipole moment of 7-ketocholesterol, due to the tilted orientation of the molecule, in the liquid disordered (l_d) phase with respect to the liquid ordered (l_o) phase. In the following figures, the changes in the dipole potential when α-tocopherol is incorporated with 7-ketocholesterol into egg-PC vesicles are investigated. A comparison is made with the results of the α-tocopherol/cholesterol/egg-PC vesicle system of the previous section as cholesterol and 7-ketocholesterol show some similarity in their phase behaviours in PC membranes.

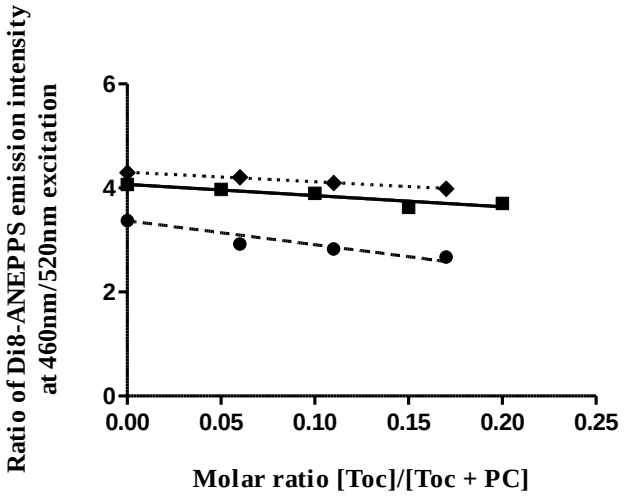

Figure 3.2.7: The ratio of Di-8-ANEPPS fluorescence intensity at 460nm and 520nm excitation ($R=I_{460}/I_{520}$ λ_{em}=580nm) with increasing α-tocopherol concentration, represented as the ratio of % mol concentration [Toc]/[Toc +PC], in PC (■), PC-10mol%cholesterol (♦), and PC-10mol%7-ketocholesterol (●) vesicles . Each data point is the average of 3 repeats with the standard error of the mean as error bars. The linear fits to the α-tocopherol-PC (—) and cholesterol-PC (**…**) vesicle ratios are described in Figure.3.2.2. A straight line was also fitted to the mixed PC/α-tocopherol/7-ketocholesterol vesicle ratios (----) yielding r^2=0.86 and slope=-4.6±0.3 which is significantly non-zero (P=0.0036, one sample t-test).

Figure 3.2.7 shows the decrease in the dipole potential of a series of PC-10mol%7-ketocholesterol vesicles with increasing concentration of α-tocopherol (5-20mol%). Also shown is the decrease in dipole potential with increasing α-tocopherol concentration in PC and PC-cholesterol vesicles. The relationships are fitted with a linear regression and the different ratios of the y-intercepts reflect the differences in the initial dipole potential of the PC, PC-cholesterol and PC-7-ketocholesterol vesicles. The slopes of the linear relationships reflect the efficacy of α-tocopherol in changing the dipole potential in the different vesicle systems. A one-way ANOVA ($P<0.0001$, $F=70.07$, $R^2=0.96$) followed by Tukey's multiple comparison test on the slopes reveals the decrease in dipole potential on increasing α-tocopherol concentration to be significantly greater in PC-7-ketocholesterol vesicles than in PC vesicles ($P<0.001$). The slopes for the PC and PC-cholesterol vesicle series are not significantly different and it follows that the slope for the PC-7-ketocholesterol vesicle series is significantly greater from that of the cholesterol containing vesicles ($P<0.001$). This reveals that the presence of 10mol% cholesterol does not alter the effect of α-tocopherol on the dipole potential of egg-PC vesicles, but the

presence of 10mol% 7-ketocholesterol influences α-tocopherol such that it has a greater effect in decreasing the dipole potential.

The differences in the influence of α-tocopherol, in cholesterol or 7-ketocholesterol containing vesicles may be due to differences in the localisation of α-tocopherol in the membrane relative to the sterols. Cholesterol associates with both saturated lipids promoting the formation of the highly ordered l_o domains and unsaturated lipids ordering the l_d phase. The data presented in the previous section suggests that this behaviour with 10mol% cholesterol may not significantly alter the phases formed by α-tocopherol in these vesicles.

7-ketocholesterol has a lower tendency to form ordered domains with saturated lipids so a greater proportion localises in the l_d phase, resulting in a decrease in the proportion of l_o to l_d phases, compared with cholesterol. 7-ketocholesterol orders the l_d phase to less of an extent than cholesterol due to its tilted orientation in this phase. It is likely that these effects may alter the position of α-tocopherol in the membrane, its partitioning between ordered and disordered phases, and its ability to influence lipid ordering in the 7-ketocholesterol-PC membrane relative to the cholesterol-PC membrane altering its influence on the dipole potential.

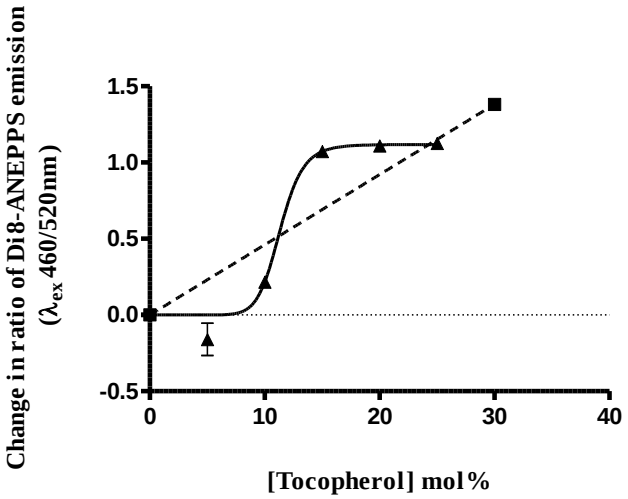

Figure 3.2.8: The change in ratio of Di-8-ANEPPS fluorescence intensity at 460nm and 520nm excitation from a PC-30mol%7-ketocholesterol reference as the concentration of α-tocopherol is increased (5-25mol%)whilst maintaining a fixed 30mol% of non-PC component. The data is fit to a sigmoidal curve showing the greatest change in dipole potential per unit increase in α-tocopherol concentration to occur between 10 and 15mol% α-tocopherol corresponding to 15-20mol% 7-ketocholesterol. A straight line fit between PC-30mol% 7-ketocholesterol and PC-30mol%α-tocopherol (----) denotes the relationship expected if the change in ratio caused by 7-ketocholesterol and α-tocopherol were simply additive.

Figure 3.2.8 shows the change in ratio of Di-8-ANEPPS fluorescence at 460nm and 520nm excitation for a series of vesicles consisting of 70mol% PC and varying concentrations of α-tocopherol (0-25%) and 7-ketocholesterol (5-30%). As the non-PC component is fixed at 30mol%, the concentration of α-tocopherol increases relative to that of 7-ketocholesterol. The dotted line denotes the expected relationship if the effects of 7-ketocholesterol and α-tocopherol

on the dipole potential were additive. The data follows a sigmoidal relationship as was observed in the parallel experiment with cholesterol and α-tocopherol containing vesicles. The inflection lies between 10mol% and 15mol%, whereas in the presence of cholesterol this occurred from 5-10mol%, and this difference may reflect the different affinities for cholesterol and 7-ketocholesterol to form l_o domains. The inflection is also less broad with 7-ketocholesterol than with cholesterol occurring over a smaller range of α-tocopherol concentrations, perhaps reflecting the relative stability of the l_o phases formed by the sterols.

This data, plotted with the molar fraction of 7-ketocholesterol to (7-ketocholesterol + PC) in the abscissa (figure 3.2.9), can be fitted to two linear relationships of distinct slopes indicating the existence of different phase landscapes when the concentration of 7-KC is less than or greater than α-tocopherol. This is in contrast to the single linear regression of the data from the PC-7-ketocholesterol vesicle series where no distinct change in the trend of the dipole potential decrease with 7-ketocholesterol concentration is apparent. The molar fraction at which the lines intersect is lower for 7-ketocholesterol than for cholesterol and again may reflect their different tendencies to form l_o phases and differences in the influence of α-tocopherol on their phase behaviour.

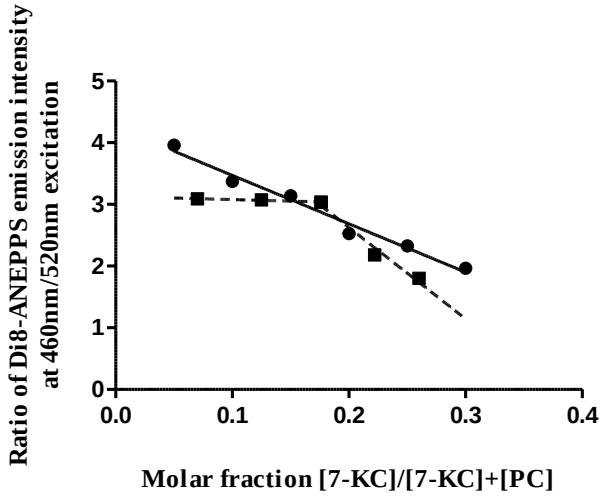

Figure 3.2.9: The ratio of Di-8-ANEPPS fluorescent intensity at 460nm and 520nm excitation in PC- 7-ketocholesterol vesicles (●) and PC- 7-ketocholesterol- α-tocopherol vesicles (■) represented as a molar fraction of 7-ketocholesterol in total (7-ketocholesterol + PC) concentrations. The 7-ketocholesterol-PC vesicles are fit to a straight line as originally shown in figure 3.2.6. The PC-7-ketocholesterol-α-tocopherol data can be fit to two straight lines of distinct slopes which is thought to be as a result of a phase transition.

Presenting this data in terms of the molar fraction of α-tocopherol in each of the α-tocopherol and 7-ketocholesterol containing vesicles (Figure 3.2.10) demonstrates the influence of α-tocopherol on the dipole potential to follow two distinct trends in the presence of 7-ketocholesterol compared with only one in PC alone. At lower molar fractions α-tocopherol significantly increases the dipole potential in the presence of 7-ketocholesterol in contrast to its effects in PC vesicles without the sterol. At higher molar fractions the trend with increasing α-

tocopherol concentration is still to increase the dipole potential but with a considerably smaller effect per unit concentration increase. This indicates that the extent of the influence of α-tocopherol on the dipole potential depends on the relative proportion of 7-ketocholesterol to α-tocopherol in the membrane.

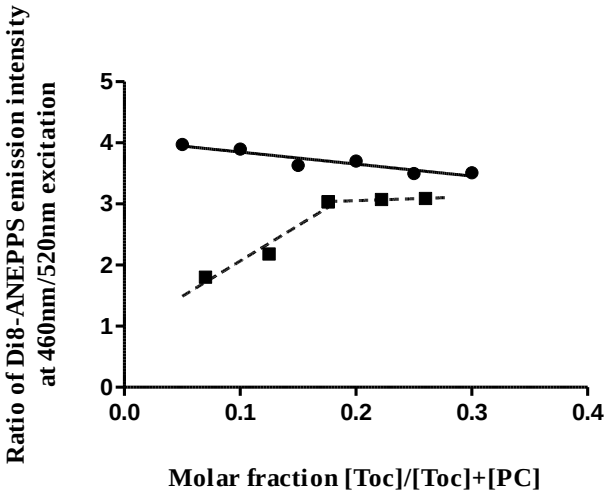

Figure 3.2.10: The ratio of Di-8-ANEPPS fluorescent intensity at 460nm and 520nm excitation in PC- α-tocopherol vesicles (●) and PC- 7-ketocholesterol- α-tocopherol vesicles (■) represented as a molar fraction of α-tocopherol in total (α-tocopherol + PC) concentrations. The α-tocopherol-PC vesicles are fit to a straight line as originally shown in figure 3.2.6. The PC-7-ketocholesterol-α-tocopherol data can be fit to two straight lines of distinct slopes which is thought to be as a result of a phase transition.

To further investigate the possibility that Di-8-ANEPPS is reflecting a significant change in the phase environment within the vesicles as the relative proportion of α-tocopherol to cholesterol (Figure 3.2.4) or 7-ketocholesterol (Figure 3.2.8) changes, a second derivative analysis[1] was conducted on the excitation spectra of Di-8-ANEPPS in selected composition vesicles featured in Figure 3.2.8. In all composition vesicles (70%PC-30%7-KC, 70%PC-20%7-KC-10%A-tocopherol, 70%PC-10%7-KC-20%α-tocopherol and 70%PC-30%α-tocopherol) two components were identified suggesting that Di-8-ANEPPS was present in two environments of different dipole potential. An unconstrained two-component curve-fit[1] of the Di-8-ANEPPS excitation spectra in each vesicle composition identified the long- and short- wavelength peak positions (λ_l and λ_s respectively) of the two component spectra (shown in Figure 3.2.11). A further parameter investigated was the ratio of the areas of the short- and long- wavelength spectral components (A_s/A_l), which are also given in Figure 3.2.11. The ratio of the areas, assuming Di-8-ANEPPS distributes homogeneously in the membranes, could reflect the relative extent of the two environments of different dipole potential detected.

[1] Many thanks to C.Peter Winlove and Ellen M. Green of the Biomedical Physics Group, University of Exeter for performing the second derivative and curve fitting analyses using WiRE 3.0 software by Renishaw (available at http://www.renishaw.com/raman)

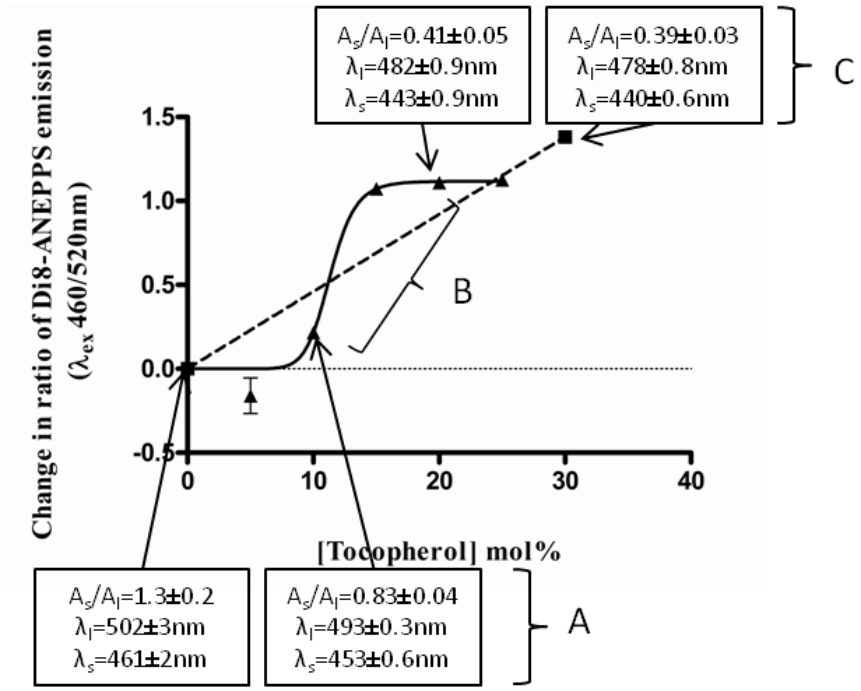

Figure 3.2.11: The graph of Figure 3.2.8 representing the spectral shift of Di-8-ANEPPS on increasing the proportion of α-tocopherol to 7-ketocholesterol within a fixed 30mol% non-PC component in 70% PC vesicles. Data points within the graph are annotated with the peak wavelengths and ratio of the area of the two spectral components identified within the corresponding Di-8-ANEPPS excitation spectrum. The pairs of data points whose excitation spectra parameters are compared using a t-test (Table 3.2.1) are annotated: **A** in the initial part, **B** either side of the inflection and **C** within the plateau of the sigmoidal relationship.

These parameters are compared for pairs of vesicle compositions that, on the plot of their change in ratio of Di-8-ANEPPS fluorescence against α-tocopherol concentration (Figure 3.2.8 and 3.2.11), fall within the initial part of the sigmoidal relationship (labelled A), either side of the inflection (B) or within the following plateau (C). Table 3.2.1 summarises the results of t-tests between these pairs. Interestingly, the area ratios within group A or group C are not significantly different however; the area ratios for vesicle compositions falling either side of the inflection (group B) are very significantly different. This indicates that a significant change in the proportion of Di-8-ANEPPS residing in higher and lower dipole potential regions occurs at this point. This may reflect a change in the relative proportion of domains of higher or lower dipole potential and therefore a significant change in the phase profile of the vesicles. The peak wavelengths of the spectra representing the higher and lower dipole potential regions are just significantly different in groups A and C. This indicates that the replacement of 10mol% 7-KC with α-tocopherol results in a significant change in the dipole potential of the two environments detected from PC-30mol% 7-KC vesicles. Likewise the dipole potential of the two environments is also significantly different between PC-20mol% α-tocopherol- 10mol% 7-KC and PC-30mol% α-tocopherol vesicles. Interestingly, both long- and short- wavelength peaks are significantly different to a much greater degree in group B with shifts in the peak positions of ~10nm. This could suggest that α-tocopherol is influencing the dipole potential in both environments and, although it is not possible to directly attribute the higher and lower dipole

potential environments to specific phases present, suggests α-tocopherol could affect both phases detected.

	A	**B**	**C**
Area Ratio A_s/A_l	ns	**	ns
Long wavelength λ_l	*	***	*
Short wavelength λ_s	*	***	*

Table 3.2.1: The results of a unpaired two-tailed t-tests comparing the ratio of areas, long wavelength peak and short wavelength peak of the two spectral components identified within each Di-8-ANEPPS excitation spectrum for pairs of data points annotated in figure 3.2.11. **A** represents a pair of data point in the initial part of the sigmoidal relationship, **B** a pair of data points either side of the sigmoidal inflection and **C** a pair of data points within the plateau after the inflection. Significant differences are denoted by *** ($P<0.001$), ** ($P<0.01$) or * ($P<0.05$) and 'ns' denotes a difference that was not significant.

This analysis has confirmed that there is a significant difference in the environments detected by Di-8-ANEPPS in the initial and latter part of the sigmoidal relationship of Figure 3.2.8 (and 3.2.11) which suggests that the corresponding vesicles could have different phase profiles with the sigmoidal inflection reflecting a transition between them. The comparison of area ratios of the long- and short- wavelength spectra to indentify changes in the proportion of the lower and higher dipole potential environments does, however, have its limitations. This relies on the assumption that Di-8-ANEPPS is distributed homogeneously in the membrane which is unlikely to be the case. It is also possible that other factors, such as changes in the fluidity of the membrane in the environment of the probe, may alter the shape of the spectra which will also influence the area ratios.

3.3. The interaction of α-tocopherol succinate with phosphatidylcholine vesicles

α-Tocopherol succinate is a structural analogue of α-tocopherol with the addition of a succinate ester moiety bonded through the hydroxyl present on the chromanol group of α-tocopherol. This gives the molecule greater water solubility compared with α-tocopherol (Halliwell and Gutteridge, 1999) facilitating the study of its interaction with membranes when added to the external environment. This section investigates the concentration dependent interaction of α-tocopherol succinate with phosphatidylcholine (PC) vesicles through measurement of the membrane surface and dipole potentials. Comparison of the changes in dipole and surface potentials with equivalent α-tocopherol succinate treatment to 100%PC vesicles and PC vesicles with various molar fractions of cholesterol and 7-ketocholesterol provides insight into the position of α-tocopherol succinate in the membrane and preference for specific lipids or lipid phases which may result in heterogeneity of its lateral localisation in the membrane. The effect of α-tocopherol succinate on the dipole potential is also compared to that of α-tocopherol to confirm this effect is shared by both anti-oxidant and non-antioxidant structural analogues.

3.3.1. The effects of α-tocopherol succinate on the surface potential

The succinate ester moiety of α-tocopherol succinate consists of a free carboxyl group at the end of a 4-carbon chain. The pK_a for this is 5.64 (Neuzil et al., 2002) and, using the Henderson-Hasselbach equation, it can be deduced that, at pH7.4, the greater proportion of α-tocopherol succinate is in a deprotonated form. This endows α-tocopherol succinate with a negative charge which can be used to detect its binding to membranes through its effect on the membrane surface potential (Wall et al., 1995b). As a charged molecule approaches and binds to the membrane surface the charge landscape of the membrane, and therefore the surface potential, is altered. This can be detected using FPE which has a quantum yield dependent on its ionisation state and, when incorporated in the membrane and at constant pH, reflects changes in the surface potential (Wall et al., 1995b).

Figure 3.3.1 shows the decrease in intensity of FPE labelled PC vesicles (λ_{ex}=490nm λ_{em}=520nm) on addition of α-tocopherol succinate. The addition of an equivalent volume of ethanol, the solvent used for α-tocopherol succinate, causes no significant change in the intensity of FPE. Calcium ions, having the opposite charge to α-tocopherol succinate, cause an increase in the intensity.

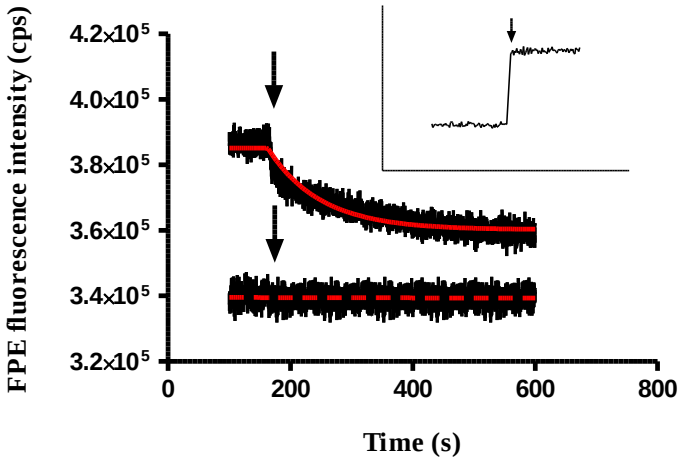

Figure 3.3.1: *Main* The change in emission intensity of FPE labelled 100% PC vesicles on addition of 3.77μM α-tocopherol succinate (*upper trace*) which is partially unprotonated (negatively charged) at pH 7.4. The trace is fit to an exponential decay (—). The change in intensity observed for an equivalent volume addition of the solvent (ethanol, *lower trace*) is also shown as a control and fits a straight horizontal line (----). This is placed at a lower intensity for clarity. The arrows indicate the point at which the addition was made. *Inset* the change in intensity on addition of 2mM calcium (positively charged) displaying an opposite effect.

FPE is located in the membrane such that the carboxyl and hydroxyl moieties, whose ionisation state dictates the quantum yield of the fluorophore, sit at the lipid water interface. Here the surface potential is at its largest before decaying exponentially with distance along the normal from the membrane surface. A free charge must, therefore, be in very close proximity to the lipid-water interface of the membrane surface to induce a change in the surface potential resulting in a change in FPE fluorescence intensity. The change in intensity of FPE on addition of α-tocopherol succinate therefore confirms that the molecule is, at least partially, deprotonated and the carboxyl group of the succinate moiety is located at the lipid-water interface. This is in agreement with Massey (Massey, 2001) who performed a similar experiment using a ratiometric technique to determine changes in the spectral properties of 4-heptadecyl-7-hydroxy-coumarin (HC) in response to changes in the surface potential.

The exponential-type decrease in FPE intensity following the addition of α-tocopherol succinate is in contrast to the instantaneous increase in intensity on Ca^{2+} addition (see Figure 3.3.1). This reflects the nature of the interaction of these charged moieties with the membrane. Ca^{2+} enters the lipid-water interface changing the FPE intensity seemingly instantaneously due to its rapid diffusion. The intensity profile after addition of α-tocopherol succinate suggests this molecule binds and inserts into the membrane with an equilibrium intensity being reached once the molecule is fully inserted placing its charged moiety at the membrane surface. This is consistent with the positioning of the hydrophobic phytyl chain among the lipid acyl chains in the hydrophobic region of the membrane, orienting the molecule parallel to the membrane normal (Massey, 2001).

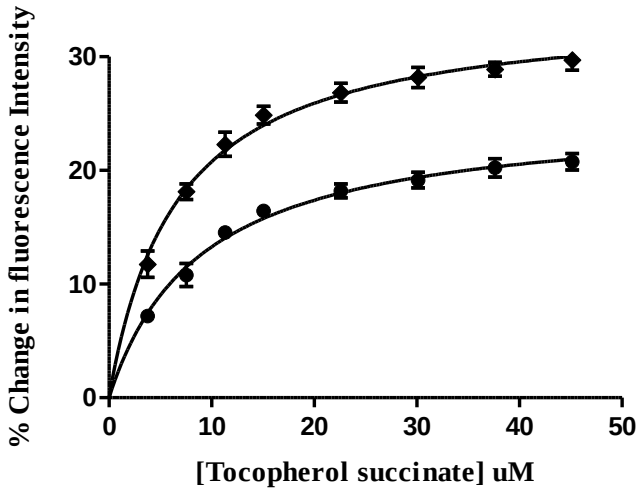

Figure 3.3.2: The percentage change in emission intensity of FPE (λ_{ex}=490nm λ_{em}=520nm) labelled 100%PC (♦) and 70mol%PC-30mol%cholesterol (●) vesicles on addition of α-tocopherol succinate. Measurements were taken once equilibrium in intensity was achieved following each addition and are the average of 3 repeats with error bars reflecting the standard error of the mean. The data is corrected for the change in surface potential due to the addition of the solvent, ethanol, and, as the intensity decreases with each addition, the *magnitude* of the change is plotted allowing the fit of a hyperbolic saturation binding equation, the results of which are shown in table 3.3.1.

The change in FPE intensity as the surface potential is changed with α-tocopherol succinate binding can be used to form a binding curve for this interaction. Figure 3.3.2 shows such binding curves for α-tocopherol succinate to 100%PC and 70%PC-30% cholesterol vesicles. The curves are fitted to a hyperbolic saturation binding model (Equation 3.3.1) where B_{max} is the maximum percentage change in intensity when a saturation concentration of α-tocopherol succinate has bound and k_d is the concentration (in μM) at which half this intensity is reached. The B_{max} and k_d values for α-tocopherol succinate titration to 100%PC and 70%PC-30% cholesterol vesicles are given in Table 3.3.1.

$$y = \frac{B_{max}x}{k_d+x} \qquad \textit{Equation 3.3.1}$$

The K_d values are not significantly different, but the B_{max} value for α-tocopherol succinate binding to 70%PC-30%cholesterol vesicles is significantly higher than for 100%PC vesicles (one way ANOVAs and Tukey's tests, see table 3.3.2).This suggests that there is little difference in the binding affinity of α-tocopherol succinate to each membrane, however, the effect on the surface potential is significantly different. This can be quantified by calculating K_{eff}, a parameter denoting the effectiveness of unit molar concentration of α-tocopherol succinate in changing the surface potential, by dividing B_{max} by K_d. K_{eff} values are shown in Table 3.3.1 and the K_{eff} for α-tocopherol succinate in 70%PC-30%cholesterol vesicles is significantly higher than in 100%PC vesicles (One way ANOVA and Tukey's test, table 3.3.2.). Both PC and cholesterol are overall electrostatically neutral, therefore the change in surface potential on addition of α-tocopherol succinate is purely due to the addition of its charge at the lipid-water interface and any interactions with lipids are not likely to additionally contribute to

the surface potential. In view of the similarity in K_d values, the significantly different K_{eff} values are surprising.

One possible explanation involves the heterogeneous distribution of FPE in the membrane and the colocalization of α-tocopherol succinate with FPE. FPE consists of a fluorescein moiety conjugated to DPPE with 16 carbon-chain saturated fatty acid tails. DPPE has a transition temperature of 63°C (Silvius, 1982) and, although the presence of the fluorescein conjugate will likely affect this, in 30mol% cholesterol containing egg-phosphatidylcholine vesicles it is known to preferentially partition into cholesterol-rich l_o domains with other saturated lipids (Wall et al., 1995a, Duggan et al., 2008). The increased K_{eff} in vesicles with cholesterol is therefore potentially explained by the localization of α-tocopherol succinate in FPE-rich regions where a greater number of FPE molecules are influenced per α-tocopherol succinate molecule.

α-tocopherol succinate is therefore potentially binding to two different environments of PC-cholesterol membranes, one of which has an increased concentration of FPE relative to the other. In this case the binding curve shown in figure 3.3.2 is the sum of the profiles of α-tocopherol succinate binding to each of the environments or 'binding sites'. Fitting a two-site saturation binding hyperbolic equation (Equation 3.3.2) allows the relative affinity of α-tocopherol succinate for the two environments to be determined. The first and second term of this equation represent the saturation binding profiles to the first and second binding sites, respectively.

$$y = \frac{B_{max1}\,x}{k_{d1}+x} + \frac{B_{max2}\,x}{k_{d2}+x} \qquad \textit{Equation 3.3.2}$$

In the PC-cholesterol membrane the first binding site can be assigned to the PC regions that are not perturbed by cholesterol, and can be assumed to yield a closely similar binding profile to that of the 100%PC membrane. The second binding site represents the region(s) of high FPE concentration occurring with the presence of cholesterol that is not present in the 100%PC membrane. Fitting equation 3.3.2 to the binding curve for 70%PC-30% cholesterol vesicles, with the B_{max} and K_d values for the binding profile to 100%PC vesicles (table 3.3.1) as B_{max1} and K_{d1}, gives K_{d2}=3±1 which is significantly lower than K_{d1} (unpaired two-tailed t-test P=0.022). This indicates that the binding affinity of α-tocopherol succinate for the second binding site, most likely cholesterol-rich l_o domains, is significantly higher than the affinity for the rest of the membrane.

This analysis, however, has limitations; it does not take into account the differences in: PC concentration (mol %), in the occurrence of gel-phase domains, or in the heterogeneous localisation of FPE, between the membranes. Not constraining B_{max1} to equal the B_{max} value

returned from the simple hyperbolic fit to 100%PC vesicles would improve the consideration of these factors in this model. The result, however, is ambiguous in the returned values of B_{max1} and $K_{d1,2}$ as there are many combinations of values for these parameters leading to curves with equally good fits to the data. A reason for this is the nature of the data; the data fits the simpler one-site hyperbolic model (Equation 3.3.1) very well and there is no evidence to suggest a second component (supported by inspection of figure 3.3.2), therefore there is no apparent indication for fitting the more complex two-site hyperbolic model. In this case, although the data doesn't display a requirement for a two-site binding model, it is scientifically valid to apply one based on the argument of the differences in α-tocopherol succinate colocalisation with FPE between membranes (indicated by different K_{eff}s) discussed above.

The binding affinity of α-tocopherol succinate to the membrane has been shown to have a strong dependence on cholesterol and, in cholesterol-containing PC membranes, α-tocopherol succinate is likely to have two binding affinities representative of its binding to cholesterol-rich l_o domains and PC l_d domains. Previously in this chapter it has been shown that 7-ketocholesterol, an oxidised form of cholesterol, has dramatically different effects on the membrane dipole potential. In the case of cholesterol, the increase in dipole potential it elicits is partly attributed to the increase in lipid order and packing density which define the l_o phase. It follows that the oxidation of cholesterol to 7-ketocholesterol is likely to alter the interaction of α-tocopherol succinate with membranes. To investigate this, cholesterol oxidation was modelled by a series of PC vesicles in which the ratio of 7-ketocholesterol to cholesterol was increased whilst keeping the concentration of PC constant. The binding curves of α-tocopherol succinate to these vesicles are shown in figure 3.3.3.

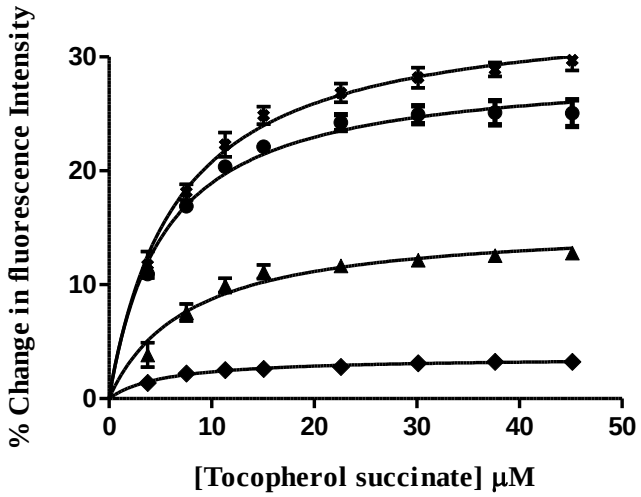

Figure 3.3.3: The percentage change in emission intensity of FPE (λ_{ex}=490nm λ_{em}=520nm) labelled 100%PC (▼), 70mol%PC-30mol%cholesterol (■), 70mol%PC-25mol%cholesterol-5mol%7-ketocholesterol (●), 70mol%PC-15mol%cholesterol-15mol%7-ketocholesterol (▲) and 70mol%PC-30mol%7-ketocholesterol (♦) vesicles on addition of α-tocopherol succinate. The data are fit to a hyperbolic saturation binding equation the results of which are shown in Table 3.3.1.

The curves are firstly fitted to the one-site hyperbolic saturation binding model (Eq. 3.3.1) and the B_{max}, K_d and calculated K_{eff} values are given in table 3.3.1. One-way ANOVAS followed by Tukey's multiple comparison tests show K_d is not significantly different between vesicle compositions, but B_{max} is significantly different in all cases and decreases as the mol% cholesterol decreases and mol% 7-ketocholesterol increases (see Table 3.3.2).

The change in K_{eff} values with vesicle composition reveals more evidence for the binding of α-tocopherol succinate to cholesterol-rich l_o domains. There is no significant difference between the K_{eff} values for 70mol%PC-30mol%cholesterol and 70mol%PC-25mol%cholesterol-5mol%7-ketocholesterol. In the latter membrane the l_o phase domains are still likely to be present and not much perturbed by the presence of a low concentration of 7-ketocholesterol and the similar K_{eff} values suggest that α-tocopherol succinate binds the l_o domains in this membrane also. When the vesicles consist of an equal molar ratio of cholesterol to 7-ketocholesterol the K_{eff} is significantly reduced together with the extent of cholesterol-rich l_o domains, due to the lower concentration of cholesterol and disruption by 7-ketocholesterol (Massey 2005). The K_{eff} of this composition is not significantly different from 100%PC vesicles suggesting similar co-localisation of FPE and α-tocopherol succinate in both systems and the absence of a secondary binding site for α-tocopherol succinate.

Vesicle composition	B_{max} (%)	K_d (μM)	K_{eff} (μM^{-1})	R^2
PC_{100}	25.13±0.82	8.94±0.94	2.31±0.31	0.948
$PC_{70}Chol_{30}$	34.41±0.87	6.57±0.62	5.24±0.51	0.947
$PC_{70}Chol_{25}7\text{-}KC_5$	29.15±0.72	5.41±0.55	5.39±0.56	0.858
$PC_{70}Choll_{15}7\text{-}KC_{15}$	15.46±0.82	7.77±1.40	2.35±0.26	0.958
$PC_{70}7\text{-}KC_{30}$	3.64±0.22	5.53±1.32	0.66±0.16	0.716

Table 3.3.1: The parameters of fit of a hyberbolic saturation binding model to data of figures 3.3.1 and 3.3.2 representing the percentage change in emission intensity of FPE in the given composition vesicles on titration of α-tocopherol succinate. Vesicle compositions are expressed as the mol% of each component as a numerical subscript (e.g. $PC_{70}Chol_{15}7\text{-}KC_{15}$ represents a 70mol%PC-15mol%cholesterol-15mol% 7-ketocholesterol vesicle). R^2 is the goodness of fit, B_{max} (%) the % change in intensity when a saturation concentration of α-tocopherol succinate has bound and K_d (μM) is the concentration of α-tocopherol succinate at which half this % change in intensity is achieved. K_{eff}, calculated by dividing B_{max} by K_d, is a measure of the effectiveness of molar concentration of α-tocopherol succinate in decreasing the surface potential.

	B_{max}	K_d (μM)	K_{eff} $(\mu M)^{-1}$
PC vs $PC_{70}Cholesterol_{30}$	***	ns	**
PC vs $PC_{70}Cholesterol_{25}7\text{-}KC_5$	*	ns	**
PC vs $PC_{70}Cholesterol_{15}7\text{-}KC_{15}$	***	ns	ns
PC vs $PC_{70}7\text{-}Ketocholesterol_{30}$	***	ns	*
$PC_{70}Cholesterol_{30}$ vs $PC_{70}Cholesterol_{25}7\text{-}KC_5$	**	ns	ns
$PC_{70}Cholesterol_{30}$ vs $PC_{70}Cholesterol_{15}7\text{-}KC_{15}$	***	ns	**
$PC_{70}Cholesterol_{30}$ vs $PC_{70}7\text{-}Ketocholesterol_{30}$	***	ns	***
$PC_{70}Cholesterol_{25}7\text{-}KC_5$ vs $PC70Cholesterol_{15}7\text{-}KC_{15}$	***	ns	**
$PC_{70}Cholesterol_{25}7\text{-}KC_5$ vs $PC_{70}7\text{-}Ketocholesterol_{30}$	***	ns	***
$PC_{70}Cholesterol_{15}7\text{-}KC_{15}$ vs $PC_{70}7\text{-}Ketocholesterol_{30}$	***	ns	ns

Table 3.3.2: The results of Tukey's multiple comparison test following one-way ANOVAS on the B_{max}, (R^2=0.99, P<0.0001, F=368.2) k_d (R^2=0.90, P=0.0002, F=25.07) and K_{eff} (R^2=0.97, P<0.0001, F=90.21) values given in table 3.3.1 which reflect α-tocopherol succinate titrations to various composition vesicles labelled with FPE. Significant differences are represented by *** (P<0.001), ** (P<0.01) or * (P<0.05) and 'ns' denotes a difference that was not significant.

The two-site hyperbolic saturation binding model (Equation 3.3.2) can be fitted to the binding profile to 70%PC-25% cholesterol-5% 7-ketocholesterol membrane but does not well represent the binding profile to 70%PC-15% cholesterol-15% 7-ketocholesterol membrane supporting the suggestion that the secondary binding site of α-tocopherol succinate in cholesterol containing PC membranes are l_o domains.

Interestingly, fitting the two-site hyperbolic model to the binding profile to 70%PC-30% 7-ketocholesterol membrane yields a B_{max} value for the secondary binding site (B_{max2}) that is

negative. This suggests that in the presence of 7-ketocholesterol the percentage change in FPE fluorescence caused by the binding of a saturating concentration of α-tocopherol succinate is less than in 100%PC. 7-ketocholesterol also forms ordered l_o-like domains in mixed saturated/unsaturated lipid systems {Mintzer, 2010, Interaction of two oxysterols`, 7-ketocholesterol and 25-hydroxycholesterol`, with phosphatidylcholine and sphingomyelin in model membranes}such as the egg-PC liposome system used here. The lower B_{max} value may be due to a low binding affinity of α-tocopherol succinate for these domains or they may also serve as a domain environment capable of sequestering FPE from α-tocopherol succinate.

3.3.2. α-Tocopherol succinate and the dipole potential

This section investigates the effect of α-tocopherol succinate on the membrane dipole potential and investigates whether this potential can similarly be used to monitor the association of α-tocopherol succinate with membranes.

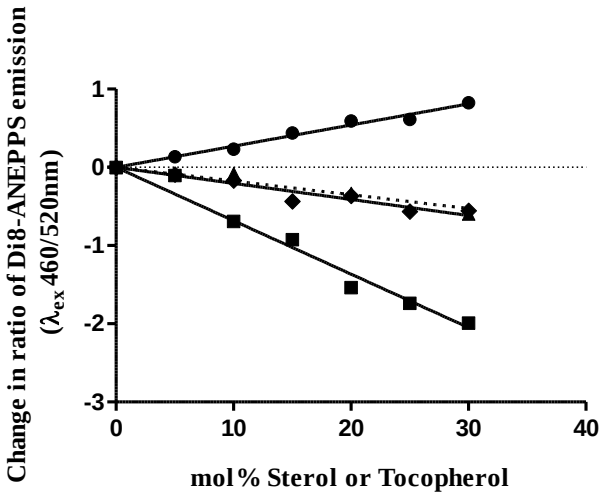

Figure 3.3.4: A comparison of the change in ratio of Di-8-ANEPPS fluorescence intensity at 460nm and 520nm excitation with increasing α-tocopherol succinate (▲) vs α-tocopherol (♦) concentration. The change in ratio with increasing cholesterol (●) and 7-ketocholesterol (■) concentration from Section 3.1.1 are also shown. Increasing the α-tocopherol succinate concentration linearly decreases the change in ratio in the same way as α-tocopherol indicating a similar decrease in dipole potential is caused by both molecules. The data is fit to a straight line constrained to intercept at the origin yielding r^2=0.92, slope= -0.018±0.001mol%$^{-1}$ which is not significantly different from that of α-tocopherol, slope= -0.0206±0.0008, (P=0.09, two-tailed t-test).

Figure 3.3.4 compares the change in dipole potential, through change in the ratio of Di-8-ANEPPS intensity at 460nm and 520nm excitation ($R=I_{460}/I_{520}$), as the molar concentration of α-tocopherol succinate is increased in egg-PC vesicles with that due to increasing concentration of α-tocopherol. The data are both fit to a straight line equation and the slopes are not significantly different (P=0.09, unpaired two-tailed t-test) confirming that the succinate ester analogue causes an equivalent change in the dipole potential.

Previous studies that compare the behaviour of α-tocopherol succinate with α-tocopherol in membranes, by observation of changes in physical parameters other than the dipole potential, show their effects to be different (Lai et al., 1985, Massey, 2001).

The effects of α-tocopherol and α-tocopherol succinate on the polarity at the lipid-water interface of DPPC and POPC membranes are investigated using polarisation studies with prodan and laurdan by Massey (Massey, 2001). α-Tocopherol was shown to decrease interfacial polarity of the membranes in the liquid crystalline (l_c) phase which was thought to be the result of a decrease in hydration. α-Tocopherol succinate caused no change in the spectral properties of prodan, which is sensitive to polarity changes at the membrane surface, due to the negligible perturbation of hydration by the hydrophilic succinate moiety positioned at the membrane surface. The effects on laurdan fluorescence depended on the protonation state of α-tocopherol succinate; when protonated its behaviour is similar to that of α-tocopherol and when deprotonated, no change in polarity is detected from that of the pure lipid bilayer. The ability to detect α-tocopherol succinate interaction with membranes by FPE fluorescence (figure 3.3.1) suggest the molecule is, at least partially, deprotonated at the pH and temperature used in both FPE and Di-8-ANEPPS vesicle experiments in this chapter. α-Tocopherol and α-tocopherol succinate are, therefore, expected to have very different effects on hydration under these conditions, which is thought to be a contributing factor of the dipole potential (Gawrisch et al., 1992). The fact that both have been shown to cause an equivalent change to the fluorescence of Di-8-ANEPPS supports the argument of Robinson *et al*. (Robinson et al., 2010) that this dipole potential probe is not sensitive to changes in hydration.

Massey also investigates variation of DPH polarisation in DPPC and POPC membranes as an indicator of lipid order. α-Tocopherol was found to order lipids in the l_c phase whereas α-tocopherol succinate had little effect on DPH polarisation (Massey, 2001). This was attributed to differences in the depth of the chromanol group of α-tocopherol and α-tocopherol succinate in the bilayer. The chromanol group of α-tocopherol is thought to sit beside the upper, most ordered, part of the lipid acyl chains where it is likely to hydrogen bond thus increasing order, whereas that of α-tocopherol succinate (due to the increase in length of the molecule with the addition of the succinate positioned at the lipid-water interface) is thought to sit deeper where it is likely to have less of an effect on ordering. A change in lipid order, by changing the extent to which lipid dipoles are oriented parallel to the membrane normal, can affect the dipole potential. The change in the dipole potential of PC vesicles by α-tocopherol and α-tocopherol succinate was equivalent suggesting that either there are no differences in the effect of these molecules on lipid order or the effect may be subtle, in comparison to other factors affecting the dipole potential, and not detected by changes in Di-8-ANEPPS fluorescence.

α-Tocopherol succinate was then titrated to Di-8-ANEPPS labelled liposome suspensions with the aim of observing its insertion into the membrane through its perturbation of the dipole potential. Comparing the resulting titration curves with those obtained with FPE labelled vesicles should give further insight into the positioning of α-tocopherol succinate in the membrane and preference for specific lipids or lipid phases resulting in heterogeneity in lateral localisation in membranes of mixed lipid composition.

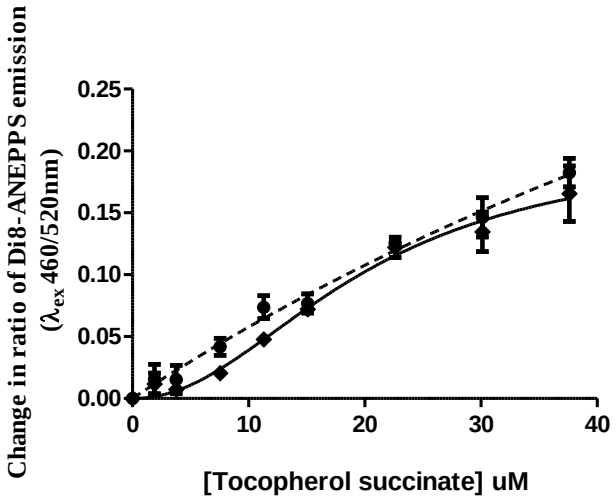

Figure 3.3.5: The change in ratio of Di-8-ANEPPS fluorescence intensity at 460nm and 520nm excitation with serial addition of α-tocopherol succinate to PC (●) and 70mol%PC-30mol%cholesterol (♦) vesicles. Control values obtained by serial addition of equal volume of the solvent (ethanol) were subtracted from the data. The data is fit to either a hyperbolic saturation binding model or sigmoidal binding model the results of which are shown in Table 3.3.3.

Figure 3.3.5 shows the change in ratio of Di-8-ANEPPS fluorescence intensity at 460nm and 520nm excitation in 100%PC and 70mol%PC-30mol%cholesterol vesicles on titration of α-tocopherol succinate. The titration to 100% PC vesicles best fits a hyperbolic binding model whereas that to 70mol%PC-30mol%cholesterol fits best to a sigmoidal binding model, the results of which are shown in Table 3.3.3. There are several explanations for the fit of a sigmoidal binding model. There could be a degree of cooperativity in the binding of α-tocopherol succinate, for example changes in membrane properties by bound α-tocopherol succinate could facilitiate further binding to the membrane. The effect may be concentration dependent such that little response in Di-8-ANEPPS fluorescence is seen at lower concentrations with increasing response as the concentration of α-tocopherol succinate in the membrane is increased. The sigmoidal relationship may also be due to the localisation of α-tocopherol succinate between different regions of the membrane and its relative colocalisation with Di-8-ANEPPS. A region with a higher concentration of α-tocopherol succinate may undergo a larger change in the dipole potential due to the high density of α-tocopherol succinate molecular dipoles. A region with a low concentration of α-tocopherol succinate (and Di-8-ANEPPS) may not report a significant change in Di-8-ANEPPS fluorescence if the change in

dipole potential is below the sensitivity limit of the probe. It is also likely, through changes in lipid packing, molecular orientation, and hydrogen bonding, that α-tocopherol succinate may alter the dipole potential of different lipid phases differently. An example of this is the larger effect of 7-KC in changing the dipole potential of the liquid disordered (l_d) phase than the liquid ordered (l_o) phase due to the tilted orientation it adopts in the former ((Massey, 2001, Starke-Peterkovic et al., 2006) and section 3.1.2).

The K_d value for α-tocopherol succinate binding to PC-cholesterol vesicles is considerably lower than that for PC vesicles indicating a large increase in the affinity of α-tocopherol succinate for the membrane in the presence of cholesterol. This suggests that α-tocopherol succinate may have a high affinity for cholesterol-rich l_o domains supporting the original suggestion made following α-tocopherol succinate titrations to FPE labelled vesicles (section 3.3.1).

Liposome composition	**R^2**	**B_{max}**	**h**	**K_d (μM)**
PC_{100}	0.94	0.8±0.4	-	130±80
$PC_{70}Cholesterol_{30}$	0.96	0.21±0.04	2.1±0.5	20±5

Table 3.3.3: The parameters of fit of a hyberbolic or sigmoidal binding model to data of Figure 3.3.5 representing the change in ratio of Di -8-ANEPPS fluorescence intensity at 460nm and 520nm excitation in the 100%PC or 70mol%PC30mol%cholesterol vesicles on serial addition of α-tocopherol succinate. R^2 is the goodness of fit, B_{max} the change in ratio when a saturation concentration of α-tocopherol succinate has bound, K_d (μM) is the concentration of α-tocopherol succinate at which half this change in ratio is achieved and h is the hill coefficient for the sigmoidal fit.

3.4. Summary

Tocopherol has a well documented antioxidant action and, due to the lipophilicity of the molecule, it is reported to exert this effect in membranes protecting unsaturated lipids from oxidation (Quinn, 2004, Atkinson et al., 2010). Tocopherol has been observed to elicit a host of biological effects which are not directly associated with its free radical scavenging ability and it has been recently proposed that some of these effects may occur as a result of the influence of tocopherol within the membrane (Azzi and Stocker, 2000, Azzi et al., 2002, Brigelius-Flohe, 2009). This chapter explored the influence of tocopherol on the membrane dipole potential of egg-phosphatidylcholine vesicles. To place this effect in some context, the effect of cholesterol oxidation on the membrane dipole potential was first explored.

7-ketocholesterol, an oxidised form of cholesterol, was demonstrated to cause a significant decrease in the dipole potential of PC vesicles. This effect, opposite to that elicited by cholesterol and of a significantly greater magnitude, is thought to arise from the opposing molecular dipole moment of 7-ketocholesterol relative to its unoxidised form and the differences in lipid ordering and hydration as a result of the additional polar moiety. The increase and decrease in the dipole potential demonstrated with cholesterol and 7-ketocholesterol are consistent with the observations of Starke-Peterkovic *et al.* (Starke-Peterkovic et al., 2006) with dimyristoylphosphatidylcholine (DMPC) vesicles, however, the relative magnitudes of the change in dipole potential by these sterols is different. In egg-PC vesicles 7-ketocholesterol induces an approximately 2.5x greater change in the dipole potential than cholesterol whereas in the DMPC vesicles of Starke-Peterkovic *et al.* the sterols cause an approximately equivalent magnitude of change (Starke-Peterkovic et al., 2006). This difference may be partly due to the greater sensitivity of the ratiometric technique used here than by Starke-Peterkovic arising from the excitation wavelengths chosen, or variation in the lipid packing density and proportion of ordered domains formed by cholesterol in the DMPC and egg-PC vesicles. The molecular dipole moment of 7-ketocholesterol is thought to contribute significantly to the decrease in the dipole potential induced by this sterol. The relative difference in the effect of cholesterol and 7-ketocholesterol in the egg-PC and DMPC vesicles therefore suggests that the mixed unsaturated/saturated lipids of egg-PC vesicles may provide an environment that is not present in the saturated DMPC vesicles in which the dipole moment of 7-ketocholesterol may exert a greater effect on the dipole potential. This is consistent with the hypothesis of Massey *et al.* that 7-ketocholesterol has a tilted orientation in the presence of unsaturated lipids (Massey and Pownall, 2005, Smondyrev and Berkowitz, 2001) which is thought to increase the contribution of the molecules dipoles to the dipole potential (Starke-Peterkovic et al., 2006).

It seems likely then, that the phases present in the membrane as a result of the lipid composition influence the effect of 7-ketocholesterol on the dipole potential. Further experiments confirmed

this idea by demonstrating that the presence of cholesterol in the membrane increases the effect of 7-ketocholesterol on the dipole potential. This effect is most pronounced when the concentration of cholesterol in the membranes exceeds ~25mol% where a significant proportion of l_o phase domains are expected to occur. The presence of cholesterol in the membrane, and the resulting phase landscape, is likely to influence the effect of 7-ketocholesterol on lipid packing and hydration as well as determine the proportion of 7-ketocholesterol in the tilted orientation, and therefore influence the extent of its effect on the membrane dipole potential.

Membrane cholesterol oxidation, simulated by increasingly replacing a 30mol% cholesterol fraction within PC vesicles with 7-ketocholesterol, demonstrates a dramatic decrease in the dipole potential which does not conform to a single linear regression. The bi-phasic nature of this decrease is thought to result from differences in the influence of 7-ketocholesterol on the dipole potential in the presence of higher or lower proportions of the l_o phase occurring with higher or lower concentrations of cholesterol.

Tocopherol is shown to decrease the dipole potential, causing the opposite effect of cholesterol with approximately 75% of the magnitude of the change. Tocopherol is known to form ordered domains with unsaturated lipids which would modulate lipid packing and hydration in a similar way to cholesterol among unsaturated lipids. The opposing effect on the dipole potential may therefore reflect possible disordering of saturated lipid rich domains which may be associated with observations of a lowering of the gel-to-liquid transition temperature and enthalpy of transition (Massey et al., 1982) which is not pronounced in unsaturated lipid membranes (Fukuzawa et al., 1979). Alternatively, this result may suggest that tocopherol has a molecular dipole moment opposite to the membrane normal which is the explanation put forward by Bechinger and Seelig (Bechinger and Seelig, 1991) for the decrease in dipole potential elicited by phloretin at concentrations where it negligibly perturbs lipid ordering and hydration. Tocopherol has also been suggested to form hydrogen bonds with dipolar groups of phospholipids (Atkinson et al., 2008), and may also perturb the polarised water surrounding these dipoles, which would contribute to a change in the dipole potential. This contribution could be explored using methods similar to those used by Diaz *et al.* to explore the contribution of water hydrogen bonded to the carboxyl dipole of phospholipids to the dipole potential and the effect of the neutralization of this dipole by phloretin (Diaz et al., 1999).

The influence of tocopherol on the dipole potential in the presence of cholesterol was then explored. At low concentrations of cholesterol the effect of tocopherol on the dipole potential was very similar to that in PC vesicles with no cholesterol. This suggests that concentrations of cholesterol up to about 20mol% may not significantly alter the localisation of tocopherol in the membrane and the changes in the phase landscape it causes. Above ~25mol% cholesterol, however, tocopherol decreases the dipole potential to a significantly greater extent which may

be indicative of the disordering of l_o domains due to the partitioning of tocopherol into these regions which represent a larger proportion of the membrane at higher cholesterol concentrations.

Considering this data from the perspective of the effect of tocopherol on the influence of cholesterol on the dipole potential it is shown that cholesterol elicits the same effect as in PC vesicles at lower concentrations but a vastly greater increase in the dipole potential with increasing concentration above ~25mol%. The dipole potential increases at a steady rate over the equivalent concentration range in PC vesicles and the onset of the regime of steeper increase in the presence of tocopherol may reflect a phase transition. For example, tocopherol lowers the gel-to-liquid transition temperature and the presence of tocopherol in the membrane may reduce the concentration of cholesterol required for this transition.

Tocopherol causes a similarly bi-phasic effect on the influence of 7-ketocholesterol on the dipole potential. The point of transition between the two regions demonstrating distinctly different effects of 7-ketocholesterol on the dipole potential occurs at a lower concentration of 7-ketocholesterol than for cholesterol. This may reflect differences in the tendencies of sterols to form l_o domains and the stability of these domains.

The effect of 7-ketocholesterol on the influence of tocopherol on the dipole potential is quite different from that of cholesterol. At low ratios of tocopherol to 7-ketocholesterol, increasing tocopherol concentration causes a dramatic increase in the dipole potential which is in sharp contrast to the much slighter decrease it elicits in PC vesicles with no 7-ketocholesterol. At higher concentrations of tocopherol the dipole potential still increases but with considerably smaller effect per unit concentration increase.

This data indicates that the influence of tocopherol on the dipole potential depends on the phase domain landscape of the membrane which is likely to be as a result of changes in the localisation of tocopherol and its subsequent influence on lipid ordering and hydration. Similarly, the presence of tocopherol alters the effect of cholesterol and 7-ketocholesterol on the membrane dipole potential. These conclusions have arisen from the fact that Di-8-ANEPPS molecules in different domains are likely to report different spectral shifts according to the lipid ordering and hydration, and resulting dipole potential, of their environment. Any significant changes in the trend of the spectral shifts reported as the compositions of membranes are stepwise altered are therefore likely to reflect significant changes in the domain landscape of the membrane.

To investigate the possibility that Di-8-ANEPPS can detect changes in the domain landscape of a membrane, a second derivative analysis was performed on the excitation spectra of Di-8-ANEPPS in a series of phosphatidylcholine vesicles of increasing ratio of tocopherol to 7-

ketocholesterol which were previously observed to demonstrate spectral shifts following a sigmoidal relationship (Figure 3.2.8). This confirmed that the probe was reflecting two environments of different dipole potential in each vesicle composition. Further analysis of the spectra corresponding to each detected environment demonstrated a point of significant change in the proportion of the higher and lower dipole potential environments identified by the probe which coincided with the inflection of the sigmoidal relationship. This suggests that Di-8-ANEPPS could be reflecting differences in the phase profile of the vesicles. A simple experiment to initially determine if this is the case would be to repeat these experiments, conducted at 37^{o}C, at a higher or lower temperature, for example <20^{o}C or >45^{o}C. If the transition point between regimes on the resulting graphs occur at different sterol or tocopherol concentrations to those shown in this chapter this indicates that the temperature of the system, as well as the composition, alters the trend in the change in spectral shift of Di-8-ANEPPS, suggesting sensitivity to the phase behaviour. This can be explored in detail using a membrane system of well defined phase behaviour over a given temperature range. The phase behaviour of tocopherol in the systems studied in this chapter are not currently well characterised and it would be interesting to gain further insight by comparison of the data presented here with phase information obtained using methods such as differential scanning calorimetry (DSC), X-ray diffraction and deuterium nuclear magnetic resonance (^{2}H NMR).

The modulation of the dipole potential by tocopherol could be a non-antioxidant action of this molecule in membranes that may later prove to underly some of the biological effects of the vitamin that cannot be attributed to its free radical scavenging capability. In support of this notion tocopherol succinate, a structural analogue with no antioxidant action, was shown to modulate the membrane dipole potential of PC liposomes causing a closely similar concentration dependent decrease to that of tocopherol. It is possible that both molecules localise similarly in the membrane to elicit similar changes in the dipole potential.

Tocopherol succinate also possesses a charged moiety enabling its interaction with membranes to be observed through changes in the surface potential. The molar efficacy of tocopherol succinate in changing the surface potential was found to be significantly higher in PC membranes containing cholesterol. As the overall binding affinity is not significantly different between the membranes the greater increase in the surface potential in the presence of cholesterol is thought to occur due to the localisation of tocopherol succinate in l_o phases where the density of FPE is greater. Interestingly, the effect of gradually replacing the cholesterol fraction with 7-ketocholesterol was to reduce the molar efficacy of tocopherol succinate in increasing the surface potential. At equal molar concentrations of cholesterol and 7-ketocholesterol the molar efficacy was not significantly different from that in PC vesicles suggesting 7-ketocholesterol may prevent the localisation of tocopherol succinate in l_o domains. At higher concentrations of 7-ketocholesterol the molar efficacy reduced further still suggesting

that the microdomain landscape promoted by the sterol may sequester FPE into regions inaccessible to tocopherol succinate.

It is possible that the affinity of tocopherol succinate for l_o domains is different to that of the bulk l_d phase of the membrane. To explore this, the titration curve of tocopherol succinate to cholesterol-containing vesicles was fitted to a two-term hyperbolic binding model where the parameters of the first term were constrained to match those yielded by a single hyperbolic fit to the equivalent titration in PC vesicles. The resulting affinity of tocopherol succinate for the hypothesized second binding site, correlated with l_o domains, was significantly higher. This result is supported by the significantly higher binding affinity of tocopherol succinate for PC-cholesterol vesicles relative to PC vesicles determined using the changes in the dipole potential on binding.

4. Interactions of α-tocopherol succinate with cell membranes

In the previous chapter, evidence is presented to suggest the oxidation of membrane cholesterol causes a substantial modulation of the membrane dipole potential. The presence of cholesterol in egg phophatidylcholine vesicles increased the dipole potential whereas 7-ketocholesterol, a common oxidative product of cholesterol, decreased the dipole potential and to greater effect than cholesterol despite the only relatively minor differences in their molecular structures. This is proposed to be due to the larger and opposing molecular dipole moment of 7-ketocholesterol as well as arising from differences in its lateral distribution, and subsequent lateral organisation of membrane lipids. In the eukaryotic cell membrane the highly ordered phase separated domains formed by cholesterol, stabilised through protein and lipid interactions, are known as lipid rafts (Pike, 2006). These are considered to act as 'functional platforms' supporting the function of many membrane proteins by means of their unique physical properties (Brown and London, 1998a, Simons and Ikonen, 1997, Simons and Toomre, 2000). Lipid rafts have an elevated dipole potential with respect to the bulk membrane and modulating the cell membrane dipole potential has been demonstrated to alter the function of raft-associated receptors (Asawakarn et al., 2001), (Luker et al., 2001). It therefore seems likely that modulation of the membrane dipole potential by cholesterol oxidation could be involved in initiating some of the deleterious effects associated with 7-ketocholesterol in cells.

α-Tocopherol is well known as a free-radical scavenger capable of localising in membranes and protecting lipids from oxidation (Diplock, 1983, Fukuzawa et al., 1993, Wolf, 2005) but is has long been thought likely to have a structural role in membranes also (Diplock, 1983, Azzi et al., 2002, Zingg and Azzi, 2004). In the previous chapter α-tocopherol was demonstrated to modulate the membrane dipole potential, an effect that was mirrored by its non-antioxidant counterpart, α-tocopherol succinate. This is attributed, as for cholesterol and 7-ketocholesterol, to its localisation and ordering of membrane lipids as well as its molecular dipole. The effect of α-tocopherol on the dipole potential in the presence of cholesterol and 7-ketocholesterol differed and is suggested to depend on the initial dipole potential, reflecting the microdomain landscape, of the membrane.

In this chapter the effects of cholesterol and 7-ketocholesterol on the dipole potential of cell membranes are assessed and compared with their effects in the artificial membrane vesicles of the previous chapter. The modulation of the cell membrane dipole potential by α-tocopherol is then investigated in the context of oxidative stress. Given the potent free radical scavenging action of α-tocopherol, focus is given to the possibility that the physical behaviour of α-tocopherol in the membrane may counter the effects of 7-ketocholesterol lending a secondary, indirect, anti-oxidant role for α-tocopherols.

Jurkat T-lymphocytes are used as a simple cell membrane model and, as a suspension culture, are ideal for the spectroscopy based investigations of the changes in the membrane dipole potential on interaction of cholesterol, 7-ketocholesterol or α-tocopherol.

4.1. Modulation of the cell membrane dipole potential by cholesterol, 7-ketocholesterol and α-tocopherols

In this section cholesterol, its oxidised counterpart 7-ketocholesterol, the antioxidant α-tocopherol and a structurally similar but more soluble analogue, α-tocopherol succinate, are titrated to a suspension of Di-8-ANEPPS labelled Jurkat T-lymphocytes to investigate the modulation of the membrane dipole potential on interaction of these molecules with the cell membrane. The resulting titration curves give information regarding the affinity of these molecules for the cell membrane and the maximum change in the dipole potential they elicit on saturation of the membrane. Together with consideration to their estimated lipophilicity, these parameters indicate the localisation of these molecules in the membrane and the molecular nature of the dipole potential change they elicit.

4.1.1. The effect of cholesterol and 7-ketocholesterol on the T-Lymphocyte membrane dipole potential

Cholesterol is a significant component of cell membranes reported to be present at concentrations of 25-45mol% of total lipid in erythrocyte plasma membranes (Cooper, 1978, Yeagle, 2005). As such, its effect on the dipole potential can be investigated in two ways; firstly the effect of its partial extraction from the membrane by methyl-β-cyclodextrin treatment can be observed. Secondly, as membranes can support up to a 1:1 ratio of cholesterol to lipids (Yeagle, 2005), it can be added at known concentrations to the external aqueous environment of cells where, due to its hydrophobicity, cholesterol will insert into the membranes.

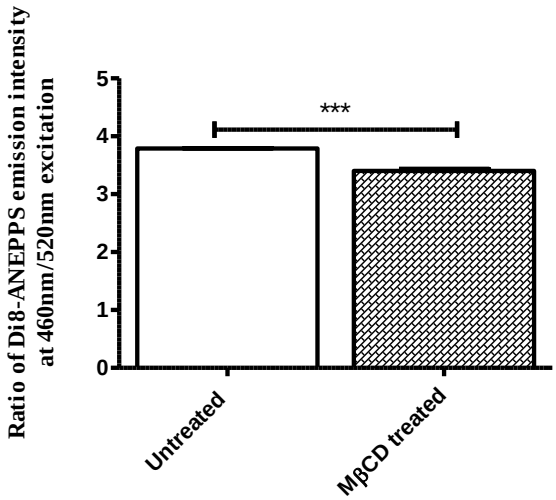

Figure 4.1.1: The ratio of the emission intensities of Di-8-ANEPPS at 460nm and 520nm excitation ($R=I_{460}/I_{520}$) in the membranes of untreated (unshaded bar) and methyl-β-cyclodextrin (10mM, 2min) treated (shaded bar) Jurkat T-lymphocytes. The ratio is significantly lower following methyl-β-cyclodextrin treatment and *** denotes $P<0.005$ (two tailed t-test).

Methyl-β-cyclodextrin depletion of membrane cholesterol results in a decrease in the dipole potential of the cell membrane as demonstrated in figure 4.1.1 which compares the fluorescence ratio, R, of Di-8-ANEPPS labelled cells following treatment with 10mM methyl-β-cyclodextrin

for 2 minutes, after (Rouquette-Jazdanian et al., 2006), with that for untreated cells. A decrease in the dipole potential was similarly seen by Starke-Peterkovic *et al.* (Starke-Peterkovic et al., 2006) after methyl-β-cyclodextrin depletion of cholesterol from vesicles formed from kidney- and brain- extracted natural lipids. Asawakarn *et al.* (Asawakarn et al., 2001) also report a decrease in the dipole potential of the Caco2 epithelial cell line on methyl-β-cyclodextrin cholesterol extraction. The decrease in the dipole potential is consistent with the reduction in lipid dipole density and increased hydration following the disruption of domains, such as rafts, that exhibit the high lipid ordering promoted by cholesterol in membranes. The removal of the molecular dipole moment of cholesterol, which also contributes to the increased dipole potential of lipid rafts, further adds to the decrease in the dipole potential.

Figure 4.1.2 shows the resulting change in dipole potential on the insertion of cholesterol to Jurkat T-lymphocyte membranes. This demonstrates the opposite effect as the addition of cholesterol to the cell membranes further promotes the formation of rafts with characteristic high lipid order and density, and reduced hydration, resulting in an increase in the dipole potential.

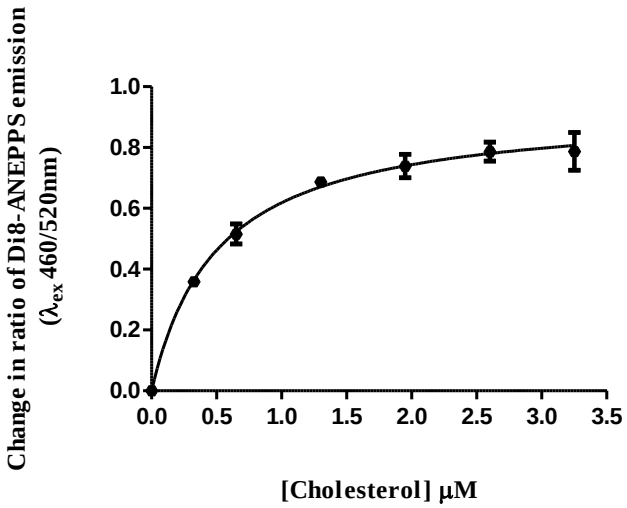

Figure 4.1.2: The change in the ratio, R, of Di-8-ANEPPS fluorescence intensity at 460nm and 520nm($R=I_{460}/I_{520}$) excitation as cholesterol is titrated to Jurkat-T-lymphocytes. The change in ratio on addition of equal volumes of the solvent, ethanol, is subtracted from the data which is the average of 3 repeats, the error bars representing the standard error of the mean. The data is fit to a hyperbolic saturation binding model with $R^2=0.97$ $B_{max}=0.93\pm0.04$ and $K_d=0.51\pm0.07\mu M$.

Repeating this experiment now adding 7-ketocholesterol to the cells in aqueous solution gives the titration curve shown in figure 4.1.3. 7-ketocholesterol decreases the ratio of Di-8-ANEPPS fluorescence intensity at 460nm and 520nm excitation, however, the modulus of this decrease in ratio is taken (as shown on the right y-axis of Figure 4.1.3) to enable fit of a hyperbolic saturation binding model.

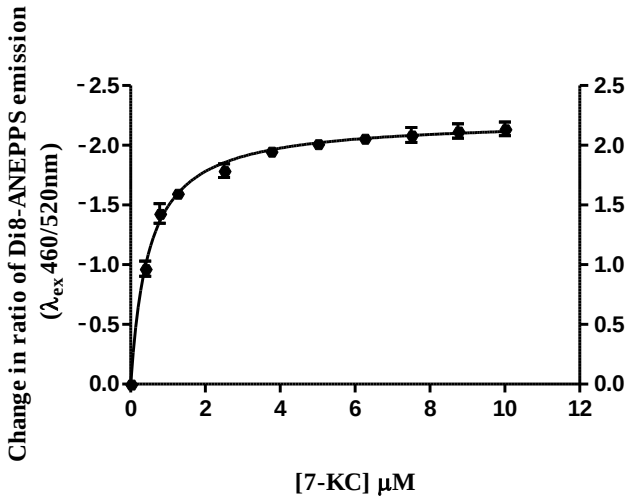

Figure 4.1.3: The change in the ratio (ΔR) of Di-8-ANEPPS fluorescence intensity at 460nm and 520nm excitation as 7-ketocholesterol is titrated to Jurkat T-lymphocytes. The data is the average of 3 repeats, the error bars representing the standard error of the mean (SEM), and is controlled for the change in ratio due to addition of the solvent, ethanol. The modulus of ΔR is taken (right y-axis) enabling the fit of a hyperbolic saturation binding model with R^2=0.99 B_{max}=2.22±0.03 and K_d=0.49±0.03μM.

7-ketocholesterol also forms ordered domains in mixed saturated/unsaturated lipid systems, however, it increases lipid packing density and reduces hydration to a lesser extent than cholesterol despite having the same orientation in the membrane in ordered saturated lipid- rich domains (Massey and Pownall, 2005, Aussenac et al., 2003, Phillips et al., 2001). These 7-ketocholesterol-enriched domains exhibit resistance to detergent solubilisation, a characteristic also shared by rafts, although these detergent resistant membrane (DRM) domains occur at higher sterol concentrations for 7-ketocholesterol than cholesterol in sphingomyelin containing membranes (Mintzer et al., 2010). This is consistent with the lower tendency of 7-ketocholesterol to form ordered domains with saturated lipids than cholesterol (Massey and Pownall, 2005). In cell membranes 7-ketocholesterol has been reported to localise in rafts (Myers and Stanley, 1999, Berthier et al., 2004, Royer et al., 2009). This has been determined by analysis of detergent extracted membrane and it should be noted that, as 7-ketocholesterol also forms DRMs independently of cholesterol (Mintzer et al., 2010, Massey and Pownall, 2005), this technique may not differentiate between 7-ketocholesterol residing in rafts or within its own ordered domains alongside rafts. If 7-ketocholesterol does partition into rafts its perturbation of the high lipid packing and higher affinity for liquid disordered (l_d) phase regions is likely to result in its ability to destabilise rafts (Massey and Pownall, 2005). The incorporation of 7-ketocholesterol into a membrane raft would be likely to reduce the dipole potential of the raft not only due to the subsequent increase in hydration and decrease in lipid packing, but also due to the presence of its molecular dipole which opposes that of cholesterol thus reducing the dipole potential.

7-ketocholesterol will also be present in the l_d phase regions where it adopts a tilted orientation (Smondyrev and Berkowitz, 2001, Massey and Pownall, 2005) thus increasing the proportion of

the magnitude of its molecular dipole resolved in the direction anti-parallel to the positive axis perpendicular to the bilayer (Starke-Peterkovic 2006). This orientation is due to increased hydration of 7-ketocholesterol and results in a lower lipid packing density than achieved by cholesterol in the l_d phase (Wang et al., 2004). 7-Ketocholesterol, therefore, is also expected to decrease the dipole potential of the l_d phase domains in the cholesterol-containing cell membrane. The decrease in the dipole potential of cell membranes on addition of 7-ketocholesterol (and increase with cholesterol) is reflected in the difference spectra of figure 4.1.4.

Comparing the K_d values obtained by fitting a hyperbolic saturation binding model to the data of figures 4.1.2 and 4.1.3 reveals that they are not significantly different between cholesterol and 7-ketocholesterol suggesting a similar affinity of cholesterol and its oxidised form for the membrane. However, the LogP values, an indicator of the lipophilicity of a molecule, are 9.62±0.28 for cholesterol and 7.13±0.03 for 7-ketocholesterol (ACD/LogP 12.0) suggesting cholesterol has a higher affinity for lipidic membranes than 7-ketocholesterol. The lack of significant difference in the K_d values may indicate that 7-ketocholesterol has a concentration-wise greater effect on the dipole potential than cholesterol and the greater maximum change in the dipole potential, B_{max}, caused by 7-ketocholesterol is consistent with this. The molar efficacy of each sterol in changing the dipole potential, K_{eff}, can be found by dividing B_{max} by K_d. For cholesterol K_{eff}=1.83±0.28μM^{-1} and for 7-ketocholesterol K_{eff}=4.36±0.35 μM^{-1} and, taking their ratio, it is shown that 7-ketocholesterol is a factor of 2.4±0.4 more effective per mole in changing the membrane dipole potential. This factor, a measure of the relative magnitude of the effects of cholesterol and 7-ketocholesterol, allows comparison with their effects in the egg-PC liposome systems of Chapter 3. Here, the ratio of Di-8-ANEPPS fluorescence at 460nm and 520nm excitation was recorded for a set of vesicles containing an increasing molar fraction of cholesterol or 7-ketocholesterol to PC. This produced a linear graph (Figure 3.1.3), the slope of which represents the efficacy per mol of the sterol in changing the dipole potential. The ratio of the slopes is 2.52±0.06 which is not significantly different from the ratio of K_{eff}s for cells. 7-ketocholesterol therefore has an approximately 2.5x greater effect on the magnitude of change of the dipole potential than cholesterol in both the vesicle and cell systems.

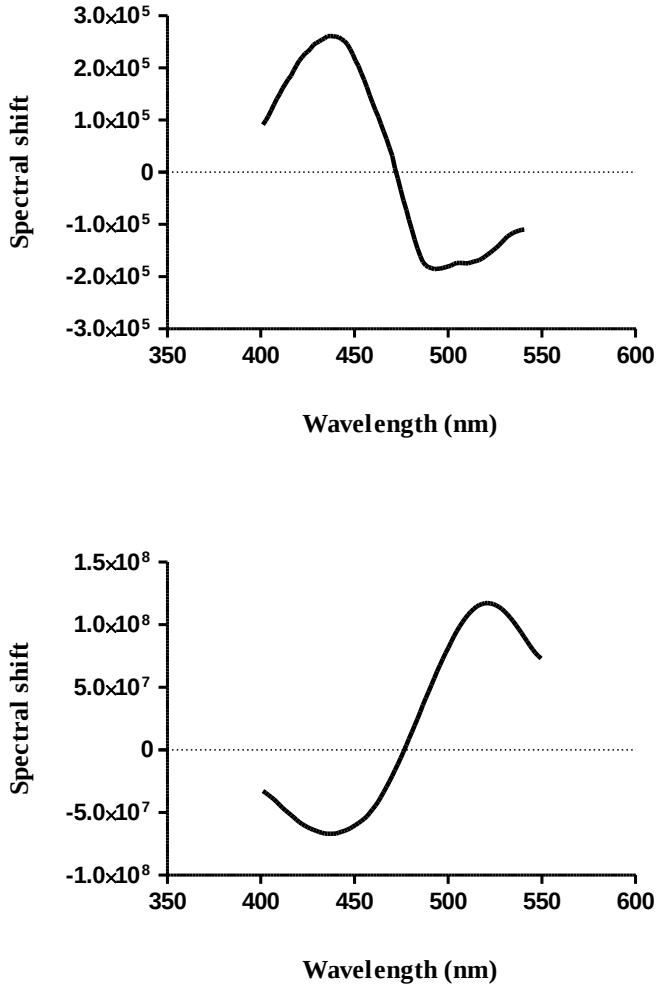

Figure 4.1.4: *Upper:* The difference spectra obtained by subtracting the excitation spectrum of Di-8-ANEPPS in Jurkat T-lymphocytes from that taken after titration up to 3.25μM cholesterol (n=3). This demonstrates a blue-shift in the excitation spectrum on insertion of cholesterol into the Jurkat T-Lymphocyte membrane representing an increase in the dipole potential. *Lower:* The difference spectra following titration up to 12.5μM 7-ketocholesterol (n=3) demonstrating a red-shift of the excitation spectra and decrease in the dipole potential.

This result seems counterintuitive as when 7-ketocholesterol enters cell membranes it reduces lipid packing and increases hydration in both rafts and cholesterol enriched l_d regions whereas when added to PC vesicles it will form l_o domains and orders the l_d phase increasing lipid packing and reducing hydration. Thus, contributions to the dipole potential by these factors are opposite in the cell and vesicle systems and, when coupled with the contribution from the molecular dipole of 7-ketocholesterol, one would expect the dipole potential to decrease to a lesser extent in the non-raft PC vesicle system. There are several potential explanations to the similar effects seen in both systems. Changes in hydration or lipid ordering may only have minor contributions to the change in dipole potential as detected by Di-8-ANEPPS and their effect would be dwarfed by the large contributions from the molecular dipole moment of 7-ketocholesterol. As 7-ketocholesterol is only likely to disrupt the gel phase domains present in PC vesicles at relatively high concentrations, it is possible that the proportion of 7-ketocholesterol in l_o and l_d phases, and therefore at orientations parallel or tilted to the

membrane normal, is similar resulting in similar contributions from its molecular dipoles in both the cell and vesicle systems. Alternatively, if hydration and lipid ordering do form substantial contributions to changes in Di-8-ANEPPS fluorescence, differences in partitioning between l_o and l_d phases of 7-ketocholesterol in the two systems may account for the similar ratio of K_{eff}s. It should also be noted that when titrating cholesterol to cell membranes one is adding cholesterol to a membrane already abundant in cholesterol. The effect is as if observing the binding of cholesterol to a membrane in only the latter part of a saturation binding experiment; as if previous cholesterol additions have been made but are discounted and the experiment is effectively begun again part way through. The difference between this and titrating cholesterol to a cholesterol-free vesicle results in the underestimation of B_{max} in comparison to the liposome system and an error when comparing the ratio of K_{eff}s for both systems.

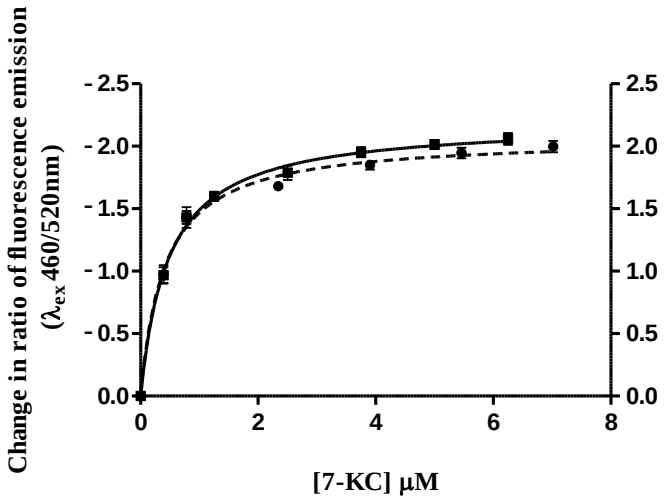

Figure 4.1.5 The change in the ratio of Di-8-ANEPPS fluorescence intensity at 460nm and 520nm excitation as 7-ketocholesterol is titrated to Jurkat T-lymphocyte treated with 10mM methyl-β-cyclodextrin for 2min (●) or untreated cells (■). The data shown is the average of 3 repeats, the error bars representing the standard error of the mean (SEM), and controlled for the change in ratio due to addition of the solvent, ethanol. The data, with the modulus of ΔR taken (right y-axis), is fit to a hyperbolic saturation binding model with R^2=0.99 B_{max}=2.07±0.04 and K_d=0.41±0.04μM for treated cells (----) and R^2=0.99 B_{max}=2.22±0.03 and K_d=0.49±0.03μM for untreated cells (─).

To further understand the effect of 7-ketocholesterol on the dipole potential of membrane rafts, 7-ketocholesterol was titrated to Jurkat T-lymphocytes following methyl-β-cyclodextrin treatment (10mM 2min) (see figure 4.1.5) previously reported to deplete 100% of raft cholesterol and virtually none of the non-raft cholesterol in Jurkat T-lymphocytes (Rouquette-Jazdanian et al., 2006).

Following methyl-β-cyclodextrin treatment, the maximum change in the dipole potential by 7-ketocholesterol at saturation concentration, B_{max}, is slightly but significantly lower than that for untreated cells (two-tailed t-test, $P<0.05$) suggesting the maximum change in the dipole potential that 7-ketocholesterol can effect is higher in the presence of rafts. As the dipole

potential of rafts is higher than that of the rest of the membrane this is consistent with 7-ketocholesterol entering rafts, disrupting the high lipid ordering and inserting an opposing molecular dipole moment (Massey and Pownall, 2005). The small magnitude of the difference between B_{max} in methyl-β-cyclodextrin treated and untreated cells is possibly due to the incomplete disruption of rafts by methyl-β-cyclodextrin or reformation of rafts by cholesterol replenishment in the short time post treatment and before 7-ketocholesterol addition (Zidovetzki and Levitan, 2007).

Interestingly, the K_{eff} values (K_{eff}=5.0±0.5μM^{-1} and K_{eff}=4.5±0.3μM^{-1} for treated and untreated cells respectively), are not significantly different (two tailed t-test, P=0.29) suggesting that the molar efficacy of 7-ketocholesterol in changing the dipole potential is similar in the presence and absence of rafts. 7-ketocholesterol forms ordered domains with saturated lipids and, in the absence of rafts due to the extraction of raft cholesterol by methyl-β-cyclodextrin treatment, it is likely these domains will be formed with the saturated lipids that would otherwise be present in rafts. In untreated cells 7-ketocholesterol may partition into rafts and do so to an extent that the dipole potential of the raft would approach that of the 7-ketocholesterol-saturated lipid ordered domains of the treated cells. If a similar proportion of 7-ketocholesterol partitions into ordered domains (either 7-ketocholesterol-saturated lipid domains or rafts) in both treated and untreated cells the overall effect of 7-ketocholesterol on the dipole potential in both cases would be similar, resulting in similar K_{eff} values.

The K_d values for treated and untreated cells are not significantly different (two-tailed t-test, P=0.18) suggesting a similar affinity of 7-ketocholesterol in binding to both raft- and non-raft containing membranes. The small, yet significant, difference in B_{max}, therefore, may reflect subtle differences in lipid ordering effects of 7-ketocholesterol and its affinity to partition into ordered domains such as rafts.The small variation in dipole potential reflecting these subtle differences are perhaps lost within the errors on calculating K_{eff} rendering B_{max} values significantly different but K_{eff} values not.

4.1.2. Does α-tocopherol bind to the T-lymphocyte membrane?

In Chapter 3 it was shown that α-tocopherol, when incorporated into phosphatidylcholine (PC) vesicles, decreased their dipole potential with respect to a α-tocopherol-free PC vesicle reference. In order to observe if α-tocopherol has a similar effect on the dipole potential of cell membranes it was added at increasing concentrations to a suspension of Di-8-ANEPPS labelled Jurkat-T-lymphocytes in aqueous solution (Figure 4.1.6). α-Tocopherol has an octanol-water partition coefficient (LogP) of 11.2±0.4 (calculated using ACD/LogP12.0) suggesting it is a lipophilic molecule and, like cholesterol, will insert into the cell membrane changing the dipole potential.

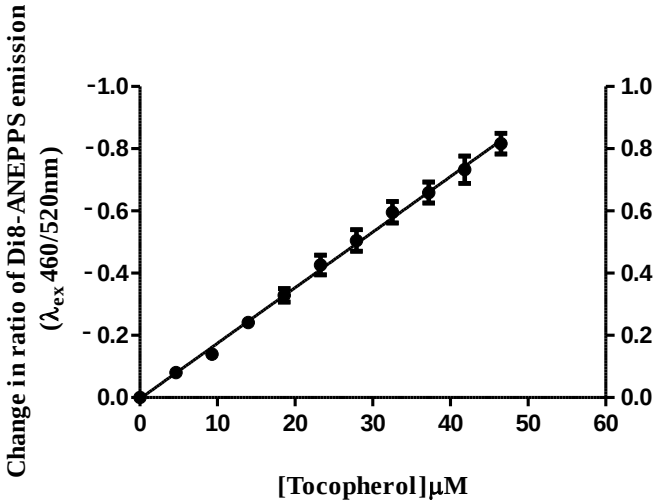

Figure 4.1.6: The change in ratio (ΔR) of fluorescence intensity at 460nm and 520nm excitation as α-tocopherol is added to the external aqueous environment of Di-8-ANEPPS labelled Jurkat T-lymphocytes. The data is the average of 3 repeats, the error bars representing the standard error of the mean (SEM), and is controlled for the change in the ratio due to addition of the solvent, ethanol. The modulus of the change in ratio is shown by the right y-axis. The data best follows a linear fit with R^2= 0.98.

Figure 4.1.6 shows that α-tocopherol titration to Jurkat T-lymphocytes causes a change in the ratio of Di-8-ANEPPS intensity at 460nm and 520nm excitation indicative of a change in the dipole potential of the cell membrane. However, the effect does not approach saturation over a concentration range ten times that of cholesterol titration to cells, despite their similar efficacies in changing the dipole potential in PC vesicles and the higher lipophilicity of α-tocopherol (LogP=11.19±0.35 ACD/LogP 12.0). Observing the excitation spectra of Di-8-ANEPPS labelled cells after the addition of 50μM and 100μM α-tocopherol (Figure 4.1.7) reveals that α-tocopherol distorts the shape of the excitation spectra to an increasing extent as the concentration of α-tocopherol is increased. α-Tocopherol is known to have very low aqueous solubility of approximately 0.012 μM at pH7.4 (ACD/Aqueous Solubility 12.0), therefore is very likely to have formed aggregates when titrated to the aqueous suspension of cells. These aggregates will scatter light that is incident on them over the wavelength range of the excitation spectra causing the distortion. The intensity of scattered light and wavelength of incident light that is scattered can be roughly correlated with the number and size of scattering particles, so as the concentration of α-tocopherol is increased the spectra become more distorted by scattering effects.

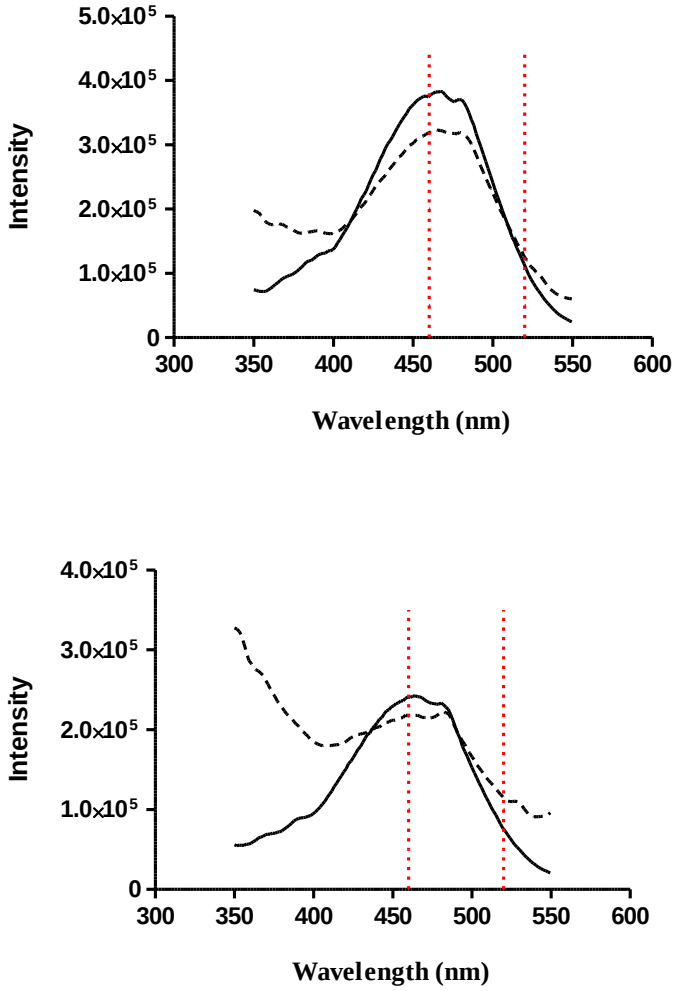

Figure 4.1.7: The excitation spectra (n=3) of Di-8-ANEPPS in Jurkat T lymphocyte cell membranes before (—) and after (----) addition of 50μM α-tocopherol (*top*) or 100μM α-tocopherol (*bottom*) to the external aqueous environment of the cells. Addition of α-tocopherol distorts the excitation spectrum and the higher the concentration the greater the distortion. The dotted red lines (**…**) lie at 460nm and 520nm, the excitation wavelengths used in the dual excitation intensity ratiometric method for changes in the dipole potential.

The excitation wavelengths (460nm and 520nm) at which the ratio of fluorescence intensities is taken in order to plot the change in ratio in figure 4.1.6 are indicated by red dotted lines on the excitation spectra (Figure 4.1.7). It can be seen that the distortion in the spectra by α-tocopherol impacts the ratio. This means that the change in ratio presented in figure 4.1.6 does not solely represent a change in the cell membrane dipole potential but also the increasing scattering of α-tocopherol aggregates. To ensure scattering effects on the ratio are avoided, the titration experiment should be conducted below the aqueous solubility limit of α-tocopherol in the presence of cells. The LogP and aqueous solubility are both significantly higher than those for cholesterol suggesting a higher aqueous solubility in the presence of cells, however, with only a ~0.2 change in ratio at 15μM of α-tocopherol it is unlikely a useful binding curve can be attained in this range.

α-Tocopherol succinate is a structural analogue of α-tocopherol with a succinate group ester linked through the phenol hydroxyl group of the α-tocopherol molecule. This addition increases the number of polar moieties within the headgroup of the molecule which are readily hydrated, resulting in the dramatically increased aqueous solubility of $5.4x10^{6}$ mol L^{-1} at pH 7.4. (ACD/Aqueous Solubility 12.0). α-Tocopherol succinate has been shown in Chapter 3 to cause very similar change in the dipole potential of PC vesicles as α-tocopherol and is therefore a good substitute enabling the effect on the dipole potential of cell membranes to be studied.

α-Tocopherol has a hydrophobic 14-carbon tail so the addition of the polar succinate ester, increasing the hydrophilicity of the headgroup, means that α-tocopherol succinate is likely to have an increased tendency to form micelles in solution. If α-tocopherol succinate micelles are present when titrating to a Di-8-ANEPPS labelled cell suspension, free Di-8-ANEPPS, normally non-fluorescent in solution, will partition into the micelles becoming fluorescent and contributing to the fluorescence signal detected. The excitation spectrum of Di-8-ANEPPS in α-tocopherol succinate micelles is likely to be different to that in cell membranes causing an error in the ratio measurement of the cell membrane dipole potential so it is crucial to find the concentration of α-tocopherol succinate at which micelles will be formed in aqueous solution, known as the critical micelle concentration (CMC).

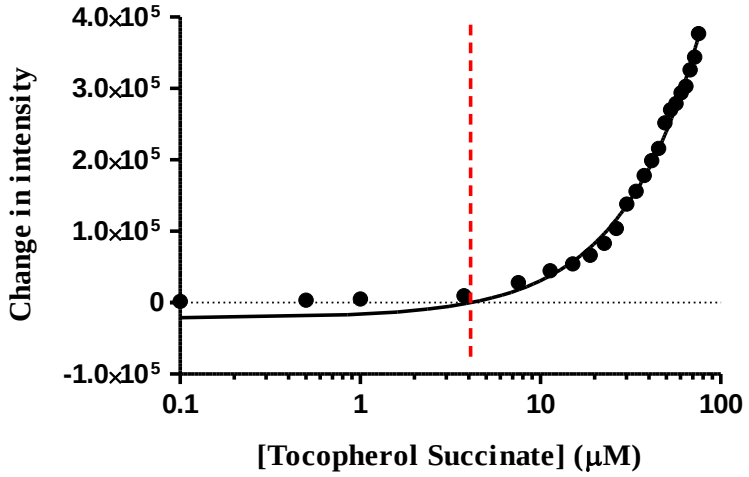

Figure 4.1.8: The detection of micelles as the concentration of α-tocopherol succinate in aqueous solution is increased by the degree of scattering of 400nm light at a 90° angle to the incident. The concentration of α-tocopherol succinate is given on a log scale and the sudden increase in the change of intensity, detected at 400nm with 400nm excitation, from the baseline intensity (intensity before α-tocopherol succinate is added) is due to the formation of micelles which cause scattering. The data shown is the average of 3 repeats and is fit to a linear regression (R^2=0.99) that intercepts the x-axis at 4.1±0.9μM which is the critical micelle concentration (CMC), indicated by the dotted red line (**…**).

The CMC has been determined experimentally using the 90° light scattering technique (Davis et al., 2011 *submitted*), the results of which are shown in figure 4.1.8. Below CMC, as the concentration of α-tocopherol succinate in aqueous solution is increased, very little change in

the intensity of light collected at 90^{o} to the incident beam is detected. Above CMC, micelles are present which scatter the incident light, detected as an increase in intensity at 90^{o} to the incident beam that is directly proportional to the number of micelles present. Fitting a linear regression to this latter regime allows the CMC to be extrapolated and for α-tocopherol succinate in aqueous solution at pH7.4 this was found to be 4.1±0.9μM.

4.1.3. The effect of α-tocopherol succinate on the T-lymphocyte membrane dipole potential

In the previous section it was shown that modulation of the cell membrane dipole potential measured through Di-8-ANEPPS spectral shifts could not be determined for α-tocopherol due to its low aqueous solubility. α-Tocopherol succinate, a more soluble form which causes similar change in the dipole potential of phosphatidylcholine vesicles (see Figure 3.3.4) to α-tocopherol, is deemed an appropriate alternative. However, α-tocopherol succinate has a propensity to form micelles in the aqueous solution and the critical micelle concentration, above which micelles are present, was found to be approximately 4μM in the osmotically balanced aqueous buffer used in the cell studies described in this chapter. Free Di-8-ANEPPS in the labelled cell suspension is likely to partition into micelles adding an error that is not easily quantified to the measured fluorescence. It is important, therefore, to remain in the non-micelle regime below CMC when investigating the effects of α-tocopherol succinate added to a cell suspension on the membrane dipole potential.

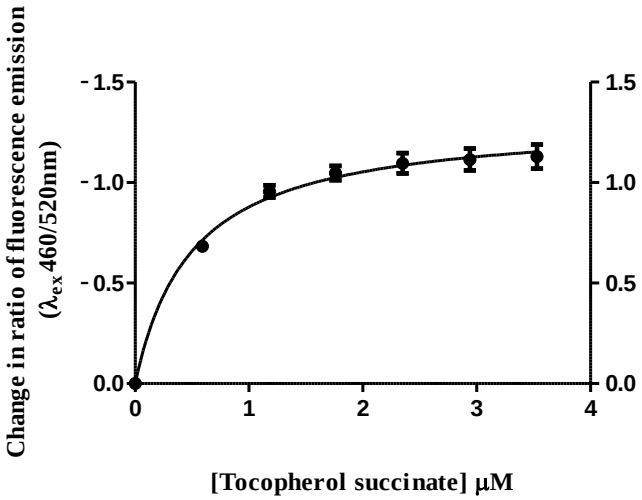

Figure 4.1.9: The change in the ratio of Di-8-ANEPPS fluorescence intensity at 460nm and 520nm excitation as α-tocopherol succinate is titrated to Jurkat T-lymphocytes. The data shown is the average of 3 repeats, the error bars representing the standard error of the mean (SEM), and is controlled for the change in ratio due to addition of the solvent, ethanol. The modulus of the data (right y-axis) is fit to a hyperbolic saturation binding model with R^2=0.97 B_{max}=1.32±0.05 and K_d=0.48±0.08μM.

Figure 4.1.9 shows the change in the dipole potential of Jurkat T-lymphocyte cell membranes when α-tocopherol succinate is titrated to Di-8-ANEPPS labelled cells. As can be seen in the red shift of the excitation spectrum and resulting difference spectrum in figure 4.1.10, α-tocopherol succinate decreases the cell membrane dipole potential.

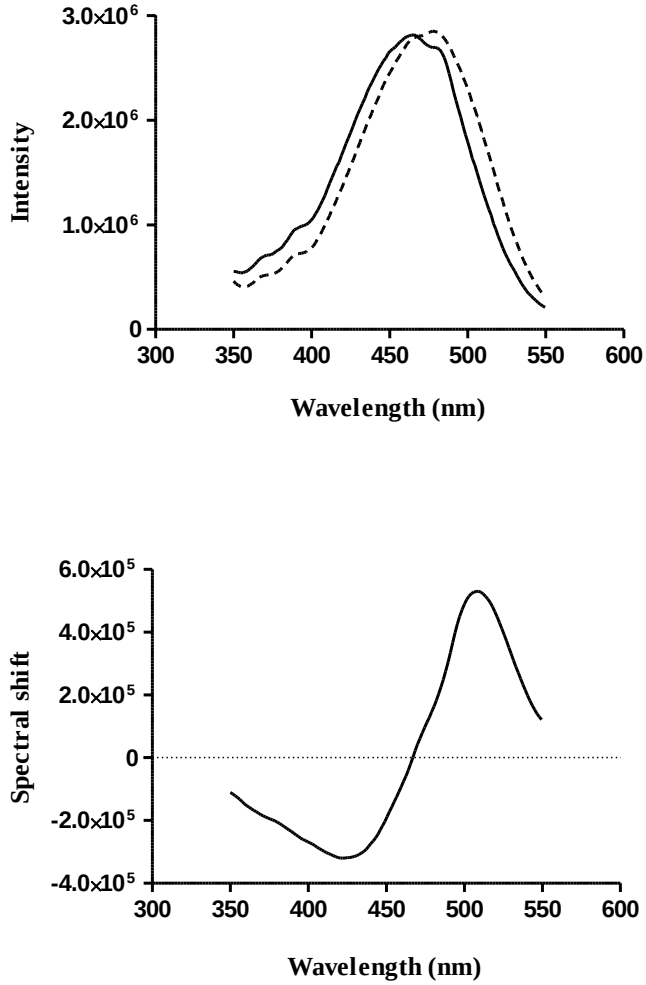

Figure 4.1.10 *Above*: The excitation spectra of Di-8-ANEPPS in Jurkat T-lymphocyte membranes before (—) and after (----) addition of a total of 3.77μM in the titration represented in figure 4.1.9. The data shown are an average of 3 spectra that have been normalised with respect to the area under the curve such that they are intensity matched. The difference spectra (*below*), resulting from the subtraction of the spectrum before from that after α-tocopherol succinate addition, then best represents the spectral red shift of a decrease in dipole potential.

α-Tocopherol succinate was also shown to decrease the dipole potential when incorporated into phosphatidylcholine vesicles (Section 3.3.2). Massey *et al*. (Massey, 2001) have demonstrated little effect on ordering of the liquid crystalline (l_c) phase of DOPC or DMPC membranes by α-tocopherol succinate and its effects on polarity to depend on its protonation state. At pH 7.4, the pH of the buffer in which labelled cells were suspended for this experiment, α-tocopherol succinate is expected to be in a deprotonated form where it has no reported effect on polarity (Massey, 2001). If the decrease in dipole potential is to be consistent with the reported lack of effect of polarity or order of liquid crystalline membranes, it must be attributed to the molecular dipole moment of α-tocopherol succinate. However, the phase landscape of the cell membrane is complex including, for example, an additional phase separation into l_o domains not present in the membranes studied by Massey *et al.* and it is likely α-tocopherol succinate will influence ordering and hydration in the cell membrane (particularly considering its structural similarity with α-tocopherol) that will affect the dipole potential.

4.1.4. α-Tocopherol succinate interactions with the cell membrane observed through changes in the surface potential

The negative charge of α-tocopherol succinate at pH7.4 allows its binding to the cell membrane to be studied through its modulation of the membrane surface potential. This is detected by changes in FPE fluorescence, which has a quantum yield dependent on its ionisation state, reflecting the surface potential in the local environment of the membrane bound probe (Wall et al., 1995b). α-Tocopherol succinate was added in a concentration-wise manner, to a suspension of FPE labelled Jurkat T-lymphocytes in aqueous solution and the resulting titration curve is shown in figure 4.1.11.

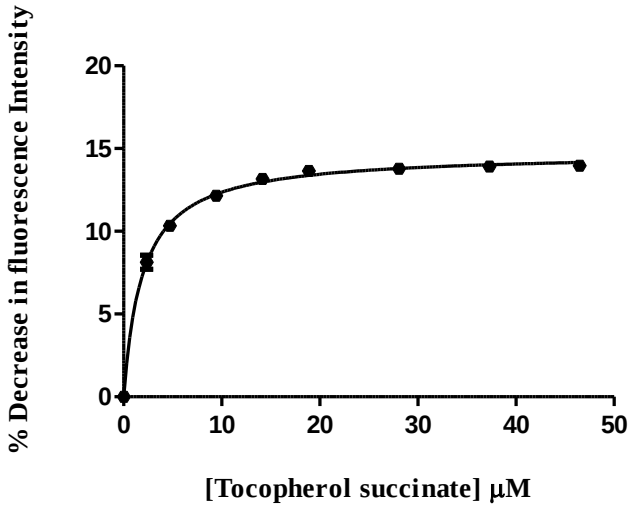

Figure 4.1.11 The percentage change in emission intensity of FPE (λ_{ex}=490nm λ_{em}=520nm) labelled Jurkat T-lymphocytes on serial addition of α-tocopherol succinate. The data shown is the average of 3 repeats and error bars reflect the standard error of the mean. The data is corrected for the change in surface potential due to the addition of the solvent, ethanol, and, as the intensity decreases with each addition, the magnitude of the change is plotted allowing the fit of a hyperbolic saturation binding equation, R^2=0.99, yielding B_{max}=14.8±0.1, K_d=1.9±0.1μM.

α-Tocopherol succinate increases the surface potential by introducing further negative charge to the membrane-water interface as it binds. This protonates the xanthene ring system of the membrane-bound FPE, which sits at the membrane surface decreasing the fluorescence intensity. When comparing the titration curves of α-tocopherol succinate to Di-8-ANEPPS labelled- and FPE labelled- cells (Figures 4.1.9 & 4.1.11 respectively) it is immediately evident that considerably higher concentrations of α-tocopherol succinate are required to saturate FPE labelled- than Di-8-ANEPPS labelled- cell membranes (approximately 50μM and 5μM in FPE and Di-8-ANEPPS labelled cells respectively). Furthermore, comparing the K_d values; K_d=1.9±0.1μM and K_d=0.48±0.08μM for FPE and Di-8-ANEPPS labelled cells respectively, indicates that FPE detectable α-tocopherol succinate binding has an approximately four times higher tendency to dissociate from the membrane than α-tocopherol succinate binding detected by Di-8-ANEPPS. It is possible that there are two distinct populations of α-tocopherol succinate interacting with cell membranes; of which both modulate the surface potential but only one elicits change in the dipole potential. These populations could be one in which α-tocopherol

succinate molecules bind and insert into the membrane, changing both the surface and dipole potential, and one that binds only to the membrane surface thus having no detectable effect on the dipole potential. This is consistent with the differences in K_d; α-tocopherol succinate that has inserted into the membrane is likely to have a much stronger interaction with the membrane than that on the membrane surface which would have a higher tendency to dissociate.

In Chapter 3 α-tocopherol succinate was shown to change the dipole potential when titrated to pure phosphatidylcholine vesicles suggesting it inserts into the membrane and so it is likely the first population is one that binds and inserts directly to the lipid bilayer of the cell membranes. The second population may be α-tocopherol succinate binding the membrane surface and unable to insert. For example α-tocopherol succinate entangled with the glycocalyx may experience steric or electrostatic hindrance, preventing it from reaching the bilayer. Alternatively, as the concentration range of the titration exceeds CMC, the second population may represent the transient interaction of α-tocopherol succinate micelles with the membrane surface. Both of these considerations would result in a weaker interaction with the membrane than associated with the insertion (and dipole potential modulation) of the molecule which is consistent with the higher tendency towards dissociation identified by the K_d values.

It is also possible that α-tocopherol succinate may bind receptors on the membrane surface. If the receptor does not undergo any conformational change that elicits a change in dipole potential but the charge of α-tocopherol succinate contributes to the cell surface charge when bound to the receptor this will give a population that modulates the surface potential only.

The α-tocopherol succinate titrations to FPE labelled Jurkat T-lymphocytes can also be compared with titrations to the compositionally simpler FPE labelled phosphatidylcholine (PC) vesicles discussed in Chapter 3. The higher K_{eff} value for titrations to 30mol%Cholesterol-70mol%PC than 100%PC vesicles, showing a greater efficacy of α-tocopherol succinate in changing the surface potential in the presence of cholesterol, led to the suggestion that α-tocopherol succinate localises, at least partially, in l_o domains where the change in surface potential elicited has a much greater effect on the fluorescence signal due to the higher density of FPE. In the cell system, $k_{eff}=7.8\pm0.4\mu M^{-1}$, which is closer to that of PC-cholesterol vesicles ($k_{eff}=5.2\pm0.5\mu M^{-1}$) than that of PC vesicles ($k_{eff}=2.3\pm0.3\mu M^{-1}$) suggesting that α-tocopherol succinate is also localising, at least partially, in areas of high FPE density i.e., domains rich in saturated phospholipids such as rafts. The K_{eff} value in cells is significantly higher than that in PC-cholesterol vesicles which may reflect an increased preference of α-tocopherol succinate for l_o domains, or a wider diversity of saturated-lipid containing ordered microdomains into which α-tocopherol succinate may partition resulting from the complex phase behaviour and domain stabilising effects of a variety of proteins and lipids in the cell membrane.

It is also possible, therefore, that the two populations of α-tocopherol succinate interacting with the membrane identified above correlate with α-tocopherol succinate binding to raft and non-raft domains. In titrations to Di-8-ANEPPS labelled PC vesicles in Section 3.3.2 the binding affinity of α-tocopherol succinate to vesicles containing 30mol% cholesterol was shown to be significantly greater than that for 100%PC vesicles suggesting the tendency for α-tocopherol succinate bound to l_o domains to dissociate is considerably less. The binding of α-tocopherol succinate to raft and non-raft domains is therefore also consistent with the strongly and weakly interacting populations identified.

4.2. The effects of Cholesterol and 7-ketocholesterol on the interactions of α-tocopherol succinate with Jurkat-T-lymphocyte membranes

In the previous section α-tocopherol succinate was shown to modulate both the dipole and surface potentials of Jurkat T-lymphocyte membranes (Figures 4.1.9 & 4.1.11) in a similar manner to that of phosphatidylcholine vesicles. Studies with cholesterol containing vesicles in Chapter 3 indicate a possible association of α-tocopherol succinate with the cholesterol enriched liquid ordered (l_o) phase in both the FPE and Di-8-ANEPPS based investigations (Figures 3.3.2 & 3.3.5). Recently, through characterisation of detergent extracted lipid fractions, α-tocopherol has been reported to partition into lipid rafts in cell membranes (Royer et al., 2009). This section investigates any similar association of α-tocopherol succinate with lipid rafts through its interaction with Jurkat T-lymphocyte cell membranes which contain either added cholesterol or are depleted of rafts by methyl-β-cyclodextrin treatment.

Previously in this chapter, 7-ketocholesterol was found to cause a greater effect on the dipole potential of cell membranes in the presence of lipid rafts compared to the raft-depleted membranes of methyl-β-cyclodextrin treated cells (Figure 4.1.5). This is consistent with reports that 7-ketocholesterol partitions into and disrupts rafts through perturbation of their characteristic high lipid packing and order (Myers and Stanley, 1999, Berthier et al., 2004, Massey and Pownall, 2005, Royer et al., 2009). If α-tocopherol succinate does associate with rafts, 7-ketocholesterol is likely to modulate the interaction of α-tocopherol succinate with the membrane. In PC vesicles 7-ketocholesterol also altered the interaction of α-tocopherol succinate with both FPE and Di-8-ANEPPS labelled membranes, in the absence of cholesterol enriched l_o phase domains. The following section therefore also investigates the interaction of α-tocopherol succinate on Jurkat T-lymphocyte membranes with added 7-ketocholesterol, which has potential to modulate the effect of α-tocopherol succinate on the dipole potential in both raft and non-raft domains.

4.2.1. The effect of cholesterol on the interactions of α-tocopherol succinate with Jurkat T-lymphocyte membranes

FPE labelled Jurkat T-lymphocytes were treated with a single addition of cholesterol, previously shown to cause significant increase in the dipole potential (Figure 3.1.3 Figure 4.1.2) suggestive of further raft formation, prior to titration of α-tocopherol succinate.

The concentration of cholesterol used was below the K_d determined by the titration of cholesterol to Di-8-ANEPPS labelled cells (Figure 4.1.2) in order to minimize the effects of the compensating actions of cells whose finely tuned membrane cholesterol concentration is perturbed. For example, cells have been shown to endocytose rafts when the proportion of raft to non-raft regions increase beyond that required for normal function of the membrane (Lajoie

and Nabi, 2010), an effect which could greatly alter the subsequent interaction of α-tocopherol succinate. Figure 4.2.1 compares the titration of α-tocopherol succinate to cholesterol treated cells with untreated cells. Both the maximum percentage change in FPE fluorescence, B_{max}, and the tendency toward dissociation after binding, K_d, are significantly decreased after cholesterol treatment (unpaired t-tests, R^2=0.93 P=0.019 and R^2=0.82 P=0.0058 for B_{max} and K_d values respectively). Saturation of the decrease in FPE fluorescence is also reached at approximately half the concentration of α-tocopherol succinate in cholesterol treated compared to untreated cells. This suggests that the association of α-tocopherol succinate with the membrane is greatly increased when the proportion of rafts is increased, but the total amount binding to the membrane is reduced resulting in a lower maximum percentage change in FPE fluorescence.

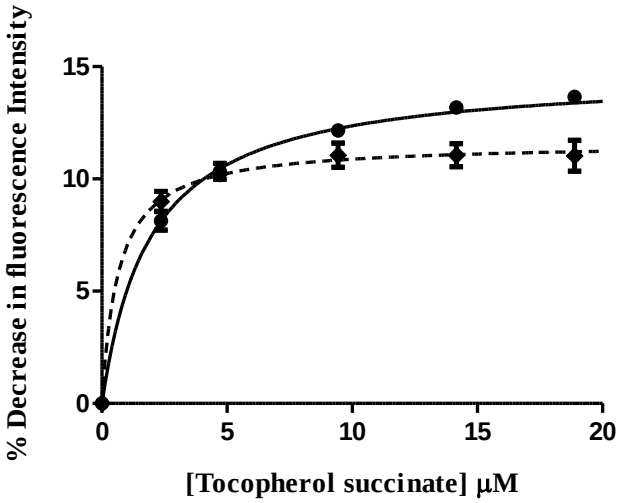

Figure 4.2.1: The percentage change in FPE fluorescence on titration of α-tocopherol succinate to untreated (●) and cholesterol (0.325μM, 10min) treated (♦) Jurkat T-lymphocytes. The data represents the average of 3 repeats (error bars are the standard error of the mean) and is corrected for the percentage change in intensity caused by addition of the solvent, ethanol. A hyperbolic saturation binding model is fitted to both data sets yielding B_{max}=14.8±0.1 K_d=1.9±0.1μM with R^2=0.99 for untreated cells (—) and B_{max}=11.6±0.3 K_d=0.7±0.2μM with R^2=0.97 for cholesterol treated cells (----).

The relative changes in B_{max} and K_d of α-tocopherol succinate titrations between cholesterol treated and untreated cells can be compared with those for titrations to phosphatidylcholine vesicles with and without 30mol% cholesterol (Figure 3.3.2). In vesicles the presence of cholesterol increased B_{max} by 37% but did not significantly alter K_d. In this system the comparison is being made between PC vesicles containing no l_o-phase domains and vesicles with 30mol% cholesterol which do have l_o domains. The increase in B_{max} was ascribed to the partition of some α-tocopherol succinate into l_o domains where the higher concentration of FPE (relative to l_d domains) causes α-tocopherol succinate to have a greater effect on fluorescence in these domains (see section 3.3.1).

In the cell system the comparison is being made between untreated cells which have membrane rafts and cholesterol treated cells which are expected to have an increased proportion of rafts. The relative change in K_d is a 60% decrease on cholesterol treatment of cells which is much

greater than the insignificant decrease with the presence of cholesterol in PC vesicles. The increase in proportion of rafts after cholesterol treatment of cells cannot be determined however, it is likely to be less than the increase in l_o phase domains with the inclusion of 30mol% cholesterol to PC vesicles. This indicates that the binding affinity of α-tocopherol succinate is much more sensitive to an increase in the proportion of rafts in cells than l_o phase domains in PC vesicles suggesting that the interaction may be sensitive to a property of rafts not possessed by the l_o phase domains promoted by cholesterol in PC vesicles.

The relative changes in B_{max} in the cell and liposome systems are also very different with a 21% decrease between untreated and cholesterol treated cells and a 37% increase between PC and PC-cholesterol vesicles. The decrease in the total amount of α-tocopherol succinate binding when cells are treated with cholesterol suggests the number of available binding sites is reduced as the proportion of rafts increases. This may be due to the decrease in the proportion of l_d phase domains; α-tocopherol is known to preferentially localise in l_d regions and, as α-tocopherol and α-tocopherol succinate cause similar change in the dipole potential, α-tocopherol succinate may also be assumed to preferentially locate in these regions. Increasing the proportion of rafts in the cell membrane is likely to reduce the extent of l_d domains reducing the binding sites for α-tocopherol succinate associated with these regions.

It is possible that the differences in α-tocopherol succinate binding behaviour in the presence of cholesterol between cells and vesicles indicates that α-tocopherol succinate may bind a cell-surface receptor and the affinity for this interaction is sensitive to the presence of rafts. The relative changes in B_{max} and K_d on cholesterol treating cells would therefore reflect changes in the binding affinity and localisation of both lipid-binding and receptor-binding α-tocopherol succinate whereas in the liposome system only changes in lipid-binding are observed. The relationship between the presence of lipid rafts and the binding behaviour of α-tocopherol succinate can be further investigated by depletion of membrane rafts with methyl-β-cyclodextrin.

Figure 4.2.2 compares the titration of α-tocopherol succinate to methyl-β-cyclodextrin (MβCD) treated- and untreated- Di-8-ANEPPS labelled cells. The parameters returned from fitting hyperbolic saturation binding models to the data are compared in table 4.1.1. The dissociation constant, K_d, for MβCD treated cells is significantly higher indicating a reduced binding affinity of α-tocopherol succinate to raft depleted cells. This is consistent with the localisation of α-tocopherol succinate in l_d regions of raft-depleted cells where the lower lipid packing and reduced order, in comparison to the l_o phase lipid rafts of untreated cells, causes a greater tendency for α-tocopherol succinate to dissociate from the membrane. This is reflected in the substantially higher concentration of α-tocopherol succinate required to reach saturation in

MβCD compared with untreated cells. The B_{max} value is also significantly lower resulting in a lower K_{eff}, the efficacy of α-tocopherol succinate in changing the dipole potential, in MβCD treated raft depleted cells.

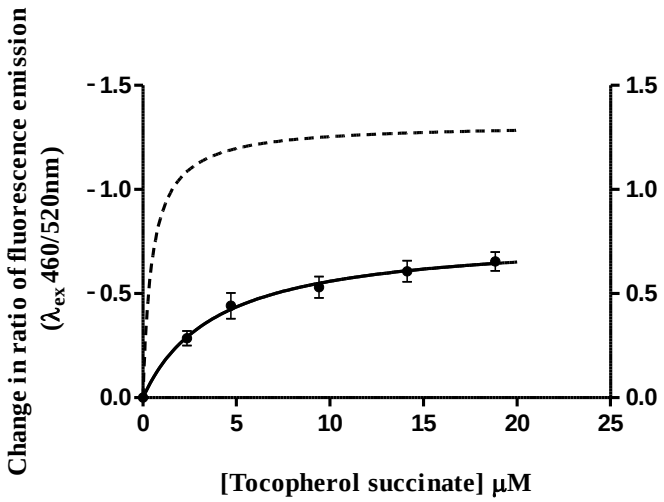

Figure 4.2.2: The change in the ratio, ΔR, of Di-8-ANEPPS fluorescence intensity at 460nm and 520nm excitation ($R=I_{460}/I_{520}$) as α-tocopherol succinate is titrated to methyl-β-cyclodextrin treated Jurkat T-lymphocytes (●). The change in ratio on addition of equal volumes of the solvent, ethanol, is subtracted from the data which is the average of 3 repeats, the error bars representing the standard error of the mean. The modulus of the data (right y-axis) is fitted to a hyperbolic saturation binding model (R^2=0.93, ─) and the fit for α-tocopherol succinate titration to untreated cells (----) is also shown for comparison. The resulting fitting parameters are shown in Table 4.2.1.

Di-8-ANEPPS detects the population of α-tocopherol succinate that inserts into the membrane and is therefore able to change the dipole potential. This is true of the lipid-binding fraction of α-tocopherol succinate and the trends in K_d, B_{max} and K_{eff} are consistent with the behaviour of α-tocopherol succinate in vesicle systems (Section 3.3). The increase in K_d on raft depletion is comparable to the relatively large, albeit not significant, decrease in the K_d of α-tocopherol succinate binding to PC-cholesterol vs PC vesicles which differ by the presence and absence, respectively, of l_o phase domains. The lower B_{max} and K_{eff} in raft-depleted cells compared with untreated cells is consistent with the notion that α-tocopherol succinate, by perturbing the tight lipid packing, decreases the dipole potential to a much greater extent in the l_o phase than the l_d phase. In a raft depleted membrane the proportion of α-tocopherol succinate localising in l_d phase domains increases and therefore the extent to which α-tocopherol succinate modulates the dipole potential decreases.

Quantity	*Untreated*	*MβCD treated*	R^2	*P value*
B_{max}	1.32±0.05	0.79±0.05	0.92	0.002
K_d (μM)	0.50±0.08	4.1±0.9	0.90	0.004
K_{eff} (μM^{-1})	2.6±0.4	0.17±0.03	0.89	0.005

Table 4.2.1: The maximum change in Di-8-ANEPPS ratio ($R=I_{460}/I_{520}$), B_{max}, and the concentration of α-tocopherol succinate at which half this change is achieved, K_d, resulting from the hyperbolic saturation binding models fitted to the data of Figure 4.2.2. K_{eff} values, the molar efficacy of α-tocopherol succinate in changing the dipole potential, are calculated by dividing B_{max} by K_d. Unpaired two-tailed t-tests were performed to compare values from untreated and methyl-β-cyclodextrin treated Jurkat T-lymphocytes showing all values to be significantly different with $P<0.01$.

In the discussion following Figure 4.2.1, however, the possibility that α-tocopherol succinate binds a membrane receptor was suggested. The binding of a ligand to a receptor has been shown to change the membrane dipole potential. For example, Asawakarn *et al.* observed modulation of the dipole potential on the binding of saquinavir with Caco-2 epithelial cell membrane receptors (Asawakarn et al., 2001). The changes in the dipole potential detected here may, therefore, reflect not only the direct insertion of α-tocopherol succinate into the bilayer but also the binding of α-tocopherol succinate to a receptor. In this case the increase in K_d and decrease in B_{max} reflect a decreased affinity of α-tocopherol succinate to bind to the receptor after raft depletion by MβCD suggesting that any potential receptor-binding of α-tocopherol succinate is raft-mediated. The receptor binding, if it does occur, may be sensitive to the concentration of cholesterol, and therefore proportion of rafts, in the membranes. As shown previously here (Figures 4.1.1 & 4.1.2) and elsewhere (Asawakarn et al., 2001) lipid rafts possess a higher dipole potential than non-raft regions of the membrane, therefore it is possible that the receptor is sensitive to the dipole potential of its environment.

4.2.2. The effect of 7-ketocholesterol on the interaction of α-tocopherol succinate with Jurkat-T-lymphocyte membranes

In the previous section the interaction of α-tocopherol succinate with Jurkat T-lymphocyte membranes was shown to be influenced by the extent of lipid rafts in the cell membrane. 7-ketocholesterol is known to insert into lipid rafts (Myers and Stanley, 1999, Berthier et al., 2004, Massey and Pownall, 2005, Royer et al., 2009) where it disrupts the characteristic high lipid packing density and dramatically decreases the membrane dipole potential (Figure 4.1.3). The presence of 7-ketocholesterol in the cell membrane is therefore likely to have an effect on subsequent interactions of α-tocopherol succinate.

To investigate this effect, FPE labelled Jurkat T-lymphocytes were treated with a pre-K_d concentration of 7-ketocholesterol, previously determined by titration to Di-8-ANEPPS labelled cells (Figure 4.1.5), prior to titration of α-tocopherol succinate. This concentration was chosen to minimise any compensating response of the cell to the physical perturbation of the membrane by 7-ketocholesterol whilst still causing significant decrease in the membrane dipole potential. It has also been shown to have no significant effect on cell viability over the time course of the α-tocopherol succinate titration (data shown in Appendix A).

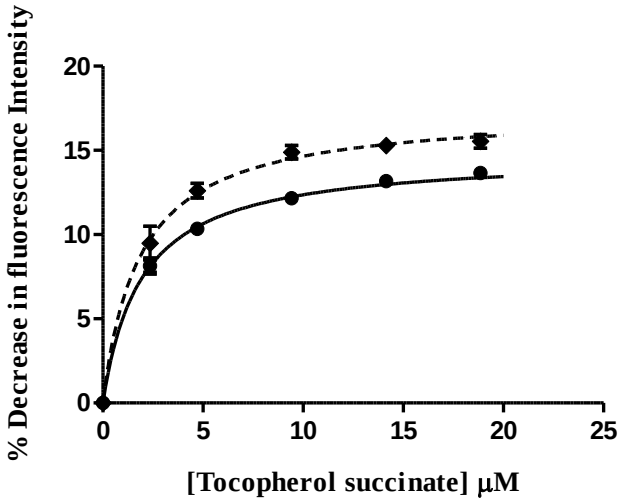

Figure 4.2.3 The percentage change in FPE fluorescence on titration of α-tocopherol succinate to untreated (●) and 7-ketocholesterol (0.325μM, 10min) treated (♦) Jurkat T-lymphocytes. The data represents the average of 3 repeats (error bars are the standard error of the mean) and is corrected for the percentage change in intensity caused by addition of the solvent, ethanol. A hyperbolic saturation binding model is fitted to both data sets yielding B_{max}=14.8±0.1 K_d=1.9±0.1μM with R^2=0.99 for untreated cells (─) and B_{max}=17.4±0.5 K_d=1.9±0.3μM with R^2=0.98 for 7-ketocholesterol treated cells (----).

Figure 4.2.3 shows the resulting binding curves of α-tocopherol succinate to 7-ketocholesterol treated and untreated cells through its modulation of the membrane surface potential. The K_d value, representing and tendency towards dissociation once bound, of α-tocopherol succinate is not significantly different after 7-ketocholesterol treatment. The maximum percentage change in FPE fluorescence, B_{max} however, is significantly increased (one-way ANOVA P=0.0001 and Tukey's multiple comparison test) indicating that the presence of 7-ketocholesterol in the cell membrane causes α-tocopherol succinate to have a greater effect on FPE fluorescence without altering its affinity to bind to the membrane. An interpretation of this result is that 7-ketocholesterol may modulate the lateral distribution of FPE and/or the extent of partitioning of α-tocopherol succinate between raft and non-raft domains. If FPE is laterally redistributed by the introduction of 7-ketocholesterol to the membrane, a higher concentration of FPE may reside in regions experiencing a significant increase in the surface potential when α-tocopherol succinate is added. This would result in the protonation of a greater number of FPE molecules by the surface potential increase induced by α-tocopherol succinate leading to a greater decrease in the fluorescence intensity of FPE in 7-ketocholesterol treated cells compared with untreated cells on exposure to α-tocopherol succinate. 7-ketocholesterol may also alter the localisation of α-tocopherol succinate in the membrane resulting in a greater partitioning into regions of higher FPE concentration, such as rafts.

The introduction of 7-ketocholesterol into the composition of phosphatidylcholine- (PC) and cholesterol- containing vesicles, labelled with FPE, resulted in a decrease in B_{max} of α-tocopherol succinate titration compared to PC-cholesterol vesicles (Figure 3.3.3). This is in contrast to the increase observed here in 7-ketocholesterol treated cells, indicating that the

mechanism by which α-tocopherol succinate interacts with cells differs from the lipid-binding interaction observed with vesicles. Modulation of the surface potential on the binding of α-tocopherol succinate to cell membrane receptor(s) may account for this difference. Another consideration is that the ratio of 7-ketocholesterol:cholesterol in the membrane is likely to be lower in cells than in the vesicles so that 7-ketocholesterol in cells will exert less of an effect on rafts than on l_o domains in vesicles. Where 7-ketocholesterol disrupted l_o phase domains in vesicles it may modulate the lipid packing of cell membrane rafts to a much lesser extent, perhaps altering their dipole potential without entirely disrupting the raft, resulting in differences in the interaction of α-tocopherol succinate with 7-ketocholesterol containing cell and vesicle membranes.

The effect of 7-ketocholesterol on the interaction of α-tocopherol succinate with cell membranes can also be observed through modulation of the membrane dipole potential. α-Tocopherol succinate was titrated to Di-8-ANEPPS labelled Jurkat T-lymphocytes treated with 7-ketocholesterol as described above and the resulting binding curve is shown in figure 4.2.4. The binding curve if α-tocopherol succinate to untreated cells is also shown for comparison.

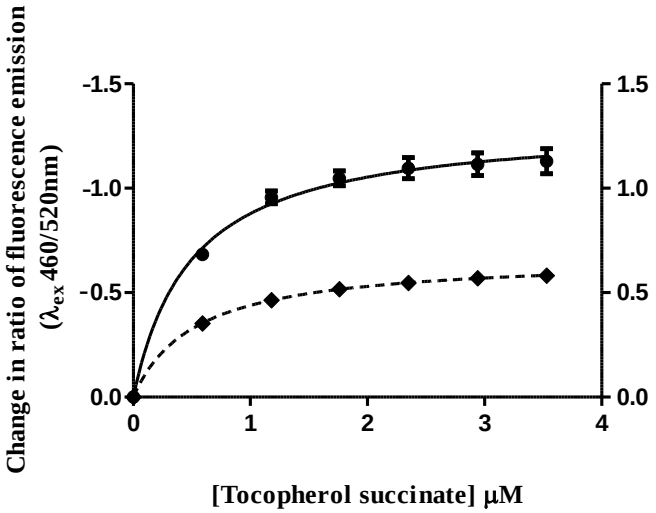

Figure 4.2.4: The change in the ratio, ΔR, of Di-8-ANEPPS fluorescence intensity at 460nm and 520nm excitation ($R=I_{460}/I_{520}$) as α-tocopherol succinate is titrated to untreated (●) and 7-ketocholesterol (0.325μM, 10min) treated (♦) Jurkat T-lymphocytes. The data represents the average of 3 repeats (error bars are the standard error of the mean) and is corrected for the change in ratio caused by addition of the solvent, ethanol. The modulus of the data (right y-axis) is fitted to a hyperbolic saturation binding model yielding B_{max}=1.32±0.05 K_d=0.50±0.08μM with R^2=0.97 for untreated cells (─) and B_{max}=0.67±0.02 K_d=0.53±0.07μM with R^2=0.98 for 7-ketocholesterol treated cells (----).

The k_d values for α-tocopherol succinate titration to untreated and 7-ketocholesterol treated cells are not significantly different indicating that the binding affinity of α-tocopherol succinate for the membrane is not altered by the presence of 7-ketocholesterol. The same result was reported for the parallel experiment with FPE labelled cells above. The maximum change in dipole potential, B_{max}, and subsequently the efficacy in changing the dipole potential, K_{eff}, of α-tocopherol succinate in untreated and 7-ketocholesterol treated cells is significantly different

(unpaired two tailed t-test, P=0.0003 and P=0.04 for B_{max} and K_{eff} respectively). The presence of 7-ketocholesterol therefore causes α-tocopherol succinate to have a much reduced effect on the dipole potential despite the extent of insertion into the membrane remaining unchanged. α-Tocopherol succinate localises, at least partially, in lipid rafts where it induces a significant reduction in the dipole potential, as demonstrated above by the reduction in the efficacy of α-tocopherol succinate in changing the dipole potential after methyl-β-cyclodextrin depletion of rafts (Figure 4.2.2). This suggests that a possible explanation for the reduced K_{eff} of α-tocopherol succinate in 7-ketocholesterol treated cells may be its reduced localisation in rafts. Royer *et al*. (Royer et al., 2009) report a 10% reduction in the relative proportion of α-tocopherol in detergent extracted raft fractions when A7R5 cells were pre-treated with 7-ketocholesterol (20μg ml^{-1}, 1hr). It is possible that, like α-tocopherol, the relative proportion of α-tocopherol succinate in rafts of 7-ketocholesterol treated Jurkat-T-lymphocytes similarly decreases. Another consideration is that the magnitude of the dipole potential of rafts is lower due to the effect of 7-ketocholesterol in reducing the lipid ordering. This means that α-tocopherol succinate subsequently localising in the 7-ketocholesterol containing raft will not disrupt lipid packing to the extent that it would in the rafts of untreated cells and would therefore be less effective in decreasing the dipole potential in 7-ketocholesterol treated cells.

Comparisons drawn previously between the binding curves of α-tocopherol succinate to cells and cholesterol-containing phosphatidylcholine vesicles, both Di-8-ANEPPS and FPE labelled, have lead to the suggestion that α-tocopherol succinate may bind to a receptor. It is possible such a receptor binding event may change the dipole potential of the membrane surrounding the receptor. In this case, the reduced efficacy of α-tocopherol succinate in decreasing the dipole potential following 7-ketocholesterol treatment suggests that the dipole potential change associated with the receptor-α-tocopherol succinate complex is different in the presence of 7-ketocholesterol (K_d is not significantly different with or without 7-ketocholesterol treatment suggesting that changes in the affinity of α-tocopherol succinate for the receptor is not responsible for the reduced efficacy). This effect has been observed by Asawakarn *et al.*(Asawakarn et al., 2001) where the change in dipole potential upon the interaction of the human immunodeficiency virus protease inhibitor, Saquinavir, with Caco-2 cells differed significantly when cells were treated with agents known to increase or decrease the dipole potential. In their investigation the nature of the interaction with Caco-2 cells in comparison to that of phosphatidylcholine vesicles implied that Saquinavir binds a membrane receptor. As the affinity of Saquinavir for the receptor was found not to change as the initial dipole potential was varied, differences in the effect of Saquinavir binding to Caco-2 membranes of differing initial dipole potential suggest the influence of the Saquinavir-receptor complex on the dipole potential varies according to the initial dipole potential of the membrane.

4.3. The influence of α-tocopherol succinate on the effect of 7-ketocholesterol on the membrane dipole potential of Jurkat T-lymphocytes

In the previous section it was demonstrated that the presence of 7-ketocholesterol in the membrane significantly influences the subsequent effect of α-tocopherol succinate on the membrane dipole potential. This is thought to result from differences in the localisation of α-tocopherol succinate in the membrane following 7-ketocholesterol treatment. Lemaire-Ewing *et al.* (Lemaire-Ewing et al., 2010) hypothesize that the localisation of α-tocopherol in lipid rafts is crucial to its ability to inhibit 7-ketocholesterol induced apoptosis by the exclusion of the latter from rafts. This chapter aims to investigate if α-tocopherol succinate alters the subsequent effect of 7-ketocholesterol on the dipole potential reflecting changes in the partitioning of 7-ketocholesterol between liquid ordered (raft-like) and liquid-disordered domains in the presence of α-tocopherol succinate. The influence of α-tocopherol succinate on the dipole potential change elicited by 7-ketocholesterol is then compared between normal cells and cells with a lowered initial dipole potential associated with oxidative stress.

4.3.1. α-Tocopherol succinate treatment and the efficacy of 7-ketocholesterol in modulating the membrane dipole potential

The effect of the presence of α-tocopherol succinate in cell membranes on the subsequent modulation of the dipole potential by 7-ketocholesterol was investigated by incubating cells with α-tocopherol succinate prior to 7-ketocholesterol titration. Jurkat-T-lymphocytes, labelled with Di-8-ANEPPS, were treated with α-tocopherol succinate for 10 minutes; the time required to reach a stable reading in the ratio of Di-8-ANEPPS fluorescence ($R=I_{460}/I_{520}$) after a single addition of α-tocopherol succinate at 37^{o}C suggesting equilibrium in the insertion and partitioning of α-tocopherol succinate between different membrane phases has been reached. The concentration chosen was below the K_d concentration determined by titration to FPE labelled cells (figure 4.1.11), but shown to cause near-maximal change in the dipole potential (figure 4.1.9).

From figure 4.3.1 it is evident that treating cells with α-tocopherol succinate has a profound effect on the change in dipole potential elicited by the subsequent 7-ketocholesterol titration. The maximum change in the dipole potential by 7-ketocholesterol, B_{max}, is significantly decreased and the concentration at which half this change occurs, K_d, is significantly increased, in cells that are pre-treated with α-tocopherol succinate (unpaired two-tailed t-test, $P<0.005$ for both k_d and B_{max}). The efficacy of 7-ketocholesterol in modulating the dipole potential, K_{eff}, calculated by the division of B_{max} by K_d, is decreased over 4-fold after α-tocopherol succinate treatment (unpaired two-tailed t-test, $P=0.0003$). The much reduced efficacy of 7-ketocholesterol may be due to differences in the extent it partitions into regions of different phase in the presence of α-tocopherol succinate. Due to differences in its effect on lipid order

and the relative contribution from its molecular dipole in the unsaturated-lipid rich liquid disordered (l_d) and cholesterol-rich lipid ordered (l_o) phases, 7-ketocholesterol alters the dipole potential of lipid rafts (l_o) and l_d regions to different extents. Previous experiments (Section 4.2) have lead to the suggestion that α-tocopherol succinate may localise in lipid rafts and it is possible that this may alter the extent to which 7-ketocholesterol, added after α-tocopherol succinate, can partition into rafts. Royer *et al.* (Royer et al., 2009) have demonstrated this effect in α-tocopherol treated A7R5 cells. 7-ketocholesterol was found at lower concentrations in detergent-extracted raft fractions after α-tocopherol treatment than in the absence of α-tocopherol. As well as partitioning into lipid rafts of cells, α-tocopherol has been shown to localise with, and increase the order of, unsaturated lipids in the l_d phase (Atkinson et al., 2010, Atkinson et al., 2008, SanchezMigallon et al., 1996, Quinn, 2004) and α-tocopherol succinate may behave similarly (Figure 3.3.4). The increased lipid packing and reduced hydration resulting from the increase in order of the l_d phase has potentially significant consequences on the extent to which 7-ketocholesterol modulates the dipole potential. In an untreated membrane 7-ketocholesterol slightly increases lipid packing in the l_d phase, but if the l_d phase is already ordered by the presence of α-tocopherol succinate, the relative effect on lipid packing on introducing 7-ketocholesterol is likely to be quite different. 7-ketocholesterol is considered to have a tilted orientation in the l_d phase (Massey, 2001), promoted by the hydration of its two polar moieties, which serves to increase the proportion of its molecular dipole that is resolved anti-parallel to the membrane normal (Starke-Peterkovic et al., 2006). This increases the contribution of 7-ketocholesterol in decreasing the dipole potential in the l_d phase relative to the l_o phase. The effect of the lipid ordering action of α-tocopherol succinate, along with the effect of its polar succinate moiety on hydration, is likely to perturb the hydration-promoted tilted orientation of 7-ketocholesterol and thus its contribution to the dipole potential. A parallel has been drawn between the lipid-ordering effect of α-tocopherol with unsaturated lipids in the l_d phase and that of cholesterol with saturated lipids forming the l_o phase (Atkinson et al., 2010, Atkinson et al., 2008). It is possible that 7-ketocholesterol may have the same non-tilted orientation in α-tocopherol-succinate-ordered phases as it does in cholesterol-ordered phases which could also account for its greatly reduced efficacy in changing the dipole potential in the presence of α-tocopherol succinate.

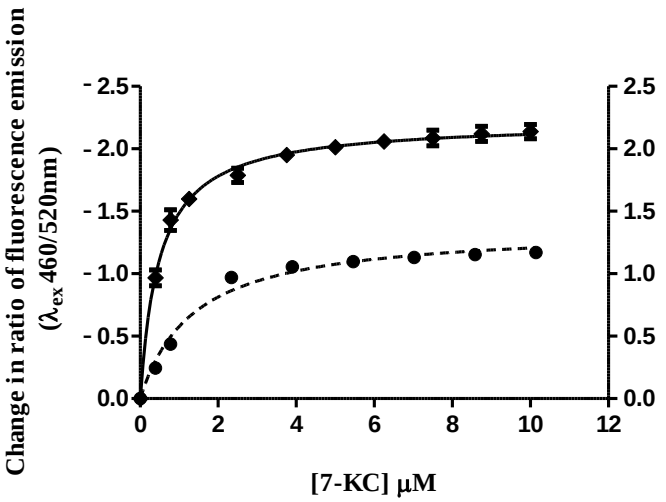

Figure 4.3.1: The change in the ratio, ΔR, of Di-8-ANEPPS fluorescence intensity at 460nm and 520nm($R=I_{460}/I_{520}$) excitation as 7-ketocholesterol (7-KC) is titrated to Di-8-ANEPPS labelled Jurkat T-lymphocytes treated with α-tocopherol succinate (2.36μM, 10min 37°C) (●). The titration to untreated cells (♦) is also shown for comparison. The change in ratio on addition of equal volumes of the solvent, ethanol, is subtracted from the data which is the average of 3 repeats, the error bars representing the standard error of the mean. The modulus of the data (right y-axis) is fitted to a hyperbolic saturation binding model with R^2=0.98 B_{max}=1.37±0.03 K_d=1.4±0.1μM for α-tocopherol succinate treated cells (----) and R^2=0.99 B_{max}=2.22±0.03 K_d=0.49±0.03μM for untreated cells (─).

4.3.2. α-Tocopherol succinate influences the effect of 7-ketocholesterol on the dipole potential differently in a cell membrane dipole potential based model of oxidative stress.

The use of α-tocopherol as an antioxidant to prevent or reduce the oxidative stress associated with insulin resistance and cardiovascular disease yields contradictory outcomes (e.g. (Celik et al., 2010, De Rosa et al., 2010, Saremi and Arora, 2010)), but the reasons for these differences are unknown. This work has shown that 7-ketocholesterol, the oxidation product of cholesterol, significantly reduces the membrane dipole potential. As cholesterol forms a crucial component of functionally important lipid rafts and the modulation of the dipole potential has been shown to alter the behaviour of membrane-bound receptors, it is likely that the altered dipole potential as a result of membrane oxidation contributes to the state of oxidative stress. α-Tocopherol succinate treatment was shown to reduce the effect of subsequent exposure of cells to 7-ketocholesterol on the dipole potential in the previous section (Section 4.3.1). However, Section 4.2.2 demonstrated that the influence of α-tocopherol succinate on the membrane is itself altered by the presence of 7-ketocholesterol. It therefore seems likely that the influence of α-tocopherol succinate on the effect of 7-ketocholesterol on the dipole potential may depend on the existing oxidative state of the membrane and the associated initial dipole potential.

A dipole potential based model of oxidative stress in Jurkat T-lymphocytes was achieved by incubating the cells with 0.3125μM 7-ketocholesterol (10min, 37°C) which causes a significant decrease in the dipole potential but is far below the concentration that would saturate the membrane. 7-ketocholesterol titration was then performed following subsequent treatment with

α-tocopherol succinate or an equal volume of the solvent without α-tocopherol succinate. The resulting titration curves are shown in Figure 4.3.2.

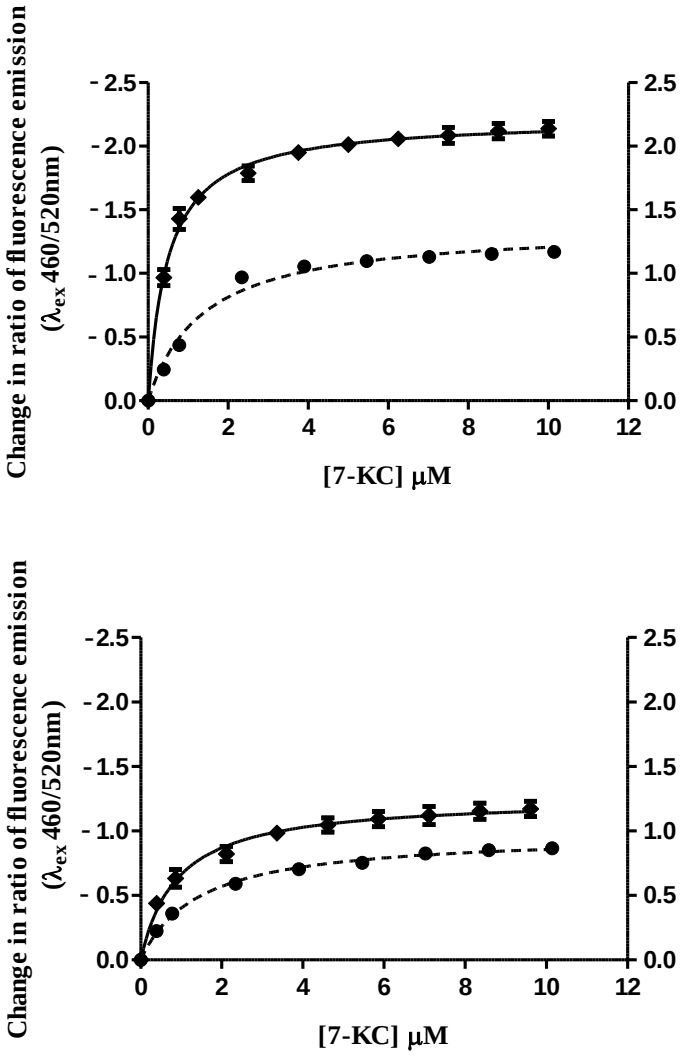

Figure 4.3.2: The change in the ratio, ΔR, of Di-8-ANEPPS fluorescence intensity at 460nm and 520nm excitation ($R=I_{460}/I_{520}$) as 7-ketocholesterol (7-KC) is titrated to Di-8-ANEPPS labelled Jurkat T-lymphocytes. The *Top* graph shows the titration curves to cells that have not been exposed to 7-KC and the *bottom* graph shows the titration curves to cells that have been exposed to 7-KC (0.3125μM, 10min, 37°C). In both graphs titrations to cells that have been treated with 2.36μM (10min 37°C) α-tocopherol succinate (●) and to those that have been treated with an equal volume of solvent without α-tocopherol succinate (♦) are shown. All data is corrected for the change in ratio on titration of equal volumes of the solvent, ethanol, and represents the average of 3 repeats with the standard error of the mean shown as error bars. The modulus of the data (right y-axis) is fitted to a hyperbolic saturation binding model (─ and ---- for untreated and α-tocopherol succinate treated cells respectively).

The data is fitted to a hyperbolic saturation binding model and the values returned for the change in the dipole potential due to a saturation concentration of 7-ketocholesterol in the membrane, B_{max}, and the concentration at which half of this maximum change occurs , K_d, are shown in table 4.3.1.

	B_{max}	k_d (μM)	K_{eff} (μM^{-1})
Normal cells, untreated	2.22±0.03	0.49±0.03	4.5±0.3
Normal cells, TS treated	1.37±0.03	1.4±0.1	0.98±0.07
7-KC exposed cells, untreated	1.26±0.03	0.9±0.1	1.4±0.07
7-KC exposed cells, TS treated	0.98±0.02	1.4±0.1	0.70±0.05

Table 4.3.1: The B_{max} and K_d values yielded by fitting a hyperbolic saturation binding model to the data of figure 4.3.2 showing 7-ketocholesterol (7-KC) titration curves with and without α-tocopherol succinate (TS) treatment for normal cells and cells exposed to 7-KC representing a membrane dipole potential based model of oxidative stress. The K_{eff} values, calculated by dividing B_{max} by K_d, are also shown.

Comparison of the change in B_{max} values between untreated and α-tocopherol succinate treated cells in both the normal and 7-ketocholesterol exposed cell models shows that the maximum change in the dipole potential elicited by 7-ketocholesterol is reduced to a greater extent by α-tocopherol treatment in normal cells than in cells of the oxidative stress model. The effectiveness of 7-ketocholesterol in changing the dipole potential, K_{eff}, is calculated by dividing B_{max} by K_d for each of the cell membranes. A two-way ANOVA of the K_{eff} values confirms that the influence of α-tocopherol succinate on the molar effectiveness of 7-ketocholesterol in changing the dipole potential is significantly different in normal and oxidative stress cell models ($P=0.0001$). Bonferroni post tests show that the difference in K_{eff} values for 7-ketocholesterol in untreated and α-tocopherol treated cells in the normal cell model is very significant ($P<0.001$). In the oxidative stress cell model the K_{eff} of 7-ketocholesterol following α-tocopherol succinate treatment is not significantly different from the K_{eff} without treatment ($P>0.05$).

The influence of α-tocopherol succinate on the subsequent effect of 7-ketocholesterol on the dipole potential differs significantly between normal cells and the oxidative stress model cells that are pre-exposed to 7-ketocholesterol. α-Tocopherol succinate treatment may act to reduce the effect of oxidation on the membrane dipole potential where cells are not yet under significant oxidative stress. In cases where cells are already under significant oxidative stress, α-tocopherol treatment may not be of any benefit in reducing the effect of further oxidation on the membrane dipole potential.

The difference in the initial dipole potential between untreated and α-tocopherol succinate treated normal cells is greater than that for the oxidative stress model cells. This correlates with the larger ΔK_{eff} of 7-ketocholesterol between α-tocopherol succinate treated and untreated normal cells than for the oxidative stress model cells, suggesting that the initial magnitude of the membrane dipole potential may determine the K_{eff} of 7-ketocholesterol in that membrane.

The differences in the initial magnitude of the dipole potential between untreated and α-tocopherol succinate treated cells in the two cell models above may be due to difference in the localisation of α-tocopherol succinate in membranes with or without 7-ketocholesterol. In previous discussions it was suggested that α-tocopherol succinate treatment may alter the

localisation and orientation of 7-ketocholesterol in the membrane (Figure 4.3.1) and likewise 7-ketocholesterol treatment may affect the localisation of α-tocopherol succinate in membranes (figure 4.2.3), in both cases reducing K_{eff}. Based on these arguments, the presence of 7-ketocholesterol may alter the localisation of α-tocopherol succinate in the membrane, with respect to that in the absence of 7-ketocholesterol, such that its ability to reduce the extent of the dipole potential change by subsequently added 7-ketocholesterol is lower. For example Lemaire-Ewing *et al.* (Lemaire-Ewing et al., 2010) proposed the hypothesis that α-tocopherol localises in lipid rafts and prevents the incorporation of 7-ketocholesterol into rafts. However, when 7-ketocholesterol is present in the membrane before α-tocopherol the localisation of α-tocopherol in lipid rafts is reduced and further 7-ketocholesterol is not prevented from disrupting rafts. It is possible that α-tocopherol succinate behaves in a similar manner and the exclusion and non-exclusion of titrated 7-ketocholesterol from rafts in normal and oxidative stress model cells, respectively, accounts for the differences of K_{eff} of 7-ketocholesterol in these two models.

4.3.3. The involvement of lipid rafts in the influence of α-tocopherol succinate on the effect of 7-ketocholesterol on the membrane dipole potential

This section investigates the involvement of lipid rafts in the mechanism by which α-tocopherol succinate reduces the effect of subsequently added 7-ketocholesterol on the dipole potential. This can be done by comparing the effect of 7-ketocholesterol on the dipole potential, with and without prior α-tocopherol succinate treatment, in normal cells and cells treated with methyl-β-cyclodextrin to deplete lipid rafts. 7-ketocholesterol was titrated to Di-8-ANEPPS labelled Jurkat T-lymphocytes following methyl-β-cyclodextrin treatment (10mM 2min, reported to deplete 100% of raft cholesterol (Rouquette-Jazdanian et al., 2006)) with or without subsequent α-tocopherol succinate treatment. The resulting titration curves are shown in Figure 4.3.3 as well as those for 7-ketocholesterol titration to normal cells with or without prior α-tocopherol succinate treatment.

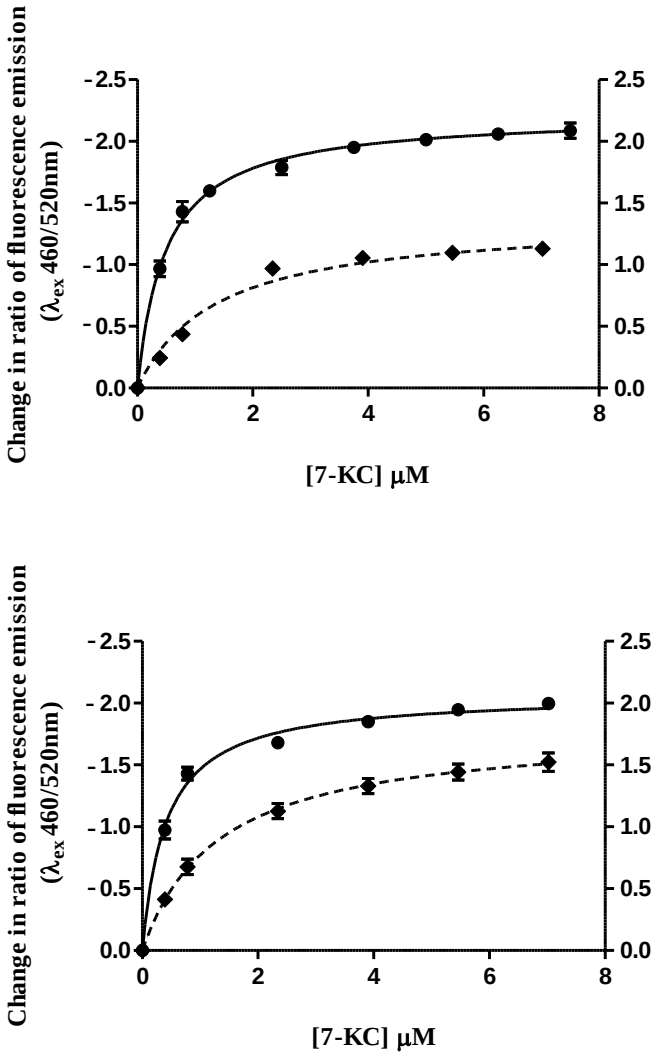

Figure 4.3.3: The change in the ratio, ΔR, of Di-8-ANEPPS fluorescence intensity at 460nm and 520nm excitation ($R=I_{460}/I_{520}$) as 7-ketocholesterol (7-KC) is titrated to Di-8-ANEPPS labelled Jurkat-T-lymphocytes. The top graph shows the titration curves to normal cells and the bottom graph shows the titration curves to cells that have been exposed to methyl-β-cyclodextrin (10mM, 2min). In both graphs titrations to cells that have been treated with 2.36μM (10min 37°C) α-tocopherol succinate (●) and to those that have been treated with an equal volume of solvent without α-tocopherol succinate (♦) are shown. All data is corrected for the change in ratio on titration of equal volumes of the solvent, ethanol, and represents the average of 3 repeats with the standard error of the mean shown as error bars. The modulus of the data (right y-axis) is fitted to a hyperbolic saturation binding model (─ and ---- for untreated and α-tocopherol succinate treated cells respectively).

The data is fitted to a hyperbolic saturation binding model and the values returned for the change in the dipole potential due to a saturation concentration of 7-ketocholesterol in the membrane, B_{max}, and the concentration at which half of this maximum change occurs , K_d, are shown in table 4.3.2.

	B_{max}	K_d (μM)	K_{eff} $(\mu M)^{-1}$
Normal cells, untreated	2.23± 0.03	0.49± 0.03	4.5± 0.3
Normal cells, TS treated	1.37± 0.03	1.4± 0.1	0.1± 0.1
MβCD exposed cells, untreated	2.07± 0.04	0.41± 0.04	5.0± 0.5
MβCD exposed cells, TS treated	1.79± 0.07	1.3± 0.2	1.4± 0.2

Table 4.3.2: The B_{max} and K_d values yielded by fitting a hyperbolic saturation binding model to the data of figure 4.3.3 showing 7-ketocholesterol (7-KC) titration curves with and without α-tocopherol succinate (TS) treatment for normal cells and cells exposed to MβCD to deplete lipid rafts. The K_{eff} values, calculated by dividing B_{max} by K_d, are also shown.

Comparison of the change in B_{max} values between untreated and α-tocopherol succinate treated cells in both the normal and methyl-β-cyclodextrin exposed cell models shows that the maximum change in the dipole potential elicited by 7-ketocholesterol is reduced approximately three times less by α-tocopherol treatment in raft depleted cells than in normal cells. The changes in B_{max} can be due to changes in the amount of 7-ketocholesterol that is binding or due to changes in the effect equal amounts of 7-ketocholesterol have in each membrane due to the different orientations exhibited by 7-ketocholesterol in different lipid domains. To investigate the latter, the effectiveness of 7-ketocholesterol in changing the dipole potential, K_{eff}, is calculated by dividing B_{max} by K_d for each of the cell membranes (values shown in table 4.3.2).

A two-way ANOVA of the K_{eff} values shows that the influence of α-tocopherol succinate on the molar efficacy of 7-ketocholesterol in changing the dipole potential is not significantly different in normal and raft depleted cells ($P=0.9$). Bonferroni post tests show that the difference in K_{eff} values for 7-ketocholestel with or without α-tocopherol succinate treatment in normal cells and raft depleted cells are equally significant ($P<0.001$ both cases).

As the α-tocopherol succinate induced change in the efficacy of 7-ketocholesterol in modulating the dipole potential is not significantly different in raft-containing and raft depleted cells, the differences in B_{max} between these cell models may purely reflect changes in the capacity of the membranes to bind 7-ketocholesterol. A two way ANOVA of the B_{max} values therefore shows that the influence of α-tocopherol succinate on the capacity of the membrane for 7-ketocholesterol is significantly different in normal and raft-depleted cells. Bonferroni post tests show the binding capacity of normal cells for 7-ketocholesterol is significantly reduced by α-tocopherol succinate treatment ($P<0.001$). α-Tocopherol succinate treatment also significantly reduces the binding capacity of raft depleted cells for 7-ketocholesterol but to a lesser degree than in normal cells ($P<0.01$).

Lemaire-Ewing *et al.* (Lemaire-Ewing et al., 2010) suggest that α-tocopherol inhibits the localisation of 7-ketocholesterol in lipid rafts. A possible explanation for the effect seen above is that α-tocopherol succinate similarly reduces the localisation of 7-ketcholesterol in lipid rafts thereby decreasing the binding capacity by reducing the proportion of the membrane accessible to 7-ketocholesterol. On the depletion of lipid rafts with methyl-β-cyclodextrin, however, this effect was diminished but not completely abolished. The concentration and duration of methyl-β-cyclodextrin treatment used has been reported to remove negligible amounts of non-raft cholesterol in Jurkat T-lymphocytes (Rouquette-Jazdanian et al., 2006) suggesting that non-raft cholesterol enriched domains may also be involved in this mechanism. However, due to the variability of the technique, it is also possible that rafts were not entirely depleted or were

partially reformed in the short time between methyl-β-cyclodextrin treatment and the experiment (Zidovetzki and Levitan, 2007). Another possibility is that α-tocopherol succinate may also form domains that are capable of excluding 7-ketocholesterol or decreasing the effect of 7-ketocholesterol on the dipole potential. For example, α-tocopherol is known to increase order in the unsaturated lipid rich liquid disordered (l_d) phase (Urano et al., 1988b, SanchezMigallon et al., 1996) and may form ordered domains which exclude 7-ketocholesterol and consequentially reduces the localisation of 7-ketocholesterol in the phase. Alternatively, this ordering my cause 7-ketocholesterol to adopt a similar orientation to that in l_o domains as opposed to the tilted orientation it is reported to adopt in the l_d phase (Massey and Pownall, 2006). This tilted orientation results in an increased contribution from the molecular dipole moment of 7-ketocholesterol in decreasing the dipole potential in the l_d phase, therefore both of these effects will reduce the influence of 7-ketocholesterol on the dipole potential.

In summary, α-tocopherol succinate significantly reduces the efficacy of 7-ketocholesterol in changing the dipole potential of Jurkat T-lymphocyte cell membranes. This significant reduction in the efficacy of 7-ketocholesterol following α-tocopherol succinate treatment does not occur in cells where the effect of oxidative stress on the dipole potential is modelled by pre-exposure of the cells to 7-ketocholesterol. This suggests that the efficacy of 7-ketocholesterol in modulating the dipole potential may depend on the initial magnitude of the dipole potential of the membrane which varies between untreated and α-tocopherol succinate treated cells in the normal and oxidative stress models. This variation may be due to differences in the localisation of α-tocopherol succinate in the membranes of normal and oxidative stress model cells which in turn leads to differences in the partitioning of subsequently titrated 7-ketocholesterol between lipid phases and the effect it then elicits on the dipole potential.

α-Tocopherol has previously been proposed to exert its protective action against 7-ketocholesterol induced apoptosis by inhibiting the partitioning of 7-ketocholesterol into lipid rafts (Royer et al., 2009, Lemaire-Ewing et al., 2010). The involvement of lipid rafts in a mechanism by which α-tocopherol succinate influences on the effect of 7-ketocholesterol on the dipole potential was therefore investigated. Methyl-β-cyclodextrin treatment was used to deplete lipid rafts and the influence of α-tocopherol succinate on the efficacy of 7-ketocholesterol in modulating the dipole potential in raft depleted cells was not found to be significantly different from that in normal cells. α-Tocopherol succinate treatment did, however, differently affect the binding capacity for 7-ketocholesterol in normal and raft depleted cells causing a significant decrease in normal cells and a lesser decrease in raft depleted cells. The differences in the decrease in binding capacity due to α-tocopherol succinate in normal and raft depleted cells could be due to differences in the exclusion of 7-ketocholesterol from membrane microdomains such as lipid rafts.

4.4. Summary

In Chapter 3 it was observed that inclusion of the cholesterol oxidation product, 7-ketocholesterol, and the anti-oxidant, α-tocopherol, significantly altered the dipole potential of phosphatidylcholine membrane vesicles. This chapter investigated the effects of α-tocopherol succinate on the membrane dipole potential of Jurkat T-lymphocyte membranes, a simple cell membrane model, in the context of oxidative stress.

The first section of this chapter firstly confirmed that cholesterol and 7-ketocholesterol cause similar increase and decrease respectively in the membrane dipole potential of Jurkat T-lymphocytes than in the phosphatidylcholine vesicles of Chapter 3. 7-ketocholesterol elicited a 2.4 fold greater effect on the dipole potential per μM of sterol than cholesterol and affected the dipole potential oppositely, influencing the cell membrane similarly to phosphatidylcholine vesicles. This result suggests that the oxidation of membrane cholesterol is likely to have a profound effect on the dipole potential of the cell membrane. Increasing or depleting the extent of lipid rafts in the membrane by cholesterol or methyl-β-cyclodextrin treatment, respectively, showed 7-ketocholesterol to cause a greater decrease in the dipole potential in the presence of lipid rafts. This is consistent with the observation that 7-ketocholesterol localises in rafts (Myers and Stanley, 1999, Berthier et al., 2004, Royer et al., 2009) as the resulting disruption of the lipid packing density in these highly ordered domains, and associated changes in hydration, would account for the greater decrease in the dipole potential in raft-containing membranes. Lipid rafts are considered 'functional platforms' supporting the function of many membrane proteins by means of their unique physical properties (Pike, 2006, Brown and London, 1998a, Simons and Ikonen, 1997, Simons and Toomre, 2000). The highly ordered nature of these cholesterol enriched microdomains results in their elevated dipole potential with respect to the bulk membrane and changes in the dipole potential have previously been demonstrated to modulate the function of a raft-associated receptor (Asawakarn et al., 2001). It is therefore possible that cholesterol oxidation and the associated decrease in dipole potential of lipid rafts could be involved in some of the deleterious effects observed with oxidative stress.

α-Tocopherol has long been thought to have structural, as well as free-radical scavenging, effects in biological membranes (Diplock, 1983) and in Chapter 3 it was shown to modulate the dipole potential of artificial membranes to a similar extent, but opposite direction, to cholesterol. The low aqueous solubility of α-tocopherol meant that the binding of α-tocopherol with cell membranes could not be detected with Di-8-ANEPPS in part due to the noise added to the excitation spectra due to scattering of incident light from α-tocopherol aggregates. α-Tocopherol succinate, however, has a much higher aqueous solubility and was shown in Chapter 3 to modulate the dipole potential of artificial membranes to the same extent as α-tocopherol. α-Tocopherol succinate was found to have a critical micelle concentration of

approximately 4±1μM and its binding to cell membranes through its effect on the dipole potential was detected below this concentration. α-Tocopherol succinate decreased the dipole potential in Jurkat T-lymphocyte cell membranes. Changing the membrane dipole potential has previously been shown to modulate the activity of membrane receptors (Asawakarn et al., 2001) and so this result highlights an alternative mechanism by which some of the cellular effects of α-tocopherols, which cannot be linked to its free radical scavenging activity (Brigelius-Flohe, 2009, Azzi et al., 2002), may occur.

α-Tocopherol succinate has a significantly higher molar efficacy in changing the dipole potential in normal cells than raft depleted cells suggesting it, like 7-ketocholesterol, may localises in lipid rafts. Pre-treatment of cells with 7-ketocholesterol reduced the efficacy of α-tocopherol succinate in changing the dipole potential which may be due to an altered localisation of α-tocopherol succinate in the membrane with 7-ketocholesterol present. For example, 7-ketocholesterol may inhibit the partitioning of α-tocopherol succinate into lipid rafts, as was observed by Royer *et al.* (Royer et al., 2009) for α-tocopherol in 7-ketocholesterol pre-treated cells. Alternatively, the presence of 7-ketocholesterol in a raft would mean α-tocopherol succinate is likely to have less of an effect on the lipid packing, and therefore dipole potential, of the raft.

It should be noted that there has been evidence in both sections 4.1 and 4.2 to indicate the possibility that α-tocopherol succinate may bind a cell membrane receptor. For example, comparison of the interaction of α-tocopherol succinate with cell membranes observed through its modulation of the dipole potential and of the surface potential reveals a considerably higher binding affinity and capacity of α-tocopherol succinate with the latter technique. This suggests that there is a population of α-tocopherol succinate that binds the membrane surface but does not insert into the membrane and therefore does not modulate the dipole potential. Further comparison of the interaction of α-tocopherol succinate to FPE labelled cells with FPE labelled cholesterol-containing lipid vesicles shows that the binding affinity of α-tocopherol succinate is much more sensitive to the increase in l_o phase domains in cells than in vesicles. These effects are consistent with the binding of α-tocopherol succinate to a raft-associated membrane receptor. However, it is also possible that the increased complexity of the cell membrane due to its lipid composition compared to that of the artificial vesicles account for these differences.

Oxidative stress is likely to involve considerable change to the membrane dipole potential which may negatively impact the cell. The effect of α-tocopherol succinate on the dipole potential of the membrane in the context of oxidative stress was therefore investigated in view of a possible alternative protective mechanism of α-tocopherols should α-tocopherol succinate have the ability to negate the effects of oxidation on the dipole potential.

Treating Jurkat T-lymphocytes with α-tocopherol succinate caused a four-fold reduction in the efficacy of subsequently titrated 7-ketocholesterol in changing the dipole potential. This effect may be due to differences in the localisation of 7-ketocholesterol in the membrane, for example the partitioning between raft and non-raft regions of the membrane, in the presence of α-tocopherol succinate. Royer *et al.* (Royer et al., 2009) observed that α-tocopherol localises in lipid rafts inhibiting the partitioning of 7-ketocholesterol into rafts and α-tocopherol succinate may behave in a similar manner. Previously in this chapter, however, it was shown that the influence of α-tocopherol succinate itself on the dipole potential was altered by the presence of 7-ketocholesterol in the membrane and it seemed likely that the influence of α-tocopherol succinate on the effect of 7-ketocholesterol on the dipole potential may depend on the existing oxidative state of the membrane and the associated initial magnitude of the dipole potential. A cell model of cholesterol oxidation in terms on the dipole potential of the membrane, achieved by pre-exposure of the cells to 7-ketocholesterol, was used to demonstrate that the influence of α-tocopherol succinate on the molar efficacy of 7-ketocholesterol in changing the dipole potential is significantly different in normal cells and cells with a lower initial dipole potential associated with oxidative stress. α-Tocopherol succinate was able to significantly decrease the effect of 7-ketocholesterol in normal cells but had no significant influence on the effect of 7-ketocholesterol in decreasing the dipole potential in the cholesterol oxidation model cells.

This suggests that α-tocopherols may play an important role in reducing the effect of cholesterol oxidation on the dipole potential, thus reducing some of the subsequent negative effects of oxidative stress, but can only exert this protective effect when cells membranes are not significantly oxidised prior to α-tocopherol treatment. If cells have undergone significant oxidation, α-tocopherols exert no protective effect against the influence of further cholesterol oxidation in decreasing the dipole potential and may even attenuate this effect by the further decrease in the dipole potential elicited by α-tocopherol itself. This result may, in part, explain the contradictory outcomes of α-tocopherol treatment used to decelerate the onset or progression of diabetic complications as a result of oxidative stress, such as insulin resistance and cardiovascular disease, which is not consistent with its free radical scavenging action (Golbidi et al., 2011, Saremi and Arora, 2010, Pazdro and Burgess, 2010, Celik et al., 2010).

A mechanism by which this protective effect of α-tocopherol occurs in normal but not significantly oxidised membranes may involve differences in the localisation of α-tocopherol in these membranes and the subsequent changes in the partitioning of the oxidised sterol, 7-ketocholesterol, between membrane domains. Lemaire-Ewing *et al.* (Lemaire-Ewing et al., 2010) hypothesize that the localisation of α-tocopherol in lipid rafts reduces the partitioning of 7-ketocholesterol into rafts and this mechanism enables α-tocopherol to inhibit 7-

ketocholesterol induced apoptosis via the Bad dephosphorylation pathway. However, when 7-ketocholesterol is present in the membrane before α-tocopherol is added the localisation of the latter in lipid rafts is inhibited and it is therefore unable to exert the protective effect (Royer et al., 2009, Lemaire-Ewing et al., 2010). The involvement of lipid rafts in the influence of α-tocopherol succinate in reducing the effect of oxidation on the dipole potential of the membrane was investigated using methyl-β-cyclodextrin treated Jurkat T lymphocytes as a raft-depleted cell model. The influence of α-tocopherol succinate on the binding capacity of the membrane for 7-ketocholesterol was found to be significantly less in raft depleted cells but a significant reduction in the binding capacity was still observed. This suggests that lipid rafts may not be the only species of microdomains from which 7-ketocholesterol is excluded by α-tocopherol succinate.

A mechanism is proposed by which α-tocopherol succinate protects against the deleterious effects of cholesterol oxidation in cell membranes by excluding 7-ketocholesterol from specific microdomains. This acts to preserve the dipole potential of the microdomain maintaining the function of the proteins it supports. An example of a microdomain species which may benefit in this mechanism are lipid rafts. These are thought to act a 'functional platforms' for many membrane proteins (Brown and London, 1998a, Simons and Ikonen, 1997, Simons and Toomre, 2000) which is likely, in part, due to their unique dipole potential attributed to their highly ordered cholesterol-rich composition (Asawakarn et al., 2001). The exclusion of 7-ketocholesterol from microdomains may also act to exclude the oxidant from lipids that are highly susceptible to oxidation. For example, α-tocopherol forms complexes with poly-unsaturated fatty acids and this preferential association is believed to place the anti-oxidant where it is most needed in the membrane (Quinn, 2004, Atkinson et al., 2010). In protecting polyunsaturated lipids from oxidation the dipole potential of the liquid disordered phases of the membrane are also preserved.

In membranes in which significant cholesterol oxidation has already occurred it is suggested that α-tocopherol succinate is unable to exclude further 7-ketocholesterol from these microdomains. In this situation α-tocopherol succinate is unable to counteract the effects of further oxidation on the dipole potential of the microdomains and inhibit some of the deleterious effects that occur under conditions of oxidative stress. This effect may, in part, explain the contradictory outcomes of the use of α-tocopherol treatment in delaying the onset or progression of diabetic complications associated with oxidative stress, such as insulin resistance and cardiovascular disease, which are not consistent with its direct anti-oxidant action.

α-Tocopherol, alongside its free-radical scavenging activity, may play a vital structural role in preserving the dipole potential of cell membrane microdomains, limiting the deleterious effects of oxidation.

5. Effect of 7-KC and α-tocopherol succinate on receptor function

In the previous chapter it was concluded that oxidation of cell membrane cholesterol is likely to have a profound effect on the dipole potential of the membrane. 7-ketocholesterol, an oxidised form of cholesterol, was observed to significantly modulate the membrane dipole potential but had a lesser effect in cell membranes depleted of cholesterol rich lipid rafts. This suggests that the partitioning of 7-ketocholesterol into lipid rafts (Berthier et al., 2004, Royer et al., 2009, Myers and Stanley, 1999) induces a significant decrease in the dipole potential of these structures. Rafts are considered to hold an important role as "functional platforms" supporting the activity of a host of membrane proteins (Simons and Ikonen, 1997, Brown and London, 1998a, Simons and Toomre, 2000). Changes in the dipole potential have previously been shown to modulate the behaviour of P-glycoprotein (P-gp) (Asawakarn et al., 2001), a cell membrane receptor known to associate with lipid rafts (Demeule et al., 2000, Hinrichs et al., 2004). It is possible, therefore, that the decrease in dipole potential due to cholesterol oxidation, particularly of lipid rafts, could be a mechanism underlying some of the deleterious effects associated with oxidative stress.

In this chapter this hypothesis is initially explored by investigating the effect of 7-ketocholesterol induced dipole potential modulation on P-gp and the involvement of lipid rafts in this effect (section 5.1.2 & 5.1.4). α-Tocopherol succinate was shown to reduce the effect of 7-ketocholesterol on the dipole potential in the previous chapter (section 4.3.1). This was suggested to occur by the modulation of the localisation and orientation of 7-ketocholesterol in the membrane and its subsequent effect in changing the dipole potential of raft and non-raft domains. An investigation of the influence of α-tocopherol succinate on the effect of 7-ketocholesterol on P-gp then follows in section 5.1.5.

In section 5.2 attentions are focussed on the influence of α-tocopherol succinate on the effect of cholesterol oxidation on the dipole potential in the context of insulin resistance. Oxidative stress is proposed to be an underlying mechanism linking insulin resistance with both type II diabetes and cardiovascular disease (Ceriello and Motz, 2004, Stern, 2005). α-Tocopherol is well known as an antioxidant (Brigelius-Flohe and Traber, 1999, Wolf, 2005), but its use as a therapeutic agent in oxidative stress associated diabetic complications and cardiovascular disease has demonstrated little benefit (see e.g. (Golbidi et al., 2011, Pazdro and Burgess, 2010, Saremi and Arora, 2010). This section aims to explore the involvement of the dipole potential modulation by 7-ketocholesterol, the oxidation product of cholesterol, in insulin resistance and identify any potential benefit in reducing the effect of 7-ketocholesterol on the dipole potential. The effect of 7-ketocholesterol on insulin binding and the influence of α-tocopherol succinate treatment are investigated in sections 5.2.2.4-6 following exploration of several methods to observe insulin

binding, including the modulation of the surface potential detected by fluorescein-phosphatidylethanolamine and flow cytometry with fluorophore-tagged insulins. The influence of α-tocopherol succinate, a non-antioxidant but structurally similar analog, on the effects of membrane cholesterol oxidation on the dipole potential is discussed in the context of insulin resistance in section 5.2.2.7.

5.1. The effect of 7-ketocholesterol and α-tocopherol on the binding of Saquinavir through modulation of the membrane dipole potential

The interaction of the antiretroviral agent Saquinavir with its receptor, P-glycoprotein (P-gp), has been previously demonstrated by our group to be influenced by the membrane dipole potential with 6-ketocholestanol and phloretin, agents increasing and decreasing the dipole potential respectively, causing an increase and decrease in Saquinavir binding (Asawakarn et al., 2001). P-gp is associated with membrane microdomains (Demeule et al., 2000, Hinrichs et al., 2004) and its presence in these structures is thought to modulate its activity (Orlowski et al., 2006, Klappe et al., 2009). Asawakarn *et al.* (Asawakarn et al., 2001) propose that the modulation is mediated by changes in the membrane dipole potential.

5.1.1. The interaction of Saquinavir with P-glycoprotein

Saquinavir modulates the dipole potential on binding P-gp and this is used to determine its concentration dependent interaction with the receptor expressed on the cell membranes of Jurkat T lymphocytes through changes in the ratio of emission intensity of Di-8-ANEPPS on dual excitation (Figure 5.1.1). The data is initially fitted to both a hyperbolic saturation binding model (Equation 5.1.1) and a sigmoidal cooperative binding model (Equation 5.1.2). The models describe the change in the ratio, R, of Di-8-ANEPPS fluorescence intensity at two excitation wavelengths (a quantity describing the shift of the excitation spectrum) with increasing Saquinavir concentration where B_{max} is the maximum change in ratio when a saturation concentration of Saquinavir has bound and K_d is the concentration (in μM) at which half this change is achieved.

$$\Delta R = \frac{B_{max}[Saquinair]}{K_d + [Saquinavir]} \qquad \text{Hyperbolic binding model (}\textit{Equation 5.1.1}\text{)}$$

$$\Delta R = \frac{B_{max}[Saquinavir]^{\boldsymbol{h}}}{K_d^{\boldsymbol{h}} + [Saquinavir]^{\boldsymbol{h}}} \qquad \text{Sigmoidal binding model (}\textit{Equation 5.1.2}\text{)}$$

The sigmoidal model includes a further term, the Hill coefficient, ***h***, and was first devised to describe the cooperative binding of oxygen to haemoglobin (Hill, 1910). When ***h***>1 or ***h***<1 a positive or negative cooperativity, respectively, in the binding of a ligand to a receptor exists. When ***h***=1 the binding is independent of the presence of other ligands and Equation 5.1.2 can be seen to reduce to Equation 5.1.1. The Hill coefficient cannot be considered to exceed the number of interaction sites present on the receptor for the ligand. However, it has been observed to do so, for example, as discussed by Shiner and Solaro (Shiner and Solaro, 1984) for the interaction of Ca^{2+} with troponin and is thought to result from the non-equilibrium state of the system.

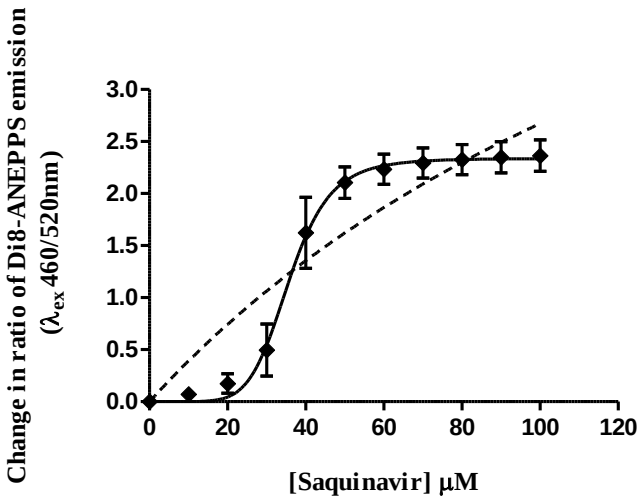

Figure 5.1.1: The change in the ratio, R, of Di-8-ANEPPS fluorescence intensity at 460nm and 520nm($R=I_{460}/I_{520}$) excitation as Saquinavir is titrated to Di-8-ANEPPS labelled Jurkat T lymphocytes. The change in ratio on addition of equal volumes of the solvent, DMSO, is subtracted from the data. Each data point is the average of 3 repeats with the error bars representing the standard error of the mean. The data is fitted to both hyperbolic (----) and sigmoidal (─) binding models, the latter of which is demonstrated to best represent the data by a sum-of-squares F-test.

The change in Di-8-ANEPPS emission ratio on titration of Saquinavir to Jurkat T-lymphocytes appears to better fit the sigmoidal binding model on inspection of Figure 5.1.1 ($R^2_{hyperbolic}$=0.8251, $R^2_{sigmoidal}$=0.9410). As this model contains an extra parameter (the Hill coefficient) in comparison to the hyperbolic model it possesses one fewer degree of freedom (DF) when both models are fit to an identical data set (in this case $DF_{sigmoidal}$=(33 data points-3 parameters)=30 and $DF_{hyperbolic}$=(33-2)=31). This intrinsically improves the fit of the sigmoidal model, when determined by the R^2 value, and so a sum of squares F-test was performed to account for the effect of the differences of the degrees of freedom (as described in section 2.5.6). The F ratio, calculated using Equation 2.4 with the residual sum of squares determined in Prism v5.02 ($SS_{sigmoidal}$=2.014, $SS_{hyperbolic}$=5.970), is 58.94 and P<0.0001 confirming the sigmoidal binding model best represents the data. The sigmoidal binding model determines the maximum change in the ratio on binding of a saturation concentration of Saquinavir, B_{max}, as 2.34± 0.07 with 36±1μM of Saquinavir required to achieve a change in ratio of half this value. The Hill coefficient for Saquinavir binding to Jurkat T-lymphocytes is relatively high (***h***=7±1) and the number of interaction sites for Saquinavir on the cell membrane is unknown so this quantity cannot be easily interpreted.

5.1.2. The involvement of membrane rafts in Saquinavir binding

The involvement of membrane rafts in the binding of Saquinavir to P-gp has been demonstrated by the effect of membrane cholesterol depletion by methyl-β-cyclodextrin in the Caco2 epithelial cell line on Saquinavir binding (Asawakarn et al., 2001). To confirm this effect in the Jurkat T-lymphocyte cell line, Di-8-ANEPPS labelled cells were treated with 10mM methyl-β-cyclodextrin for 2 minutes, a concentration and length of treatment previously reported to

remove 100% of raft-associated cholesterol and virtually none of the non-raft cholesterol in this cell line (Rouquette-Jazdanian et al., 2006). Figure 5.1.2 compares the binding of Saquinavir to untreated and methyl-β-cyclodextrin treated cells through its modulation of the membrane dipole potential.

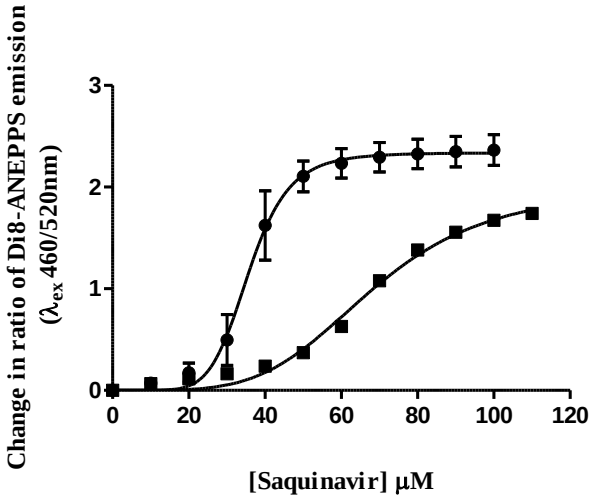

Figure 5.1.2: The change in the ratio, R, of Di-8-ANEPPS fluorescence intensity at 460nm and 520nm($R=I_{460}/I_{520}$) excitation as Saquinavir is titrated to Di-8-ANEPPS labelled Jurkat T-lymphocytes. Cells are either untreated (●) or treated with methyl-β-cyclodextrin (10mM 2min) (■) to remove raft-associated cholesterol. The change in ratio on addition of equal volumes of the solvent, DMSO, is subtracted from the data. Each data point is the average of 3 repeats with the error bars representing the standard error of the mean (not visible for treated cells). The data is fitted to a sigmoidal binding model (Eq.5.2) with R^2= 0.94, K_d= 36±1μM B_{max}= 2.34± 0.07 h= 7±1 for untreated cells and R^2= 0.9879, K_d= 68±2μM B_{max}= 2.00± 0.09 h= 4.4± 0.4 for MβCD treated cells.

The maximum change in fluorescence ratio, B_{max}, is significantly lower following methyl-β-cyclodextrin treatment (unpaired two-tailed t test R^2=0.6713 P=0.0460) suggesting that the maximum change in the dipole potential effected by the Saquinavir-P-gp interaction is reduced in the absence of membrane rafts. This result is difficult to interpret as there is some ambiguity surrounding the factors contributing to the maximum change in dipole potential in this case. The decrease in B_{max} may be representative of a decrease in the binding capacity of P-gp for Saquinavir as a result of a reduction in the number of active receptors. In this case the result is consistent with the decreased binding capacity of P-gp for Saquinavir reported by Asawakarn *et al*. following methyl-β-cyclodextrin treatment of Caco-2 cells (Asawakarn et al., 2001). The decrease in B_{max} may also reflect a decrease in the effect on the dipole potential elicited by the receptor on binding Saquinavir. The mechanism by which the binding interaction causes change in the dipole potential, and the sensitivity of this mechanism to its environment, is unknown so the origin of the change in B_{max} cannot be determined unambiguously.

The dissociation constant K_d, reflecting the concentration at which half the change in the ratio indicated by B_{max} occurs, is also significantly higher (unpaired two-tailed t test R^2=0.9793 P=0.0002) in methyl-β-cyclodextrin treated cells. This quantity, representing the affinity of Saquinavir for P-gp, is not affected by the ambiguity in the molecular origins of B_{max}. This

result indicates that the affinity of Saquinavir for P-gp is approximately twice greater in the presence of rafts which is consistent with the suggestions of Orlowski *et al.* and Klappe *et al.* (Orlowski et al., 2006, Klappe et al., 2009) that the activity of P-gp is dependent on these structures. This was not observed by Asawakarn *et al.* (Asawakarn et al., 2001) who found no change in the affinity of Saquinavir for P-gp following methyl-β-cyclodextrin treatment. The discrepancy in these results may be due to differences in the method of methyl-β-cyclodextrin treatment. The extent of cholesterol depletion and the degree to which it is removed from raft and non-raft domains of the cell membrane is dependent on the cell type and the conditions of methyl-β-cyclodextrin treatment such as concentration and incubation duration. Longer incubations and higher concentrations can result in significant cholesterol depletion from non-raft membrane regions as well as alter the distribution of cholesterol between the plasma membrane and intracellular membranes (Zidovetzki and Levitan, 2007). Following the overnight treatment of Caco-2 cells with 30mM methyl-β-cyclodextrin, the cholesterol distribution in the cell membrane to which Saquinavir binding was observed by Asawakarn *et al.* (Asawakarn et al., 2001) is likely to have been quite different from that of the methyl-β-cyclodextrin treated Jurkat T-lymphocytes in this study. The concentration and duration of treatment used in this study is preferred as, whether or not it does in fact deplete 100% of raft cholesterol as reported by Rouquette-Jazdanian *et al.*(Rouquette-Jazdanian et al., 2006), it nevertheless does remove some membrane cholesterol whilst the short duration of treatment minimally perturbs intracellular cholesterol. Although the difficulty in direct visualisation of these structures does not enable the entire depletion of rafts to be confirmed, this concentration and duration of treatment does alter the microdomain landscape of the membrane as evidenced by the decrease in dipole potential following treatment (Section 4.1.1). Figure 5.1.2 therefore demonstrates that the interaction of Saquinavir with P-gp is sensitive to the microdomain environment of the receptor and significantly altered following the partial depletion of membrane cholesterol indicating the involvement of the cholesterol enriched microdomains known as rafts. Specifically, the binding of Saquinavir to P-gp is likely to be sensitive to the dipole potential of such microdomains (Asawakarn et al., 2001).

5.1.3. The effect of Saquinavir on the interaction of α-tocopherol succinate with cell membranes

The interaction of α-tocopherol succinate with membranes, and its effect on the dipole potential, has been demonstrated to be influenced by the pre-existing dipole potential of the membrane in the previous chapters (Section 4.2). To investigate whether the change in the dipole potential associated with the binding of Saquinavir to its receptor influences the interaction of α-tocopherol succinate with the cell membrane, Jurkat T-lymphocytes labelled with Di-8-ANEPPs were treated with Saquinavir immediately prior to α-tocopherol succinate titration.

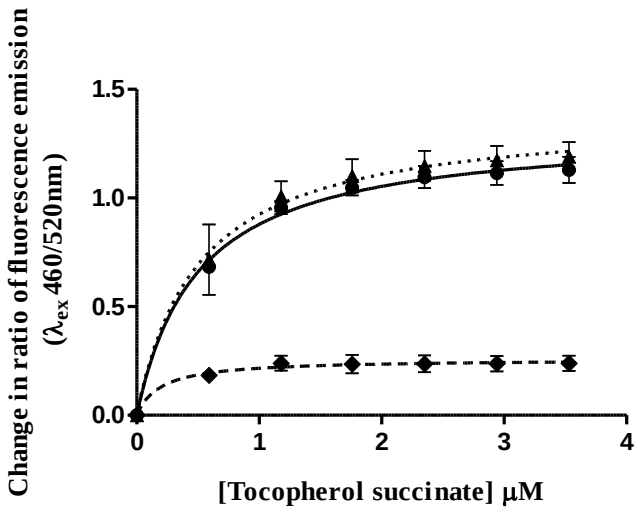

Figure 5.1.3: The change in the ratio, R, of Di-8-ANEPPS fluorescence intensity at 460nm and 520nm($R=I_{460}/I_{520}$) excitation as α-tocopherol succinate is titrated to Di-8-ANEPPS labelled Jurkat T-lymphocytes. Cells are untreated (●) or treated with 30μM (▲) or 50μM (♦) Saquinavir (1min 37°C). The change in ratio on addition of equal volumes of the solvent, ethanol, is subtracted from the data. Each data point is the average of 3 repeats with the error bars representing the standard error of the mean. The data is fitted to a hyperbolic binding model (Eq.5.1) where K_d=0.50±0.08 B_{max}=1.32±0.05 for untreated cells (—), K_d=0.50±0.2 B_{max}=1.39±0.09 for 30μM treated cells (…) and K_d=0.2±0.2 B_{max}=0.26±0.03 for 50μM treated cells (----).

Treating cells with 30μM Saquinavir did not significantly alter the maximum change in the dipole potential elicited by α-tocopherol succinate or the concentration at which this occurs (P=0.54 and P=0.98 respectively, two tailed t tests). This concentration of Saquinavir elicits a small change in the dipole potential (ΔR=0.5) and is at the beginning of the steep increase of the sigmoidal relationship (see Figure 5.1.1) indicating the point where the Saquinavir concentration is just high enough to support cooperative binding and to facilitate a change in the dipole potential. Treating cells with 50μM Saquinavir, a concentration eliciting a near maximum change in the dipole potential (ΔR~2) at the point where the sigmoidal relationship begins to plateau following the steep increase, significantly decreases α-tocopherol succinate binding. The affinity of α-tocopherol succinate for the membrane is increased, however this change is not significant (P=0.17 two tailed t test) due to the high error in K_d most likely resulting from the low number of data points around this concentration. The maximum change in dipole potential caused by α-tocopherol succinate is significantly lower following 50μM Saquinavir treatment (P<0.0001, two tailed t test).

There does, therefore, appear to be a dependence of the maximum change in the dipole potential elicited by α-tocopherol succinate on the extent to which the Saquinavir pre-treatment modulates the dipole potential. A possible explanation is that the decrease in B_{max} following 50μM Saquinavir treatment is due to a decrease in the amount of α-tocopherol succinate able to bind the membrane. The reduction in the number of binding sites available to α-tocopherol succinate on the membrane following Saquinavir treatment can be interpreted as the result of two potential effects. It is possible that the raft-localised decrease in the dipole potential caused

by Saquinavir, as mentioned above, influences the affinity of α-tocopherol succinate for specific membrane domains. This may effectively reduce the overall number of binding sites available to α-tocopherol succinate on the membrane if, for example, the affinity of α-tocopherol succinate for rafts is rendered negligible following the decrease in the dipole potential of these structures by Saquinavir. Alternatively, the decrease in available binding sites is consistent with the competitive binding of α-tocopherol succinate with P-gp in the presence of Saquinavir. However, as mentioned previously, some ambiguity surrounds the interpretation of B_{max} which does not necessarily reflect the number of available binding sites, for example the number of receptors binding the ligand. A similar ambiguity was found in the interpretation of B_{max} for 7-ketocholesterol interaction with cell membranes (Section 4.1.1 & 4.3.1) as the sterol contributes to the dipole potential to different extents in different regions of the membrane (Starke-Peterkovic et al., 2006) such that the change in dipole potential cannot be quantised per molecule of 7-ketocholesterol inserting in the membrane. In that situation the molar efficacy of 7-ketocholesterol in changing the dipole potential provided the best means of comparison of the influence of 7-ketocholesterol in differently treated membranes and this is also the most appropriate method of interpreting the data presented here.

The efficacy, K_{eff}, is measured by the ratio B_{max}/K_d and decreases from $2.6\pm0.4\mu M^{-1}$ in normal cells to $1\pm1\mu M^{-1}$ for treated cells, although the change is not statistically significantly different ($P=0.2$ two tailed t test) again due to the large error in K_d for treated cells. It is likely that the acquisition of further data points at concentrations of α-tocopherol succinate in the region of the K_d concentration following 50μM Saquinavir treatment will significantly reduce this error rendering the K_{eff} values for treated and untreated cells significantly different. An alternative interpretation is, therefore, that the change in the dipole potential resulting from the binding of Saquinavir influences the efficacy of α-tocopherol succinate in changing the dipole potential of the membrane. Like Saquinavir, α-tocopherol has also been shown to localise in rafts (Royer et al., 2009) and as both α-tocopherol and α-tocopherol succinate change the dipole potential to similar extents (Section 3.3.2) it may be assumed that they localise similarly in the membrane. The reduced effect of α-tocopherol succinate on the dipole potential can therefore be considered likely to arise from the change in the dipole potential of rafts due to Saquinavir. This may result, for example, in the altered localisation of α-tocopherol succinate in the membrane thus altering the extent to which it changes the dipole potential.

5.1.4. The effect of 7-ketocholesterol on Saquinavir binding

The binding of Saquinavir to its receptor is influenced by the dipole potential of the membrane (Asawakarn et al., 2001, Luker et al., 2001). 7-ketocholesterol, the oxidation product of cholesterol, has been shown to significantly modulate the dipole potential of the Jurkat T-lymphocyte membrane (Section 4.1) and so the binding of Saquinavir to 7-ketocholesterol

treated cells is compared with that to untreated cells to observe if it similarly influences Saquinavir binding (Figure 5.1.4).

The effect of 7-ketocholesterol treatment (*0.325μM, 10min* shown previously to cause a significant decrease in the dipole potential, but not saturate the membrane (Section 4.1.1) is to significantly decrease the affinity of Saquinavir for its receptor (unpaired two-tailed t test P=0.0037 R^2=0.9021). The degree of cooperativity in the binding of Saquinavir to its receptor is not significantly different between treated and untreated cells (P=0.4549 R^2=0.1459). The maximum change in fluorescence ratio, B_{max}, associated with the binding of Saquinavir with its receptor is significantly decreased (P= 0.0015 R^2=0.9376) which is also seen by Asawakarn *et al.* (Asawakarn et al., 2001) on decreasing the membrane dipole potential with phloretin suggesting that 7-ketocholesterol is influencing the interaction of Saquinavir with its receptor through modulation of the membrane dipole potential.

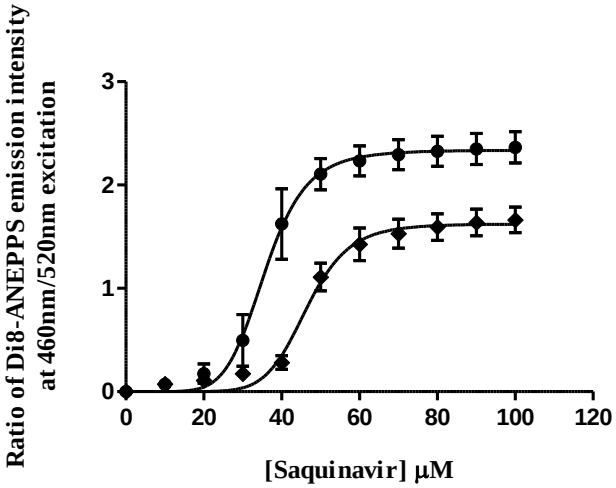

Figure 5.1.4: The change in the ratio, R, of Di-8-ANEPPS fluorescence intensity at 460nm and 520nm($R=I_{460}/I_{520}$) excitation as Saquinavir is titrated to Di-8-ANEPPS labelled Jurkat T-lymphocytes. Cells are either untreated (●) or treated with 7-ketocholesterol (7-KC) (0.325μM, 10min) (♦). The change in ratio on addition of equal volumes of the solvent, DMSO, is subtracted from the data. Each data point is the average of 3 repeats with the error bars representing the standard error of the mean. The data is fitted to a sigmoidal binding model (Eq.5.2) with R^2= 0.94, K_d= 36±1 μM B_{max}= 2.34± 0.07 h= 7±1 for untreated cells and R^2= 0.9485, K_d= 47±1μM B_{max}= 1.62±0.05 h= 8±2 for 7-KC treated cells.

Despite the ambiguity in the molecular origin of the change in B_{max}, it is interesting to note that the decrease in B_{max} of Saquinavir titration following methyl-β-cyclodextrin or 7-ketocholesterol treatment from that of untreated cells is 14% and 31% respectively. This correlates well with the relative effects of 7-ketocholesterol and methyl-β-cyclodextrin treatment on the dipole potential; methyl-β-cyclodextrin treatment reduces the dipole potential of the cell membrane by approximately half as much as 7-ketocholesterol (ΔR=0.4 and ΔR=0.9 respectively). This suggests that the binding capacity of the receptor for Saquinavir, or the change in dipole potential elicited by the Saquinavir-receptor interaction, depends on the initial magnitude of the membrane dipole potential. The lower the initial dipole potential of the membrane, the smaller the change in fluorescence induced on subsequent saturation of the membrane with Saquinavir.

Comparing the decrease in the binding affinity of Saquinavir (increase in K_d) after methyl-β-cyclodextrin or 7-ketocholesterol treatment shows that methyl-β-cyclodextrin causes a three times greater decrease in the binding affinity than 7-ketocholesterol (91% and 30% respectively). This does not correlate with the differences in the initial dipole potential of the membranes following each treatment (ΔR~0.38 and ΔR~0.88 for MβCD or 7KC treated cells, respectively, deduced from Figures 4.1.1.1 & 4.1.1.3) suggesting that the binding affinity is sensitive to parameters, other than the dipole potential, that vary between the treated membranes. The phases of the domains present are an example of the differences between methyl-β-cyclodextrin treated and 7-ketocholesterol treated membranes. The methyl-β-cyclodextrin treatment conditions used have been shown to remove 100% of raft cholesterol and very little non-raft cholesterol (Rouquette-Jazdanian et al., 2006) which entirely disrupts the high lipid packing of the liquid-ordered (l_o) phase membrane rafts with minimal change to the non-raft liquid disordered (l_d) regions. 7-ketocholesterol, however, partitions into both the l_o and l_d phases of the membrane. In the l_o phase membrane rafts 7-ketocholesterol reduces the lipid packing but still maintains l_o phases with a higher lipid packing and order than the l_d phase non-raft regions. 7-ketocholesterol localising in the non-raft phases acts to increase the order and lipid packing, but to a lesser extent than it does in the l_o phase. Correlating the phase profile of the membrane with the affinity of Saquinavir for its receptor we see that the binding affinity is dramatically reduced in the absence of cholesterol-rich l_o phases following methyl-β-cyclodextrin treatment. The decrease in binding affinity is three-fold smaller following perturbation, but not total disruption, of the l_o phases by 7-ketocholesterol. This suggests that the binding affinity of Saquinavir for its receptor may not rely purely on the dipole potential of the environment of the receptor but is also sensitive to the presence of l_o phases.

5.1.5. Modulation of the effect of 7-ketocholesterol on Saquinavir binding by α-Tocopherol Succinate

In the previous chapter it was shown that the effect of 7-ketocholesterol on the membrane dipole potential can be influenced by the presence of α-tocopherol succinate. As the dipole potential is known to modulate the interaction of Saquinavir with membrane receptors it is possible that the presence of α-tocopherol succinate in the cell membrane alters the influence of 7-ketocholesterol on the subsequent binding of Saquinavir with its receptors.

Figure 5.1.5 shows the effect of 7-ketocholesterol on the binding of Saquinavir in α-tocopherol succinate treated Jurkat T-lymphocytes. Note the difference in scale of the ratio changes compared with Figure 5.1.4. The variation between the sigmoidal binding curves is very different to that due to 7-ketocholesterol treatment in cells that have not been exposed to α-tocopherol succinate, shown in Figure 5.1.4. To compare the influence of 7-ketocholesterol on Saquinavir binding in the α-tocopherol succinate- exposed cell system and the non-exposed cell

system a two way ANOVA was performed on the K_d values derived from these four titration curves.

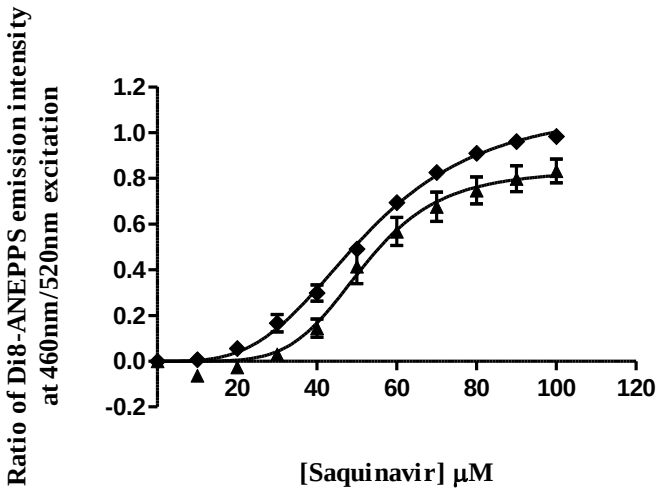

Figure 5.1.5: The change in the ratio, R, of Di-8-ANEPPS fluorescence intensity at 460nm and 520nm($R=I_{460}/I_{520}$) excitation as Saquinavir is titrated to Di-8-ANEPPS labelled Jurkat T-lymphocytes. Cells are treated with α-tocopherol succinate (TS) (2.36μM, 10min 37°C) with (▲) or without (♦) subsequent 7-ketocholesterol (7-KC) (0.325μM, 10min 37°C) treatment. The change in ratio on addition of equal volumes of the solvent, DMSO, is subtracted from the data. Each data point is the average of 3 repeats with the error bars representing the standard error of the mean. The data is fitted to a sigmoidal binding model (Eq.5.2) with R^2= 0.9924, K_d= 52±2μM B_{max}= 1.11± 0.04 h= 3.4± 0.2 for TS treated cells and R^2= 0.9569, K_d= 52±2μM B_{max}= 0.84± 0.04 h= 5.4± 0.9 for cells exposed to 7-KC following TS treatment.

There is significant interaction (P=0.006) between the effects of α-tocopherol succinate and 7-ketocholesterol on the K_d value of Saquinavir titration. This suggests that α-tocopherol succinate significantly influences the effect of 7-ketocholesterol on the binding affinity of Saquinavir for its receptor. Bonferroni post tests confirm a significant difference in K_d due to 7-ketocholesterol treatment in normal cells ($P<0.05$) but no significant difference in α-tocopherol succinate treated cells ($P>0.05$).

Previously in this section P-gp was shown to be significantly affected by the depletion of lipid rafts and it seems likely that the influence of 7-ketocholesterol on P-gp involves the modulation of the dipole potential of lipid rafts by this oxidised sterol. α-Tocopherol succinate reduces the effect of 7-ketocholesterol on the dipole potential, potentially by inhibiting the localisation of 7-ketocholesterol into domains such as lipid rafts. It is by this mechanism that Lemaire-Ewing *et al.* hypothesize α-tocopherol is able to protect against 7-ketocholesterol induced apoptosis via the Akt-Bad signalling pathway associated with rafts (Lemaire-Ewing et al., 2010). It is possible that the attenuation of the effect of 7-ketocholesterol on the affinity of Saquinavir for P-gp by α-tocopherol succinate may also occur by a similar mechanism.

To fully appreciate the influence of α-tocopherol succinate on the effect of 7-ketocholesterol on P-gp the effect of α-tocopherol succinate itself on the binding of Saquinavir must also be considered. A one way ANOVA comparing the K_d values for Saquinavir titration to normal

cells, 7-ketocholesterol treated cells and α-tocopherol succinate treated cells ($P=0.0004$ $R^2=0.93$ $F=38.5$) demonstrates that α-tocopherol succinate significantly decreases the affinity of Saquinavir for P-gp ($P<0.05$) and does so to a greater extent than 7-ketocholesterol ($P<0.05$ Tukey's multiple comparisons test). This is not consistent with the extent to which α-tocopherol succinate decreases the dipole potential relative to 7-ketocholesterol. 7-ketocholesterol has a greater effect on the dipole potential than α-tocopherol succinate and, although this does not necessarily correspond to the relative effects of these molecules on the dipole potential of microdomains where P-gp are localised, the large discrepancy between this and their relative effects on K_d should not be entirely dismissed. This highlights the possibility that α-tocopherol succinate may cause this effect by a mechanism not directly associated with the dipole potential, for example, by binding P-gp as mentioned previously.

The ambiguity in the interpretation of B_{max} in the context of the experiments performed has led to no conclusion being drawn regarding the potential binding of α-tocopherol succinate to this receptor. Future experiment to resolve this ambiguity could include observing the changes to α-tocopherol succinate binding following Saquinavir treatment through its modulation of the surface potential using fluorescein-phosphatidylethanolamine (FPE). Due to the nature of this technique, the maximum change in fluorescence, B_{max}, found on fitting a binding curve would correlate directly with the binding capacity of the membrane for α-tocopherol succinate. To clarify if the reduced interaction of α-tocopherol succinate with the membrane following Saquinavir pre-treatment arises specifically from the decreased availability of receptor binding sites, and not the associated decrease in dipole potential, a ligand for P-gp that does not perturb the dipole potential on binding must be used in place of Saquinavir.

Regardless of the mechanism, it is clear that α-tocopherol succinate significantly influences the activity of P-gp. This receptor acts as a multi-drug efflux pump so this effect may have significant consequences on the toxicity of various native or xenobiotic compounds but could also be used to positively influence the efficacy of therapeutic agents due to the reduced capacity with which they are removed from cells.

5.2. The influence of 7-ketocholesterol and α-tocopherol succinate on the interaction of insulin with cell membranes

The close relationship between type II diabetes mellitus and cardiovascular disease lead Stern to propose the "common soil hypothesis" which postulates that these diseases must share common antecedents such as insulin resistance (Stern, 2005). Ceriello and Motz later suggested oxidative stress to be the underlying mechanism linking insulin resistance with the cellular dysfunction that results in diabetes and cardiovascular disease (Ceriello and Motz, 2004). Oxidative stress has been observed to be present before the occurrence of insulin resistance (Ceriello, 2000, Evans et al., 2005) and therefore anti-oxidants such as α-tocopherol have received much attention as potential therapeutic agents for the prevention or amelioration of insulin resistance. The benefit of α-tocopherol in cardiovascular disease has also been widely investigated (see (Saremi and Arora, 2010, Farbstein et al., 2010, De Rosa et al., 2010, Clarke et al., 2008) for reviews). Despite the wealth of in vitro and animal models confirming the anti-oxidant activity of α-tocopherol and signifying the potential benefits of α-tocopherol treatment, this has not been substantiated in clinical trials (Golbidi et al., 2011, Pazdro and Burgess, 2010, Saremi and Arora, 2010, Robinson et al., 2006, Brigelius-Flohe et al., 2002). The need for a more comprehensive understanding of the molecular actions of tocopherols is recognised and, with the emergence of several effects of the antioxidant which are not directly associated with its free-radical scavenging capability (Brigelius-Flohe, 2009, Zingg and Azzi, 2004), it has become clear that viewing α-tocopherol principally as an antioxidant may lead to significant underestimation of its functions.

α-Tocopherol has long been suggested to have roles within the membrane other than that of an antioxidant (Diplock, 1983) and, due to its structure and lipophilic nature is considered likely to perturb the physical properties of biological membranes. In the previous chapters both α-tocopherol and a non-antioxidant analogue, α-tocopherol succinate, were demonstrated to cause significant modulation of the membrane dipole potential. In chapter 4 (section 4.3.1) α-tocopherol succinate treatment was shown to significantly reduce the dramatic effect of 7-ketocholesterol on the dipole potential. This suggested that α-tocopherol may ameliorate the effects of oxidative stress on the dipole potential of the cell membrane, potentially reducing the physiological consequences of such perturbation. This section aims to investigate the effect of the dipole potential modulation of 7-ketocholesterol on the insulin receptor and the consequences of α-tocopherol succinate treatment. Changes in the surface potential and flow cytometry using fluorescently tagged insulin are used to observe the binding of insulin to its receptor and explore its relationship to dipole potential measurements.

5.2.1. Jurkat T-lymphocytes

5.2.1.1. *Surface potential measurements*

Insulin has an isolelectric point at pH 5.31 (Calculated using Protein Calculator v3.3 and UniProtKB/Swiss-prot database (Nicol and Smith, 1960)) and is therefore negatively charged at pH7.4, suggesting its binding to insulin receptors is likely to modulate the membrane surface potential and may therefore be detected through changes in the quantum yield of membrane-bound FPE. Figure 5.1.1 shows the fluorescence intensity of FPE labelled Jurkat T-lymphocytes suspended in HEPES buffered sucrose solution (10mM HEPES 280mM sucrose, pH7.4, 37^{o}C) on addition of an excess of insulin (1μM, human, recombinant from *Saccharomyces cerevisiae*). The increase in fluorescence intensity on addition of 2mM positively charged calcium ions was used to confirm the responsiveness of the membrane-bound FPE and this data is also shown.

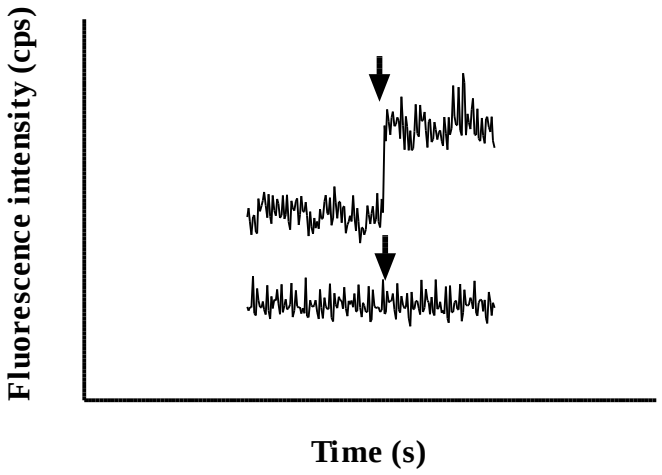

Figure 5.2.1: The change in emission intensity of FPE labelled Jurkat T-lymphocytes (40,000 cells ml^{-1} in 10mM HEPES 280mM sucrose solution, pH7.4 37^{o}C) on addition of 2mM calcium ions (positively charged) in the form of calcium carbonate (upper trace) or 1μM Insulin (lower trace) which is negatively charged at pH7.4.

The increase in intensity on addition of calcium ions is consistent with the decreased surface potential due to the introduction of positive ions to the membrane surface leading to deprotonation of membrane-bound FPE and an increase in its quantum yield. This confirms that the FPE labelling the cell membrane is responsive to changes in the surface potential, however, the addition of an excess of insulin did not detectably perturb FPE fluorescence. This may be due to the limited binding capacity of the membrane for insulin or the low affinity of insulin for its receptor. The charge of an insulin molecule at pH7.4 is -3.4e and this is increased in magnitude with increasing pH. Figure 5.2.2 shows the fluorescence intensity of FPE on addition of insulin or calcium ions to labelled Jurkat T-lymphocytes at pH8.2 where the negative charge per insulin molecule is increased to -5.7e. The calcium response is increased, showing the enhanced sensitivity of the FPE under these conditions, but still no effect of insulin is observed.

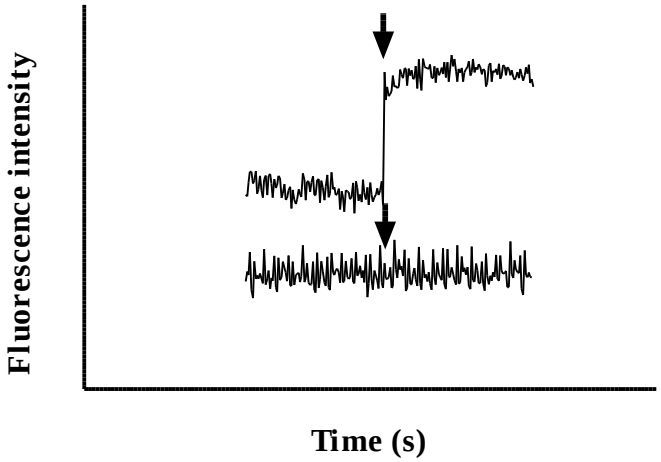

Figure 5.2.2 The change in emission intensity of FPE labelled Jurkat T-lymphocytes (40,000 cells ml^{-1} in 10mM HEPES 280mM sucrose solution, pH8.2 37^{o}C) on addition of 2mM calcium ions (positively charged) in the form of calcium carbonate (upper trace) or 1μM Insulin (lower trace). The traces are displayed on the same intensity and time scale as Figure 5.2.1.

In further experiments the cells were serum starved for 12hrs, removing insulin and insulin-like growth factor-1 from the culture environment, to increase the binding capacity of the cell membranes for insulin by promoting the expression of insulin-receptors on the cell surface and minimising the pre-bound insulin and IR-insulin complex internalisation prior to the experiment (Traxinger and Marshall, 1990, Livingston and Moxley, 1982, Moxley et al., 1981, De Pirro et al., 1979, Muggeo et al., 1977). During this time and throughout the experiment cells were maintained in 10mM glucose to further increase the affinity of insulin for its receptor (Traxinger and Marshall, 1990, Whitesell and Gliemann, 1979, Garvey et al., 1986). However, there was still no detectable change in the surface potential. It is possible that the insulin receptors expressed on the Jurkat T-lymphocyte membrane are still not sufficiently numerous or the insulin-insulin receptor interaction does not significantly alter the charge landscape of the membrane. For instance the Debye length, over which ions in solution effectively screen the effects of the membrane surface charge, is under approximately 0.5nm (O'Shea, 2005), whereas proteins, such as insulin and its receptor, are of the order of 5-50nm in size so it is possible that the charged moieties of insulin bound to its receptor are positioned too far from the membrane to perturb the surface charge landscape.

5.2.1.2. ***Flow cytometry using fitc-insulin***

Jurkat T-lymphocytes were labelled with fitc-insulin (from bovine pancreas, ≥1mol fitc per mol insulin) according to Murphy *et al.* (Murphy et al., 1982) and the resulting shift of the fluorescence histogram of a 10,000 cell sample in comparison with unlabelled cells (excitation at 488nm line detection with a 530nm filter of 30nm bandwidth) is shown in figure 5.2.3. A significant increase in average fluorescence intensity of the cell population occurs with fitc-insulin labelling and to determine the extent to which this can be attributed to receptor-bound

fitc-insulin cells were treated with an excess of unlabelled insulin prior to, and during, fitc-insulin labelling.

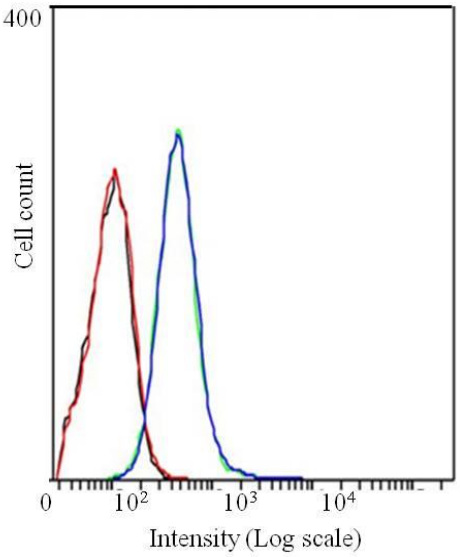

Figure 5.2.3: Typical fluorescence histograms obtained by flow cytometry of Jurkat T-lymphocytes labelled with fitc-insulin (1μM 30min 37°C) (green) and with fitc-insulin in the presence of, and following prior treatment with, unlabelled insulin (10μM 30min 37°C) (blue). Also shown are the histograms for unlabelled cells (black) and cells treated with unlabelled insulin only (red). Data was collected for 10,000 cells in each sample and the fluorescence histogram plotted for the live cell population identified in a forward scatter vs side scatter plot (as discussed in section 2.6.3). The live cell population contained >85% of cells and of this >95% were labelled with fitc-insulin.

Figure 5.2.3 shows that the presence of unlabelled insulin does not affect the fluorescence intensity of unlabelled or labelled cells suggesting no detectable difference in the extent of fitc-insulin labelling of cells despite blocking insulin binding sites with unlabelled insulin. This suggests that the majority of the fluorescence signal detected is not due to fitc-insulin bound to the insulin receptors. Murphy *et al.* found approximately 70% of the total fluorescence to be due to internalised fitc-insulin using similar labelling conditions with Swiss 3T3 cells (Murphy et al., 1982). Of this, 75% is attributed to fluorophores internalised via non-insulin receptor specific mechanisms. It is therefore possible that non-specific internalised fluorescence may mask any insulin-receptor specific changes in the fluorescence intensity following fitc-insulin incubation in the presence of excess unlabelled insulin.

In order to distinguish the contributions of internalised and surface-bound fitc-insulin to the total fluorescence intensity detected, trypan blue was used to quench fitc-insulin on the surface of viable cells, which are impermeable to the dye (Loike and Silverstein, 1983, Ma and Lim, 2003). Figure 5.2.4 demonstrates the ability of trypan blue to quench the fluorescence of fitc-insulin in solution.

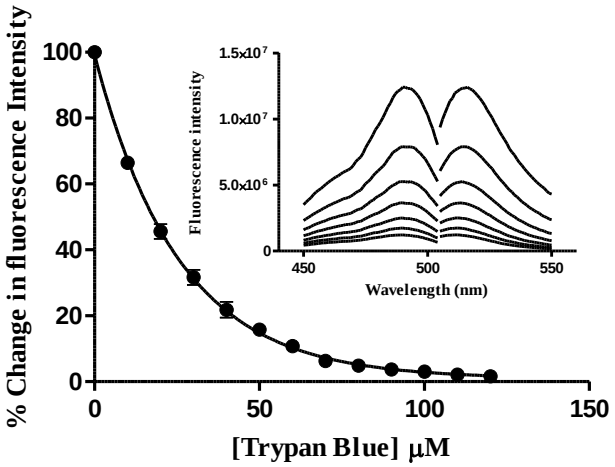

Figure 5.2.4: (*main*) The percentage decrease in fluorescence intensity of fitc-insulin (1µM in DPBS, room temperature) on titration of trypan blue (0.4% solution) detected at 520nm (λ_{ex}=490). Data represents the average of 3 repeats with the standard error of the mean represented as error bars. (*inset*) The excitation and emission spectra of fitc-insulin before addition of trypan blue and following each of the first 6 additions shown on the quenching curve.

Both the excitation and emission spectra are suppressed with trypan blue quenching suggesting the mechanism is the static quenching of ground state complex formation between trypan blue and fitc. Once these complexes have formed, excess trypan blue can be washed from the cells in preparation for flow cytometry without compromising the quenched state. Figure 5.2.5 shows the total fluorescence intensity of fitc-insulin labelled cells treated with increasing concentrations of trypan blue prior to flow cytometry.

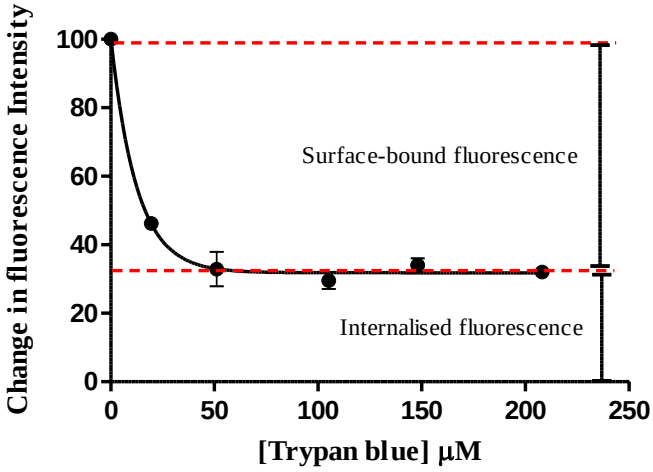

Figure 5.2.5: The change in fluorescence intensity of fitc-insulin labelled Jurkat T-lymphocytes (1µM 30min 37°C) treated with increasing concentrations of Trypan Blue (1min, RT) prior to flow cytometry analysis. Data was taken for 10,000 cells and intensity histograms were plotted for the live cell population determined from a forward scatter vs side scatter plot. The median fluorescence intensity of the resulting normal distribution was taken for each sample and normalised between that of unlabelled cells (0%) and fitc-insulin labelled cells with no trypan blue treatment (100%). Complete quenching of accessible fitc fluorescence was achieved with >50µM of trypan blue indicating approximately 30% of the total fluorescence signal to be due to internalised fluorophore. Data represents the average of 3 repeats with the standard error of the mean represented as error bars.

Fitc-insulin internalisation is decreased with temperature; Murphy *et al.* (Murphy et al., 1982) observe a 5 fold decrease in internalisation between 37°C and 4°C which is shown to be, at least partially, insulin(-analogue) specific. This is consistent with the later findings of Hachiya *et al.* (Hachiya et al., 1987) who report little internalisation of ^{125}I-Insulin in vascular endothelial cells at 10°C but significant internalisation at 37°C. Trypan blue quenching of Jurkat T-lymphocytes incubated with fitc-insulin at 4°C and 37°C should therefore reveal a significant difference in internalisation of fitc-insulin due to an expected reduced rate of insulin receptor internalisation at the lower temperature. Figure 5.2.6 shows the result of this experiment.

The percentage of internalised fluorescence is not significantly different (P=0.97 R^2=0.0005, unpaired two-tailed t test) at 4°C and 37°C. Murphy *et al.* (Murphy et al., 1982) found fitc-insulin to have a decreased specificity for the insulin receptor at 4°C (possibly due to insulin dimerisation) suggesting a lower concentration would be bound to the membrane surface at 4°C than at 37°C. This suggests that in our cells non-receptor specific binding masks receptor binding. However, it should be noted that fitc self-quenches its fluorescence through homo resonance energy transfer with a Forster distance of 47Å (Lakowicz et al., 2003). It is therefore possible that the fluorescence intensities are affected by self-quenching resulting through insulin dimerisation, colocalisation of insulin receptors in domains of the membrane (Schlessinger et al., 1980) and close proximity of non-specifically bound fitc-insulin the extent of which would change with temperature.

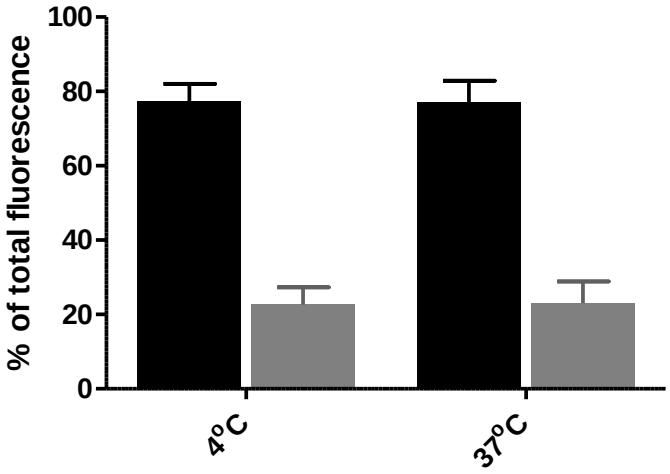

Figure 5.2.6: The percentage fluorescence intensity of surface-bound (black shaded) and internalised (grey shaded) fitc-insulin determined by trypan blue quenching of surface fluorescence (100µM, 1min RT) of Jurkat T-lymphocytes labelled with fitc-insulin (1µM, 30min) at 4°C and 37°C. Data was taken for 10,000 cells and intensity histograms were plotted for the live cell population determined from a forward scatter vs side scatter plot. The median intensity of the resulting normal distribution was taken for each sample and normalised between that of unlabelled cells (0%) and fitc-insulin labelled cells with no trypan blue treatment (100%). The % internalised fluorescence represents the % decrease in fluorescence following trypan blue treatment and the % surface-bound fluorescence is the total fluorescence (100%) minus % internalised fluorescence. Data represents the average of 3 repeats with the standard error of the mean represented as error bars.

To investigate whether separating the total fitc-insulin fluorescence into components corresponding to surface-bound and internalised fitc-insulin would reveal a receptor-bound factor, cells were labelled with fitc-insulin, with and without excess unlabelled insulin, followed by trypan blue quenching prior to flow cytometry.

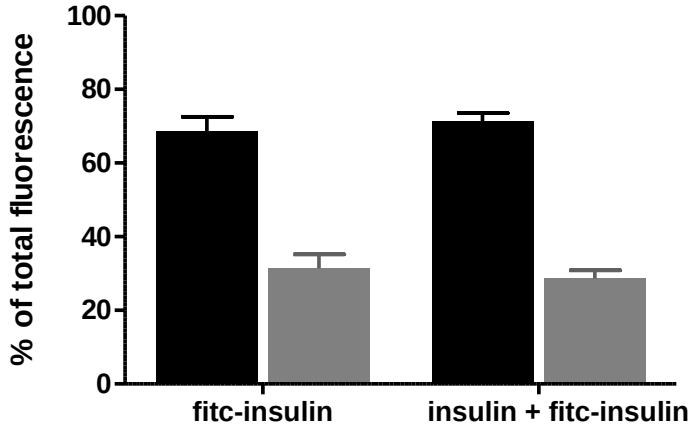

Figure 5.2.7: The percentage fluorescence intensity of surface-bound (black shaded) and internalised (grey shaded) fitc-insulin determined by trypan blue quenching of surface fluorescence (100μM, 1min RT) of Jurkat T-lymphocytes labelled with fitc-insulin (1μM, 30min) or with fitc-insulin in the presence of, and following prior treatment with, unlabelled insulin (10μM 30min 37^{o}C). The same protocol as outlined in the legend of Figure 5.2.6 was used.

Figure 5.2.7 shows the percentage contributions of surface-bound and internalised fitc-insulin in cells labelled in the presence and absence of unlabelled insulin. The total fluorescence (normalised to 100%) is the same in both cases; the percentage of fluorescence attributed to surface-bound fitc-insulin is not significantly different (unpaired two-tailed t test P=0.58 R^2=0.08) confirming that the signal is due principally to the non-specific binding and non-receptor mediated (non-specific) internalisation.

Ziegler *et al.* also report significant non-specific binding of fitc-insulin to lymphocytes labelled with 1μM fitc-insulin. Figure 5.2.8 shows the fluorescence histogram of cells labelled with 10^{-8}M fitc-insulin which is demonstrated to minimize non-specific binding under the conditions outlined in (Ziegler et al., 1994) (90min 15^{o}C in assay buffer: 100mM HEPES, 120mM $NaCl_2$, 5mM KCl, 1.2mM $MgSO_4$, 10mM NaN_3, 10mM D-glucose, 1%BSA, pH7.8).

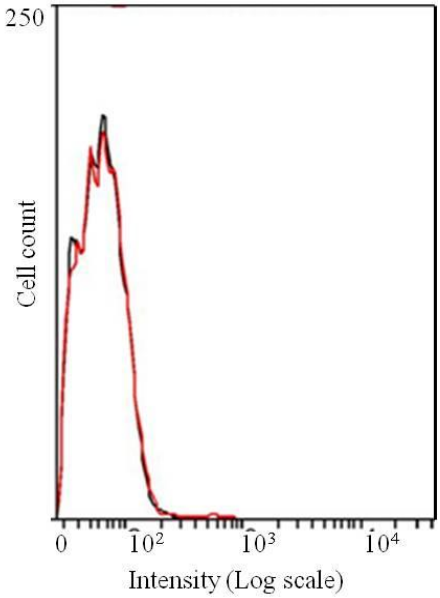

Figure 5.2.8: Typical fluorescence histograms obtained by flow cytometry of Jurkat T-lymphocytes unlabelled (black) and labelled with fitc-insulin (red) at a concentration minimising non-specific binding (10nM 90min 15°C) after Ziegler *et al.*(Ziegler 1994) Data was collected for 10,000 cells in each sample and the fluorescence histogram plotted for the live cell population identified in a forward scatter vs side scatter plot (>80% of total cells).

No detectable fluorescence above the autofluorescence of unlabelled cells is observed. This suggests that fitc-insulin may have a low affinity for insulin receptors and/or the number of insulin receptors expressed on the membrane may be relatively low compared to the cell lines used by others in similar studies (Murphy et al., 1982, Ziegler et al., 1994, Bohn, 1980).

Murphy *et al.* find fitc-insulin to stimulate protein and DNA synthesis by only 1.5% and 56%, respectively, of that by native insulin in Swiss 3T3 cells (Murphy et al., 1984) and Tietze *et al.*(Tietze et al., 1962) found fitc-insulin to produce 60-80% of the hypoglycaemic response of native insulin in fasted rabbits. It is possible that fluorescence labelling of insulin may interfere with its transport and function within the cells and, although the conjugation site of fitc with insulin is not involved with receptor binding, steric hindrance due to the large fitc group may reduce the binding affinity (Tietze et al., 1962). Further experiments were conducted using biotinylated insulin to circumvent this problem.

5.2.1.3. ***Flow cytometry using biotinylated insulin***

To determine if the low affinity of fitc-insulin for the receptor is responsible for the undetectable fluorescence using fitc-insulin, biotinylated insulin was used with post-labelling with a fluorescent streptavidin. Biotinylated insulin (biotin-insulin, BI) has a significantly higher (23% greater) affinity for the insulin receptor than fitc-insulin, only slightly less than that of native insulin (Ziegler et al., 1994). It also shows high specificity for the insulin receptor with very low non-specific binding at concentrations $\leq 10^{-7}\mu M$ (Ziegler et al., 1994). The careful selection of the fluorophore conjugated to avidin or streptavidin can also increase the sensitivity

of this technique. Both avidin and streptavidin can bind to biotin with a ratio of up to 4mol/mol biotin (Chaiet and Wolf, 1964). This has potential to produce a four-fold increase in fluorescence intensity per insulin-biotin molecule however this depends on the nature of the fluorophore conjugated to the avidin/streptavidin. Fitc, as mentioned earlier, self quenches (Lakowicz et al., 2003) and decreases in fluorescence when conjugated to protein at high concentrations; Alexa Fluor 488 (AF 488), a fluorophore with very similar spectral properties and quantum yield to fitc (Panchuk-Voloshina et al., 1999), is much less sensitive to self-quenching ("Advantages of the Alexa Fluor 488 dye conjugates"www.invitrogen.com/site/us/en/home/brands/Molecular-Probes/Key-Molecular-Probes-Products/alexa-fluor/Alexa-Fluor-488-Secondary-Antibodies.html 06/03/2011). Jurkat T-lymphocytes were therefore labelled sequentially with 10^{-7}µM biotin-insulin and streptavidin-Alexa fluor 488.

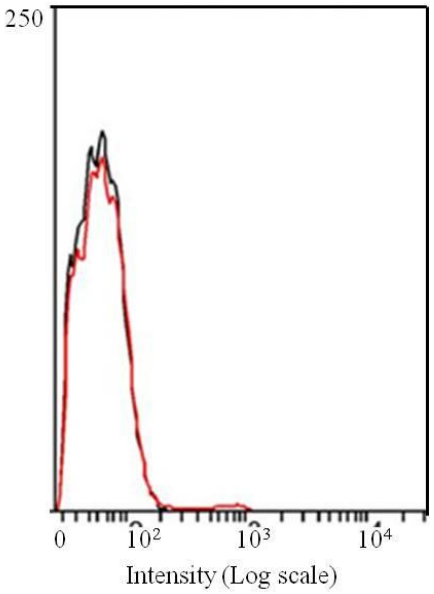

Figure 5.2.9: Typical fluorescence histograms obtained by flow cytometry of Jurkat T-lymphocytes unlabelled (black) and labelled with biotin-insulin (0.1µM 90min 15°C) followed by streptavidin-Alexa Fluor 488 (1mg ml^{-1} streptavidin diluted 1:500, 30min 4°C) (red) after Ziegler *et al.* (Ziegler 1994). Data was collected for 10,000 cells in each sample and the fluorescence histogram plotted for the live cell population identified in a forward scatter vs side scatter plot (>80% of total cells).

Figure 5.2.9 is an example representative of the resulting fluorescence histograms and, despite the increased sensitivity, there is no increase in average fluorescence of the labelled cells above the background. This confirms that Jurkat T-lymphocytes do not express insulin receptors extensively enough to detect the binding of insulin to them using a fluorescence based assay.

5.2.2. IM9 B-Lymphocytes

IM9 B-lymphocytes express relatively high levels of insulin receptors (Brunetti et al., 2001) and have been used to study the binding of insulin using radiolabelled and fluorescent insulin including the methods described above (Maron and Kahn, 1985, Jehle et al., 1996, Ziegler et al.,

1994). To confirm the presence of detectable levels of the receptor on these cells the binding of biotinylated insulin was assessed using flow cytometry.

5.2.2.1. ***Detection of insulin receptors on IM9 cells by flow cytometry***

IM9 B-lymphocytes were labelled with biotinylated insulin (biotin-insulin, BI) at 15°C for 90 minutes and subsequently with streptavidin-Alexa Fluor 488 (S488) at 4°C for 30 minutes after Ziegler *et al.* (Ziegler et al., 1994). The fluorescence histogram resulting from flow cytometry of the labelled cells, compared to that of the background fluorescence of unlabelled cells, is shown in Figure 5.2.10

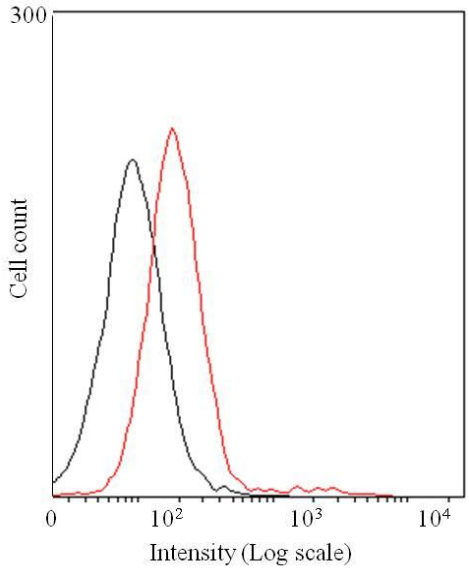

Figure 5.2.10: Typical fluorescence histograms obtained by flow cytometry of IM9 B-lymphocytes unlabelled (black) and labelled with biotin-insulin (BI) (0.1μM 90min 15°C) followed by streptavidin-Alex Fluor 488 (S488) (1mg ml^{-1} streptavidin diluted 1:500, 30min 4°C) (red) after Ziegler *et al.* (Ziegler 1994). Propidium iodide (*PI*) (3μM) was added to all samples at least 5mins prior to flow cytometry. Data was collected for 10,000 cells in each sample and the fluorescence histogram plotted for the live cell population identified in a forward scatter vs side scatter plot (excluding >75% *PI* positive cells).

The separation of the median intensities of the normal distributions of fluorescence for unlabelled and labelled cells is in good agreement with that reported by Ziegler *et al.* (Ziegler et al., 1994). Figure 5.2.11 shows the median fluorescence expressed as a percentage of the separation of the median intensities of unlabelled (0%) and biotin-insulin with streptavidin-Alexa Fluor 488 labelled (100%) cells. As expected, biotin-insulin does not contribute to the fluorescence signal but streptavidin-Alexa Fluor 488 demonstrated non-specific binding amounting to ~12% of the signal from cells labelled with both biotin-insulin and streptavidin-Alexa Fluor 488 which is considered insignificant.

In fact, in the presence of biotin-insulin, due to the high affinity of streptavidin for biotin, the non-specific binding associated with streptavidin-Alexa Fluor 488 is likely to be lower than that seen in Figure 5.2.11. The non-specific binding of biotin-insulin, to which the fluorophore

binds, should also be considered. To investigate this, cells were labelled in the presence of an excess of unlabelled insulin. The fluorescence histograms for cells labelled in the presence and absence of unlabelled insulin are shown in Figure 5.2.12.

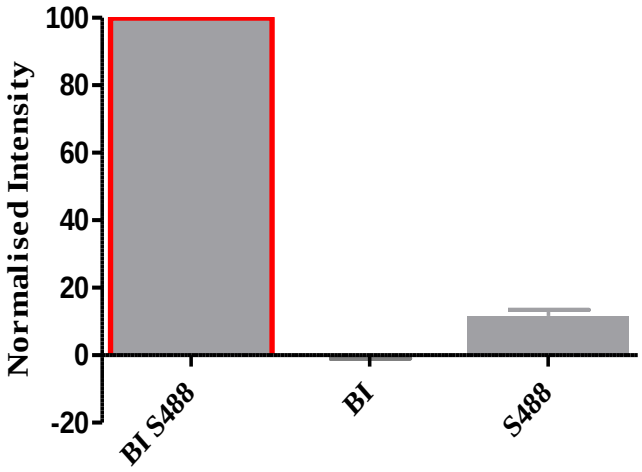

Figure 5.2.11: The percentage fluorescence intensity of IM9 B-lymphocytes labelled with biotin-insulin (BI) (0.1µM 90min 15°C) or streptavidin-Alexa Fluor 488 (S488) (1mg ml^{-1} streptavidin diluted 1:500, 30min 4°C) compared to cells labelled with both BI and S488. Propidium iodide (*PI*, 3µM) was added to all samples at least 5mins before flow cytometry. Data was taken for 10,000 cells and intensity histograms were plotted for the live cell population determined from a forward scatter vs side scatter plot (excluding >75% *PI* positive cells). The median intensity of the resulting normal distribution was taken for each sample and normalised between that of unlabelled cells (0%) and cells labelled with both BI and S488 (100%) corresponding to the black and red histograms of figure 5.2.2.11 respectively. Data represents the average of 3 repeats with the standard error of the mean represented as error bars.

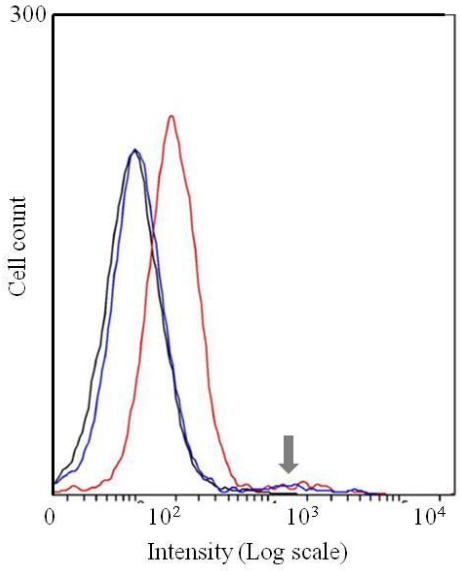

Figure 5.2.12: Typical fluorescence histograms obtained by flow cytometry of IM9 B-lymphocytes labelled with biotin-insulin (BI) (0.1µM 90min 15°C) followed by streptavidin-Alex Fluor 488 (S488) (1mg ml^{-1} streptavidin diluted 1:500, 30min 4°C) (red) and with biotin-insulin in the presence of, and following prior treatment with, unlabelled insulin (10µM 90min 15°C) preceeding streptavidin-Alexa Fluor 488 labelling (blue). The histogram for unlabelled cells is also shown (black). Propidium iodide (*PI*, 3µM) was added to all samples at least 5mins prior to flow cytometry. Data was collected for 10,000 cells in each sample and the fluorescence histogram plotted for the live cell population identified in a forward scatter vs side scatter plot (excluding >75% *PI* positive cells).

Unlabelled insulin significantly reduces the fluorescence intensity indicating that the majority of the fluorescence corresponds to surface-bound molecules. Interestingly, the small higher-intensity secondary peak (indicated by the arrow in Figure 5.2.12) is not affected by labelling in the presence of excess insulin suggesting this to be associated with non-receptor specific bound fluorophore.

Figure 5.2.13 shows the median fluorescence determined in these experiments. The fluorescence signal is reduced by >90% in cells labelled in the presence of unlabelled insulin suggesting that >90% of the fluorescence signal can be attributed to insulin-receptor bound biotin-insulin. This is greater than the ~80% specificity of biotin-insulin for insulin receptors reported by Ziegler *et al.* (Ziegler et al., 1994) which may be due to differences in the non-specific binding of the different fluorescent streptavidins used. In fact, the percentage fluorescence due to non-specific binding in Figure 5.2.11 is not significantly different from that of cells labelled with biotin-insulin streptavidin-AF 488 in the presence of unlabelled insulin shown in Figure 5.2.13 (unpaired two-tailed t test, $P=0.22$, $R^2=0.35$). This suggests that the non-specific binding observed in the latter may be principally due to the non-specific binding of streptavidin-AF 488 and not biotin-insulin. Interestingly, practically no fluorescence signal above the background fluorescence of unlabelled cells originated from cells labelled with streptavidin-AF 488 following insulin treatment. This suggests that insulin may inhibit the non-specific binding of streptavidin-AF 488, but not in the presence of biotin-insulin indicating that biotin-insulin is involved, to some degree, in non-specific binding. More likely, however, the increase in fluorescence of insulin and streptavidin-AF 488 labelled cells in the presence of biotin-insulin may be due to the incomplete blocking of insulin receptors by the unlabelled insulin and so corresponds to a small amount of specific binding (Ziegler et al., 1994).

These data demonstrate that IM9 B-lymphocytes, unlike Jurkat T-lymphocytes, do express levels of the insulin receptor that are detectable using fluorescent insulin. These cells were therefore employed in a further series of experiments to establish an effect of insulin binding on the surface potential.

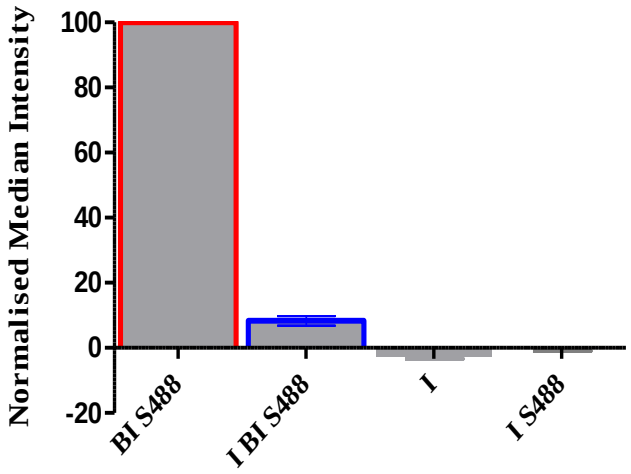

Figure 5.2.13: The percentage fluorescence intensity of IM9 B-lymphocytes labelled with biotin-insulin (BI) (0.1µM 90min 15°C) in the presence of, and following prior treatment with, unlabelled insulin (10µM 90min 15°C) followed by streptavidin-Alex Fluor 488 (S488) (1mg ml^{-1} streptavidin diluted 1:500, 30min 4°C) (blue) compared to cells labelled with biotin-insulin without unlabelled insulin (I) prior to streptavidin-alexa fluor 488 (red). Also shown is the percentage fluorescence intensity from cells labelled with insulin only or insulin followed by streptavidin-alexa fluor 488. The same protocol as outlined in the legend of Figure 5.2.11 was used.

5.2.2.2. *Surface potential experiments*

IM9 B-lymphocytes were labelled with fluorescein-phosphatidylethanolamine (FPE) to report changes in the surface potential. Cells were serum starved for 12hrs prior to the experiment and also maintained in 10mM glucose increasing the binding capacity of the membrane and the affinity of insulin for the receptors, respectively, as described in section 5.2.1.1. Labelled cells were suspended in HEPES-buffered sucrose solution (10mM HEPES, 10mM glucose 270mM sucrose) at pH8.2 to maximise both the charge per insulin molecule and the sensitivity of FPE to changes in the surface potential (described in section 5.2.1.1). FPE within the labelled cell membranes responded to the addition of 2mM calcium ions in the same manner as shown in figure 5.2.2, however, no change in intensity of FPE fluorescence was detected on the addition of 1µM insulin. Since this negative result is unlikely to be due to insufficient binding it is concluded that the interaction of insulin with the receptor does not modify the charge landscape of the membrane.

5.2.2.3. *A return to flow cytometry using biotinylated insulin*

As the surface potential could not be used to explore the binding of insulin to its receptor, flow cytometry using biotinylated insulin post-labelled with streptavidin-Alexa Fluor 488 was instead used to investigate the effect of 7-ketocholesterol and α-tocopherol on insulin binding. Prior to this, the use of trypan blue quenching to distinguish the contributions of surface-bound and internalised fluorophore, as discussed in section 5.2.1.2 for fitc-insulin, was assessed.

Figure 5.2.14 demonstrates that streptavidin-AF 488 fluorescence can be quenched by trypan blue. The significantly reduced height of the excitation spectrum, as well as the emission spectrum, is indicative of a static mechanism of quenching such as that seen with fitc.

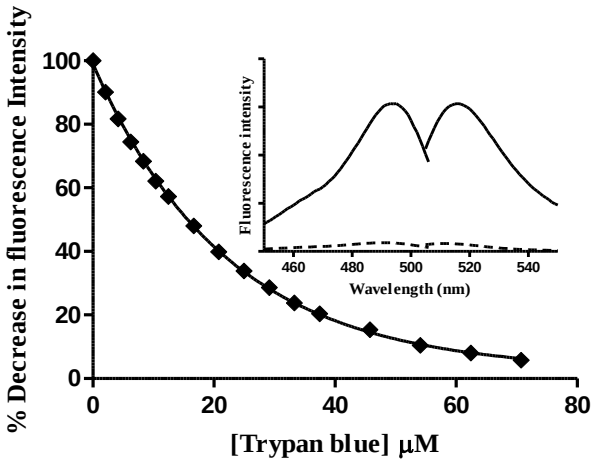

Figure 5.2.14: (*main*) The percentage decrease in fluorescence intensity of streptavidin-Alexa Fluor 488 (1mg ml^{-1} streptavidin diluted 1:500 in DPBS, room temperature) on titration of trypan blue (0.4% solution) detected at 520nm (λ_{ex}=490). Data represents the average of 3 repeats with the standard error of the mean represented as error bars. (*inset*) The excitation and emission spectra of streptavidin-Alexa Fluor 488 at the start and end points of the titration shown.

Figure 5.2.15 gives examples of the typical fluorescence histograms obtained on flow cytometry of cells that have been labelled with biotin-insulin and streptavidin-AF 488 with or without subsequent trypan blue treatment (100μM 1min RT). Interestingly, trypan blue treatment does not reduce the intensity of the principle peak of the fluorescence histogram for labelled cells and, as demonstrated more clearly in Figure 5.2.16, actually increases the median fluorescence of labelled cells although not significantly (one-tailed t-test P=0.06). The secondary peak at higher intensity, thought to correspond to non-specifically bound streptavidin-AF 488, however, is eliminated following trypan blue treatment (indicated by the arrow in Figure 5.2.15). This suggests that streptavidin-AF 488 that is bound to biotin-insulin is protected from static quenching by trypan blue whereas that not associated with biotin is susceptible to quenching.

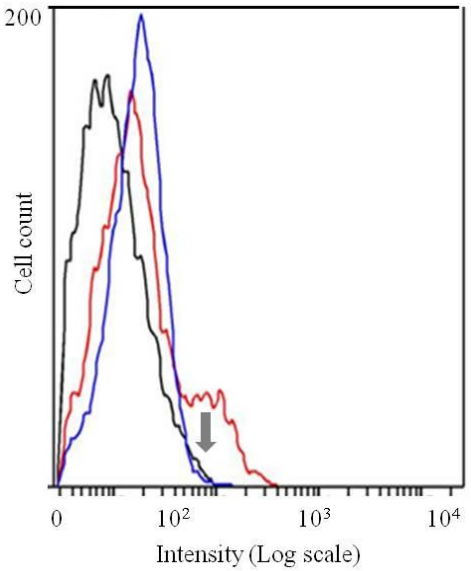

Figure 5.2.15: Typical fluorescence histograms obtained by flow cytometry of IM9 B-lymphocytes labelled with biotin-insulin (BI) (0.1µM 90min 15°C) followed by streptavidin-Alexa fluor 488 (S488) (1mg ml^{-1} streptavidin diluted 1:500, 30min 4°C) with (blue) and without (red) trypan blue treatment (100µM 1min, RT). The same protocol as outlined in the legend of Figure 5.2.11 was used. Trypan blue treatment visibly quenched the fluorescence of a population with intensity to the right of the main peak (arrow) and increased the median intensity of the main peak.

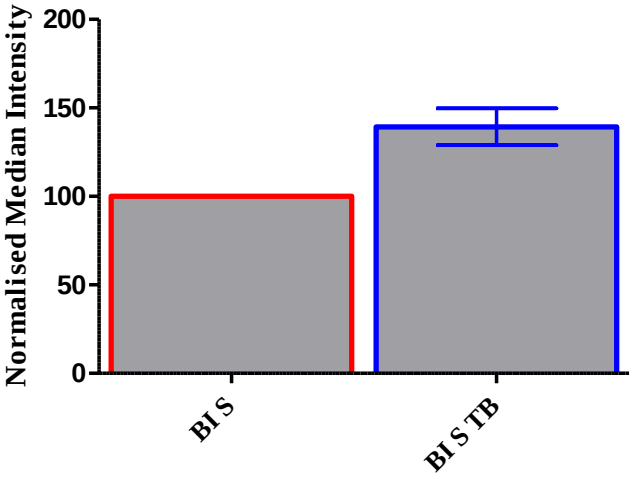

Figure 5.2.16: The percentage fluorescence intensity of IM9 B-lymphocytes labelled with biotin-insulin (BI) (0.1µM 90min 15°C) and streptavidin-Alexa fluor 488 (S488) (1mg ml^{-1} streptavidin diluted 1:500, 30min 4°C) followed by trypan blue treatment (100µM 1min, RT) (blue) compared with untreated labelled cells (red). The same protocol as outlined in the legend of Figure 5.2.11 was used. Data represents the average of 3 repeats with the standard error of the mean represented as error bars.

The trypan blue quenching technique is, therefore, not able to distinguish between internalised and surface-bound fluorescence where streptavidin-AF 488 is used. Labelling with streptavidin-AF 488 is performed at 4°C and it is widely reported that receptor internalisation is significantly reduced at this temperature (Murphy et al., 1982, Hachiya et al., 1987) suggesting that a significantly larger proportion of the total fluorescence from labelled cells is likely to arise from surface-bound fluorophore than is due to internalised fluorophore. Further experiments therefore assume that the total fluorescence corresponds to surface-bound molecules.

5.2.2.4. *The effect of 7-ketocholesterol on insulin binding*

The influence of 7-ketocholesterol on the binding of insulin to IM9 B-lymphocytes was investigated by pre-treating cells with 7-ketocholesterol at a concentration and with the incubation conditions previously found to cause maximum change in the dipole potential. The concentration of 7-ketocholesterol and duration of exposure used were much less than the incubation conditions reported to induce apoptosis (Lizard et al., 1997, Palozza et al., 2010, Royer et al., 2009).

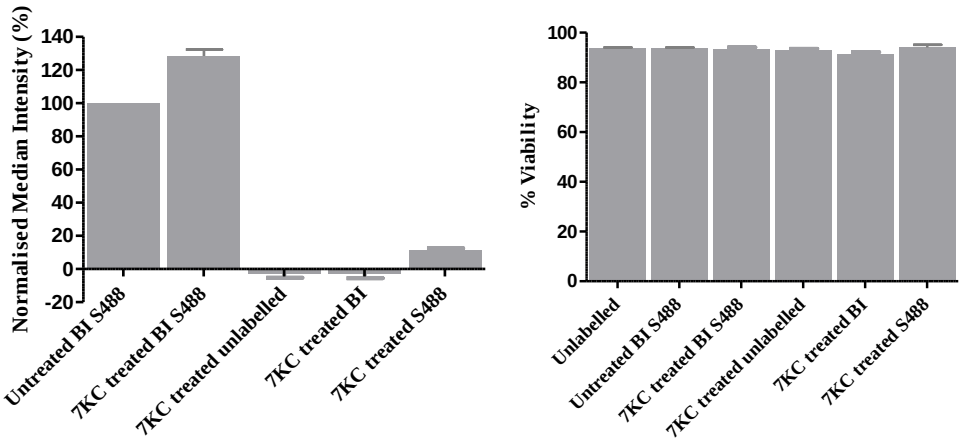

Figure 5.2.17: *(left)* The percentage fluorescence intensity of IM9 B-lymphocytes labelled with biotin-insulin (BI) (0.1μM 90min 15^{o}C) and streptavidin-Alexa fluor 488 (S488) (1mg ml^{-1} streptavidin diluted 1:500 30min 4^{o}C) with or without 7-ketocholesterol (7KC) treatment (10μM 10min 37^{o}C prior to, and 10μM during, subsequent labelling). Propidium iodide (*PI*, 3μM) was added to all samples at least 5mins prior to flow cytometry. Also shown are the percentage fluorescence intensities of 7KC treated cells that are unlabelled or labelled with BI or S-488 as controls. The same protocol as outlined in the legend of Figure 5.2.11 was employed with the live cell population excluding >90% *PI* positive cells. *(Right)* The percentage viability of the population assessed in each sample with respect to an unlabelled and untreated control. Data represents the average of 6 repeats (n=3 for controls) with the standard error of the mean represented as error bars.

The presence of 7-ketocholesterol significantly increased the average fluorescence intensity of cells labelled with biotin-insulin and streptavidin-Alexa Fluor 488 (one tailed t test, P=0.0006). Figure 5.2.17 also shows the average fluorescence intensity for control samples treated with 7-ketocholesterol and either unlabelled or labelled with biotin-insulin to be not significant (P>0.05 one tailed t tests). The 7-ketocholesterol treated control labelled with streptavidin-Alexa Fluor 488 only, however, shows a significant average fluorescence (P=0.011 one tailed t test) associated with non-specific binding. This is not significantly different from that shown in Figure 5.2.11 (P=0.88 two tailed t test) suggesting that the degree of non-specific binding is not altered by 7-ketocholesterol treatment. The viability of the cells assessed was determined by propidium iodide exclusion, and was not significantly different following 7-ketocholesterol treatment (P=0.28 F=1.3 R2=0.24 one way anova followed by Dunnetts multiple comparisons test). Fluorescence from non-viable cells was not included in the calculated average fluorescence intensity. The increase in fluorescence intensity therefore represents an increase in insulin specific binding in healthy cells. As cells were labelled at 4^{o}C where receptor-mediated

internalisation of the fluorophore is minimised, the increase in average fluorescence can be attributed to surface-bound biotin-insulin streptavidin-Alexa Fluor 488 complexes. Together with evidence in the previous section (Figure 5.2.13) suggesting the majority of surface-bound fluorescence to be associated with insulin receptor binding, this suggests that 7-ketocholesterol treatment causes significant modulation of the membrane dipole potential and increases the receptor binding of biotin-insulin. This increase in binding may be due to an increased receptor expression on the membrane. Interestingly the opposite effect, a decrease in receptor expression, was observed following treatment of neuronal cultures with cholesterol by Taghibiglou *et al.* (Taghibiglou et al., 2009). They exposed cells to 2mM cholesterol for 30minutes at 37^{o}C which, according to data presented in Chapter 4 (Section 4.1.1), is likely to cause a significant increase in the membrane dipole potential. Taghibiglou *et al.* found the decrease in receptor expression to correlate with an increase in facilitated receptor endocytosis and it would be interesting to determine if the membrane dipole potential, altered by cholesterol or 7-ketocholesterol, can be correlated with this. The extent of receptor mediated endocytosis on 7-ketocholesterol treatment could be determined using the current fluorescence assay either by finding a suitable quencher of surface-bound fluorescence or using trypsin to remove surface-bound insulin-fluorophore complexes (Murphy et al., 1982).

The increase in surface-bound fluorescence following 7-ketocholesterol treatment may also reflect an increased affinity of (biotin-)insulin for the receptor. The influence of the dipole potential on the affinity of biotin-insulin for the receptor could be explored using a competitive binding assay with another detectable insulin analogue (e.g. ^{125}I-Insulin or another fluorescently tagged insulin) as used by Ziegler *et al*. (Ziegler et al., 1994) after Freychet (Freychet, 1979).

5.2.2.5. ***The influence of α-tocopherol succinate and 7-ketocholesterol on insulin binding***

In Chapter 4 (Section 4.3.2) it was demonstrated that α-tocopherol succinate treatment significantly reduced the effect of 7-ketocholesterol on the cell membrane dipole potential. If 7-ketocholesterol was already present lowering the dipole potential of the membrane, simulating the effects of oxidative stress on the membrane, then α-tocopherol succinate treatment was found to have no significant effect.

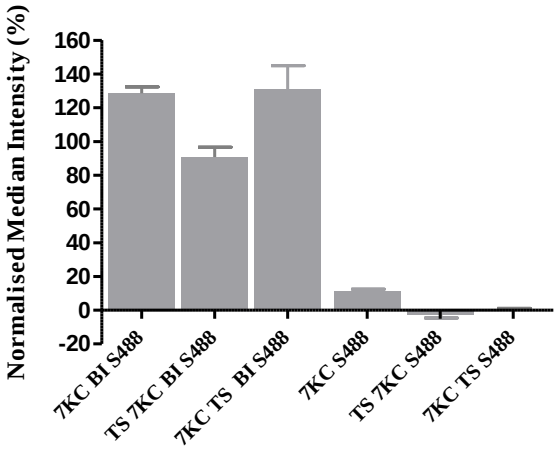

Figure 5.2.18: The percentage fluorescence intensity of 7-ketocholesterol treated (10μM 10min 37°C prior to, and 10μM during, subsequent labelling) IM9 B-lymphocytes labelled with biotin-insulin (BI) (0.1μM 90min 15°C) and streptavidin-Alexa fluor 488 (S488) (1mg ml^{-1} streptavidin diluted 1:500 30min 4°C) without further treatment or with α-tocopherol succinate treatment (TS)(3.77μM 10min 37°C prior to, and 3.77μM during, subsequent labelling) immediately before or after 7KC exposure. Propidium iodide (*PI*, 3μM) was added to all samples at least 5mins prior to flow cytometry. Also shown are the percentage fluorescence intensities of 7KC and TS treated cells that are labelled with S488 only. The same protocol as outlined in the legend of Figure 5.2.11 was employed with the live cell population excluding >90% *PI* positive cells. Data represents the average of 6 repeats (n=3 for 7KC S488 control) with the standard error of the mean represented as error bars.

The combined influence of α-tocopherol succinate and 7-ketocholesterol on insulin binding, when α-tocopherol succinate is given prior to or following exposure of the cells to 7-ketocholesterol, is shown in Figure 5.2.18. α-Tocopherol succinate treatment before exposure to 7-ketocholesterol significantly decreased insulin binding with respect to 7-ketocholesterol exposed cells (one way anova followed by Dunnetts multiple comparison test $P<0.05$). If cells were treated with α-tocopherol succinate after initial exposure to 7-ketocholesterol this effect was abolished and insulin binding was not significantly different from that to untreated 7-ketocholesterol exposed cells ($P>0.05$). Comparing the insulin binding of cells exposed to 7-ketocholesterol, with or without prior α-tocopherol succinate treatment, with normal cells demonstrates α-tocopherol succinate treatment to inhibit the effect of 7-ketocholesterol and maintain the same extent of insulin binding occurring in normal cells (one way anova followed by Dunnetts multiple comparison test $P>0.05$ for TS then 7-KC treated and $P<0.05$ for 7-KC treated).

These data suggest that the altered dipole potential of the membrane associated with oxidative stress is associated with increased insulin binding. α-Tocopherol succinate is able to inhibit this increase, maintaining insulin binding at normal levels, but its influence is dependent on the pre-existing oxidative state of the membrane. If the dipole potential of the membrane is lowered as a result of oxidative stress prior to α-tocopherol succinate treatment, it has no influence.

Insulin receptors have been associated with lipid rafts (Vainio et al., 2005, Vainio et al., 2002, Bickel, 2002, Cohen et al., 2003) and it is possible that the effect of 7-ketocholesterol, and α-tocopherol succinate, involve these structures. In a hypothesis proposed by Lemaire-Ewing *et al.* (Lemaire-Ewing et al., 2010) α-tocopherol, when present in the cell membrane prior to exposure to 7-ketocholesterol, inhibits the sterol from localising in rafts. If α-tocopherol treatment occurs after 7-ketocholesterol exposure, the sterol partitions into rafts and the addition of α-tocopherol, now unable to localise in rafts to the same extent, does not effect this. It is possible a similar effect is occurring with α-tocopherol succinate and the increase of insulin binding on 7-ketocholesterol treatment may be due to the disruption of the highly ordered rafts, lowering the dipole potential. When α-tocopherol succinate treatment occurs prior to 7-ketocholesterol exposure, the partitioning of 7-ketocholesterol into rafts is inhibited and the increase in insulin binding is avoided. Where cells are exposed to 7-ketocholesterol before α-tocopherol succinate treatment the increase in insulin binding is not prevented as α-tocopherol succinate does not decrease the extent of 7-ketocholesterol localising in the rafts.

5.2.2.6. ***The effect of α-tocopherol succinate on insulin binding***

The effect of α-tocopherol succinate on insulin binding, without 7-ketocholesterol, was investigated.

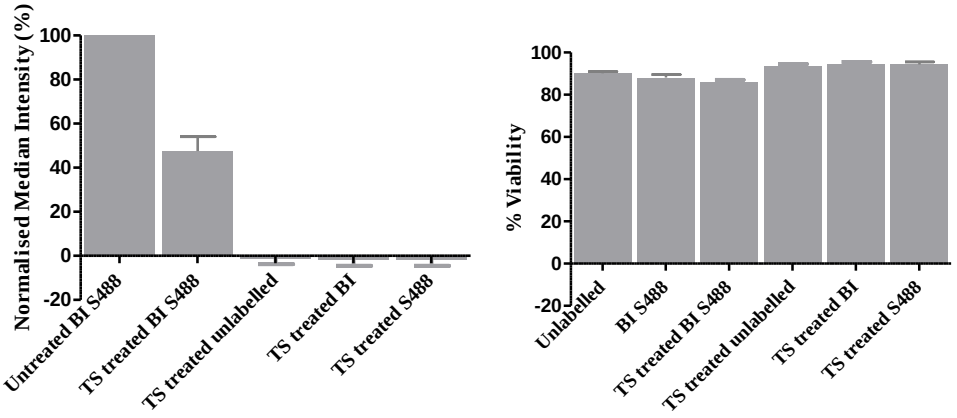

Figure 5.2.19: *(left)* The percentage fluorescence intensity of IM9 B-lymphocytes labelled with biotin-insulin (BI) (0.1μM 90min 15°C) and streptavidin-Alexa fluor 488 (S488) (1mg ml^{-1} streptavidin diluted 1:500 30min 4°C) with or without α-tocopherol succinate (TS) treatment (3.77μM 10min 37°C prior to, and 3.77μM during, subsequent labelling). Propidium iodide (*PI*, 3μM) was added to all samples at least 5mins prior to flow cytometry. Also shown are the percentage fluorescence intensities of TS treated cells that are unlabelled or labelled with BI or S-488 as controls. The same protocol as outlined in the legend of Figure 5.2.11 was employed with the live cell population excluding >92% *PI* positive cells. Data represents the average of 6 repeats (n=3 for controls) with the standard error of the mean represented as error bars.

The presence of α-tocopherol succinate in cell membranes significantly lowered the extent of insulin binding to cell surface receptors (Figure 5.2.19). Interestingly, α-tocopherol succinate and 7-ketocholesterol cause opposite effects on insulin binding despite both molecules eliciting a decrease in the dipole potential. Furthermore, α-tocopherol succinate, which causes the

smaller decrease in dipole potential relative to 7-ketocholesterol, causes the greater change in insulin binding. This suggests that insulin binding may not be influenced by the membrane dipole potential *per se* but the underlying effects responsible for the dipole potential change, such as the degree of lipid packing and order in the various microdomains occurring in the membrane.

Taghibiglou *et al.* (Taghibiglou et al., 2009) found the increase in rafts occurring with cholesterol treatment of cell membranes to result in a decrease in insulin binding. α-Tocopherol is thought to form ordered domains with unsaturated lipids in a parallel manner to the cholesterol-induced formation of ordered domains with saturated lipids (Atkinson et al., 2008, Atkinson et al., 2010). As both α-tocopherol and α-tocopherol succinate were shown to cause closely similar effects on the dipole potential in Chapter 3 (Section 3.3.2) it may be assumed that they have similar effects on the ordering of membrane lipids. α-Tocopherol succinate may, therefore, form ordered domains in which insulin receptors have similar behaviour to those in cholesterol-enriched rafts. The effects of α-tocopherol succinate treatment would be to increase the extent of domains in which the insulin receptors exhibit behaviour resulting in reduced insulin binding in a similar mechanism to the reduction of insulin binding due to cholesterol treatment suggested by Taghibiglou *et al*. (Taghibiglou et al., 2009). Alternatively, the presence of α-tocopherol succinate in non-raft domains may promote the partitioning of insulin receptors into rafts. This would increase the proportion of receptors whose subsequent activity is affected by these cholesterol-enriched domains promoting the further decrease in insulin binding observed. Further investigation on the sensitivity of insulin receptor binding to the microdomain landscape of a membrane, in particular the composition and subsequent physical properties (e.g. dipole potential) of these domains is warranted. This can be achieved by the reconstitution of insulin receptors in model membranes, such as the lipid vesicles of Chapter 3, where the lipidic composition and resulting phase separation into microdomains can be controlled.

5.2.2.7. ***The influence of the membrane dipole potential on insulin resistance in the context of oxidative stress- future work***

Insulin resistance occurs on a cellular level as a result of downregulation and decreased signalling of the insulin receptor causing insulin to become less effective in stimulating the process necessary to lower blood glucose. The results presented in the above section (5.2.2.4) suggest that the decrease in dipole potential associated with cholesterol oxidation in oxidative stress, modelled by the incorporation of 7-ketocholesterol in the membrane, is associated with an increase in insulin binding. Oxidative stress, however, has been reported as a cause of insulin resistance (Ceriello and Motz, 2004) and the increase in insulin binding on 7-ketocholesterol treatment presented here appears to be in contradiction with these observations. Oxidative stress can inhibit several stages of the insulin signalling and glucose transport cascade (Ceriello, 2000)

suggesting that insulin receptor expression is by no means a sole indicator of the effect of 7-ketocholesterol in the membrane on insulin resistance. In fact, increasing the extent of lipid rafts in the membrane by cholesterol treatment downregulates insulin receptors (Taghibiglou et al., 2009) yet the activation of insulin receptors has been reported to be dependent on lipid rafts (Vainio et al., 2002, Vainio et al., 2005, Bickel, 2002, Cohen et al., 2003) and inhibited by cholesterol removal with methyl-β-cyclodextrin treatment (Vainio et al., 2002, Parpal et al., 2001). A suggested mechanism for this reliance on rafts includes the direct interaction of resident rafts proteins such as caveolins (see (Inokuchi, 2010)) and flotillins (see (Bickel, 2002)) with insulin signalling molecules resulting in the spatial and temporal organisation of these molecules for correct insulin signalling (Bickel, 2002). Disruption of rafts may sequester insulin receptors from these molecules inhibiting signalling. It has also been reported that the localisation of insulin bound insulin receptors in detergent resistant domains is prevented by the clustering of the GM2 ganglioside (Vainio et al., 2002) and increased levels of the GM3 ganglioside have also been associated with the elimination of insulin receptors from detergent resistant domains, sequestering the receptor from caveolins and flotillins that remain in the domains (Kabayama et al., 2005, Kabayama et al., 2007).

Conflicting results have been reported on the presence of insulin receptors in detergent resistant membrane fractions (see (Inokuchi, 2010) for discussion) perhaps depending on the concentration and length of Triton X-100 treatment used. This technique has led to the suggestion that insulin receptors associate with both low and high density membrane fractions (raft and non-raft associated, respectively) and that, if insulin receptors are considered not to localise in rafts, intermediate molecules are involved in the caveolin dependent signalling mechanism (Mastick et al., 1995). It is nevertheless evident that insulin signalling is sensitive to the microdomain environments of the membrane and to the accessibility of the insulin receptor to molecules involved in signalling which these microdomains can enable or inhibit.

7-ketocholesterol dramatically alters the membrane dipole potential both as a result of lipid dipole density and hydration changes resulting from the modulation of the microdomain landscape and by influencing the local dipole potential by introducing its own molecular dipole moment (Section 3.1.2, Section 4.1.1) which can itself influence the behaviour of membrane proteins (Section 5.1, (Asawakarn et al., 2001)). It is highly likely that cholesterol oxidation, by its perturbation of the membrane, may dramatically alter insulin signalling and play a role in insulin resistance offering a previously not widely considered mechanism by which oxidative stress may induce insulin resistance. Future work should therefore aim to correlate the effects of 7-ketocholesterol on the membrane dipole potential with insulin signalling. This can be initially approached by investigating the effects of 7-ketocholesterol on insulin receptor activation using a tyrosine phosphorylation assay as outlined by Whiteman and Birnbaum (Whiteman and

Birnbaum, 2003). The detection of the subsequent phosphorylation of the insulin receptor substrates, responsible for assembling signalling complexes, would then indicate the occurrence of insulin signalling.

α-Tocopherol and α-tocopherol succinate have also been demonstrated to modulate the membrane dipole potential (Section 3.3.2) and influence the effect of 7-ketocholesterol through a suggested mechanism involving altering the localisation of 7-ketocholesterol in the membrane (Section 4.3.1). Further understanding of the influence of α-tocopherol on insulin signalling, and its influence on the effect of 7-ketocholesterol on insulin signalling in the context of this mechanism, may indicate alternative non-antioxidation based actions of α-tocopherol in the context of oxidation and insulin resistance. This improved understanding may highlight any potential benefits or negative effects of α-tocopherol treatment in oxidative stress induced insulin resistance and the situations in which this treatment may or may not be recommended.

5.3. Summary

This chapter aimed to investigate whether the modulation of the dipole potential concurrent with the oxidation of cell membrane cholesterol alters the function of receptors in the membrane. Cholesterol rich lipid rafts are shown to be susceptible to the decrease in dipole potential due to 7-ketocholesterol, the oxidation product of cholesterol (section 4.1.1), and as they act as 'functional platforms' supporting the activity of a host of membrane proteins (Simons and Ikonen, 1997, Brown and London, 1998a, Simons and Toomre, 2000) it is likely that this effect may have significant consequences on raft-associated receptors.

To explore this concept the interactions of the antiretroviral agent Saquinavir with its receptor P-glycoprotein (P-gp), previously shown to be sensitive to the dipole potential (Asawakarn et al., 2001) and known to associate with rafts (Demeule et al., 2000, Hinrichs et al., 2004) was investigated. The influence of the modulation of the dipole potential due to cholesterol oxidation on the binding of insulin to the insulin receptor, whose activity is also thought to be reliant upon rafts (Vainio et al., 2002, Vainio et al., 2005, Bickel, 2002, Cohen et al., 2003), was then explored. For clarity the influence of the dipole potential modulation by 7-ketocholesterol and α-tocopherol succinate on these two receptors are discussed under separate headings.

5.3.1. The influence of 7-ketocholesterol, α-tocopherol succinate and the dipole potential on P-glycoprotein

The reliance of the activity of P-gp on rafts (Orlowski et al., 2006, Klappe et al., 2009) was confirmed by demonstrating a significant reduction in the binding of Saquinavir following raft depletion by methyl-β-cyclodextrin treatment. The affinity of Saquinavir for P-gp was significantly lowered and a decrease in the influence of P-gp on the dipole potential on saturation of the receptor with Saquinavir was also observed. This second observation reflects either a decrease in the binding capacity of the membrane for Saquinavir, a decrease in the effect on the dipole potential elicited by P-gp on binding Saquinavir which may be sensitive to the environment of the receptor, or a combination of these effects.

7-ketocholesterol treatment, at a concentration previously shown to cause significant modulation of the dipole potential, also decreased the affinity of Saquinavir for P-gp and the dipole potential modulation elicited by the interaction. Oxidation of membrane cholesterol is therefore likely to significantly influence the activity of P-gp. Comparison with the effects of methyl-β-cyclodextrin suggest that the decrease in dipole potential of lipid rafts is a likely mechanism involved in the influence of 7-ketocholesterol in modifying the behaviour of P-gp. This mechanism was first suggested by Asawakarn *et al.* in explanation of the effect of phloretin and 6-ketocholestanol, agents that affect a decrease and increase in the dipole potential respectively, on the receptor (Asawakarn et al., 2001).

α-Tocopherol succinate has been shown to attenuate the effect of 7-ketocholesterol on the dipole potential (section 4.3.1) which is suggested to occur by the modulation of the localisation and orientation of 7-ketocholesterol in the membrane by α-tocopherol succinate. A hypothesis proposed by Lemaire-Ewing *et al.* (Lemaire-Ewing et al., 2010) suggests that α-tocopherol prevents the localisation of 7-ketocholesterol in rafts and by this mechanism inhibits 7-ketocholesterol induced apoptosis via the raft-associated Akt-Bad pathway. A similar mechanism may occur in which α-tocopherol succinate may ameliorate the effect of 7-ketocholesterol on the affinity of Saquinavir for P-gp. This idea was explored by comparing the influence of 7-ketocholesterol on the Saquinavir-P-gp interaction in α-tocopherol succinate treated cells with that in untreated cells. α-Tocopherol succinate significantly influences the effect of 7-ketocholesterol on the affinity of Saquinavir for P-gp; following α-tocopherol succinate treatment, 7-ketocholesterol does not cause a significant change in the affinity in contrast to its effect in the absence of α-tocopherol succinate.

α-Tocopherol succinate, however, was observed to significantly influence the interaction of Saquinavir with P-gp itself and with greater effect than 7-ketocholesterol. This effect does not correlate with the relative extents to which α-tocopherol succinate and 7-ketocholesterol change the membrane dipole potential; α-tocopherol succinate decreases the dipole potential to a lesser extent than 7-ketocholesterol. However, this does not necessarily correspond to the relative effects of these molecules on the dipole potential of microdomains where P-gp are localised. Future work should therefore aim to correlate the function of P-gp with its localisation in a heterogeneous membrane and how this is affected by the modulation of the microdomain and associated dipole potential landscape of the membrane with these molecules.

This discrepancy between the influence of 7-ketocholesterol and α-tocopherol succinate on the dipole potential and their relative effects on the affinity of Saquinavir for P-gp does highlight the possibility that α-tocopherol succinate may elicit its effect by a mechanism not directly associated with the dipole potential. α-Tocopherol succinate may bind P-gp affecting the interaction of Saquinavir with the receptor. In this case Saquinavir, by binding P-gp, would likewise alter the interaction of subsequently added α-tocopherol succinate with the membrane. This effect was observed and, although it could be attributed to the decrease in the dipole potential elicited by Saquinavir, the ambiguity in the interpretation of the results presented here means the possibility that α-tocopherol succinate binds P-gp cannot be dismissed without further investigation. This could include observing the influence of Saquinavir on the interaction of α-tocopherol succinate with the membrane though its modulation of the surface potential, where the maximum change in fluorescence, B_{max}, would correlate directly with the binding capacity of the membrane for α-tocopherol succinate, resolving the ambiguity. The dipole potential of the membrane influences the interaction of α-tocopherol succinate (Section 4.2) and

should α-tocopherol succinate be found to bind P-gp further investigation would be required to separate the influence of Saquinavir excluding P-gp binding sites from α-tocopherol succinate and the effect of the dipole potential change associated with the binding of Saquinavir with P-gp on α-tocopherol succinate binding.

Regardless of whether the decrease in affinity of Saquinavir for P-gp due to α-tocopherol succinate is due to the direct interaction of α-tocopherol succinate with P-gp or its effects on the microdomains of the membrane and their dipole potential, it is clear that α-tocopherol succinate significantly influences the activity of P-gp. P-gp is an ATP dependent multi-drug efflux pump that acts to lower the intracellular concentration of xenobiotic cytotoxic compounds. It has been demonstrated to remove from cells a host of chemically unrelated drugs including antibiotics, anti-cancer agents, steroids, antihistamines, calcium channel blockers and anti-HIV peptomimetics (such as Saquinavir) (Endicott and Ling, 1989, Gottesman and Pastan, 1993, Dintaman and Silverman, 1999). This activity, in conjunction with the fact that P-gp is localised, for example, in epithelial cells of the intestine and endothelial cells of the blood-brain barrier, has led to the hypothesis of the physiological function of P-gp as a protective barrier and xenobiotic export mechanism (Schinkel et al., 1994, vanAsperen et al., 1997). The activity of P-gp has also been associated with multidrug resistance; for example increased expression of P-gp is observed in cancerous tumour cells (Goldstein, 1996) and the consequent increase in drug resistance is associated with the failure of chemotherapy (Gottesman and Pastan, 1993, Gottesman, 1993, Endicott and Ling, 1989). Interestingly, α-tocopherol succinate has been shown to increase the efficacy of some chemotherapeutic agents (Ripoll et al., 1986, Prasad et al., 1994, Prasad and Kumar, 1996, Prasad et al., 2003)) and this may occur due to the effect of α-tocopherol succinate on P-gp through its modulation of the dipole potential or otherwise.

Tocopheryl polyethylene glycol 1000 succinate (TPGS) has also been shown to inhibit the activity of P-gp. Dintaman and Silverman (Dintaman and Silverman, 1999) demonstrated TPGS to increase the cytotoxicity of several known P-gp ligands in 3T3 cells. They were also able to inhibit the increased resistance to these xenobiotics of MDR1 cDNA transfected 3T3 cells with upregulated P-gp expression by TPGS treatment. TPGS, however, has not been directly demonstrated to bind P-gp and, due to its structural similarities with α-tocopherol succinate, it very likely to insert into the lipid bilayer and perturb the dipole potential of cell membranes. The influence of TPGS on the dipole potential relative to α-tocopherol succinate could be investigated and correlated with their relative effects on Saquinavir binding, and that of the ligands studied by Dintaman and Silverman, to further explore the role of the dipole potential as a regulatory mechanism of P-gp activity.

Interestingly, α-tocopherol succinate is thought to be the most effective form of vitamin E for use as an adjuvant in anti-cancer therapy (Prasad et al., 2003), even more so than α-tocopherol (Weber et al., 2002), and conjugation of the molecule with polyethylene glycol further enhances this effect (Youk et al., 2005).

Further investigation into the mechanism underlying the inhibition of P-gp activity by α-tocopherol succinate and TPGS, and the involvement of the membrane dipole potential, may lead to a better understanding of the beneficial use of these compounds against multi-drug resistance. However, it is also important to further understanding of their potential negative effects against the protective barrier against xenobiotics to which P-gp contributes.

5.3.2. The influence of 7-ketocholesterol, α-tocopherol succinate and the dipole potential on the insulin receptor

The first technique employed to investigate the interaction of insulin with cell membranes relied on the perturbation of the membrane surface potential on interaction of this charged molecule with the membrane detected using fluorescein phosphatidylethanolamine (FPE). Insulin interaction with the membranes of Jurkat T-lymphocytes or IM9 B-lymphocytes, which have greater insulin receptor expression, could not be detected with this technique. The binding of fluorescein isothiocyanate (fitc) labelled insulin to the membrane could be detected by flow cytometry (Murphy et al., 1982). However, high levels of non-specific binding led to the use of biotinylated insulin with greater affinity for the insulin receptor. This was fluorescently tagged with streptavidin-Alexa Fluor 488 which exhibited high specificity for biotin-insulin and minimal non-specific binding with the additional advantage of increased sensitivity as up to four streptavidin molecules may bind per biotin molecule (Ziegler et al., 1994). This method enabled the binding of insulin with receptors on the surface of IM9 B-lymphocytes, but not Jurkat T-lymphocytes, to be determined. This suggests that Jurkat T-lymphocytes must express a relatively low number of insulin receptors below the sensitivity limit of this technique. Even with IM9 B-lymphocytes no modulation of the membrane surface potential by human insulin could be detected suggesting that the nature of the insulin-receptor interaction screens the charge of insulin such that its presence on the membrane is not detected by FPE.

The common soil hypothesis suggests that insulin resistance is a precursor to both diabetes and cardiovascular disease (Stern, 2005) and oxidative stress has been proposed as the underlying mechanism linking insulin resistance with the cellular dysfunction that results in the onset of these diseases (Ceriello and Motz, 2004). Oxidative stress has been observed to be present even prior to the occurrence of insulin resistance and is suggested to influence the activity of the insulin receptor (Ceriello, 2000, Evans et al., 2005). 7-ketocholesterol, the oxidised form of cholesterol, was shown to significantly modulate the membrane dipole potential (Section 3.1.2

& 4.1.1). In the first part of this chapter (section 5.1) it was demonstrated that cholesterol oxidation is likely to have significant consequences on the raft-associated receptor P-gp through modulation of the dipole potential of rafts. The activity of the insulin receptor is also thought to be dependent on rafts and may similarly be affected by the change in the dipole potential associated with cholesterol oxidation.

The binding of insulin to receptors on the surface of IM9 B-lymphocytes was found to be most sensitively detected using biotinylated insulin and streptavidin-Alexa Fluor 488 with flow cytofluorometry. 7-ketocholesterol treatment of the cells, at a concentration and under conditions previously verified to significantly alter the dipole potential, significantly increased the average fluorescence of viable cells indicating an increase in insulin-receptor binding. This could result from an increase in the binding capacity of insulin receptors for insulin or an increase in the affinity of (biotinylated)-insulin for the receptor when the oxidised sterol is present in the membrane. As the activity of the insulin receptor is thought to be raft-dependent (Vainio et al., 2005, Vainio et al., 2002, Bickel, 2002, Cohen et al., 2003) this effect may occur by a similar mechanism proposed for the influence of 7-ketocholesterol on P-gp involving the modulation of the dipole potential of microdomains. Interestingly Taghibiglou *et al.* observed the opposite effect, a decrease in receptor expression, on cholesterol treatment of neuronal cultures (Taghibiglou et al., 2009) which is correlated with increased facilitated receptor endocytosis. The conditions of cholesterol treatment used suggest this is likely to cause a significant increase in the membrane dipole potential (see Section 4.1.1) and further supports the hypothesis that the dipole potential may be a factor associated with the extent of insulin receptor expression on the cell membrane.

The increase in insulin binding following the incorporation of 7-ketocholesterol into the membrane, simulating the decrease in dipole potential associated with cholesterol oxidation, appears to be in contrast with reports indicating oxidative stress as a causative factor in insulin resistance (Ceriello and Motz, 2004, Meigs et al., 2007, Urakawa et al., 2003). Insulin resistance occurs on a cellular level as a result of downregulation and decreased signalling of the insulin receptor and oxidative stress has been shown to inhibit several stages of the insulin signalling and glucose transport cascade (Ceriello, 2000). This suggests that the binding capacity and affinity of the insulin- receptor interaction do not provide a complete indication of the effect of 7-ketocholesterol in the membrane on insulin resistance.

Interestingly, insulin signalling has been reported to be dependent on lipid rafts (Vainio et al., 2005, Vainio et al., 2002, Bickel, 2002, Cohen et al., 2003) and inhibited by membrane cholesterol depletion with methyl-β-cyclodextrin (Vainio et al., 2002, Parpal et al., 2001). A proposed mechanism for this reliance on rafts involves the direct interaction of raft-resident

proteins with signalling molecules promoting the spatial and temporal organisation of these molecules required for insulin signalling (Bickel, 2002, Inokuchi, 2010). However, Balbis *et al.* (Balbis et al., 2004) report that insulin receptors in both detergent resistant and detergent soluble membrane become activated upon insulin stimulation suggesting insulin signalling to occur in both raft and non-raft domains.

The differences among these reports regarding the role of rafts in the activity of the insulin receptor may result from the variation in methods of methyl-β-cyclodextrin raft depletion and detergent raft extraction. The extent to which cholesterol is removed from raft and non-raft domains is sensitive to the concentration and duration of methyl-β-cyclodextrin treatment and varies with cell type (Zidovetzki and Levitan, 2007). The detergent used and the concentration at which it is used for the extraction of detergent resistant membrane fractions produces variable results. It is also worth noting that detergent resistant membranes do not exclusively include lipid rafts; other microdomains such as the highly ordered phases formed by 7-ketocholesterol with saturated lipids are also resistant to detergent solubilisation (Mintzer et al., 2010). It is clear, therefore, that the activity of insulin receptors may not rely on lipid rafts *per se*, but perhaps depend on the physical properties, such as the lipid ordering or the dipole potential, representative of a host of raft and non-raft microdomain structures of the membrane.

7-ketocholesterol dramatically alters the membrane dipole potential as a result of its modulation of the microdomain landscape of the membrane and through the influence of its molecular dipole moment within these microdomains (Sections 3.1.2 and 4.1.1). Cholesterol oxidation is therefore likely to significantly impact insulin signalling. Investigations correlating the dipole potential associated with membrane heterogeneity with insulin signalling are warranted and may include exploring the influence of the dipole potential on: the co-localisation of insulin receptors with other membrane proteins (e.g. caveolins and flotillins) potentially required for signalling, the effect on facilitated receptor endocytosis, and the activity of molecules such as protein tyrosine phophatases capable of disrupting insulin signalling. This will aid in developing a greater understanding of the role of the dipole potential in insulin resistance and may prove to offer a previously not widely considered mechanism by which oxidative stress may induce insulin resistance.

Following the association of oxidative stress with insulin resistance and the development of diabetes and cardiovascular disease (Ceriello and Motz, 2004) α-tocopherol, well known for its anti-oxidant action (Wolf, 2005, Brigelius-Flohe and Traber, 1999), has been widely explored as a potential therapeutic agent, however, has demonstrated little benefit in clinical trials (Golbidi et al., 2011, Pazdro and Burgess, 2010, Saremi and Arora, 2010, Robinson et al., 2006, Brigelius-Flohe et al., 2002). α-Tocopherol has long been considered likely to have non-

antioxidant actions (Diplock, 1983) and several effects of the antioxidant which are not related to its free-radical scavenging capability have been observed (Brigelius-Flohe, 2009, Zingg and Azzi, 2004). Previously in this thesis α-tocopherol succinate was demonstrated to reduce the dramatic effect of 7-ketocholesterol on the membrane dipole potential and in this chapter the question of whether α-tocopherol succinate could therefore ameliorate the effect of 7-ketocholesterol on insulin binding was explored (Section 5.2.2.5).

It was found that treating cells with α-tocopherol succinate prior to exposure to 7-ketocholesterol entirely inhibited the increase in insulin binding associated with 7-ketocholesterol. However, if cells were treated with α-tocopherol succinate following exposure with 7-ketocholesterol insulin binding was not significantly altered from that of 7-ketocholesterol exposed cells untreated with α-tocopherol succinate. This result suggests that the benefit of α-tocopherol treatment may depend on the pre-existing oxidative state of the membrane and may be of little benefit where oxidative stress is already apparent.

It is possible that the presence of α-tocopherol succinate in the membrane prior to 7-ketocholesterol exposure inhibits the localisation of 7-ketocholesterol in specific microdomains and therefore its effect on the dipole potential in the microenvironment of the insulin receptor. When α-tocopherol succinate exposure occurs when 7-ketocholesterol is already present in the membrane it may be unable to influence the localisation of 7-ketocholesterol in these microdomains. This hypothesis is consistent with that originally proposed by Lemaire-Ewing *et al.* (Lemaire-Ewing et al., 2010) describing the prevention of the raft-associated mechanism underlying 7-ketocholesterol induced apoptosis by α-tocopherol.

α-Tocopherol succinate itself was demonstrated to increase insulin binding (Section 5.2.2.6) opposite to the action of 7-ketocholesterol, although, interestingly, both act to decrease the dipole potential. This could be attributed to the influence of α-tocopherol succinate on microdomains. α-Tocopherol forms ordered domains with unsaturated lipids in a parallel manner to cholesterol with saturated lipids (Atkinson et al., 2010, Atkinson et al., 2008). It may be assumed that α-tocopherol succinate adopts a similar behaviour among unsaturated lipids in cell membranes. Taghibiglou *et al.* (Taghibiglou et al., 2009) report an increase in insulin receptor expression concurrent with an increase in the proportion of rafts following cholesterol treatment. It is possible that α-tocopherol succinate similarly increases the proportion of ordered domains in which insulin receptors localise. This is consistent with the idea presented previously in this discussion that microdomains other than lipid rafts may influence insulin receptors due to their specific physical properties such as the dipole potential.

Further experiments should explore the effect of tocopherols on the microdomain landscape of the membrane, and associated dipole potential microheterogeneity, on insulin receptor binding and insulin signalling. The reconstitution of insulin receptors within lipid vesicles may provide a model to study insulin binding to the receptor in various microdomain environments of different dipole potential which can be controlled through lipidic composition. It would also be interesting to visualise the localisation of the receptor in heterogeneous membranes, correlating this with insulin binding, by imaging artificial bilayers and cell membranes with fluorescently labelled insulin and receptors. This will enable the real-time effects of 7-ketocholesterol and tocopherols on the insulin receptor to be observed. For insulin signalling studies, similar investigations to those suggested above to probe the effects of 7-ketocholesterol are recommended and can be extended to explore the effects of α-tocopherol in the context of membrane oxidation.

6. Conclusions and Future work

6.1. Conclusions

Oxidative stress results in the structural alteration of susceptible cell membrane components (Halliwell and Gutteridge, 1999), altering their collective behaviour and eliciting significant changes in the physical properties of the membrane ((Megli and Sabatini, 2003, Megli et al., 2005, Ayuyan and Cohen, 2006) that are known to regulate many membrane functions (Los and Murata, 2000, Lucero and Robbins, 2004, Barenholz, 2002). Preventative measures have included treatment with the membrane-bound anti-oxidant, α-tocopherol, which is thought to co-localise in membranes with unsaturated lipids, a species highly susceptible to oxidation (Quinn, 2004, Atkinson et al., 2010). Despite its well documented free radical scavenging ability (Wolf, 2005), α-tocopherol has demonstrated negligible benefit, and occasionally even negative effects, in the prevention or treatment of oxidative stress associated disease in clinical trials (Golbidi et al., 2011, Clarke et al., 2008, Saremi and Arora, 2010, Pazdro and Burgess, 2010). The reasons underlying this outcome are currently not well understood however, α-tocopherol is known to perturb the collective behaviour of membrane lipids potentially resulting in significant non-antioxidant actions of the vitamin in cell membranes (Wang and Quinn, 2000a, Wang and Quinn, 2006, Azzi et al., 2002, Azzi and Stocker, 2000). This thesis investigated the influence of α-tocopherol on the membrane dipole potential, a physical property reflecting the collective ordering and organisation of membrane lipids, in the context of oxidative stress.

To begin with, the effect of α-tocopherol on the dipole potential was studied using phosphatidylcholine vesicles which provide a simple membrane model where the collective behaviour of lipids are well characterised. α-Tocopherol was demonstrated to decrease the dipole potential of egg-phosphatidylcholine vesicles. Interestingly, the same effect was observed with 7-ketocholesterol, an oxidised form of cholesterol, although the decrease occurred to a significantly greater extent for the oxidised sterol. The presence of α-tocopherol in the vesicles influenced the effect of both cholesterol and 7-ketocholesterol on the dipole potential. As α-tocopherol and both sterols are reported to independently alter the phase behaviour of lipids in different ways, it is thought their combined effect results in another, different, phase behaviour altering the microdomain landscape, and dipole potential, of the membrane compared with the presence of either component alone. The influence of α-tocopherol in combination with each sterol was different which is consistent with the differing phase behaviours of cholesterol and 7-ketocholesterol and their partitioning between, and orientation within, the liquid ordered and liquid disordered phases (Massey and Pownall, 2006). The converse effect, that cholesterol and 7-ketocholesterol differently influence the effect of α-tocopherol on the dipole potential, was also observed. It is hypothesized that the initial dipole

potential of a membrane, perhaps reflecting the microdomain landscape, influences the effect of species which modulate the dipole potential.

It is proposed that the modulation of the dipole potential by α-tocopherol is a non-antioxidant action of this molecule within biological membranes. This effect was confirmed to be independent of its anti-oxidant action by demonstrating that α-tocopherol succinate, a structural analogue with no free radical scavenging capability, influences the dipole potential in a closely similar manner when similarly incorporated into egg-phosphatidylcholine vesicles.

The additional succinate moiety of this structural analogue, not present on α-tocopherol, renders the molecule significantly more soluble allowing its interaction with vesicles to be studied. The modulation of both the surface potential and dipole potential on interaction of α-tocopherol succinate provide evidence to suggest that this molecule localised in the liquid ordered domains of cholesterol-enriched egg-phosphatidylcholine membranes and may bind to these regions with a greater affinity than the liquid disordered phase. Interestingly, the gradual replacement of cholesterol with 7-ketocholesterol appeared to reduce the association of α-tocopherol succinate with the saturated lipid-rich ordered phases formed by both sterols.

The influence of α-tocopherol succinate on the dipole potential was then investigated in cell membranes which, due to their greater variety in lipid composition, are expected to exhibit a significantly more complex phase behaviour and microdomain landscape. α-Tocopherol succinate, cholesterol and 7-ketocholesterol were observed to cause similar relative changes in the dipole potential of Jurkat T-lymphocyte membranes as seen with egg-phosphatidylcholine vesicles. Interestingly, pre-treating cells with α-tocopherol succinate dramatically reduced the efficacy of 7-ketocholesterol in decreasing the dipole potential. This is thought to result from the altered dipole potential, and microdomain landscape, of the membrane elicited by α-tocopherol succinate treatment. The sensitivity of the effect of α-tocopherol succinate, as well as that of 7-ketocholesterol, on the microdomain landscape of the membrane suggests that α-tocopherol succinate may behave differently in membranes where significant oxidation has occurred therefore altering its ability to influence the effect of further oxidation on the dipole potential. This idea was supported with the observation that α-tocopherol succinate had no significant influence on the effect of 7-ketocholesterol on the dipole potential in cells exposed to the oxidised sterol prior to treatment.

The involvement of microdomains in the influence of 7-ketocholesterol on the dipole potential and the ability of α-tocopherol succinate to modulate this effect was further investigated by employing methyl-β-cyclodextrin to alter the microdomain landscape by depleting raft-associated cholesterol. In raft depleted cells the influence of α-tocopherol succinate on the effect

of 7-ketocholesterol on the dipole potential was reduced. However, the oxidised sterol still significantly modulated the dipole potential suggesting that rafts may not be the only species of microdomain involved in the ability of α-tocopherol succinate to negate the effects of 7-ketocholesterol on the dipole potential.

It is hypothesized that α-tocopherol succinate may protect against the deleterious effects of cholesterol oxidation in cell membranes by excluding 7-ketocholesterol from specific microdomains, acting to preserve the dipole potential of the microdomain maintaining the function of the proteins it supports. However, where significant cholesterol oxidation has previously occurred the concurrent changes in the microdomain landscape of the membrane prevent α-tocopherol succinate from eliciting this protective effect.

Interestingly both 7-ketocholesterol and α-tocopherol succinate exhibited a greater efficiency in decreasing the dipole potential in the presence of rafts suggesting these molecules may partition into these microdomains. The decreased effect of 7-ketocholesterol following α-tocopherol succinate treatment may arise from the exclusion of the sterol from rafts. Membrane rafts are therefore a likely example of a type of microdomain involved in the proposed mechanism.

Membrane rafts are thought to act as functional platforms promoting the activity of many membrane proteins (Brown and London, 1998a, Simons and Ikonen, 1997) which has been proposed to arise, at least in part, from their elevated dipole potential with respect to the surrounding membrane (Asawakarn et al., 2001). The final chapter therefore investigated the influence of α-tocopherol succinate, in the context of membrane oxidation, on the function of two receptors that are reported to be raft associated; P-glycoprotein and the insulin receptor.

The first receptor studied was the multi-drug efflux pump, P-glycoprotein (P-gp), through the interactions of Saquinavir with this receptor which has previously been reported by our group to be sensitive to the dipole potential of the cell membrane (Asawakarn et al., 2001). Exposing Jurkat T-lymphocytes to 7-ketocholesterol significantly decreased the affinity of Saquinavir for P-gp suggesting cholesterol oxidation significantly influences this raft-associated receptor. α-tocopherol succinate also significantly modulated the interaction of Saquinavir with P-gp and, surprisingly, with much greater influence than 7-ketocholesterol which is inconsistent with their respective effects on the dipole potential. An explanation for this effect is that P-gp may associate with microdomains other than rafts in which α-tocopherol succinate has a considerable influence. However, it is also possible that this effect may occur through a mechanism not directly associated with the dipole potential, for example α-tocopherol succinate may bind P-gp. The mechanism by which α-tocopherol succinate causes this dramatic effect on P-gp warrants further investigation as it may have significant implications on the efficacy of therapeutic agents

or the cytotoxicity of xenobiotic compounds. For example, α-tocopherol succinate has been shown to increase the efficacy of some chemotherapeutic agents and its modulation of the membrane dipole potential may prove to be involved in the underlying mechanism of this action (Ripoll et al., 1986, Prasad et al., 1994, Prasad et al., 2003).

Oxidative stress has been associated with the onset of insulin resistance (Ceriello and Motz, 2004) and so the possible involvement of the change in the dipole potential associated with cholesterol oxidation was investigated through its effect on the binding of insulin. Treating IM-9 B-lymphocytes with 7-ketocholesterol significantly increased insulin binding which is in apparent contradiction with reports that oxidative stress promotes insulin resistance. This suggests that insulin binding may not be the principal indicator of any dipole potential-related effects of 7-ketocholesterol in insulin resistance. Investigation into the influence of the dipole potential on the signalling activity of the insulin receptor, which has been linked to rafts (Vainio et al., 2005, Vainio et al., 2002, Bickel, 2002, Cohen et al., 2003), is suggested.

Interestingly, α-tocopherol succinate treatment entirely inhibited the increase in insulin binding resulting from 7-ketocholesterol exposure however, it was ineffective when α-tocopherol succinate treatment followed prior 7-ketocholesterol exposure. This is consistent with our hypothesis suggesting that α-tocopherol succinate may preserve normal levels of insulin binding by protecting the microdomains inhabited by the insulin receptor from the effects of 7-ketocholesterol on the dipole potential.

6.2. Future work

A main theme of this thesis is that the dipole potential of microdomains may modulate the influence of these structures on the function of proteins that associate with them. 7-ketocholesterol and α-tocopherol, both known to alter membrane phase behaviour and demonstrated in this work to significantly modulate the membrane dipole potential, may cause some of their cellular effects by modulating the dipole potential heterogeneity of the cell membrane. The focus of future studies should be to attempt to correlate the dipole potential heterogeneity with the microdomain landscape of a membrane and investigate the sensitivity of membrane protein activity to changes in the dipole potential of their immediate environment. This section suggests some of the experimental approaches, with both artificial membrane systems and cells, which can be followed.

6.2.1. Artificial membrane studies

In Chapter 3 evidence was presented that the dipole potential probe, Di-8-ANEPPS, detects changes in the phase profile of large unilamellar vesicles of changing composition. The excitation spectra of the probe were found to be composed of two components of different peak wavelength which were taken to reflect the presence in mixed composition vesicles of two environments of different dipole potential. It remains to confirm this hypothesis and establish whether changes in peak positions or areas provide additional information about heterogeneities in membrane dipole potential. These possibilities may be further explored using both two photon fluorescence excitation and coherent anti-stokes Raman (CARS) imaging. The use of two photon excitation greatly improves the spatial resolution of the measurements (Denk et al., 1990) and CARS imaging of giant unilamellar vesicles (e.g. (Li and Cheng, 2006)) will enable direct (label-free) visualisation of the extent of each phase and the correlation of the dipole potential reported by Di-8-ANEPPS with each phase. It may also be possible to determine the excitation spectrum of the probe in each of the identified phases which can be correlated initially in vesicles of a composition with a well defined phase behaviour (for example the DOPC:DPPC:Cholesterol system whose phase behaviour is discussed in Section 1.1.3). These investigations can then be extended to the more complex egg-phosphatidylcholine with cholesterol/7-ketocholesterol/α-tocopherol systems studied in this thesis. Furthermore, it may be possible to reconstitute membrane receptors (such as P-glycoprotein and the insulin receptor) into vesicles and investigate the effects of the phases present and their dipole potential on the spatial distribution of the receptor in the membrane and its ability to bind ligands. Whether the dipole potential itself regulates protein function (as speculated in this thesis) or whether it merely reflects the phase of a microdomain that influences proteins by other means is a significant question that could be answered by this approach.

6.2.2. Cell membrane studies

Once the relationship between microdomains and the dipole potential has been investigated in artificial membranes these experiments can be translated to the cell membrane which possesses a more complex microdomain environment. Endothelial cells, being large adherent cells, are very suited for imaging of the heterogeneity of the dipole potential and the possible correlation with heterogeneity in the spatial distribution of lipid types, such as those associated with rafts, identified using CARS microscopy. This information could then be correlated with the spatial localisation and activity of membrane receptors, such as P-glycoprotein and the insulin receptor. The effects of 7-ketocholesterol and α-tocopherol succinate on both the receptors and the heterogeneity of the dipole potential can then be investigated.

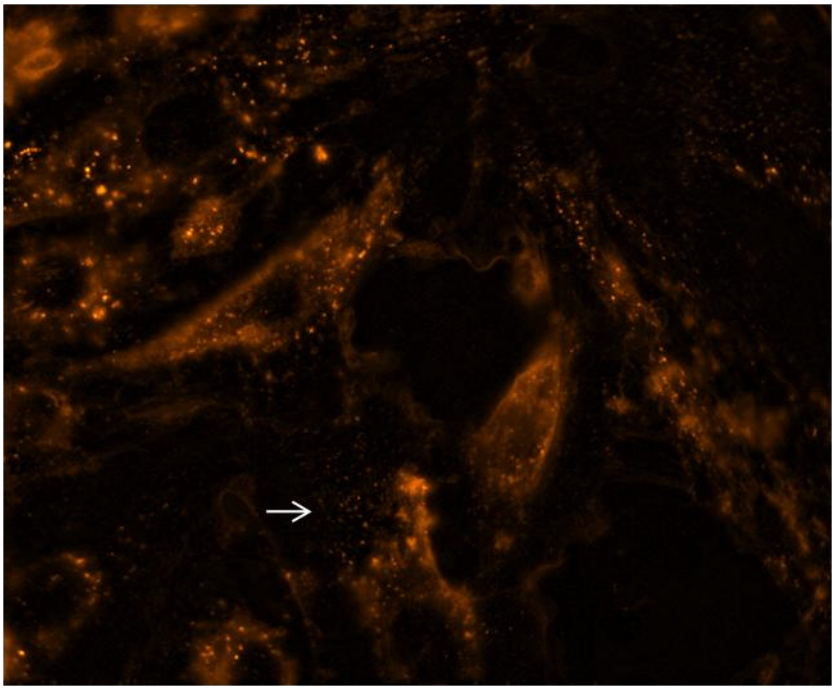

Figure 6.2.1: Preliminary imaging of human umbilical vein endothelial cells (HUVEC) labelled with Di-8-ANEPPS (2μM 90min 37°C) with a standard fluorescence microscope identifies visible 'hot-spots' of increased fluorescence intensity (e.g. those indicated by the arrow) which correspond to domains of increased dipole potential relative to the bulk membrane. Future imaging using two-photon excitation will increase spatial resolution and CARS imaging may allow identification of the lipid composition of visualised 'hot-spots'.

Although microdomains, such as rafts, are likely to be beyond the spatial resolution of CARS microscopy, it is possible to investigate the influence on receptors of the effects of 7-ketocholesterol and α-tocopherol succinate on the microdomain landscape of the cell membrane indirectly. For example, single particle tracking of fluorescently tagged receptors allows information on the microdomain environment of the receptor to be obtained by observing changes in the rate of diffusion of the receptor following 7-ketocholesterol or α-tocopherol succinate treatment of the cell (Sheets et al., 1997, Simson et al., 1998).

Cell membranes are highly dynamic and it is quite likely that the dipole potential fluctuates, temporally as well as spatially, in the healthy cell membrane. Also, it has been recently observed that changes in curvature stress of the membranes of erythrocytes alter the dipole potential in the region of the deformation (Jewell and Winlove, 2011). Considering the significant deformation experienced by erythrocytes in passing through the microcirculation this appears to suggest that healthy cells may, as a matter of course, experience significant modulation in the membrane dipole potential in vivo as well as small scale fluctuations. Endothelial cells, which line the luminal surface of blood cells, provide another example of cells that are exposed to significant physical forces in vivo (Resnick et al., 2003). The mechanical shear stress imposed by blood flow on endothelial cells has been reported to alter membrane fluidity (Haidekker et al., 2000) and cause deformation of cytoskeletal elements (Osborn et al., 2006, Choi and Helmke, 2008), both of which influence the microdomain landscape of the membrane, and it is therefore also likely to influence the dipole potential of cell membranes in vivo. In addition to the improvements in spatial resolution of the fluorescence methods alluded to above, there is also a need to increase the temporal resolution and technology now exists to achieve this.

Elements of the extracellular matrix, as well as of the cytoskeleton, are reported to stabilise membrane microdomains (Langhorst et al., 2007, Garner and Baum, 2008). The glycocalyx of endothelial cells can be considered a type of extracellular matrix and, as the barrier between flowing blood and the endothelial cell membrane, is affected by changes in the composition and flow of blood associated with cardiovascular disease (Gouverneur et al., 2006b, Gouverneur et al., 2006a) and hyperglycaemia (Nieuwdorp et al., 2006, Zuurbier et al., 2005). It would be interesting to investigate the consequences of pathological changes in the glycocalyx on the dipole potential, however initially the fundamental relationship between the physical state of the glycocalyx and the dipole potential of the underlying bilayer needs to be investigated.

In conclusion, this thesis has demonstrated that α-tocopherol, and its non-antioxidant counterpart α-tocopherol succinate, significantly modulate the membrane dipole potential. This is thought to occur as a result of their effects on the microdomain landscape of the membrane. α-tocopherol and α-tocopherol succinate decrease the effect of the oxidised cholesterol, 7-ketocholesterol, on the membrane dipole potential and are thought to do this by altering the localisation of 7-ketocholesterol in the membrane. We hypothesize that α-tocopherols may prevent the deleterious effects of cholesterol oxidation on membrane proteins by excluding 7-ketocholesterol from the microdomains in which these proteins reside thus preserving the dipole potential of their environment and their functions. The microdomain landscape promoted by α-tocopherols may also enhance the activity of therapeutic compounds by influencing the multi-drug efflux pump P-glycoprotein; however, this may also significantly influence the

cytotoxicity of xenobiotic compounds. Further investigation into the heterogeneity of the changes in dipole potential elicited by α-tocopherols in the membrane, particularly in the context of membrane oxidation, are required which can then be correlated with the activity of proteins such as the insulin receptor and P-glycoprotein. We suggest that the significant effect of α-tocopherols on the membrane dipole potential should be considered when assessing the possible benefits and potentially significant negative effects of α-tocopherol treatment.

7. Bibliography

ALAKOSKELA, J. M. I. & KINNUNEN, P. K. J. 2001. Control of a redox reaction on lipid bilayer surfaces by membrane dipole potential. *Biophysical Journal,* 80**,** 294-304.

ALAKOSKELA, J. M. I., SODERLUND, T., HOLOPAINEN, J. M. & KINNUNEN, P. K. J. 2004. Dipole potential and head-group spacing are determinants for the membrane partitioning of pregnanolone. *Molecular Pharmacology,* 66**,** 161-168.

ALBERTS, B., BRAY, D., JOHNSON, A., LEWIS, J., RAFF, M., ROBERTS, K., WATSON, J.D. 1994. *Molecular Biology of the Cell, 3rd Edition, Garlands,* New York, Garland Science.

ALMEIDA, P. F. F., VAZ, W. L. C. & THOMPSON, T. E. 1992. Lateral diffusion and percolation in 2-phase, 2-component lipid bilayers- topology of the solid-phase domains inplane and across the lipid bilayer. *Biochemistry,* 31**,** 7198-7210.

ARANDA, F. J., COUTINHO, A., BERBERANSANTOS, M. N., PRIETO, M. J. E. & GOMEZ-FERNANDEZ, J. C. 1989. Fluorescence study of the location and dynamics of alpha-tocopherol in phospholipid-vesicles. *Biochimica Et Biophysica Acta,* 985**,** 26-32.

ASAWAKARN, T., CLADERA, J. & O'SHEA, P. 2001. Effects of the membrane dipole potential on the interaction of saquinavir with phospholipid membranes and plasma membrane receptors of Caco-2 cells. *Journal of Biological Chemistry,* 276**,** 38457-38463.

ATKINSON, J., EPAND, R. F. & EPAND, R. M. 2008. Tocopherols and tocotrienols in membranes: A critical review. *Free Radical Biology and Medicine,* 44**,** 739-764.

ATKINSON, J., HARROUN, T., WASSALL, S. R., STILLWELL, W. & KATSARAS, J. 2010. The location and behavior of alpha-tocopherol in membranes. *Molecular Nutrition & Food Research,* 54**,** 641-651.

AUSSENAC, F., TAVARES, M. & DUFOURC, E. J. 2003. Cholesterol dynamics in membranes of raft composition: A molecular point of view from H-2 and P-31 solid-state NMR. *Biochemistry,* 42**,** 1383-1390.

AVANTI. Avanti Polar Lipids, Inc. Available: www.avantilipids.com [Accessed 19-03-2011 2011].

AYUYAN, A. G. & COHEN, F. S. 2006. Lipid peroxides promote large rafts: Effects of excitation of probes in fluorescence microscopy and electrochemical reactions during vesicle formation. *Biophysical Journal,* 91**,** 2172-2183.

AZZI, A. 2007. Molecular mechanism of alpha-tocopherol action. *Free Radical Biology and Medicine,* 43**,** 16-21.

AZZI, A., GYSIN, R., KEMPNA, R., MUNTEANU, A., VILLACORTA, L., VISARIUS, T. & ZINGG, J. M. 2004. Regulation of gene expression by alpha-tocopherol. *Biological Chemistry,* 385**,** 585-591.

AZZI, A., RICCIARELLI, R. & ZINGG, J. M. 2002. Non-antioxidant molecular functions of alpha-tocopherol (vitamin E). *Febs Letters,* 519**,** 8-10.

AZZI, A. & STOCKER, A. 2000. Vitamin E: non-antioxidant roles. *Progress in Lipid Research,* 39**,** 231-255.

BACKER, J. M. & DAWIDOWICZ, E. A. 1981. Transmembrane movement of cholesterol in small unilamellar vesicles detected by cholesterol oxidase. *Journal of Biological Chemistry,* 256**,** 586-588.

BALBIS, A., BAQUIRAN, G., MOUNIER, C. & POSNER, B. I. 2004. Effect of insulin on caveolin-enriched membrane domains in rat liver. *Journal of Biological Chemistry,* 279**,** 39348-39357.

BARENHOLZ, Y. 2002. Cholesterol and other membrane active sterols: from membrane evolution to "rafts". *Progress in Lipid Research,* 41**,** 1-5.

BARTON, P. G. & GUNSTONE, F. D. 1975. Hydrocarbon chain packing and molecular-motion in phospholipid bilayers formed from unsaturated lecithins- synthesis and properties of 16 positional isomers of 1,2-dioctadecenoyl-sn-glycero-3-phosphorylcholine. *Journal of Biological Chemistry,* 250**,** 4470-4476.

BECHINGER, B. & SEELIG, J. 1991. Interaction of electric dipoles with phospholipid head groups- A H-2 and P-31 NMR-study of phloretin and phloretin analogs in phosphatidylcholine membranes. *Biochemistry,* 30**,** 3923-3929.

BECKER, W. M., KLEINSMITH, L.J., HARDIN, J. 2003. *The world of the cell*, Benjamin-Cummings.

BERG, J., TYMOCZKO, J. & STRYER, L. 2002. *Biochemistry,* W H Freeman and Company.

BERTHIER, A., LEMAIRE-EWING, S., PRUNET, C., MONIER, S., ATHIAS, A., BESSEDE, G., DE BARROS, J. P. P., LAUBRIET, A., GAMBERT, P., LIZARD, G. & NEEL, D. 2004. Involvement of a calcium-dependent dephosphorylation of BAD associated with the localization of Trpc-1 within lipid rafts in 7-ketocholesterol-induced THP-1 cell apoptosis. *Cell Death and Differentiation,* 11**,** 897-905.

BERTHIER, A., LEMAIRE-EWING, S., PRUNET, C., MONTANGE, T., VEJUX, A., DE BARROS, J. P. P., MONIER, S., GAMBERT, P., LIZARD, G. & NEEL, D. 2005. 7-Ketocholesterol-induced apoptosis - Involvement of several pro-apoptotic but also anti-apoptotic calcium-dependent transduction pathways. *Febs Journal,* 272**,** 3093-3104.

BICKEL, P. E. 2002. Lipid rafts and insulin signaling. *American Journal of Physiology-Endocrinology and Metabolism,* 282**,** E1-E10.

BITTMAN, R., KASIREDDY, C. R., MATTJUS, P. & SLOTTE, J. P. 1994. Interaction of cholesterol with sphingomyelin in monolayers and vesicles. *Biochemistry,* 33**,** 11776-11781.

BJORKHEM, I. & DICZFALUSY, U. 2002. Oxysterols - Friends, foes, or just fellow passengers? *Arteriosclerosis Thrombosis and Vascular Biology,* 22**,** 734-742.

BLANCHETTE, C. D., LIN, W. C., ORME, C. A., RATTO, T. V. & LONGO, M. L. 2008. Domain nucleation rates and interfacial line tensions in supported bilayers of ternary mixtures containing galactosylceramide. *Biophysical Journal,* 94**,** 2691-2697.

BOESZE-BATTAGLIA, K. 2005. Membrane rafts. *In:* YEAGLE, P. L. (ed.) *The structure of biological membranes.* Second edition ed. Boca Raton: CRC Press.

BOHN, B. 1980. Flow-cytometry- A novel-approach for the quantitative-analysis of receptor-ligand interactions on surfaces of living cells. *Molecular and Cellular Endocrinology,* 20**,** 1-15.

BRADFORD, A., ATKINSON, J., FULLER, N. & RAND, R. P. 2003. The effect of vitamin E on the structure of membrane lipid assemblies. *Journal of Lipid Research,* 44**,** 1940-1945.

BRIGELIUS-FLOHE, R. 2009. Vitamin E: The shrew waiting to be tamed. *Free Radical Biology and Medicine,* 46**,** 543-554.

BRIGELIUS-FLOHE, R., KELLY, F. J., SALONEN, J. T., NEUZIL, J., ZINGG, J. M. & AZZI, A. 2002. The European perspective on vitamin E: current knowledge and future research. *American Journal of Clinical Nutrition,* 76**,** 703-716.

BRIGELIUS-FLOHE, R. & TRABER, M. G. 1999. Vitamin E: function and metabolism. *Faseb Journal,* 13**,** 1145-1155.

BRINK-VAN DER LAAN, E. V., KILLIAN, J. A. & DE KRUIJFF, B. 2004. Nonbilayer lipids affect peripheral and integral membrane proteins via changes in the lateral pressure profile. *Biochimica Et Biophysica Acta-Biomembranes,* 1666**,** 275-288.

BROCKMAN, H. 1994. Dipole potential of lipid membranes. *Chemistry and Physics of Lipids,* 73**,** 57-79.

BROWN, A. J. & JESSUP, W. 1999. Oxysterols and atherosclerosis. *Atherosclerosis,* 142**,** 1-28.

BROWN, D. A. & LONDON, E. 1998a. Functions of lipid rafts in biological membranes. *Annual Review of Cell and Developmental Biology,* 14**,** 111-136.

BROWN, D. A. & LONDON, E. 1998b. Structure and origin of ordered lipid domains in biological membranes. *Journal of Membrane Biology,* 164**,** 103-114.

BROWN, D. A. & LONDON, E. 2000. Structure and function of sphingolipid- and cholesterol-rich membrane rafts. *Journal of Biological Chemistry,* 275**,** 17221-17224.

BROWN, D. A. & ROSE, J. K. 1992. Sorting of GPI-anchored proteins to glycolipid-enriched membrane subdomains during transport to the apical cell-surface. *Cell,* 68**,** 533-544.

BRUNETTI, A., MANFIOLETTI, G., CHIEFARI, E., GOLDFINE, I. D. & FOTI, D. 2001. Transcriptional regulation of human insulin receptor gene by the high-mobility group protein HMGI(Y). *Faseb Journal,* 15**,** 492-500.

BULLEN, A. & SAGGAU, P. 1999. Fast quantitative measurements with voltage-sensitive dyes and high-speed, random-access fluorescence microscopy. *Biophysical Journal,* 76**,** A97-A97.

BUZON, V. & CLADERA, J. 2006. Effect of cholesterol on the interaction of the HIV GP41 fusion peptide with model membranes. Importance of the membrane dipole potential. *Biochemistry,* 45**,** 15768-15775.

BUZON, V., CLADERA, J., 2006. Effect of cholesterol on the interaction of the HIV GP41 fusion peptide with model membranes. Importance of the membrane dipole potential. *Biochemistry,* 45**,** 15768-15775.

CATALA, A. 2010. A synopsis of the process of lipid peroxidation since the discovery of the essential fatty acids. *Biochemical and Biophysical Research Communications,* 399**,** 318-323.

CATTELOTTE, J., TOURNIER, N., RIZZO-PADOIN, N., SCHINKEL, A. H., SCHERRMANN, J. M. & CISTERNINO, S. 2009. Changes in dipole membrane potential at the mouse blood-brain barrier enhance the transport of (99m)Technetium Sestamibi more than inhibiting Abcb1, Abcc1, or Abcg2. *Journal of Neurochemistry,* 108**,** 767-775.

CELIK, T., YUKSEL, C. & IYISOY, A. 2010. Alpha tocopherol use in the management of diabetic cardiomyopathy: lessons learned from randomized clinical trials. *Journal of Diabetes and Its Complications,* 24**,** 286-288.

CERIELLO, A. 2000. Oxidative stress and glycemic regulation. *Metabolism-Clinical and Experimental,* 49**,** 27-29.

CERIELLO, A. & MOTZ, E. 2004. Is oxidative stress the pathogenic mechanism underlying insulin resistance, diabetes, and cardiovascular disease? The common soil hypothesis revisited. *Arteriosclerosis, thrombosis, and vascular biology* 24**,** 816-823.

CEVC, G. 1990. Membrane electrostatics. *Biochimica Et Biophysica Acta,* 1031**,** 311-382.

CEVC, G., WATTS, A. & MARSH, D. 1981. Titration of the phase-transition of phosphatidylserine bilayer- membranes - effects of pH, surface electrostatics, ion binding, and headgroup hydration. *Biochemistry,* 20**,** 4955-4965.

CHAIET, L. & WOLF, F. J. 1964. Properties of streptavidin biotin-binding protein producd by streptomycete. *Archives of Biochemistry and Biophysics,* 106**,** 1-&.

CHANDLER, D. 2005. Interfaces and the driving force of hydrophobic assembly. *Nature,* 437**,** 640-647.

CHAPMAN, D. 1975a. Fluidity and phase transitions of cell membranes. *Biomembranes,* 7**,** 1-9.

CHAPMAN, D. 1975b. Phase-transitions and fluidity characteristics of lipids and cell-membranes. *Quarterly Reviews of Biophysics,* 8**,** 185-235.

CHEN, S. C., STURTEVANT, J. M. & GAFFNEY, B. J. 1980. Scanning calorimetric evidence for a 3rd phase-transition in phosphatidylcholine bilayers. *Proceedings of the National Academy of Sciences of the United States of America-Biological Sciences,* 77**,** 5060-5063.

CHEN, Z. & RAND, R. P. 1997. The influence of cholesterol on phospholipid membrane curvature and bending elasticity. *Biophysical Journal,* 73**,** 267-276.

CHERNOMORDIK, L. V. & ZIMMERBERG, J. 1995. Bending membranes to the task-structural intermediates in bilayer fusion. *Current Opinion in Structural Biology,* 5**,** 541-547.

CHIU, S. W., JAKOBSSON, E., MASHL, R. J. & SCOTT, H. L. 2002. Cholesterol-induced modifications in lipid bilayers: A simulation study. *Biophysical Journal,* 83**,** 1842-1853.

CHOI, C. K. & HELMKE, B. P. 2008. Short-term shear stress induces rapid actin dynamics in living endothelial cells. *Molecular and Cellular Biomechanics,* 5**,** 247-258.

CLADERA, J., MARTIN, I. & O'SHEA, P. 2001. The fusion domain of HIV gp41 interacts specifically with heparan sulfate on the T-lymphocyte cell surface. *Embo Journal,* 20**,** 19-26.

CLADERA, J., MARTIN, I., RUYSSCHAERT, J. M. & O'SHEA, P. 1999. Characterization of the sequence of interactions of the fusion domain of the simian immunodeficiency virus with membranes - Role of the membrane dipole potential. *Journal of Biological Chemistry,* 274**,** 29951-29959.

CLADERA, J. & O'SHEA, P. 1998. Intramembrane molecular dipoles affect the membrane insertion and folding of a model amphiphilic peptide. *Biophysical Journal,* 74**,** 2434-2442.

CLARKE, M. W., BURNETT, J. R. & CROFT, K. D. 2008. Vitamin E in human health and disease. *Critical Reviews in Clinical Laboratory Sciences,* 45**,** 417-450.

CLARKE, R. J. 1997. Effect of lipid structure on the dipole potential of phosphatidylcholine bilayers. *Biochimica Et Biophysica Acta-Biomembranes,* 1327**,** 269-278.

CLARKE, R. J. 2001. The dipole potential of phospholipid membranes and methods for its detection. *Advances in Colloid and Interface Science,* 89**,** 263-281.

CLARKE, R. J. & KANE, D. J. 1997. Optical detection of membrane dipole potential: Avoidance of fluidity and dye-induced effects. *Biochimica Et Biophysica Acta-Biomembranes,* 1323**,** 223-239.

COHEN, A. W., COMBS, T. P., SCHERER, P. E. & LISANTI, M. P. 2003. Role of caveolin and caveolae in insulin signaling and diabetes. *American Journal of Physiology-Endocrinology and Metabolism,* 285**,** E1151-E1160.

COOPER, R. A. 1978. Influence of increased membrane cholesterol on membrane fluidity and cell-function in human red blood-cells. *Journal of Supramolecular Structure,* 8**,** 413-430.

CULLIS, P. R. & DE KRUIJFF, B. 1978. Polymorphic phase behaviour of phosphatidylethanolamines of natural and synthetic origin- P-31 NMR-study. *Biochimica Et Biophysica Acta,* 513**,** 31-42.

CULLIS, P. R. & DE KRUIJFF, B. 1979. Lipid polymorphism and the functional roles of lipids in biological-membranes. *Biochimica Et Biophysica Acta,* 559**,** 399-420.

DANIELLI, J. F. & DAVSON, H. 1935. A contribution to the theory of permeability of thin films. *Journal of cellular and comparative physiology,* 5**,** 495-508.

DAVIS, B., RICHENS, J. & O'SHEA, P. 2011 *submitted.* Probe-free critical micelle concentration determination of bacterial quorum sensing molecules. *Biophysical Journal*.

DAVIS, B. M. 2011. *Interactions of bacterial quorum sensing signalling molecules with membranes and their in vivo transport.* Doctor of Philosophy, University of Nottingham.

DAVIS, B. M., JENSEN, R., WILLIAMS, P. & O'SHEA, P. 2010. The Interaction of N-Acylhomoserine Lactone Quorum Sensing Signaling Molecules with Biological Membranes: Implications for Inter-Kingdom Signaling. *Plos One,* 5.

DE ALMEIDA, R. F. M., BORST, J., FEDOROV, A., PRIETO, M. & VISSER, A. 2007. Complexity of lipid domains and rafts in giant unilamellar vesicles revealed by combining imaging and microscopic and macroscopic time-resolved fluorescence. *Biophysical Journal,* 93**,** 539-553.

DE ALMEIDA, R. F. M., FEDOROV, A. & PRIETO, M. 2003. Sphingomyelin/phosphatidylcholine/cholesterol phase diagram: Boundaries and composition of lipid rafts. *Biophysical Journal,* 85**,** 2406-2416.

DE ALMEIDA, R. F. M., LOURA, L. M. S., FEDOROV, A. & PRIETO, M. 2005. Lipid rafts have different sizes depending on membrane composition: A time-resolved fluorescence resonance energy transfer study. *Journal of Molecular Biology,* 346**,** 1109-1120.

DE KRUIJFF, B. 1997. Lipid polymorphism and biomembrane function. *Current Opinion in Chemical Biology,* 1**,** 564-569.

DE PIRRO, R., BERTOLI, A., GRECO, A. V., GELLI, A. S. & LAURO, R. 1979. The effect of food intake on insulin receptor in man. *Acta Endocrinologica,* 90**,** 473-480.

DE ROSA, S., CIRILLO, P., PAGLIA, A., SASSO, L., DI PALMA, V. & CHIARIELLO, M. 2010. Reactive Oxygen Species and Antioxidants in the Pathophysiology of Cardiovascular Disease: Does the Actual Knowledge Justify a Clinical Approach? *Current Vascular Pharmacology,* 8**,** 259-275.

DE WEER, P. 2000. A century of thinking about cell membranes. *Annual Review of Physiology,* 62**,** 919-926.

DEMEL, R. A. & DE KRUIJFF, B. 1976. The function of sterols in membranes. *Biochimica Et Biophysica Acta,* 457**,** 109-132.

DEMEL, R. A., PALTAUF, F. & HAUSER, H. 1987. Monolayer characteristics and thermal-behaviour of natural and synthetic phosphatidylserines. *Biochemistry,* 26**,** 8659-8665.

DEMEULE, M., JODOIN, J., GINGRAS, D. & BELIVEAU, R. 2000. P-glycoprotein is localized in caveolae in resistant cells and in brain capillaries. *Febs Letters,* 466**,** 219-224.

DENK, W., STRICKLER, J. H. & WEBB, W. W. 1990. 2-photon laser scanning fluorescence microscopy. *Science,* 248**,** 73-76.

DIAZ, S., AMALFA, F., DE LOPEZ, A. C. B. & DISALVO, E. A. 1999. Effect of water polarized at the carbonyl groups of phosphatidylcholines on the dipole potential of lipid bilayers. *Langmuir,* 15**,** 5179-5182.

DINTAMAN, J. M. & SILVERMAN, J. A. 1999. Inhibition of P-glycoprotein by D-alpha-tocopheryl polyethylene glycol 1000 succinate (TPGS). *Pharmaceutical Research,* 16**,** 1550-1556.

DIPLOCK, A. T. 1983. The role of vitamin-E in biological membranes. *Ciba Foundation Symposia,* 101**,** 45-55.

DIPLOCK, A. T. & LUCY, J. A. 1973. Biochemical modes of action of vitamin-E and selenium- hypothesis. *Febs Letters,* 29**,** 205-210.

DIPLOCK, A. T., LUCY, J. A., VERRINDER, M. & ZIELENIEWSKI, A. 1977. Alpha-tocopherol and permeability to glucose and chromate of unsaturated liposomes. *Febs Letters,* 82**,** 341-344.

DOMENE, C., BOND, P. J., DEOL, S. S. & SANSOM, M. S. P. 2003. Lipid/protein interactions and the membrane/water interfacial region. *Journal of the American Chemical Society,* 125**,** 14966-14967.

DRAGSTED, L. O. 2008. Biomarkers of exposure to vitamins A, C, and E and their relation to lipid and protein oxidation markers. *European Journal of Nutrition,* 47**,** 3-18.

DUGGAN, J., JAMAL, G., TILLEY, M., DAVIS, B., MCKENZIE, G., VERE, K., SOMEKH, M. G., O'SHEA, P. & HARRIS, H. 2008. Functional imaging of microdomains in cell membranes. *European Biophysics Journal with Biophysics Letters,* 37**,** 1279-1289.

EKIEL, I. H., HUGHES, L., BURTON, G. W., JOVALL, P. A., INGOLD, K. U. & SMITH, I. C. P. 1988. Structure and dynamics of alpha-tocopherol in model membranes and in solution- A broad-line and high-resolution NMR study. *Biochemistry,* 27**,** 1432-1440.

ELLIOTT, R., KATSOV, K., SCHICK, M. & SZLEIFER, I. 2005. Phase separation of saturated and mono-unsaturated lipids as determined from a microscopic model. *Journal of Chemical Physics,* 122.

ENDICOTT, J. A. & LING, V. 1989. The biochemistry of P-glycoprotein-mediated multidrug resistance. *Annual Review of Biochemistry,* 58**,** 137-171.

ENGELMAN, D. M. 2005. Membranes are more mosaic than fluid. *Nature,* 438**,** 578-580.

EPAND, R. M. 1998. Lipid polymorphism and protein-lipid interactions. *Biochimica Et Biophysica Acta-Reviews on Biomembranes,* 1376**,** 353-368.

ERIN, A. N., SKRYPIN, V. V. & KAGAN, V. E. 1985. Formation of alpha-tocopherol complexes with fatty-acids- nature of complexes. *Biochimica Et Biophysica Acta,* 815**,** 209-214.

ERIN, A. N., SPIRIN, M. M., TABIDZE, L. V. & KAGAN, V. E. 1984. Formation of alpha-tocopherol complexes with fatty-acids- A hypothetical mechanism of stabilization of biomembranes by vitamin-E. *Biochimica Et Biophysica Acta,* 774**,** 96-102.

EVANS, H. M. & BISHOP, K. S. 1922. On the existence of a hitherto unrecognized dietary factor essential for reproduction. *Science,* 56**,** 650-651.

EVANS, J., MADDUX, B. & GOLDFINE, I. 2005. The molecular basis for oxidative stress-induced insulin resistance. *Antioxidants and redox signalling,* 7**,** 1040-1052.

FARBSTEIN, D., KOZAK-BLICKSTEIN, A. & LEVY, A. P. 2010. Antioxidant Vitamins and Their Use in Preventing Cardiovascular Disease. *Molecules,* 15**,** 8098-8110.

FITCHEN, N., O'SHEA, P., WILLIAMS, P. & HARDIE, K. R. 2003. Electrostatic sensor for identifying interactions between peptides and bacterial membranes. *Molecular Immunology,* 40**,** 407-411.

FLEWELLING, R. F. & HUBBELL, W. L. 1986. The membrane dipole potential in a total membrane-potential model- applications to hydrophobic ion interactions with membranes. *Biophysical Journal,* 49**,** 541-552.

FLUHLER, E., BURNHAM, V. G. & LOEW, L. M. 1985. Spectra, membrane-binding, and potentiometric responses of new charge shift probes. *Biochemistry,* 24**,** 5749-5755.

FOX, C. & KEITH, A. 1972. *Membrane molecular biology,* Sinauer Associates inc.

FRANKLIN, J. C. & CAFISO, D. S. 1993. Internal Electrostatic Potentials in Bilayers - Measuring and Controlling Dipole Potentials in Lipid Vesicles. *Biophysical Journal,* 65**,** 289-299.

FREYCHET, P. 1979. Insulin receptors. *In:* BLECHER, M. (ed.) *Methods in receptor research.* New York: Marcel Dekker.

FRUHWIRTH, G. O., LOIDL, A. & HERMETTER, A. 2007. Oxidized phospholipids: From molecular properties to disease. *Biochimica Et Biophysica Acta-Molecular Basis of Disease,* 1772**,** 718-736.

FUKANO, T., SAWANO, A., OHBA, Y., MATSUDA, M. & MIYAWAKI, A. 2007. Differential ras activation between caveolae/raft and non-raft Microdomains. *Cell Structure and Function,* 32**,** 9-15.

FUKUZAWA, K., IKEBATA, W., SHIBATA, A., KUMADAKI, I., SAKANAKA, T. & URANO, S. 1992. Location and dynamics of alpha-tocopherol in model phospholipid-membranes with different charges. *Chemistry and Physics of Lipids,* 63**,** 69-75.

FUKUZAWA, K., IKEBATA, W., SHIBATA, A., SAKANAKA, T. & URANO, S. 1993. Location of alpha-tocopherol in phospholipid vesicles and its dynamics in inhibiting lipid peroxidation. *In:* MINO, M., NAKAMURA, H., DIPLOCK, A. T. & KAYDEN, H. J. (eds.) *Vitamin E- its usefulness in health and in curing diseases.* Tokyo, Japan: Japan Scientific Society Press.

FUKUZAWA, K., IKENO, H., TOKUMURA, A. & TSUKATANI, H. 1979. Effect of alpha-tocopherol incorporation on glucose permeability and phase-transition of lecithin liposomes. *Chemistry and Physics of Lipids,* 23**,** 13-22.

FULLER, N., BENATTI, C. R. & RAND, R. P. 2003. Curvature and bending constants for phosphatidylserine-containing membranes. *Biophysical Journal,* 85**,** 1667-1674.

FULLER, N. & RAND, R. P. 2001. The influence of lysolipids on the spontaneous curvature and bending elasticity of phospholipid membranes. *Biophysical Journal,* 81**,** 243-254.

GARNER, O. B. & BAUM, L. G. 2008. Galectin-glycan lattices regulate cell-surface glycoprotein organization and signalling. *Biochemical Society Transactions,* 36**,** 1472-1477.

GARVEY, W. T., OLEFSKY, J. M. & MARSHALL, S. 1986. Insulin induces progressive insulin resistance in cultured rat adipocytes- sequential effects at receptor and multiple postreceptor sites. *Diabetes,* 35**,** 258-267.

GAUS, K., DEAN, R. T., KRITHARIDES, L. & JESSUP, W. 2001. Inhibition of cholesterol efflux by 7-ketocholesterol: Comparison between cells, plasma membrane vesicles, and liposomes as cholesterol donors. *Biochemistry,* 40**,** 13002-13014.

GAUS, K., KRITHARIDES, L., SCHMITZ, G., BOETTCHER, A., DROBNIK, W., LANGMANN, T., QUINN, C. M., DEATH, A., DEAN, R. T. & JESSUP, W. 2004. Apolipoprotein A-1 interaction with plasma membrane lipid rafts controls cholesterol export from macrophages. *Faseb Journal,* 18**,** 574-.

GAWRISCH, K. 2005. The dynamics of membrane lipids. *In:* YEAGLE, P. L. (ed.) *The structure of biological membranes.* Second edition ed. Boca Raton, FL: CRC Press.

GAWRISCH, K., RUSTON, D., ZIMMERBERG, J., PARSEGIAN, V. A., RAND, R. P. & FULLER, N. 1992. Membrane dipole potentials, hydration forces, and the ordering of water at membrane surfaces. *Biophysical Journal,* 61**,** 1213-1223.

GIROTTI, A. W. 1998. Lipid hydroperoxide generation, turnover, and effector action in biological systems. *Journal of Lipid Research,* 39**,** 1529-1542.

GOLBIDI, S., EBADI, S. & LAHE, I. 2011. Antioxidants in the treatment of diabetes. *Current diabetes reviews*.

GOLDING, C., SENIOR, S., WILSON, M. T. & OSHEA, P. 1996. Time resolution of binding and membrane insertion of a mitochondrial signal peptide: Correlation with structural changes and evidence for cooperativity. *Biochemistry,* 35**,** 10931-10937.

GOLDSTEIN, L. J. 1996. MDR1 gene expression in solid tumours. *European Journal of Cancer,* 32A**,** 1039-1050.

GOMEZ-FERNANDEZ, J. C., VILLALAIN, J., ARANDA, F. J., ORTIZ, A., MICOL, V., COUTINHO, A., BERBERAN-SANTOS, M. N. & PRIETO, M. J. E. 1989. Localization of alpha-tocopherol in membranes. *Diplock, A. T., Et Al. (Ed.). Annals of the New York Academy of Sciences, Vol. 570. Vitamin E: Biochemistry and Health Implications; Conference, New York, New York, USA, October 31-November 2, 1988. Xiii+555p. New York Academy of Sciences: New York, New York, USA. Illus***,** 109-120.

GORTER, E. & GRENDEL, F. 1925. On bimolecular layers of lipoids on the chromocytes of the blood. *Journal of Experimental Medicine,* 41**,** 439-443.

GOTTESMAN, M. M. 1993. How cancer-cells evade chemotherapy- 16th Richard-and-Hinda-Rosenthal-foundation award lecture. *Cancer Research,* 53**,** 747-754.

GOTTESMAN, M. M. & PASTAN, I. 1993. Biochemistry of multidrug-resistance mediated by the multidrug transporter. *Annual Review of Biochemistry,* 62**,** 385-427.

GOUVERNEUR, M., SPAAN, J. A. E., PANNEKOEK, H., FONTIJN, R. D. & VINK, H. 2006a. Fluid shear stress stimulates incorporation of hyaluronan into endothelial cell glycocalyx. *American Journal of Physiology-Heart and Circulatory Physiology,* 290**,** H458-H462.

GOUVERNEUR, M., VAN DEN BERG, B., NIEUWDORP, M., STROES, E. & VINK, H. 2006b. Vasculoprotective properties of the endothelial glycocalyx: effects of fluid shear stress. *Journal of Internal Medicine,* 259**,** 393-400.

GROSS, E., BEDLACK, R. S. & LOEW, L. M. 1994. Dual-Wavelength Ratiometric Fluorescence Measurement of the Membrane Dipole Potential. *Biophysical Journal,* 67**,** 208-216.

GRUNER, S. 2005. Nonlamellar Lipid Phases. *In:* YEAGLE, P. (ed.) *The Structure of Biological Membranes.* Second Edition ed. Boca Raton, FL: CRC Press.

GRUNER, S. M., CULLIS, P. R., HOPE, M. J. & TILCOCK, C. P. S. 1985. Lipid polymorphism- the molecular-basis of nonbilayer phases. *Annual Review of Biophysics and Biophysical Chemistry,* 14**,** 211-238.

GUBERNATOR, J., STASIUK, M. & KOZUBEK, A. 1999. Dual effect of alkylresorcinols, natural amphiphilic compounds, upon liposomal permeability. *Biochimica Et Biophysica Acta-Biomembranes,* 1418**,** 253-260.

GUILLEN, J., KINNUNEN, P. K. J. & VILLALAIN, J. 2008. Membrane insertion of the three main membranotropic sequences from SARS-CoV S2 glycoprotein. *Biochimica Et Biophysica Acta-Biomembranes,* 1778**,** 2765-2774.

HACHIYA, H. L., TAKAYAMA, S., WHITE, M. F. & KING, G. L. 1987. Regulation of insulin-receptor internalization in vascular endothelial-cells by insulin and phorbol ester. *Journal of Biological Chemistry,* 262**,** 6417-6424.

HACQUEBARD, M. & CARPENTIER, Y. A. 2005. Vitamin E: absorption, plasma transport and cell uptake. *Current Opinion in Clinical Nutrition and Metabolic Care,* 8**,** 133-138.

HAIDEKKER, M. A., L'HEUREUX, N. & FRANGOS, J. A. 2000. Fluid shear stress increases membrane fluidity in endothelial cells: a study with DCVJ fluorescence. *American Journal of Physiology-Heart and Circulatory Physiology,* 278**,** H1401-H1406.

HALL, E. & BOSKEN, J. 2009. Measurement of oxygen radicals and lipid peroxidation in neural tissues. *Current Protocols in Neuroscience,* 48**,** 1-7.

HALLIWELL, B. & GUTTERIDGE, J. M. C. 1999. *Free Radicals in Biology and Medicine,* Oxford, New York, Clarendon Press, Oxford University Press.

HANCOCK, J. F. 2006. Lipid rafts: contentious only from simplistic standpoints. *Nature Reviews Molecular Cell Biology,* 7**,** 456-462.

HAQUE, M. E. & LENTZ, B. R. 2004. Roles of curvature and hydrophobic interstice energy in fusion: Studies of lipid perturbant effects. *Biochemistry,* 43**,** 3507-3517.

HARDER, T., SCHEIFFELE, P., VERKADE, P. & SIMONS, K. 1998. Lipid domain structure of the plasma membrane revealed by patching of membrane components. *Journal of Cell Biology,* 141**,** 929-942.

HARRISON, D., GRIENDLING, K. K., LANDMESSER, U., HORNIG, B. & DREXLER, H. 2003. Role of oxidative stress in atherosclerosis. *American Journal of Cardiology,* 91**,** 7A-11A.

HAUGLAND, R. P. 2005. *Probes for membrane potential. The Handbook- A guide to fluorescent probes and labelling technologies,* Invitrogen Molecular Probes: Eugene.

HAUSER, H. & POUPART, G. 2005. Lipid structure. *In:* YEAGLE, P. (ed.) *The structure of biological membranes.* Second edition ed. Boca Raton: CRC Press.

HERRERA, E. & BARBAS, C. 2001. Vitamin E: action, metabolism and perspectives. *Journal of Physiology and Biochemistry,* 57**,** 43-56.

HILL, A. 1910. The possible effects of the aggregation of the molecules of haemoglobin on its dissociation curves. *Journal of physiology,* 40**,** iv-vii.

HINRICHS, J. W. J., KLAPPE, K., HUMMEL, I. & KOK, J. W. 2004. ATP-binding cassette transporters are enriched in non-caveolar detergent-insoluble glycosphingolipid-enriched membrane domains (DIGs) in human multidrug-resistant cancer cells. *Journal of Biological Chemistry,* 279**,** 5734-5738.

HOBDEN, C., TEEVAN, C., JONES, L. & O'SHEA, P. 1995. Hydrophobic properties of the cell-surface of candida-albicans- A role in aggregation. *Microbiology-Uk,* 141**,** 1875-1881.

HOFSASS, C., LINDAHL, E. & EDHOLM, O. 2003. Molecular dynamics simulations of phospholipid bilayers with cholesterol. *Biophysical Journal,* 84**,** 2192-2206.

HOGBERG, C. J. & LYUBARTSEV, A. P. 2008. Effect of local anesthetic lidocaine on electrostatic properties of a lipid bilayer. *Biophysical Journal,* 94**,** 525-531.

HOSOMI, A., ARITA, M., SATO, Y., KIYOSE, C., UEDA, T., IGARASHI, O., ARAI, H. & INOUE, K. 1997. Affinity for alpha-tocopherol transfer protein as a determinant of the biological activities of vitamin E analogs. *Febs Letters,* 409**,** 105-108.

HUANG, Z. Y., LIU, Q. P., LI, W. Z., WANG, R. J., WANG, D., ZHANG, Y. B., ZHANG, F., CHI, Y., LIU, Z., MATSUURA, E., LIU, Z. B. & ZHANG, Q. M. 2010. 7-Ketocholesterol Induces Cell Apoptosis by Activation of Nuclear Factor kappa B in Mouse Macrophages. *Acta Medica Okayama,* 64**,** 85-93.

INOKUCHI, J. 2010. Membrane microdomains and insulin resistance. *Febs Letters,* 584**,** 1864-1871.

IPSEN, J. H., KARLSTROM, G., MOURITSEN, O. G., WENNERSTROM, H. & ZUCKERMANN, M. J. 1987. Phase-equilibria in the phosphatidylcholine-cholesterol system. *Biochimica Et Biophysica Acta,* 905**,** 162-172.

ISRAELACHVILI, J. N., MARCELJA, S. & HORN, R. G. 1980. Physical principles of membrane organization. *Quarterly Reviews of Biophysics,* 13**,** 121-200.

ISRAELACHVILI, J. N. & MITCHELL, D. J. 1975. Model for packing of lipids in bilayer membranes. *Biochimica Et Biophysica Acta,* 389**,** 13-19.

ISRAELACHVILI, J. N., MITCHELL, D. J. & NINHAM, B. W. 1976. Theory of self-assembly of hydrocarbon amphiphiles into micelles and bilayers. *Journal of the Chemical Society-Faraday Transactions Ii,* 72**,** 1525-1568.

JACOBSON, K. & DIETRICH, C. 1999. Looking at lipid rafts? *Trends in Cell Biology,* 9**,** 87-91.

JACOBSON, K., SHEETS, E. D. & SIMSON, R. 1995. Revisiting the fluid mosaic model of membranes. *Science,* 268**,** 1441-1442.

JANG, E. R. & LEE, C. S. 2011. 7-Ketocholesterol induces apoptosis in differentiated PC12 cells via reactive oxygen species-dependent activation of NF-kappa B and Akt pathways. *Neurochemistry International,* 58**,** 52-59.

JANIAK, M. J., SMALL, D. M. & SHIPLEY, G. G. 1979. Temperature and compositional dependence of the structure of hydrated dimyristoyl lecithin. *Journal of Biological Chemistry,* 254**,** 6068-6078.

JANMEY, P. A. & KINNUNEN, P. K. J. 2006. Biophysical properties of lipids and dynamic membranes. *Trends in Cell Biology,* 16**,** 538-546.

JEHLE, P. M., LUTZ, M. P. & FUSSGAENGER, R. D. 1996. High affinity binding sites for proinsulin in human IM-9 lymphoblasts. *Diabetologia,* 39**,** 421-432.

JENDRASIAK, G. L. & MENDIBLE, J. C. 1976a. Effect of phase-transition on hydration and electrical-conductivity of phospholipids. *Biochimica Et Biophysica Acta,* 424**,** 133-148.

JENDRASIAK, G. L. & MENDIBLE, J. C. 1976b. Phospholipid head-group orientation - effect on hydration and electrical-conductivity. *Biochimica Et Biophysica Acta,* 424**,** 149-158.

JENNER, P. 2003. Oxidative stress in Parkinson's disease. *Annals of Neurology,* 53**,** S26-S36.

JEWELL, S. A. & WINLOVE, C. P. 2011. *Unpublished data.*

JOHNSON, I. & SPENCE, M. T. Z. 2011. pH Indicators. *In:* JOHNSON, I. & SPENCE, M. T. Z. (eds.) *Molecular Probes Handbook; A guide to fluorescent probes and labelling technologies.*

KABAYAMA, K., SATO, T., KITAMURA, F., UEMURA, S., KANG, B., IGARASHI, Y. & INOKUCHI, J. 2005. TNFalpha-induced insulin resistance in adipocytes as a membrane microdomain disorder: involvement of ganglioside GM3. *Glycobiology,* 15**,** 21-29.

KABAYAMA, K., SATO, T., SAITO, K., LOBERTO, N., PRINETTI, A., SONNINO, S., KINJO, M., IGARASHI, Y. & INOKUCHI, J. I. 2007. Dissociation of the insulin receptor and caveolin-1 complex by ganglioside GM3 in the state of insulin resistance. *Proceedings of the National Academy of Sciences of the United States of America,* 104**,** 13678-13683.

KAGAN, V. E. 1989. Tocopherol stabilizes membrane against phospholipase-A, free fatty-acids, and lysophospholipids. *Annals of the New York Academy of Sciences,* 570**,** 121-135.

KAGAN, V. E. & QUINN, P. J. 1988. The interaction of alpha-tocopherol and homologs with shorter hydrocarbon chains with phospholipid-bilayer dispersions- A fluorescence probe study. *European Journal of Biochemistry,* 171**,** 661-667.

KAGAN, V. E., SERBINOVA, E. A., BAKALOVA, R. A., STOYTCHEV, T. S., ERIN, A. N., PRILIPKO, L. L. & EVSTIGNEEVA, R. P. 1990. Mechanisms of stabilization of biomembranes by alpha-tocopherol- The role of the hydrocarbon chain in the inhibition of lipid-peroxidation. *Biochemical Pharmacology,* 40**,** 2403-2413.

KAMALELDIN, A. & APPELQVIST, L. A. 1996. The chemistry and antioxidant properties of tocopherols and tocotrienols. *Lipids,* 31**,** 671-701.

KENWORTHY, A. K. & EDIDIN, M. 1998. Distribution of a glycosylphosphatidylinositol-anchored protein at the apical surface of MDCK cells examined at a resolution of < 100 angstrom using imaging fluorescence resonance energy transfer. *Journal of Cell Biology,* 142**,** 69-84.

KENWORTHY, A. K., PETRANOVA, N. & EDIDIN, M. 2000. High-resolution FRET microscopy of cholera toxin B-subunit and GPI-anchored proteins in cell plasma membranes. *Molecular Biology of the Cell,* 11**,** 1645-1655.

KINNUNEN, P. K. J. 1996. On the molecular-level mechanisms of peripheral protein-membrane interactions induced by lipids forming inverted non-lamellar phases. *Chemistry and Physics of Lipids,* 81**,** 151-166.

KLAPPE, K., HUMMEL, I., HOEKSTRA, D. & KOK, J. W. 2009. Lipid dependence of ABC transporter localization and function. *Chemistry and Physics of Lipids,* 161**,** 57-64.

LAI, M. Z., DUZGUNES, N. & SZOKA, F. C. 1985. Effects of replacement of the hydroxyl group of cholesterol and tocopherol on the thermotropic behaviour of phospholipid-membranes. *Biochemistry,* 24**,** 1646-1653.

LAJOIE, P. & NABI, I. R. 2010. Lipids rafts, caveolae, and their endocytosis. *International Review of Cell and Molecular Biology, Vol 282,* 282**,** 135-163.

LAKOWICZ, J. R., MALICKA, J., D'AURIA, S. & GRYCZYNSKI, I. 2003. Release of the self-quenching of fluorescence near silver metallic surfaces. *Analytical Biochemistry,* 320**,** 13-20.

LANGE, Y., DOLDE, J. & STECK, T. L. 1981. The rate of transmembrane movement of cholesterol in the human erythrocyte. *Journal of Biological Chemistry,* 256**,** 5321-5323.

LANGHORST, M. F., SOLIS, G. P., HANNBECK, S., PLATTNER, H. & STUERMER, C. A. O. 2007. Linking membrane microdomains to the cytoskeleton: Regulation of the lateral mobility of reggie-1/flotillin-2 by interaction with actin. *Febs Letters,* 581**,** 4697-4703.

LE GOFF, G., VITHA, M. F. & CLARKE, R. J. 2007. Orientational polarisability of lipid membrane surfaces. *Biochimica Et Biophysica Acta-Biomembranes,* 1768**,** 562-570.

LECUYER, H. & DERVICHI, D. 1969. Structure of aqueous mixtures of lecithin and cholesterol. *Journal of Molecular Biology,* 45**,** 39.

LEFEVRE, T. & PICQUART, M. 1996. Vitamin E-phospholipid interactions in model multilayer membranes: A spectroscopic study. *Biospectroscopy,* 2**,** 391-403.

LEIKIN, S., KOZLOV, M. M., FULLER, N. L. & RAND, R. P. 1996. Measured effects of diacylglycerol on structural and elastic properties of phospholipid membranes. *Biophysical Journal,* 71**,** 2623-2632.

LEMAIRE-EWING, S., DESRUMAUX, C., NEEL, D. & LAGROST, L. 2010. Vitamin E transport, membrane incorporation and cell metabolism: Is alpha-tocopherol in lipid rafts an oar in the lifeboat? *Molecular Nutrition & Food Research,* 54**,** 631-640.

LEMAIRE-EWING, S., PRUNET, C., MONTANGE, T., VEJUX, A., BERTHIER, A., BESSEDE, G., CORCOS, L., GAMBERT, P., NEEL, D. & LIZARD, G. 2005. Comparison of the cytotoxic, pro-oxidant and pro-inflammatory characteristics of different oxysterols. *Cell Biology and Toxicology,* 21**,** 97-114.

LENNE, P. F., WAWREZINIECK, L., CONCHONAUD, F., WURTZ, O., BONED, A., GUO, X. J., RIGNEAULT, H., HE, H. T. & MARGUET, D. 2006. Dynamic molecular confinement in the plasma membrane by microdomains and the cytoskeleton meshwork. *Embo Journal,* 25**,** 3245-3256.

LENTZ, B. R., BARENHOLZ, Y. & THOMPSON, T. E. 1976. Fluorescence depolarization studies of phase-transitions and fluidity in phospholipid bilayers. 2. 2-component phosphatidylcholine liposomes. *Biochemistry,* 15**,** 4529-4537.

LENTZ, B. R., BARROW, D. A. & HOECHLI, M. 1980. Cholesterol-phosphatidylcholine interactions in multilamellar vesicles. *Biochemistry,* 19**,** 1943-1954.

LEONARDUZZI, G., VIZIO, B., SOTTERO, B., VERDE, V., GAMBA, P., MASCIA, C., CHIARPOTTO, E., POLI, G. & BIASI, F. 2006. Early involvement of ROS overproduction in apoptosis induced by 7-ketocholesterol. *Antioxidants & Redox Signaling,* 8**,** 375-380.

LERAY, C., CAZENAVE, J. P. & GACHET, C. 2002. Platelet phospholipids are differentially protected against oxidative degradation by plasmalogens. *Lipids,* 37**,** 285-290.

LEWIS, R., MAK, N. & MCELHANEY, R. N. 1987a. A differential scanning calorimetric study of the thermotropic phase-behaviour of model membranes composed of phosphatidylcholines containing linear saturated fatty acyl chains. *Biochemistry,* 26**,** 6118-6126.

LEWIS, R. & MCELHANEY, R. 2005. The Mesomorphic Phase Behaviour of Lipid Bilayers. *In:* YEAGLE, P. (ed.) *The Structure of Biological Membranes.* Second Edition ed. Boca Raton, FL: CRC Press.

LEWIS, R., SYKES, B. D. & MCELHANEY, R. N. 1987b. Thermotropic phase-behaviour of model membranes composed of phosphatidylcholines containing DL-methyl anteisobranched fatty-acids.1. Differential scanning calorimetric and P-31 NMR spectroscopic studies.. *Biochemistry,* 26**,** 4036-4044.

LI, L. & CHENG, J. X. 2006. Coexisting stripe- and patch-shaped domains in giant unilamellar vesicles. *Biochemistry,* 45**,** 11819-11826.

LI, X. M., MOMSEN, M. M., BROCKMAN, H. L. & BROWN, R. E. 2003. Sterol structure and sphingomyelin acyl chain length modulate lateral packing elasticity and detergent solubility in model membranes. *Biophysical Journal,* 85**,** 3788-3801.

LIVINGSTON, J. N. & MOXLEY, R. T. 1982. Glucose-ingestion mediates a rapid increase in the insulin responsiveness of rat adipocytes. *Endocrinology,* 111**,** 1749-1751.

LIZARD, G., MOISANT, M., CORDELET, C., MONIER, S., GAMBERT, P. & LAGROST, L. 1997. Induction of similar features of apoptosis in human and bovine vascular endothelial cells treated by 7-ketocholesterol. *Journal of Pathology,* 183**,** 330-338.

LOEW, L. M., SCULLY, S., SIMPSON, L. & WAGGONER, A. S. 1979. Evidence for a Charge-Shift Electrochromic Mechanism in a Probe of Membrane-Potential. *Nature,* 281**,** 497-499.

LOIKE, J. D. & SILVERSTEIN, S. C. 1983. A fluorescence quenching technique using trypan blue to differentiate between attached and ingested glutaraldehyde-fixed red-blood-cells in phagycytosing murine macrophages. *Journal of Immunological Methods,* 57**,** 373-379.

LOS, D. & MURATA, N. 2000. Regulation of enzymatic activity and gene expression by membrane fluidity. *Science's STKE,* 62**,** pe1.

LUCERO, H. A. & ROBBINS, P. W. 2004. Lipid rafts-protein association and the regulation of protein activity. *Archives of Biochemistry and Biophysics,* 426**,** 208-224.

LUCY, J. A. 1972. Functional and structural aspects of biological-membranes- suggested structural role for vitamin-E in control of membrane-permeability and stability. *Annals of the New York Academy of Sciences,* 203**,** 4-11.

LUKER, G. D., FLAGG, T. P., SHA, Q., LUKER, K. E., PICA, C. M., NICHOLS, C. G. & PIWNICA-WORMS, D. 2001. MDR1 P-glycoprotein reduces influx of substrates without affecting membrane potential. *Journal of Biological Chemistry,* 276**,** 49053-49060.

LYONS, M. A. & BROWN, A. J. 1999. 7-ketocholesterol. *International Journal of Biochemistry & Cell Biology,* 31**,** 369-375.

MA, Z. S. & LIM, L. Y. 2003. Uptake of chitosan and associated insulin in Caco-2 cell monolayers: A comparison between chitosan molecules and chitosan nanoparticles. *Pharmaceutical Research,* 20**,** 1812-1819.

MAGGIO, B. 1999. Modulation of phospholipase A(2) by electrostatic fields and dipole potential of glycosphingolipids in monolayers. *Journal of Lipid Research,* 40**,** 930-939.

MAGNANI, E. & BETTINI, E. 2000. Resazurin detection of energy metabolism changes in serum-starved PC12 cells and of neuroprotective agent effect. *Brain Research Protocols,* 5**,** 266-272.

MAOR, I., KAPLAN, M., HAYEK, T., VAYA, J., HOFFMAN, A. & AVIRAM, M. 2000. Oxidized monocyte-derived macrophages in aortic atherosclerotic lesion from apolipoprotein E-deficient mice and from human carotid artery contain lipid peroxides and oxysterols. *Biochemical and Biophysical Research Communications,* 269**,** 775-780.

MARGUET, D., LENNE, P. F., RIGNEAULT, H. & HE, H. T. 2006. Dynamics in the plasma membrane: how to combine fluidity and order. *Embo Journal,* 25**,** 3446-3457.

MARITIM, A. C., SANDERS, R. A. & WATKINS, J. B. 2003. Diabetes, oxidative stress, and antioxidants: A review. *Journal of Biochemical and Molecular Toxicology,* 17**,** 24-38.

MARON, R. & KAHN, C. R. 1985. The insulin-receptor- characterization and regulation using insulin-antiinsulin antibody complexes as a probe for flow-cytometry. *Journal of Clinical Endocrinology & Metabolism,* 60**,** 1004-1011.

MARSH, D. 1999. Thermodynamic analysis of chain-melting transition temperatures for monounsaturated phospholipid membranes: Dependence on cis-monoenoic double bond position. *Biophysical Journal,* 77**,** 953-963.

MASSEY, J. B. 2001. Interfacial properties of phosphatidylcholine bilayers containing vitamin E derivatives. *Chemistry and Physics of Lipids,* 109**,** 157-174.

MASSEY, J. B. & POWNALL, H. J. 2005. The polar nature of 7-ketocholesterol determines its location within membrane domains and the kinetics of membrane micro solubilization by apolipoprotein A-I. *Biochemistry,* 44**,** 10423-10433.

MASSEY, J. B. & POWNALL, H. J. 2006. Structures of biologically active oxysterols determine their differential effects on phospholipid membranes. *Biochemistry,* 45**,** 10747-10758.

MASSEY, J. B., SHE, H. S. & POWNALL, H. J. 1982. Interaction of Vitamin-E with saturated phospholipid bilayers. *Biochemical and Biophysical Research Communications,* 106**,** 842-847.

MASTALOUDIS, A., TRABER, M. G., CARSTENSEN, K. & WIDRICK, J. J. 2006. Antioxidants did not prevent muscle damage in response to an ultramarathon run. *Medicine and Science in Sports and Exercise,* 38**,** 72-80.

MASTICK, C., BRADY, M. & SALTIEL, A. 1995. Insulin stimulates the tyrosine phosphorylation of caveolin. *Journal of Cell Biology,* 129**,** 1523-1531.

MATOS, P. M., GONCALVES, S. & SANTOS, N. C. 2008. Interaction of peptides with biomembranes assessed by potential-sensitive fluorescent probes. *Journal of Peptide Science,* 14**,** 407-415.

MAYER, L. D., HOPE, M. J. & CULLIS, P. R. 1986. Vesicles of variable sizes produced by a rapid extrusion procedure. *Biochimica Et Biophysica Acta,* 858**,** 161-168.

MAYOR, S. & RAO, M. 2004. Rafts: Scale-dependent, active lipid organization at the cell surface. *Traffic,* 5**,** 231-240.

MCLAUGHLIN, S. 1989. The electrostatic properties of membranes. *Annual Review of Biophysics and Biophysical Chemistry,* 18**,** 113-136.

MCMULLEN, T. P. W. & MCELHANEY, R. N. 1995. New aspects of the interaction of cholesterol with dipalmitoylphosphatidylcholine bilayers as revealed by high-sensitivity differential scanning calorimetry. *Biochimica Et Biophysica Acta-Biomembranes,* 1234**,** 90-98.

MCMULLEN, T. P. W. & MCELHANEY, R. N. 1997. Differential scanning calorimetric studies of the interaction of cholesterol with distearoyl and dielaidoyl molecular species of phosphatidylcholine, phosphatidylethanolamine, and phosphatidylserine. *Biochemistry,* 36**,** 4979-4986.

MCMURCHIE, E. J. & MCINTOSH, G. H. 1986. Thermotropic interaction of vitamin-E with dimyristoyl and dipalmitoyl phosphatidylcholine liposomes. *Journal of Nutritional Science and Vitaminology,* 32**,** 551-558.

MEGLI, F. M., RUSSO, L. & SABATINI, K. 2005. Oxidized phospholipids induce phase separation in lipid vesicles. *Febs Letters,* 579**,** 4577-4584.

MEGLI, F. M. & SABATINI, K. 2003. EPR studies of phospholipid bilayers after lipoperoxidation 1. Inner molecular order and fluidity gradient. *Chemistry and Physics of Lipids,* 125**,** 161-172.

MEIGS, J. B., LARSON, M. G., FOX, C. S., KEANEY, J. F., VASAN, R. S. & BENJAMIN, E. J. 2007. Association of oxidative stress, insulin resistance, and diabetes risk phenotypes - The framingham offspring study. *Diabetes Care,* 30**,** 2529-2535.

MENDELSOHN, R., DAVIES, M. A., BRAUNER, J. W., SCHUSTER, H. F. & DLUHY, R. A. 1989. Quantitative-determination of conformational disorder in the acyl chains of phospholipid-bilayers by infrared-spectroscopy. *Biochemistry,* 28**,** 8934-8939.

MILLANVOYE-VAN BRUSSEL, E., TOPAL, G., BRUNET, A., DO PHAW, T., DECKERT, V., RENDU, F. & DAVID-DUFILHO, M. 2004. Lysophosphatidylcholine and 7-oxocholesterol modulate Ca2+ signals and inhibit the phosphorylation of endothelial NO synthase and cytosolic phospholipase A(2). *Biochemical Journal,* 380**,** 533-539.

MINTZER, E., CHARLES, G. & GORDON, S. 2010. Interaction of two oxysterols, 7-ketocholesterol and 25-hydroxycholesterol, with phosphatidylcholine and sphingomyelin in model membranes. *Chemistry and Physics of Lipids,* 163**,** 586-593.

MONROE, E. B., JURCHEN, J. C., LEE, J., RUBAKHIN, S. S. & SWEEDLER, J. V. 2005. Vitamin E imaging and localization in the neuronal membrane. *Journal of the American Chemical Society,* 127**,** 12152-12153.

MORRIS, R., COX, H., MOMBELLI, E. & QUINN, P. 2004. Rafts, little caves and large potholes: how lipid structure interacts with membrane proteins to create functionally diverse membrane environments. *Subcellular Biochemistry,* 37**,** 35-118.

MOSMANN, T. 1983. Rapid calorimetric assay for cellular growth and survival- Application to proliferation and cyto-toxicity assays. *Journal of Immunological Methods,* 65**,** 55-63.

MOXLEY, R. T., LIVINGSTON, J. N., LOCKWOOD, D. H., GRIGGS, R. C. & HILL, R. L. 1981. Abnormal regulation of monocyte insulin-binding affinity after glucose-ingestion in patients with monocyte-dystrophy. *Proceedings of the National Academy of Sciences of the United States of America-Biological Sciences,* 78**,** 2567-2571.

MUGGEO, M., BAR, R. S. & ROTH, J. 1977. Change in affinity of insulin receptors following oral glucose in normal adults. *Journal of Clinical Endocrinology & Metabolism,* 44**,** 1206-1209.

MURPHY, R. F., BISACCIA, E., CANTOR, C. R., BERGER, C. & EDELSON, R. L. 1984. Internalization and acidification of insulin by activated human-lymphocytes. *Journal of Cellular Physiology,* 121**,** 351-356.

MURPHY, R. F., POWERS, S., VERDERAME, M., CANTOR, C. R. & POLLACK, R. 1982. Flow cytofluorometric analysis of insulin binding and internalization by swiss 3T3 cells. *Cytometry,* 2**,** 402-406.

MYERS, S. J. & STANLEY, K. K. 1999. Src family kinase activation in glycosphingolipid-rich membrane domains of endothelial cells treated with oxidised low density lipoprotein. *Atherosclerosis,* 143**,** 389-397.

MYOISHI, M., MINAMINO, T. & KITAKAZE, M. 2007. Increased endoplasmic reticulum stress in atherosclerotic plaques associated with acute coronary syndrome. *Circulation,* 116**,** 107-107.

NEUZIL, J., ZHAO, M., OSTERMANN, G., STICHA, M., GELLERT, N., WEBER, C., EATON, J. W. & BRUNK, U. T. 2002. alpha-tocopheryl succinate, an agent with in vivo anti-tumour activity, induces apoptosis by causing lysosomal instability. *Biochemical Journal,* 362**,** 709-715.

NICOL, D. & SMITH, L. F. 1960. Amino-acid sequence of human insulin. *Nature,* 187**,** 483-485.

NIEUWDORP, M., VAN HAEFTEN, T. W., GOUVERNEUR, M., MOOIJ, H. L., VAN LIESHOUT, M. H. P., LEVI, M., MEIJERS, J. C. M., HOLLEMAN, F., HOEKSTRA, J. B. L., VINK, H., KASTELEIN, J. J. P. & STROES, E. S. G. 2006. Loss of endothelial glycocalyx during acute hyperglycemia coincides with endothelial dysfunction and coagulation activation in vivo. *Diabetes,* 55**,** 480-486.

NIKI, E., YOSHIDA, Y., SAITO, Y. & NOGUCHI, N. 2005. Lipid peroxidation: Mechanisms, inhibition, and biological effects. *Biochemical and Biophysical Research Communications,* 338**,** 668-676.

NOGUCHI, N., NUMANO, R., KANEDA, H. & NIKI, E. 1998. Oxidation of lipids in low density lipoprotein particles. *Free Radical Research,* 29**,** 43-52.

O'SHEA, P. 1988. Physical fields and cellular organisation: field-dependent mechanisms of morphogenesis. *Experientia,* 44**,** 684-694.

O'SHEA, P. 2003. Intermolecular interactions with/within cell membranes and the trinity of membrane potentials: kinetics and imaging. *Biochemical Society Transactions,* 31**,** 990-996.

O'SHEA, P. 2004. Membrane potentials: measurement, occurence and roles in cellular function, In: Walz, D., Teissie, J., Milazzo, G. (Eds.), Bioelectrochemistry of membranes, Basel:Birkhauser. 23-59.

O'SHEA, P. 2005. Physical landscapes in biological membranes: physico-chemical terrains for spatio-temporal control of biomolecular interactions and behaviour. *Philosophical Transactions of the Royal Society A,* 363**,** 575-588.

OLIFERENKO, S., PAIHA, K., HARDER, T., GERKE, V., SCHWARZLER, C., SCHWARZ, H., BEUG, H., GUNTHERT, U. & HUBER, L. A. 1999. Analysis of CD44-containing lipid rafts: Recruitment of annexin II and stabilization by the actin cytoskeleton. *Journal of Cell Biology,* 146**,** 843-854.

ORLOWSKI, S., MARTIN, S. & ESCARGUEIL, A. 2006. P-glycoprotein and 'lipid rafts': some ambiguous mutual relationships (floating on them, building them or meeting them by chance?). *Cellular and Molecular Life Sciences,* 63**,** 1038-1059.

ORTIZ, A., ARANDA, F. J. & GOMEZ-FERNANDEZ, J. C. 1987. A differential scanning calorimetry study of the interaction of alpha-tocopherol with mixtures of phospholipids. *Biochimica Et Biophysica Acta,* 898**,** 214-222.

OSBORN, E. A., RABODZEY, A., DEWEY, C. F. & HARTWIG, J. H. 2006. Endothelial actin cytoskeleton remodeling during mechanostimulation with fluid shear stress. *American Journal of Physiology-Cell Physiology,* 290**,** C444-C452.

PALOZZA, P., SIMONE, R., CATALANO, A., BONINSEGNA, A., BOHM, V., FROHLICH, K., MELE, M. C., MONEGO, G. & RANELLETTI, F. O. 2010. Lycopene prevents 7-ketocholesterol-induced oxidative stress, cell cycle arrest and apoptosis in human macrophages. *Journal of Nutritional Biochemistry,* 21**,** 34-46.

PANCHUK-VOLOSHINA, N., HAUGLAND, R. P., BISHOP-STEWART, J., BHALGAT, M. K., MILLARD, P. J., MAO, F. & LEUNG, W. Y. 1999. Alexa dyes, a series of new fluorescent dyes that yield exceptionally bright, photostable conjugates. *Journal of Histochemistry & Cytochemistry,* 47**,** 1179-1188.

PARASASSI, T., DISTEFANO, M., LOIERO, M., RAVAGNAN, G. & GRATTON, E. 1994. Cholesterol modifies water concentration and dynamics in phospholipid-bilayers- A fluorescence study using Laurdan probe. *Biophysical Journal,* 66**,** 763-768.

PARPAL, S., KARLSSON, M., THORN, H. & STRALFORS, P. 2001. Cholesterol depletion disrupts caveolae and insulin receptor signaling for metabolic control via insulin receptor substrate-1, but not for mitogen-activated protein kinase control. *Journal of Biological Chemistry,* 276**,** 9670-9678.

PAZDRO, R. & BURGESS, J. R. 2010. The role of vitamin E and oxidative stress in diabetes complications. *Mechanisms of Ageing and Development,* 131**,** 276-286.

PEDRUZZI, E., GUICHARD, C., OLLIVIER, W., DRISS, F., FAY, M., PRUNET, C., MARIE, J. C., POUZET, C., SAMADI, M., ELBIM, C., O'DOWD, Y., BENS, M., VANDEWALLE, A., GOUGEROT-POCIDALO, M. A., LIZARD, G. & OGIER-DENIS, E. 2004. NAD(P)H oxidase Nox-4 mediates 7-ketocholesterol-induced endoplasmic reticulum stress and apoptosis in human aortic smooth muscle cells. *Molecular and Cellular Biology,* 24**,** 10703-10717.

PERLY, B., SMITH, I. C. P., HUGHES, L., BURTON, G. W. & INGOLD, K. U. 1985. Estimation of the location of natural alpha-tocopherol in lipid bilayers by C-13-NMR spectroscopy. *Biochimica Et Biophysica Acta,* 819**,** 131-135.

PETERSON, U., MANNOCK, D. A., LEWIS, R., POHL, P., MCELHANEY, R. N. & POHL, E. E. 2002. Origin of membrane dipole potential: Contribution of the phospholipid fatty acid chains. *Chemistry and Physics of Lipids,* 117**,** 19-27.

PHILLIPS, J. E., GENG, Y. J. & MASON, R. P. 2001. 7-Ketocholesterol forms crystalline domains in model membranes and murine aortic smooth muscle cells. *Atherosclerosis,* 159**,** 125-135.

PIKE, L. J. 2003. Lipid rafts: bringing order to chaos. *Journal of Lipid Research,* 44**,** 655-667.

PIKE, L. J. 2006. Rafts defined: a report on the Keystone Symposium on Lipid Rafts and Cell Function. *Journal of Lipid Research,* 47**,** 1597-1598.

POPIK, W. & ALCE, T. M. 2004. CD4 receptor localized to non-raft membrane microdomains supports HIV-1 entry - Identification of a novel raft localization marker in CD4. *Journal of Biological Chemistry,* 279**,** 704-712.

PRALLE, A., KELLER, P., FLORIN, E. L., SIMONS, K. & HORBER, J. K. H. 2000. Sphingolipid-cholesterol rafts diffuse as small entities in the plasma membrane of mammalian cells. *Journal of Cell Biology,* 148**,** 997-1007.

PRASAD, K. N., HERNANDEZ, C., EDWARDSPRASAD, J., NELSON, J., BORUS, T. & ROBINSON, W. A. 1994. Modification of the effect of Tamoxifen, Cisplatin, DTIC, and Interferon-alpha-2B on human-melanoma cells in culture by a mixture of vitamins. *Nutrition and Cancer-an International Journal,* 22**,** 233-245.

PRASAD, K. N., KUMAR, B., YAN, X. D., HANSON, A. J. & COLE, W. C. 2003. alpha-tocopheryl succinate, the most effective form of vitamin E for adjuvant cancer treatment: A review. *Journal of the American College of Nutrition,* 22**,** 108-117.

PRASAD, K. N. & KUMAR, R. 1996. Effect of individual and multiple antioxidant vitamins on growth and morphology of human nontumorigenic and tumorigenic parotid acinar cells in culture. *Nutrition and Cancer-an International Journal,* 26**,** 11-19.

PRIEME, H., LOFT, S., NYYSSONEN, K., SALONEN, J. T. & POULSEN, H. E. 1997. No effect of supplementation with vitamin E, ascorbic acid, or coenzyme Q10 on oxidative DNA damage estimated by 8-oxo-7,8-dihydro-2'-deoxyguanosine excretion in smokers. *American Journal of Clinical Nutrition,* 65**,** 503-507.

PRIES, A. R., SECOMB, T. W. & GAEHTGENS, P. 2000. The endothelial surface layer. *Pflugers Archiv-European Journal of Physiology,* 440**,** 653-666.

PURDON, A. D., TINKER, D. O. & NEUMANN, A. W. 1976. Detection of lipid phase-transitions by surface tensiometry. *Chemistry and Physics of Lipids,* 17**,** 344-352.

QUINN, P. J. 2004. Is the distribution of alpha-tocopherol in membranes consistent with its putative functions? *Biochemistry-Moscow,* 69**,** 58-66.

RESNICK, N., YAHAV, H., SHAY-SALIT, A., SHUSHY, M., SCHUBERT, S., ZILBERMAN, L. C. M. & WOFOVITZ, E. 2003. Fluid shear stress and the vascular endothelium: for better and for worse. *Progress in Biophysics & Molecular Biology,* 81**,** 177-199.

RIETVELD, A. & SIMONS, K. 1998. The differential miscibility of lipids as the basis for the formation of functional membrane rafts. *Biochimica Et Biophysica Acta-Reviews on Biomembranes,* 1376**,** 467-479.

RIPOLL, E. A. P., RAMA, B. N. & WEBBER, M. M. 1986. Vitamin-E enhances the chemotherapeutic effects of Adriamycin on human prostatic-carcinoma cells-invitro. *Journal of Urology,* 136**,** 529-531.

ROBINSON, D., BESLEY, N. A., VERE, K. A., O'SHEA, P. & HIRST, J. D. 2010. Order Profiles of Water on Phospholipid / Cholesterol Membrane Bilayer Surfaces.

ROBINSON, I., DE SERNA, D., GUTIERREZ, A. & SCHADE, D. 2006. Vitamin E in humans: an explanation of clinical trial failure. *Endocrine practice,* 12**,** 576-582.

ROONEY, M., TAMURALIS, W., LIS, L. J., YACHNIN, S., KUCUK, O. & KAUFFMAN, J. W. 1986. The influence of oxygenated sterol compounds on dipalmitoylphosphatidylcholine bilayer structure and packing. *Chemistry and Physics of Lipids,* 41**,** 81-92.

ROSENBLAT, M. & AVIRAM, M. 2002. Oxysterol-induced activation of macrophage NADPH-oxidase enhances cell-mediated oxidation of LDL in the atherosclerotic apolipoprotein E deficient mouse: inhibitory role for vitamin E. *Atherosclerosis,* 160**,** 69-80.

ROUQUETTE-JAZDANIAN, A. K., PELASSY, C., BREITTMAYER, J. P. & AUSSEL, C. 2006. Revaluation of the role of cholesterol in stabilizing rafts implicated in T cell receptor signaling. *Cellular Signalling,* 18**,** 105-122.

ROYER, M. C., LEMAIRE-EWING, S., DESRUMAUX, C., MONIER, S., DE BARROS, J. P. P., ATHIAS, A., NEEL, D. & LAGROST, L. 2009. 7-Ketocholesterol Incorporation into Sphingolipid/Cholesterol-enriched (Lipid Raft) Domains Is Impaired by Vitamin E- A specific role for alpha-tocopherol with consequences on cell death. *Journal of Biological Chemistry,* 284**,** 15826-15834.

SANCHEZ-MIGALLON, M., ARANDA, F. J. & GOMEZ-FERNANDEZ, J. C. 1996. Interaction between alpha-tocopherol and heteroacid phosphatidylcholines with different amounts of unsaturation. *Biochimica Et Biophysica Acta-Biomembranes,* 1279**,** 251-258.

SANKARAM, M. B. & THOMPSON, T. E. 1991. Cholesterol-induced fluid-phase immiscibility in membranes. *Proceedings of the National Academy of Sciences of the United States of America,* 88**,** 8686-8690.

SAREMI, A. & ARORA, R. 2010. Vitamin E and Cardiovascular Disease. *American Journal of Therapeutics,* 17**,** E56-E65.

SCHINKEL, A. H., SMIT, J. J. M., VAN TELLINGEN, O., BEIJNEN, J. H., WAGENAAR, E., VAN DEEMTER, L., MOL, C., VAN DERVALK, M. A., ROBANUSMAANDAG, E. C., TERIELE, H. P. J., BERNS, A. J. M. & BORST, P. 1994. Disruption of the mouse MDR1A p-glycoprotein gene leads to a deficiency in the blood-brain-barrier and to increased sensitivity to drugs. *Cell,* 77**,** 491-502.

SCHLESSINGER, J., VANOBBERGHEN, E. & KAHN, C. R. 1980. Insulin and antibodies against insulin-receptor cap on the membrane of cultured human-lymphocytes. *Nature,* 286**,** 729-731.

SCHUTZ, G. J., KADA, G., PASTUSHENKO, V. P. & SCHINDLER, H. 2000. Properties of lipid microdomains in a muscle cell membrane visualized by single molecule microscopy. *Embo Journal,* 19**,** 892-901.

SEELIG, J., MACDONALD, P. M. & SCHERER, P. G. 1987. Phospholipid head groups as sensors if electric charge in membranes. *Biochemistry,* 26**,** 7535-7541.

SEGEL, I. 1976. *Biochemical calculations: How to solve mathematical problems in general biochemistry*, John Wiley & Sons.

SEMCHYSCHYN, D. J. & MACDONALD, P. M. 2004. Conformational response of the phosphatidylcholine headgroup to bilayer surface charge: torsion angle constraints from dipolar and quadrupolar couplings in bicelles. *Magnetic Resonance in Chemistry,* 42**,** 89-104.

SEVERCAN, F. 1997. Vitamin E decreases the order of the phospholipid model membranes in the gel phase: An FTIR study. *Bioscience Reports,* 17**,** 231-235.

SHAIKH, S. R. & EDIDIN, M. A. 2006. Membranes are not just rafts. *Chemistry and Physics of Lipids,* 144**,** 1-3.

SHARMA, P., VARMA, R., MAYOR, S. 2006. The Biophysical Characterization of Lipid Rafts, chapter 3 in: Fielding, C.J. (Ed.), Lipid Rafts and Caveolae: From Membrane Biophysics to Cell Biology, Wiley-VCH.

SHEETS, E. D., LEE, G. M., SIMSON, R. & JACOBSON, K. 1997. Transient confinement of a glycosylphosphatidylinositol-anchored protein in the plasma membrane. *Biochemistry,* 36**,** 12449-12458.

SHEPHERD, J. C. W. & BULDT, G. 1978. Zwitterionic dipoles as a dielectric probe for investigating head group mobility in phospholipid membranes. *Biochimica Et Biophysica Acta,* 514**,** 83-94.

SHINER, J. S. & SOLARO, R. J. 1984. The Hill coefficient for the Ca2+-activation of striated-muscle contraction. *Biophysical Journal,* 46**,** 541-543.

SHOGOMORI, H. & BROWN, D. A. 2003. Use of detergents to study membrane rafts: The good, the bad, and the ugly. *Biological Chemistry,* 384**,** 1259-1263.

SILVIUS, J. R. 1982. Thermotropic Phase Transitions of Pure Lipids in Model Membranes and Their Modifications by Membrane Proteins. *Lipid-Protein Interactions.* New York: John Wiley & Sons, Inc.

SILVIUS, J. R., DELGIUDICE, D. & LAFLEUR, M. 1996. Cholesterol at different bilayer concentrations can promote or antagonize lateral segregation of phospholipids of differing acyl chain length. *Biochemistry,* 35**,** 15198-15208.

SIM, B., CLADERA, J. & O'SHEA, P. 2004. Fibronectin interactions with osteoblasts: Identification of a non-integrin-mediated binding mechanism using a real-time fluorescence binding assay. *Journal of Biomedical Materials Research Part A,* 68A**,** 352-359.

SIMON, S. A. & MCINTOSH, T. J. 1986. Depth of water penetration into lipid bilayers. *Methods in Enzymology,* 127**,** 511-521.

SIMON, S. A., MCINTOSH, T. J., MAGID, A. D. & NEEDHAM, D. 1992. Modulation of the interbilayer hydration pressure by the addition of dipoles at the hydrocarbon water interface. *Biophysical Journal,* 61**,** 786-799.

SIMONS, K. & IKONEN, E. 1997. Functional rafts in cell membranes. *Nature,* 387**,** 569-572.

SIMONS, K. & TOOMRE, D. 2000. Lipid rafts and signal transduction. *Nature Reviews Molecular Cell Biology,* 1**,** 31-39.

SIMSON, R., YANG, B., MOORE, S. E., DOHERTY, P., WALSH, F. S. & JACOBSON, K. A. 1998. Structural mosaicism on the submicron scale in the plasma membrane. *Biophysical Journal,* 74**,** 297-308.

SINGER, S. J. & NICOLSON, G. L. 1972. Fluid Mosaic Model of Structure of Cell-Membranes. *Science,* 175**,** 720-&.

SMITH, M. A., ROTTKAMP, C. A., NUNOMURA, A., RAINA, A. K. & PERRY, G. 2000. Oxidative stress in Alzheimer's disease. *Biochimica Et Biophysica Acta-Molecular Basis of Disease,* 1502**,** 139-144.

SMONDYREV, A. M. & BERKOWITZ, M. L. 2001. Effects of oxygenated sterol on phospholipid bilayer properties: a molecular dynamics simulation. *Chemistry and Physics of Lipids,* 112**,** 31-39.

SRIVASTAVA, S., PHADKE, R. S., GOVIL, G. & RAO, C. N. R. 1983. Fluidity, permeability and antioxidant behaviour of model membranes incorporates with alpha-tocopherol and vitamin-E acetate. *Biochimica Et Biophysica Acta,* 734**,** 353-362.

STARKE-PETERKOVIC, T. & CLARKE, R. J. 2009. Effect of headgroup on the dipole potential of phospholipid vesicles. *European Biophysics Journal with Biophysics Letters,* 39**,** 103-110.

STARKE-PETERKOVIC, T., TURNER, N., VITHA, M. F., WALLER, M. P., HIBBS, D. E. & CLARKE, R. J. 2006. Cholesterol effect on the dipole potential of lipid membranes. *Biophysical Journal,* 90**,** 4060-4070.

STERN, M. 1995. Diabetes and cardiovascular disease. The "common soil" hypothesis. *Diabetes,* 44**,** 369-374.

STILLWELL, W., DALLMAN, T., DUMAUAL, A. C., CRUMP, F. T. & JENSKI, L. J. 1996. Cholesterol versus alpha-tocopherol: Effects on properties of bilayers made from heteroacid phosphatidylcholines. *Biochemistry,* 35**,** 13353-13362.

STILLWELL, W., EHRINGER, W., WANG, L. J. & WASSALL, S. R. 1990. Effect of alpha-tocopherol on phospholipid-bilayer stability. *Biophysical Journal,* 57**,** A271-A271.

STILLWELL, W., EHRINGER, W. & WASSALL, S. R. 1992. Interaction of alpha-tocopherol with fatty-acids in membranes and ethanol. *Biochimica Et Biophysica Acta,* 1105**,** 237-244.

SUARNA, C., DEAN, R. T., MAY, J. & STOCKER, R. 1995. Human atherosclerotic plaque contains both oxidised lipids and relatively large amounts of alpha-tocopherol and ascorbate. *Arteriosclerosis Thrombosis and Vascular Biology,* 15**,** 1616-1624.

SUZUKI, Y., TSUCHIYA, M., WASSALL, S. R., CHOO, Y. M., GOVIL, G., KAGAN, V. E. & PACKER, L. 1993. Structural and dynamic membrane-properties of alpha-tocopherol and alpha-tocotrienol- Implication to the molecular mechanism of their antioxidant potency. *Biochemistry,* 32**,** 10692-10699.

TAGHIBIGLOU, C., BRADLEY, C. A., GAERTNER, T., LI, Y. P., WANG, Y. S. & WANG, Y. T. 2009. Mechanisms involved in cholesterol-induced neuronal insulin resistance. *Neuropharmacology,* 57**,** 268-276.

TANFORD, C. 1980. *The Hydrophobic Effect: Formation of Micelles and Biological Membranes,* NY, Wiley.

TARBELL, J. M. & PAHAKIS, M. Y. 2006. Mechanotransduction and the glycocalyx. *Journal of Internal Medicine,* 259**,** 339-350.

TARBELL, J. M., WEINBAUM, S. & KAMM, R. D. 2005. Cellular fluid mechanics and mechanotransduction. *Annals of Biomedical Engineering,* 33**,** 1719-1723.

THEUNISSEN, J. J. H., JACKSON, R. L., KEMPEN, H. J. M. & DEMEL, R. A. 1986. Membrane-properties of oxysterols- Interfacial orientation, influence on membrane-permeability and redistribution between membranes. *Biochimica Et Biophysica Acta,* 860**,** 66-74.

THEWALT, J. L. & BLOOM, M. 1992. Phosphatidylcholine-cholesterol phase diagrams. *Biophysical Journal,* 63**,** 1176-1181.

TIETZE, F., LOMAX, N. R. & MORTIMORE, G. E. 1962. Preparation and properties of fluorescent insulin derivatives. *Biochimica Et Biophysica Acta,* 59**,** 336-&.

TRABER, M. G. & ATKINSON, J. 2007. Vitamin E, antioxidant and nothing more. *Free Radical Biology and Medicine,* 43**,** 4-15.

TRABER, M. G. & KAYDEN, H. J. 1989. Preferential incorporation of alpha-tocopherol vs gamma-tocopherol in human lipoproteins. *American Journal of Clinical Nutrition,* 49**,** 517-526.

TRAUBLE, H. & EIBL, H. 1974. Electrostatic effects on lipid phase-transitions- Membrane structure and ionic environment. *Proceedings of the National Academy of Sciences of the United States of America,* 71**,** 214-219.

TRAXINGER, R. R. & MARSHALL, S. 1990. Glucose regulation of insulin-receptor affinity in primary cultured adipocytes. *Journal of Biological Chemistry,* 265**,** 18879-18883.

TYURIN, V. A., KAGAN, V. E., SERBINOVA, E. A., GORBUNOV, N. V., ERIN, A. N., PRILIPKO, L. L. & STOICHEV, T. S. 1986. Interaction of alpha-tocopherol with phospholipid liposomes- Absence of transbilayer mobility. *Bulletin of Experimental Biology and Medicine,* 102**,** 1677-1680.

ULRICH, A. S. & WATTS, A. 1994. Molecular response of the lipid headgroup to bilayer hydration monitored by H-2-NMR. *Biophysical Journal,* 66**,** 1441-1449.

URAKAWA, H., KATSUKI, A., SUMIDA, Y., GABAZZA, E. C., MURASHIMA, S., MORIOKA, K., MARUYAMA, N., KITAGAWA, N., TANAKA, T., HORI, Y., NAKATANI, K., YANO, Y. & ADACHI, Y. 2003. Oxidative stress is associated with adiposity and insulin resistance in men. *Journal of Clinical Endocrinology & Metabolism,* 88**,** 4673-4676.

URANO, S., IIDA, M., OTANI, I. & MATSUO, M. 1987. Membrane stabilization of vitamin-E- Interactions of alpha-tocopherol with phospholipids in bilayer liposomes. *Biochemical and Biophysical Research Communications,* 146**,** 1413-1418.

URANO, S., INOMORI, Y., SUGAWARA, T., KATO, Y., KITAHARA, M., HASEGAWA, Y., MATSUO, M. & MUKAI, K. 1992. Vitamin E- Inhibition of Retinol-induced hemolysis and membrane-stabilizing behaviour. *Journal of Biological Chemistry,* 267**,** 18365-18370.

URANO, S., MATSUO, M., SAKANAKA, T., UEMURA, I., KOYAMA, M., KUMADAKI, I. & FUKUZAWA, K. 1993. Mobility and molecular-orientation of vitamin-E in liposomal membranes as determined by F-19 NMR and fluorescence polarization techniques. *Archives of Biochemistry and Biophysics,* 303**,** 10-14.

URANO, S., SHICHITA, N. & MATSUO, M. 1988a. Interaction of vitamin-E and its model compounds with unsaturated fatty-acids in homogeneous solution. *Journal of Nutritional Science and Vitaminology,* 34**,** 189-194.

URANO, S., YANO, K. & MATSUO, M. 1988b. Membrane-stabilizing effect of vitamin-E- Effect of alpha-tocopherol and its model compounds on fluidity of lecithin liposomes. *Biochemical and Biophysical Research Communications,* 150**,** 469-475.

VAINIO, S., BYKOV, I., HERMANSSON, M., JOKITALO, E., SOMERHARJU, P. & IKONEN, E. 2005. Defective insulin receptor activation and altered lipid rafts in Niemann-Pick type C disease hepatocytes. *Biochemical Journal,* 391**,** 465-472.

VAINIO, S., HEINO, S., MANSSON, J. E., FREDMAN, P., KUISMANEN, K., VAARALA, O. & IKONEN, E. 2002. Dynamic association of human insulin receptor with lipid rafts in cells lacking caveolae. *Embo Reports,* 3**,** 95-100.

VALENTA, C., STEININGER, A. & AUNER, B. G. 2004. Phloretin and 6-ketocholestanol: membrane interactions studied by a phospholipid/polydiacetylene colorimetric assay and differential scanning calorimetry. *European Journal of Pharmaceutics and Biopharmaceutics,* 57**,** 329-336.

VAN BLITTERSWIJK, W. J., VAN DER MEER, B. W. & HILKMANN, H. 1987. Quantitative contributions of cholesterol and the individual classes of phospholipids and their degree of fatty acyl (un)saturation to membrane fluidity measured by fluorescence polarization. *Biochemistry,* 26**,** 1746-1756.

VAN DIJCK, P. W. M., DE KRUIJFF, B., VAN DEENEN, L. L. M., DEGIER, J. & DEMEL, R. A. 1976. Preference of cholesterol for phosphatidylcholine in mixed phosphatidylcholine-phosphatidylethanolamine bilayers. *Biochimica Et Biophysica Acta,* 455**,** 576-587.

VAN DIJCK, P. W. M., KAPER, A. J., OONK, H. A. J. & DEGIER, J. 1977. Miscibility properties of binary phosphatidylcholine mixtures- calorimetric study. *Biochimica Et Biophysica Acta,* 470**,** 58-69.

VAN DIJCK, P. W. M., VERVERGAERT, P., VERKLEIJ, A. J., VAN DEENEN, L. L. M. & DEGIER, J. 1975. Influence of Ca2+ and Mg2+ on thermotropic phase behaviour and permeability properties of liposomes prepared from dimyristoyl phosphatidylglycerol and mixtures of dimyristoyl phosphatidylglycerol and dimyristoyl phosphatidylcholine. *Biochimica Et Biophysica Acta,* 406**,** 465-478.

VAN GINKEL, G., MULLER, J. M., SIEMSEN, F., VANTVELD, A. A., KORSTANJE, L. J., VAN ZANDVOORT, M. A. M., WRATTEN, M. L. & SEVANIAN, A. 1992. Impact of oxidized lipids and antioxidants, such as vitamin-E and Lazaroids, on the structure and dynamics of unsaturated membranes. *Journal of the Chemical Society-Faraday Transactions,* 88**,** 1901-1912.

VAN ASPEREN, J., VAN TELLINGEN, O., SPARREBOOM, A., SCHINKEL, A. H., BORST, P., NOOIJEN, W. J. & BEIJNEN, J. H. 1997. Enhanced oral bioavailability of paclitaxel in mice treated with the P-glycoprotein blocker SDZ PSC 833. *British Journal of Cancer,* 76**,** 1181-1183.

VASILENKO, I., DEKRUIJFF, B. & VERKLEIJ, A. J. 1982. Polymorphic phase-behaviour of cardiolipin from bovine heart and from bacillus-subtilis as detected by P-31-NMR and freeze-fracture techniques- Effects of Ca-2+, Mg-2+, Ba-2+ and temperature. *Biochimica Et Biophysica Acta,* 684**,** 282-286.

VEATCH, S. L., POLOZOV, I. V., GAWRISCH, K. & KELLER, S. L. 2004. Liquid domains in vesicles investigated by NMR and fluorescence microscopy. *Biophysical Journal,* 86**,** 2910-2922.

VEJUX, A., MALVITTE, L. & LIZARD, G. 2008. Side effects of oxysterols: cytotoxicity, oxidation, inflammation, and phospholipidosis. *Brazilian Journal of Medical and Biological Research,* 41**,** 545-556.

VICKERS, T. 2007. Radical chain reaction mechanism of lipid peroxidation. *In:* PEROXIDATION.PNG, L. (ed.) *w:image:Lipid peroxidation v2.png.* v2 ed.: www.wikipedia.org.

VIOLA, A., SCHROEDER, S., SAKAKIBARA, Y. & LANZAVECCHIA, A. 1999. T lymphocyte costimulation mediated by reorganization of membrane microdomains. *Science,* 283**,** 680-682.

VIST, M. R. & DAVIS, J. H. 1990. Phase-equilibria of cholesterol and dipalmitoylphosphatidylcholine mixtures- H-2 nuclear magnetic-resonance and differential scanning calorimetry. *Biochemistry,* 29**,** 451-464.

VITHA, M. F. & CLARKE, R. J. 2007. Comparison of excitation and emission ratiometric fluorescence methods for quantifying the membrane dipole potential. *Biochimica Et Biophysica Acta*.

VOGEL, V. & MOBIUS, D. 1988. Hydrated polar groups in lipid monolayers- Effective local dipole-moments and dielectric-properties. *Thin Solid Films,* 159**,** 73-81.

VOGLINO, L., MCINTOSH, T. J. & SIMON, S. A. 1998. Modulation of the binding of signal peptides to lipid bilayers by dipoles near the hydrocarbon-water interface. *Biochemistry,* 37**,** 12241-12252.

WALL, J., AYOUB, F. & OSHEA, P. 1995a. Interactions of Macromolecules with the Mammalian-Cell Surface. *Journal of Cell Science,* 108**,** 2673-2682.

WALL, J., GOLDING, C. A., VAN VEEN, M. & O'SHEA, P. 1995b. The use of fluoresceinphosphatidylethanolamine (FPE) as a real-time probe for peptide-membrane interactions. *Molecular Membrane Biology,* 12**,** 183-192.

WANG, J. W., MEGHA & LONDON, E. 2004. Relationship between sterol/steroid structure and participation in ordered lipid domains (lipid rafts): Implications for lipid raft structure and function. *Biochemistry,* 43**,** 1010-1018.

WANG, X. Y. & QUINN, P. J. 1999. The effect of alpha-tocopherol on the thermotropic phase behaviour of dipalmitoylphosphatidylethanolamine - A synchrotron X-ray diffraction study. *European Journal of Biochemistry,* 264**,** 1-8.

WANG, X. Y. & QUINN, P. J. 2000a. Preferential interaction of alpha-tocopherol with phosphatidylcholines in mixed aqueous dispersions of phosphatidylcholine and phosphatidylethanolamine. *European Journal of Biochemistry,* 267**,** 6362-6368.

WANG, X. Y. & QUINN, P. J. 2000b. The distribution of alpha-tocopherol in mixed aqueous dispersions of phosphatidylcholine and phosphatidylethanolamine. *Biochimica Et Biophysica Acta-Biomembranes,* 1509**,** 361-372.

WANG, X. Y. & QUINN, P. J. 2000c. The location and function of vitamin E in membranes (review). *Molecular Membrane Biology,* 17**,** 143-156.

WANG, X. Y. & QUINN, P. J. 2002. Phase separations of alpha-tocopherol in aqueous dispersions of distearoylphosphatidylethanolamine. *Chemistry and Physics of Lipids,* 114**,** 1-9.

WANG, X. Y. & QUINN, P. J. 2006. The structure and phase behaviour of alpha-tocopherol-rich domains in 1-palmitoyl-2-oleoyl-phosphatidylethanolamine. *Biochimie,* 88**,** 1883-1888.

WANG, Z. Q., LIN, H. N., LI, S. S. & HUANG, C. H. 1995. Phase-transition behavior and molecular-structures of monounsaturated phosphatidylcholines- calorimetric studies and molecular mechanics simulations. *Journal of Biological Chemistry,* 270**,** 2014-2023.

WASSALL, S. R., MCCABE, M. A., EHRINGER, W. & STILLWELL, W. 1990. H-2 NMR-studies of a structural role for vitamin-E in membranes. *Biophysical Journal,* 57**,** A473-A473.

WASSALL, S. R., THEWALT, J. L., WONG, L., GORRISSEN, H. & CUSHLEY, R. J. 1986. Deuterium NMR-study of the interaction of alpha-tocopherol with a phospholipid model membrane. *Biochemistry,* 25**,** 319-326.

WASSALL, S. R., WANG, L. J., MCCABE, R. C. Y., EHRINGER, W. D. & STILLWELL, W. 1991. Electron-spin-resonance study of the interaction of alpha-tocopherol with phospholipid model membranes. *Chemistry and Physics of Lipids,* 60**,** 29-37.

WEBER, T., LU, M., ANDERA, L., LAHM, H., GELLERT, N., FARISS, M. W., KORINEK, V., SATTLER, W., UCKER, D. S., TERMAN, A., SCHRODER, A., ERL, W., BRUNK, U. T., COFFEY, R. J., WEBER, C. & NEUZIL, J. 2002. Vitamin E succinate is a potent novel antineoplastic agent with high selectivity and cooperativity with tumor necrosis factor-related apoptosis-inducing ligand (Apo2 ligand) in vivo. *Clinical Cancer Research,* 8**,** 863-869.

WENZ, J. J. & BARRANTES, F. J. 2003. Steroid structural requirements for stabilizing or disrupting lipid domains. *Biochemistry,* 42**,** 14267-14276.

WHITEMAN, E. & BIRNBAUM, M. 2003. Assaying tyrosine phosphorylation of insulin receptor and insulin receptor substrates. *In:* OZCAN, S. (ed.) *Diabetes Mellitus methods and protocols.* Humana Press.

WHITESELL, R. R. & GLIEMANN, J. 1979. Kinetic-parameters of transport of 3-O-methylglucose and glucose in adipocytes. *Journal of Biological Chemistry,* 254**,** 5276-5283.

WOLF, G. 2005. The discovery of the antioxidant function of vitamin E: The contribution of Henry A. Mattill. *Journal of Nutrition,* 135**,** 363-366.

YEAGLE, P. 1988. Cholesterol and the cell membrane. *In:* YEAGLE, P. (ed.) *Biology of Cholesterol.* Boca Raton, FL: CRC press.

YEAGLE, P. 2005. The roles of cholesterol in biological membranes. *In:* YEAGLE, P. (ed.) *The structure of biological membranes.* second edition ed. Boca Raton, FL: CRC press.

YOUK, H. J., LEE, E., CHOI, M. K., LEE, Y. J., CHUNG, J. H., KIM, S. H., LEE, C. H. & LIM, S. J. 2005. Enhanced anticancer efficacy of alpha-tocopheryl succinate by conjugation with polyethylene glycol. *Journal of Controlled Release,* 107**,** 43-52.

YOUNG, I. & MCENENY, J. 2001. Lipoprotein oxidation and atherosclerosis. *Biochemical society transactions,* 29**,** 358-362.

ZHANG, H. X., DU, G. H. & ZHANG, J. T. 2004. Assay of mitochondrial functions by resazurin in vitro. *Acta Pharmacologica Sinica,* 25**,** 385-389.

ZHANG, J., DAVIDSON, R. M., WEI, M. D. & LOEW, L. M. 1998. Membrane electric properties by combined patch clamp and fluorescence ratio imaging in single neurons. *Biophysical Journal,* 74**,** 48-53.

ZIDOVETZKI, R. & LEVITAN, I. 2007. Use of cyclodextrins to manipulate plasma membrane cholesterol content: Evidence, misconceptions and control strategies. *Biochimica Et Biophysica Acta-Biomembranes,* 1768**,** 1311-1324.

ZIEGLER, O., CANTIN, C., GERMAIN, L., DUPUIS, M., SEKALY, R. P., DROUIN, P. & CHIASSON, J. L. 1994. Insulin binding to human cultured lymphocytes measured by flow cytometry using three ligands. *Cytometry,* 16**,** 339-345.

ZINGG, J. M. 2007. Modulation of signal transduction by vitamin E. *Molecular Aspects of Medicine,* 28**,** 481-506.

ZINGG, J. M. & AZZI, A. 2004. Non-antioxidant activities of vitamin E. *Current Medicinal Chemistry,* 11**,** 1113-1133.

ZUURBIER, C. J., DEMIRCI, C., KOEMAN, A., VINK, H. & INCE, C. 2005. Short-term hyperglycemia increases endothelial glycocalyx permeability and acutely decreases lineal density of capillaries with flowing red blood cells. *Journal of Applied Physiology,* 99**,** 1471-1476.

8. Appendix A

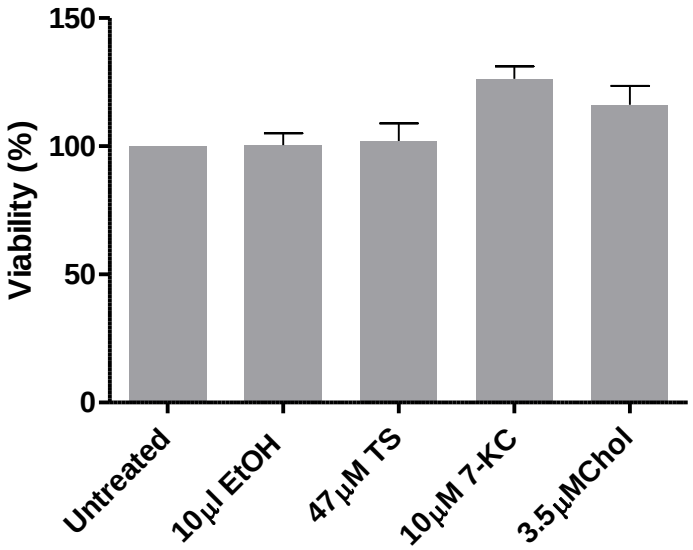

Figure 8.1.1:The percentage viability of Jurkat T-lymphocytes as determined using an AlamarBlue cell viability assay. Cells were treated with 47µM α-tocopherol succinate (TS), 10µM 7-ketocholesterol (7-KC) or 3.5µM cholesterol (Chol), which represent the maximum concentration the cells are exposed to during the titration experiments and a greater concentration that any pre-treatments applied, for 1hr at 37^{o}C prior to performing the assay as described in section 2.4.9. Cells were also treated with a 4µl/ml ethanol representing the maximum concentration of the solvent that the cells are exposure to during titration and pre-treatments. n=6 and a one-way ANOVA ($P<0.0001$, F-28.78, $R^2=0.82$) followed by Dunnett's multiple comparison test revealed that none of the treatments caused a significant decrease in viability; treatment with ethanol and α-tocopherol succinate caused no significant change in viability and treatment with 7-ketocholesterol or cholesterol significantly increased viability ($P<0.001$).